



**NOVEL ROUTES TOWARDS ANTIBIOTICS  
USING ORGANOCATALYTIC AND  
BIOCATALYTIC APPROACHES**

A Thesis Submitted to  
University College London

By

**David Steadman**

For the Degree of  
Doctor of Philosophy

Christopher Ingold Laboratories  
Department of Chemistry  
University College London  
20 Gordon Street  
London WC1H 0AJ

I, David Steadman, confirm that the work presented in this thesis is my own. Where information has been derived from other sources, I confirm that this has been indicated in the thesis.

Signature

## Abstract

Aromatic ketodiols and 2-amino-1,3-diols are present in many interesting biologically-active molecules. The aminodiol motif itself is present in the broad-spectrum antibiotics chloramphenicol and thiamphenicol. This thesis describes organocatalytic and biocatalytic approaches to this family of compounds, using organocatalysts and transketolase and transaminase enzymes.

Transketolase (TK) is a ThDP-dependent enzyme which has been used to prepare aliphatic ketodiols with good yields and high degrees of stereoselectivity. A biomimetic approach to racemic ketodiols has also been reported. Transaminases (TAMs) are a broad family of enzymes which stereoselectively form amines from ketone or aldehyde functionalities. A two-step TK/TAM pathway has already been reported which gives access to aliphatic aminodiols, but the preparation of aromatic aminodiols using this combined TK/TAM strategy has yet to be investigated.

A literature review of transketolase, transaminase and biocatalysis in general is presented in chapter 1. The substrate scope of the biomimetic TK reaction to prepare racemic aromatic ketodiols has been investigated, and an asymmetric variant developed which was used to transform aromatic aldehydes in water in up to 50% *ee* (chapter 2). A range of single TK mutants have been used to transform a small range of basic aromatic aldehydes (chapter 3) with low yields but good stereoselectivities (up to 80% *ee*). In order to create more active combination mutant TKs, a range of mutants were made and tested with aliphatic aldehydes (chapter 4) to determine what combinations of single mutants could be created without sacrificing enzyme structure and function. With knowledge gained from this and by further study of the TK active-site, a range of combination mutants were then created which accepted a range of functionalised benzaldehydes with excellent yields and stereoselectivities (<98 % *ee*, <100% yield, chapter 5). With mutant TKs in hand which could transform aromatic aldehydes, the use of two step TK/TAM strategy toward aromatic aldehydes was then investigated (chapter 5). Finally, to assess the substrate range of TK with regards to donor substrate, a range of novel donor substrates was investigated (chapter 6). Mutant TKs were shown to accept several novel donor substrates, giving access to chiral ketols with excellent stereoselectivity (>95% *ee*). Possible future work is outlined in chapter 7.

# Contents

Abstract .....	3
Contents.....	4
Table of Schemes.....	6
Table of Figures.....	8
Table of Tables .....	12
Abbreviations .....	14
Acknowledgements.....	17
1 Introduction.....	18
1.1 Enzymatic Catalysis in Synthesis .....	19
1.2 Thiamine diphosphate (ThDP) dependent enzymes .....	20
1.2.1 Pyruvate decarboxylase (PDC) (EC 4.1.1.1) .....	21
1.2.2 Benzoylformate decarboxylase (BFD) (EC 4.1.1.7) .....	24
1.2.3 Transketolase (EC 2.2.1.1).....	26
1.2.4 TK Function <i>in vivo</i> .....	27
1.2.5 Mechanism of TK catalysis.....	27
1.2.6 Sources of transketolase.....	29
1.2.7 Mutation and study of yeast transketolase .....	30
1.2.8 Mutation and study of <i>E. coli</i> TK.....	31
1.2.9 Biomimetic transketolase reaction.....	35
1.3 Use of TK in organic synthesis .....	37
1.3.1 Spinach transketolase in synthesis.....	37
1.3.2 <i>E. coli</i> transketolase in synthesis .....	38
1.3.3 Large scale process development .....	39
1.4 Transaminase.....	41
1.4.1 Function <i>in vivo</i> .....	41
1.4.2 Mechanism of catalysis.....	41
1.4.3 Classes of transaminase enzymes .....	44
1.4.4 Omega transaminases ( $\omega$ -transaminases).....	44
1.5 TAmS in organic synthesis .....	45
1.6 Aminodiol synthesis by TK and TAm .....	49
1.7 Syntheses of chloroamphenicol and thiamphenicol .....	51
1.8 Project aims and objectives .....	54
2 The Biomimetic Transketolase Reaction .....	55
2.1 Previous work carried out by the group before starting the PhD .....	56
2.2 Substrate scope of the racemic biomimetic reaction .....	57
2.3 Mechanistic study of the biomimetic transketolase reaction <sup>[79]</sup> .....	62
2.4 The asymmetric biomimetic TK reaction .....	66
2.4.1 Chiral analysis of ketodiol products from asymmetric biomimetic TK reaction .....	68
2.5 Summary of chapter 2.....	70
3 Aromatic aldehydes with single point mutant TKs.....	72

3.1	Previous work done by the group to identify active mutant TKs using a colorimetric assay .....	73
3.2	Biotransformations of aromatic aldehydes with active single mutant TKs	75
3.3	Chiral analytical methods for determining the stereoselectivities of aromatic ketodiols .....	80
3.4	Docking of benzaldehyde into D469T.....	83
3.5	Summary of chapter 3.....	86
4	Aliphatic aldehydes with single and combination mutant TKs .....	87
4.1	Creation of combination mutant libraries <sup>[88]</sup> .....	88
4.2	Biotransformations of aliphatic aldehydes with single and combination mutant TKs .....	93
4.3	Summary of chapter 4.....	100
5	Aromatic aldehydes with combination mutant TKs .....	101
5.1	Probing TK active-site with formylbenzoic acid.....	104
5.2	Screening of 3-formylbenzoic acid with TK mutants.....	108
5.3	Screening of 4-formylbenzoic acid with TK mutants.....	111
5.4	Creation of a new mutant library to improve the bioconversions with aromatic aldehydes.....	115
5.5	Biotransformation of aromatic aldehydes with combination mutant TKs	123
5.6	Aromatic substrates not accepted by combination mutant TKs .....	147
5.7	Aminodiol synthesis with TAm.....	148
5.8	Assignment of absolute stereochemistry of aromatic ketodiols using transaminase .....	153
5.9	Analysis of docking results to support assignment of absolute stereochemistry .....	158
5.10	Summary of chapter 5.....	161
6	Novel donor substrates with transketolase .....	162
6.1	Sodium pyruvate as a donor in the TK reaction.....	166
6.2	2-Ketobutyric acid as a donor in the TK reaction .....	170
6.3	2-ketoglutaric acid as a donor in the TK reaction .....	172
6.4	Determination of stereoselectivity of TK with novel donors .....	173
6.4.1	Determination of stereoselectivity of TK reaction with sodium pyruvate as donor substrate .....	173
6.4.2	Determination of stereoselectivity of TK reaction with 2-ketobutyric acid as donor substrate .....	177
6.5	Summary of chapter 6.....	180
7	Conclusions and future work.....	181
8	Experimental.....	184
9	References .....	221
	Appendix .....	227

## Table of Schemes

Scheme 1.1. Biocatalytic formation of artemisinic acid (2).....	20
Scheme 1.2. PDC catalysed formation of ( <i>R</i> )-PAC (5) .....	21
Scheme 1.3. Overall reaction scheme and mechanism for the <i>in vivo</i> decarboxylation of pyruvate (7) by PDC .....	22
Scheme 1.4. Overall reaction scheme and mechanism of pyruvate decarboxylase catalysed ketol formation .....	24
Scheme 1.5. Overall reaction scheme and mechanism of BFD catalysed ketol formation .....	25
Scheme 1.6. Crossed benzoin formation catalysed by BFD mutant, H281A .....	26
Scheme 1.7. TK-catalysed reaction <i>in vivo</i> .....	27
Scheme 1.8. TK-catalysed reaction <i>in vitro</i> with HPA as ketol donor.....	27
Scheme 1.9. Overall reaction scheme and mechanism for the <i>in vitro</i> TK reaction with HPA (23) as the ketol donor .....	29
Scheme 1.10 TK biotransformation of glycolaldehyde (26) to erythrulose (27) using HPA (23) as the donor substrate.....	32
Scheme 1.11 TK biotransformation of propanal (24) to ketodiol (25) using HPA (23) as the donor substrate.....	33
Scheme 1.12 Biotransformation of aliphatic aldehydes by D469E and H26Y TK...	34
Scheme 1.13. Overall reaction scheme and initial postulated mechanism for the NMM-catalysed biomimetic TK reaction <sup>[50]</sup> .....	36
Scheme 1.14. Synthesis of "natural-labelled" 6-deoxy-L-sorbose (32) using spinach transketolase .....	37
Scheme 1.15. Synthetic route towards a novel <i>N</i> -hydroxypyrrolidine (38) using TK mediated carbon-carbon bond formation in the first step .....	39
Scheme 1.16. Model TK catalysed carbon-carbon bond formation reaction of Li-HPA (Li-23) and glycolaldehyde (26) to generate L-erythrulose (27).....	40
Scheme 1.17 Overall reaction scheme and the combined half-reactions of the <i>in vivo</i> transaminase reaction.....	43
Scheme 1.18. Synthesis of ( <i>R</i> )-4-phenylpyrrolidin-2-one (52) via dynamic kinetic resolution catalysed by TAm.....	45
Scheme 1.19. Chemoenzymatic synthesis of ( <i>S</i> )-Rivastigmine (56).....	46
Scheme 1.20. Two catalytic routes to the synthesis of sitagliptin (61).....	48
Scheme 1.21. ABT (67) synthesis <i>via</i> a TK/TAm mediated synthetic pathway <sup>[74]</sup> ...	50
Scheme 1.22. Four possible stereoisomers of 69 resulting from chemical reductive amination of ketodiol 68 .....	51
Scheme 1.23.TAm reaction using ketodiol 68 as a substrate exclusively forming a new ( <i>S</i> ) stereocentre.....	51
Scheme 1.24. Three- step synthesis of chloramphenicol (66) <sup>[76]</sup> .....	52
Scheme 1.25. Four step synthesis of thiamphenicol (70) <sup>[76]</sup> .....	53
Scheme 1.26. 5 step Synthesis of chloramphenicol (66) using a tethered aminohydroxylation approach <sup>[77]</sup> .....	54

Scheme 2.1 Reaction scheme of buffer catalysed ketodiol formation.....	56
Scheme 2.2 Synthesis of 3,4-dimethylcyclohex-3-enecarbaldehyde (122) and its potential use as a substrate in TK biotransformations .....	60
Scheme 2.3 Possible mechanisms of formation of rearranged ketodiol (128).....	61
Scheme 2.4 Possible mechanism of the biomimetic TK reaction - Mechanisms A and B.....	63
Scheme 2.5 Possible mechanisms of the biomimetic TK reaction – Mechanisms C and D.....	64
Scheme 2.6. Biomimetic TK reaction with <sup>13</sup> C-labelled HPA and benzaldehyde ....	65
Scheme 3.1 Transketolase catalysed ketodiol formation with cyclic aldehydes and D469E TK .....	73
Scheme 3.2 Colorimetric assay used to identify active TK mutants .....	74
Scheme 3.3 Proposed mechanism for the formation of the observed double addition product 144.....	74
Scheme 3.4 Proposed mechanism for the formation of undesired rearranged ketodiol (128) in the TK reaction.....	76
Scheme 5.1 Monobenzylation of ketodiol (68) for chiral HPLC analysis .....	125
Scheme 5.2 Di-benzylation of ketodiol (103) for chiral HPLC analysis. ....	129
Scheme 5.3 Attempts to derivatise 4-FBA biotransformation product (154) .....	143
Scheme 5.4 Approach to thiamphenicol using TAm.....	149
Scheme 5.5 Stereoselectivity of aromatic aminodiol synthesis by CV2025 <sup>[75]</sup> .....	149
Scheme 5.6 Combined TK and TAm strategy to an aromatic aminodiol (69) starting from benzaldehyde (8) .....	150
Scheme 5.7 69-B of known stereochemistry, and formation of 69-B derived from the two-step biotransformation procedure .....	155
Scheme 6.1 Formation of the active ThDP-enamine intermediate in the active site of TK with pyruvate derivatives .....	165
Scheme 6.2 TK reaction using sodium pyruvate as the donor substrate.....	166
Scheme 6.3 Phenylacetylcarbinol (5) formation by pyruvate decarboxylase and transketolase .....	167
Scheme 6.4 TK reaction with 2-ketobutyric acid as the donor substrate.....	170
Scheme 6.5 Potential use of $\alpha$ -ketoglutaric acid as a donor substrate for TK.....	172

## Table of Figures

Figure 1.1. Structure of thiamine diphosphate (ThDP).....	21
Figure 1.2 Representation of ThDP adduct in the active-site of yeast TK with the function of conserved residues indicated (reproduced from <sup>[37]</sup> ).....	30
Figure 1.3. Structure of ThDP in the active site of <i>E. coli</i> TK, with 1st shell (green) and 2nd shell (cyan) amino acid residues. (Used with permission from Elsevier). <sup>[46]</sup>	32
.....	32
Figure 1.4. Structure of PLP (44) .....	42
Figure 1.5. Structures of some biologically active aminodiols .....	49
Figure 1.6. Structures of chloramphenicol (66) and thiamphenicol (70).....	52
Figure 2.1 Tertiary amines and sulfonate screened with propanal for ketodiols formation .....	56
Figure 2.2 Aldehydes screened in initial investigation into the biomimetic TK reaction.....	57
Figure 2.3 Benzaldehydes 115-119 not accepted in biomimetic TK reaction .....	59
Figure 2.4 Structure of hydroquinine 4-methyl-2-quinolyl ether (131).....	66
Figure 2.5 Chiral HPLC traces of mono-benzoylated derivatives of (105) and (106). Elution times shown in minutes.....	69
Figure 2.6 Possible rationale for the formation of the assigned <i>R</i> -stereocentre (reproduced from <sup>[79]</sup> ).....	70
Figure 3.1 Overlaid chiral HPLC traces of dibenzoylated (68) from the biomimetic reaction (blue) and F434A (black).....	81
Figure 3.2 <sup>1</sup> H NMR Mosher's ester analysis for identification of the unknown absolute stereocentre in (68).....	82
Figure 3.3. Active site of D469T TK with the ThDP enamine from the crystal structure of WT-TK (1QGD) (green) and the ThDP-enamine configuration obtained from docking into D469T (orange) overlaid. ....	84
Figure 3.4 Three binding clusters obtained from docking benzaldehyde into D469T TK with the ThDP-enamine intermediate (orange) .....	84
Figure 4.1 Structures of desired aromatic ketodiols product (68) and undesired double addition product (144).....	88
Figure 4.2 Observed trade-off between specific activity and soluble TK concentration for a range of mutants with propanal. Diamonds-previously identified single mutants, squares-combination mutants made from active single mutants, triangles-combination mutants created after guidance by statistical coupling analysis. <sup>[88]</sup> (Used with permission from Elsevier).....	89
Figure 4.3 The nine residues forming a co-evolved network within the active-site of TK. <sup>[88]</sup> (Used with permission from Elsevier). ....	91
Figure 4.4 Effect of recombining R520V and R520Q with D469 mutants. Experimental specific activities shown in black, expected specific activities from additive effects of single mutants shown in white. <sup>[88]</sup> (Used with permission from Elsevier). ....	93



Figure 5.1 Conformations obtained from the computational docking of benzaldehyde (8) into D469T. (ThDP-enamine intermediated shown in orange).....	104
Figure 5.2 Structure of R5P (20) and crystal structure of <i>E. coli</i> WT TK with R5P bound (2R5N) <sup>[90]</sup> .....	105
Figure 5.3 3-Formylbenzoic acid (3-FBA) (97) with the phosphate mimic carboxylate group highlighted.....	106
Figure 5.4 Most populated cluster obtained by docking of 3-FBA (97) into D469T. (ThDP-enamine shown in orange).....	107
Figure 5.5 Results obtained for docking 3-FBA (97) into D469T/R520Q (ThDP-enamine shown in orange).....	111
Figure 5.6 Results obtained for docking 4-FBA (153) into D469T.....	113
Figure 5.7 Additional substituted benzaldehydes screened with D469T.....	115
Figure 5.8 Substrates used for screening of R358X/D469T/R520Q and S385X/D469T/R520Q mutant libraries.....	118
Figure 5.9 Lowest energy, non-productive cluster found for docking 3-FBA (97) into S385E/D469T/R520Q. (Two non-productive conformations shown in red and green, ThDP-enamine shown in orange). .....	120
Figure 5.10 Productive cluster found for docking 3-FBA (97) into S385E/D469T/R520Q. (ThDP-enamine shown in orange).....	120
Figure 5.11 Results found for docking 4-FBA (153) into S385Y/D469T/R520Q. (ThDP enamine shown in orange). .....	122
Figure 5.12 Productive cluster found for docking 3-HBA (93) into S385Y/D469T/R520Q. (ThDP-enamine shown in orange). .....	123
Figure 5.13 Chiral HPLC traces for mono-benzoate derivatives (68-B) of ; A - racemic product, B - S385T/D469T/R520Q product, C - S385Y/D469T/R520Q product. (Elution time shown in minutes).....	126
Figure 5.14 Most populated conformation found for docking of benzaldehyde into S385T/D469T/R520Q. (Non-productive conformation shown in white, ThDP-enamine shown in orange).....	127
Figure 5.15 Chiral HPLC traces of di-benzoylated derivatives (103-B) of; A - racemic product, B - S385T/D469T/R520Q product. Elution times are shown in minutes. ....	129
Figure 5.16 Chiral HPLC traces of mono-benzoylated derivatives (105-B) of; A - Racemic product, B - S385Y/D469T/R520Q product, C – S385E/D469T/R520Q product. Elution times are shown in minutes. ....	131
Figure 5.17 Chiral HPLC traces of mono-benzoylated derivatives (107-B) of; A - Racemic product, B - S385Y/D469T/R520Q product.....	133
Figure 5.18 Chiral HPLC traces of mono-benzoylated derivatives (106-B) of; A - racemic product, B - S385T/D469T/R520Q product.....	135
Figure 5.19 Results obtained for docking of methyl-3-formylbenzoate (95) into D469T. A-Lowest energy, most highly populated cluster showing productive conformation, B-Second cluster showing non-productive conformation, C-Third cluster showing non-productive conformation, D-Fourth cluster showing non-productive conformation. ....	136

Figure 5.20 Results obtained for docking of methyl-3-formylbenzoate into S385T/D469T/R520Q. A - First low-energy, highly populated cluster, showing productive conformation, B - Second low-energy, highly populated cluster showing productive conformation .....	137
Figure 5.21 Chiral HPLC traces of di-benzoylated derivatives (108-B) of; A - Racemic product, B - S385Y/D469T/R520Q product.....	140
Figure 5.22 Chiral HPLC traces of monobenzoylated derivatives (110-B) of; A - Racemic product, B - S385T/D469T/R520Q product, C - S385Y/D469T/R520Q product .....	141
Figure 5.23 Results obtained for the docking of 4-methylsulfonylbenzaldehyde. A – Non-productive cluster found for docking into D469T. B – Non-productive, lowest energy cluster found for docking into S385E/D469T/R520Q. C – Productive cluster found for docking into S385T/D469T/R520Q. D - Productive cluster found for docking into S385T/D469T/R520Q.....	146
Figure 5.24 Structure of 1,8-naphthaldehydic acid (160) .....	147
Figure 5.25 Range of Vanillin analogues tested with TK mutants.....	147
Figure 5.26 Structure of 3-nitrobenzaldehyde (98) .....	148
Figure 5.27 Two major products isolated after acetylation of the crude TAM reaction .....	150
Figure 5.28 Range of aromatic ketodiols investigated with CV2025.....	151
Figure 5.29 Assignment of absolute stereochemistry of aliphatic ketodiols based on a modified Mosher's analysis method. (Used with permission from Elsevier). <sup>[83]</sup> ....	153
Figure 5.30 Aliphatic ketodiols containing aromatic groups used to prove validity of modified Mosher's ester analysis method .....	154
Figure 5.31 Structures of both <i>syn</i> -diastereomers of 69 .....	154
Figure 5.32 Overlaid chiral HPLC profiles of 69-B from the TK/TAM strategy and (1 <i>S</i> ,2 <i>S</i> )-69-B. Elution times shown in minutes. ....	156
Figure 5.33 Productive conformation found for docking 3-FBA (97) into D469T, where neither face of the substrate is preferentially exposed to the ThDP-enamine intermediate. ....	159
Figure 5.34 Productive conformation found from docking of 4-(methylsulfonyl)benzaldehyde into S385T/D469T/R520Q, where neither face of the aldehyde is preferentially exposed to the ThDP-enamine intermediate. ....	159
Figure 5.35 Productive conformation found from docking of methyl-3-formylbenzoate into S385T/D460T/R520Q, with the re-face preferentially exposed to the ThDP-enamine intermediate attack.....	160
Figure 6.1 Structures of two of the natural substrates for TK, xylulose-5-phosphate (19) and fructose-6-phosphate (166).....	163
Figure 6.2 Crystal structures of WT-TK (2R5N) with; A - xylulose-5-phosphate (19) and B - fructose-6-phosphate (166), bound. ....	163
Figure 6.3 Pyruvate derivatives studied as donor substrates for yeast TK <sup>[102]</sup> .....	164
Figure 6.4 Potential novel donor substrates for TK.....	166
Figure 6.5 Use of Mosher's ester analysis to determine the absolute stereochemistry of ketol products (175) <sup>[104]</sup> (Used with permission from Elsevier). ....	174

Figure 6.6 <sup>1</sup> H-NMR of <i>S</i> -Mosher's derivative (175-B) of ketol (175) from D469E reaction with hexanal and sodium pyruvate, with terminal methyl singlet region expanded .....	175
Figure 6.7 <sup>1</sup> H-NMR of <i>S</i> -Mosher's derivative (174-B) of ketol (174) from D469E reaction with pentanal and sodium pyruvate, with terminal methyl singlet region expanded .....	176
Figure 6.8 <sup>1</sup> H-NMR spectrum of <i>S</i> -Mosher's derivative (175-B) of ketol (175) from the D469E reaction of hexanal with sodium pyruvate, with terminal methyl triplet region expanded.....	178
Figure 6.9 Formation of <i>S</i> -Mosher's ester derivative (177-B) of ketol (177) from the S385T/D469T/R520Q TK reaction with hexanal and 2-ketoglutaric acid. The resulting <sup>1</sup> H-NMR is shown, with the terminal methyl triplet region expanded.....	179
Figure 7.1 Approach to biocatalytic aminodiols synthesis; above route using currently available enzymes, below ideal route using ( <i>R</i> )-selective enzymes .....	183

## Table of Tables

Table 2.1 Tertiary amine catalysts screened for ketodiol formation with propanal <sup>[50]</sup> .....	57
Table 2.2 Yields obtained for benzaldehydes screened in biomimetic TK reaction* 58	
Table 2.3 Yields obtained for aliphatic aldehydes screened in biomimetic TK reaction* .....	60
Table 2.4 Yield and stereoselectivity data for substituted benzaldehydes screened in asymmetric biomimetic TK reaction* .....	67
Table 3.1 Biotransformations of benzaldehyde by single mutant TKs* .....	75
Table 3.2 Biotransformation of heteroaromatic aldehydes by single mutant TKs* ..	77
Table 3.3 Biotransformations of phenylacetaldehyde (149) and 2-methyl phenylacetaldehyde (151) by single mutant TKs* .....	78
Table 3.4 Biotransformations of 3-hydroxybenzaldehyde (99), 4-hydroxybenzaldehyde (118) and 4-chlorobenzaldehyde (99)* .....	79
Table 4.1 Library of combination mutants made to residues with the co-evolved network in TK. Variants with >70% activity of WT shown in bold. ....	92
Table 4.2 Isolated yield and stereoselectivity data obtained for the biotransformation of propanal by single, double and triple mutant TKs* .....	94
Table 4.3 Isolated yield and stereoselectivity data for single and double mutant TKs with butanal* .....	97
Table 4.4 Isolated yield and stereoselectivity data for single and double mutant TKs with pentanal* .....	97
Table 4.5 Isolated yield data for single, double and triple mutants with 3,4-dimethylcyclohex-3-enecarbaldehyde* .....	99
Table 5.1 Isolated yields and stereoselectivities for the transformation of benzaldehyde (8) by mutant TKs* .....	102
Table 5.2 Conversions obtained for the transformation of 3-formylbenzoic acid (97) by mutant TKs* .....	108
Table 5.3 Conversions obtained for the transformation of 3-FBA (97) by TKs with mutations at phosphate binding residues* .....	109
Table 5.4 Conversions obtained for the transformation of 4-FBA (153) by mutant TKs* .....	112
Table 5.5 Conversions obtained for the transformation of 4-FBA by TKs with mutations at phosphate binding residues <sup>†</sup> .....	114
Table 5.6 Isolated yields and stereoselectivities obtained for the transformation of benzaldehyde by S385X/D469T/R520Q <sup>†</sup> .....	124
Table 5.7 Isolated yields and stereoselectivities obtained for the transformation of 3-HBA (93) by S385X/D469T/R520Q mutants* .....	128
Table 5.8 Isolated yields and stereoselectivities obtained for the transformation of 3-fluorobenzaldehyde (93) by S385X/D469T/R520Q mutants* .....	130
Table 5.9 Isolated yields and stereoselectivities obtained for the transformation of 3-vinylbenzaldehyde (96) by S385X/D469T/R520Q mutants* .....	132

Table 5.10 Isolated yields and stereoselectivities obtained for the transformation of methyl-3-formylbenzoate (95) by S385X/D469T/R520Q mutants* .....	134
Table 5.11 Conversions and stereoselectivities obtained for the transformation of 3-FBA (97) by S385X/D469T/R520Q mutants* .....	138
Table 5.12 Isolated yields and stereoselectivities obtained for the transformation by S385X/D469T/R520Q mutants* .....	140
Table 5.13 Conversions obtained for the biotransformation of 4-FBA (153) by S385X/D469T/R520Q mutants* .....	142
Table 5.14 Conversion yields and stereoselectivities obtained for the biotransformation of 4-methylsulfonylbenzaldehyde by S385X/D469T/R520Q mutants* .....	144
Table 5.15 Previously reported elution times for all four diastereoisomers of triacetylated aminodiol 69 <sup>[75]</sup> .....	155
Table 5.16 Summary of stereoselectivities obtained for mutant TKs with aromatic aldehydes. Absolute stereochemistries based on the observed selectivity for TK with benzaldehyde, from study of acetylated aminodiol from combined TK/TAM approach .....	157
Table 6.1 Kinetic parameters obtained for pyruvate derivatives and their reaction with ThDP in the active-site of yeast TK <sup>[102]</sup> .....	164
Table 6.2 Yields obtained for D469E with sodium pyruvate (Na-7) as the donor substrate* .....	167
Table 6.3 Yields obtained for D469T with sodium pyruvate (Na-7) as the donor substrate* .....	168
Table 6.4 Yields obtained for D469Y, D469E/R520Q and S385T/D469T/R520Q with sodium pyruvate (Na-7) as the donor substrate* .....	169
Table 6.5 Yields obtained for D469E with 2-ketobutyric acid as the donor substrate* .....	170
Table 6.6 Yields obtained for D469T, D469Y, D469E/R520Q and S385T/D469T/R520Q with 2-ketobutyric acid as the donor substrate* .....	171
Table 6.7 Yields obtained for D469E with $\alpha$ -ketoglutaric acid as the donor substrate* .....	172
Table 6.8 Isolated yields and stereoselectivities obtained for D469E and D469T with sodium pyruvate as the donor substrate .....	177
Table 6.9 Isolated yields and stereoselectivities obtained for mutant TKs with 2-ketobutyric acid (172) as the donor substrate .....	180

## Abbreviations

ABT	2-Amino-1,3,4-butanetriol
Ac	Acetyl
AcN	Acetonitrile
Ar	Aryl
AT	Aminotransferase
Å	Angstrom
Ala	Alanine
<i>A. Annua</i>	<i>Artemisia annua</i>
Asp	Aspartic acid
Arg	Arginine
<i>ee</i>	Enantiomeric excess
BFD	Benzoylformate decarboxylase
br	Broad
CAL-B	<i>Candida antarctica</i> lipase-B
cat	Catalytic amount
CHARMM	Chemistry at HARvard Molecular Mechanics
CI	Chemical ionisation
Conv	Conversion
d	Doublet
Da	Daltons
DIPEA	N,N-Diisopropylethylamine
DIPT	Diisopropyl tartrate
DMAP	4-(Dimethylamino)pyridine
DMSO	Dimethylsulfoxide
<i>E. coli</i>	<i>Escherichia coli</i>
ESI	Electrospray ionisation
EtOAc	Ethyl acetate
Et <sub>2</sub> O	Diethyl ether
2-FBA	2-Formylbenzoic acid
3-FBA	3-Formylbenzoic acid
4-FBA	4-Formylbenzoic acid

FPP	Farnesyl pyrophosphate
GC	Gas chromatography
Glu	Glutamic acid
Gln	Glutamine
3-HBA	3-hydroxybenzaldehyde
HEPES	4-(2-hydroxyethyl)-1-piperazineethanesulfonic acid
His	Histidine
HIV	Human immunodeficiency virus
HPA	Hydroxypyruvate
HPLC	High performance liquid chromatography
HR	High resolution
Hz	Hertz
IPA	isopropanol
ISPR	<i>In-situ</i> product removal
KPi	Potassium phosphate
m	Multiplet
menD	2-Succinyl-6-hydroxy-2,4-cyclohexadiene-1-carboxylate synthase
MeOH	Methanol
min	Minutes
MOM	Methoxymethyl ether
MOPS	3-Morpholinopropane-1-sulfonic acid
mp	Melting point
MS	Mass spectrometry
MTPA-Cl	$\alpha$ -Methoxy- $\alpha$ -(trifluoromethyl)phenylacetyl chloride
nm	Nanometre
NMM	N-methylmorpholine
NMR	Nuclear magnetic resonance
PAC	Phenylacetylcarbinol
PDC	Pyruvate decarboxylase
PLP	Pyridoxal 5'-phosphate
PMP	Pyridoxamine phosphate
ppm	Parts per million
R5P	Ribose-5-phosphate

s	singlet
SCA	Statistical coupling analysis
<i>S. cerevisiae</i>	<i>Saccharomyces cerevisiae</i>
Ser	Serine
sext	sextet
SGAT	Serine-glyoxylate aminotransferase
TAm	Transaminase
TBSOTf	tert-butyldimethylsilyltrifluoromethylsulfonate
ThDP	Thiamine diphosphate
THF	Tetrahydrofuran
Thr	Threonine
TK	Transketolase
TLC	Thin layer chromatography
TMS	Trimethylsilyl
TRIS	Tris(hydroxymethyl)aminomethane
<i>V. fluvialis</i>	<i>Vibrio fluvialis</i>
Val	Valine
WT	Wild-type
<i>Z. mobilis</i>	<i>Zymomonas mobilis</i>



## **Acknowledgements**

Many people have helped me during the course of this project and the writing of this thesis. Firstly, I would like to thank my supervisor Prof. Helen Hailes for her constant support and guidance and all of the past and present members of the Hailes and Tabor groups for making the lab such a pleasant place to work in.

I gratefully acknowledge Armando Cazares and James Galman for their help and encouragement, especially at the beginning of this project and all of the BiCE team for the helpful meetings and discussions.

This project has been truly collaborative, and for that I would like to thank Dr. Paul Dalby for his supervision and Panwajee Payongsri, for all of her molecular biology skills, and for making this such a fruitful and pleasant collaboration.

I would like to thank all of the Meaders, for putting me up and helping me find my feet during my first year, and all of my family for their support and encouragement and for providing a relaxing environment in which to escape from work.

Last but not least, I thank Lucy, for her unlimited patience and for making the writing of this thesis so much easier with her constant support, encouragement and understanding.

In addition, this thesis is dedicated to the memory of Emmie Moira Burt, who was unknowingly responsible for its existence.

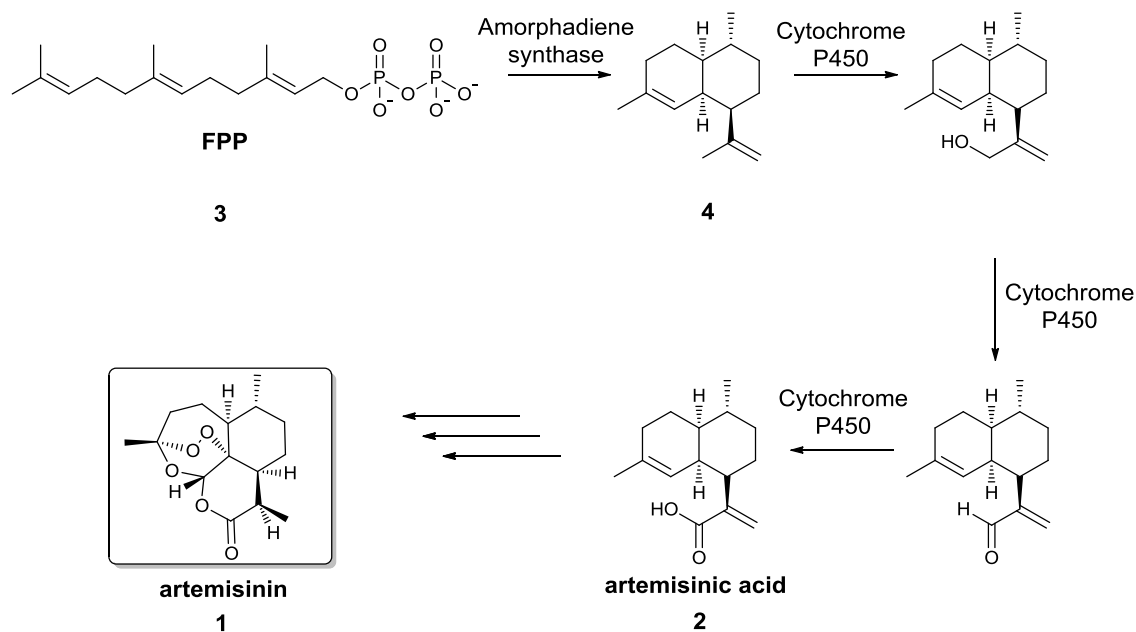
# 1 Introduction

## 1.1 Enzymatic Catalysis in Synthesis

Enzymes possess many attractive qualities for use in organic synthesis. With a current industrial focus on “Green Chemistry”,<sup>[1]</sup> alternative chemical processes are being sought which utilise more sustainable reaction conditions and reagents and produce less waste than current industrial processes. Enzymatic catalysis can fulfil many of these criteria, since many biocatalytic reactions can be performed at ambient temperature and pressure, using only water as a solvent. Enzymes are also attractive due to the exquisite levels of regio- and stereocontrol that they offer over standard chemical techniques, transforming specific chemical functionalities in the presence of other functional groups, negating the need for costly protecting group strategies. Indeed, since the first report of a biocatalytic reaction to produce (*R*)-mandelonitrile from benzaldehyde and hydrogen cyanide using a plant extract,<sup>[2]</sup> biocatalysts have been used for over 100 years to produce a wide range of useful intermediates and final compounds for the food and flavour,<sup>[3, 4]</sup> agrochemical,<sup>[5]</sup> cosmetic<sup>[6]</sup> and pharmaceutical<sup>[7, 8, 9, 10]</sup> industries.

One of the most powerful examples of biocatalysis to make pharmaceutical intermediates is in the production of a precursor of the anti-malarial compound artemisinin (**1**) by engineered baker’s yeast (Scheme 1.1).<sup>[11]</sup> In this approach toward artemisinic acid (**2**), a direct precursor for the synthesis of artemisinin, the mevalonate pathway in baker’s yeast was engineered to allow the production of large amounts of farnesyl pyrophosphate (FPP) (**3**), the required starting material for the biosynthesis of the sesquiterpene artemisinic acid (**2**). This pathway was engineered by upregulating genes responsible for FPP (**3**) production, while downregulating genes responsible for the production of sterols which use FPP to make squalene in the first step of the steroid synthetic pathway. An extra biosynthetic pathway was then introduced into *S. cerevisiae* from *A. annua* to enable the conversion of FPP into artemisinic acid (**2**) in four enzymatic steps. The first step in this ‘inserted’ pathway was the conversion of FPP into amorpha-4,11-diene (**4**) by amorphadiene synthase, followed by a three step oxidation by a novel cytochrome P450. This gave artemisinic acid (**2**) which was transported out of the yeast cells but remained on the cell surface allowing easy extraction of the product from the cell pellet after centrifugation. This process was able to produce up to 100 mg/L of product, and

coupled with existing synthetic methods to produce artemisinin from artemisinic acid offers a sustainable, commercially viable alternative to this high value anti-malarial compound, with maximum yields of 25g/L predicted.<sup>[11]</sup> This compares favourably with the shortest reported total synthesis of this compound to date, which was performed on a gram scale over 6 steps to give artemisinin (**1**) in 16% overall total yield.<sup>[12]</sup>



Scheme 1.1. Biocatalytic formation of artemisinic acid (2)

## 1.2 Thiamine diphosphate (ThDP) dependent enzymes

Thiamine diphosphate (ThDP) (Figure 1.1) is an important cofactor that assists in carbon-carbon bond breaking and formation in many different enzymatic reactions. ThDP-dependent enzymes have been widely studied for their abilities to form not only carbon-carbon bonds but also carbon-nitrogen, carbon-sulphur and carbon-oxygen bonds.<sup>[13]</sup> Most interestingly from a synthetic organic chemistry perspective is the broad substrate scope demonstrated by this family of enzymes, allowing many non-natural substrates to be accepted and useful synthetic compounds to be accessed in a sustainable, atom-efficient fashion.<sup>[13]</sup>

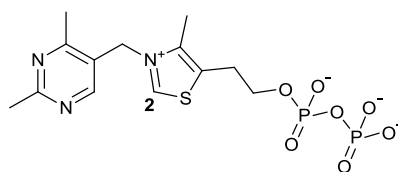
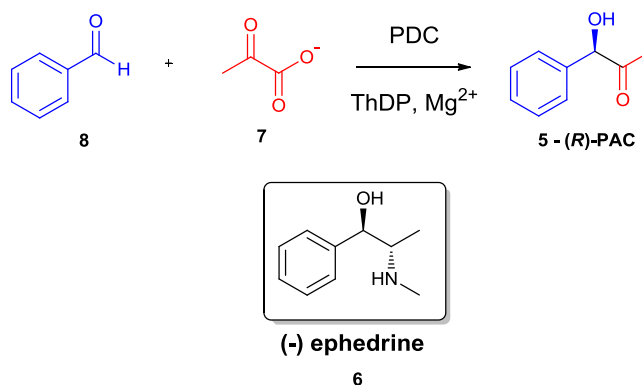


**Figure 1.1. Structure of thiamine diphosphate (ThDP)**

Many ThDP dependent enzymes demonstrate similar reaction mechanisms. Indeed, the reactivity of this family of enzymes derives from the initial reaction of a donor substrate (either a ketoacid or aldehyde) with the C-2 atom of thiazolium ring of ThDP (Figure 1.1), forming an enamine intermediate. This reactive species can couple to an acceptor substrate, forming an asymmetric carbon-carbon bond. The diversity of products which can be made by these enzymes is defined by the broad, yet distinct, substrate spectrum exhibited by each enzyme within the family, examples are given below.<sup>[14]</sup>

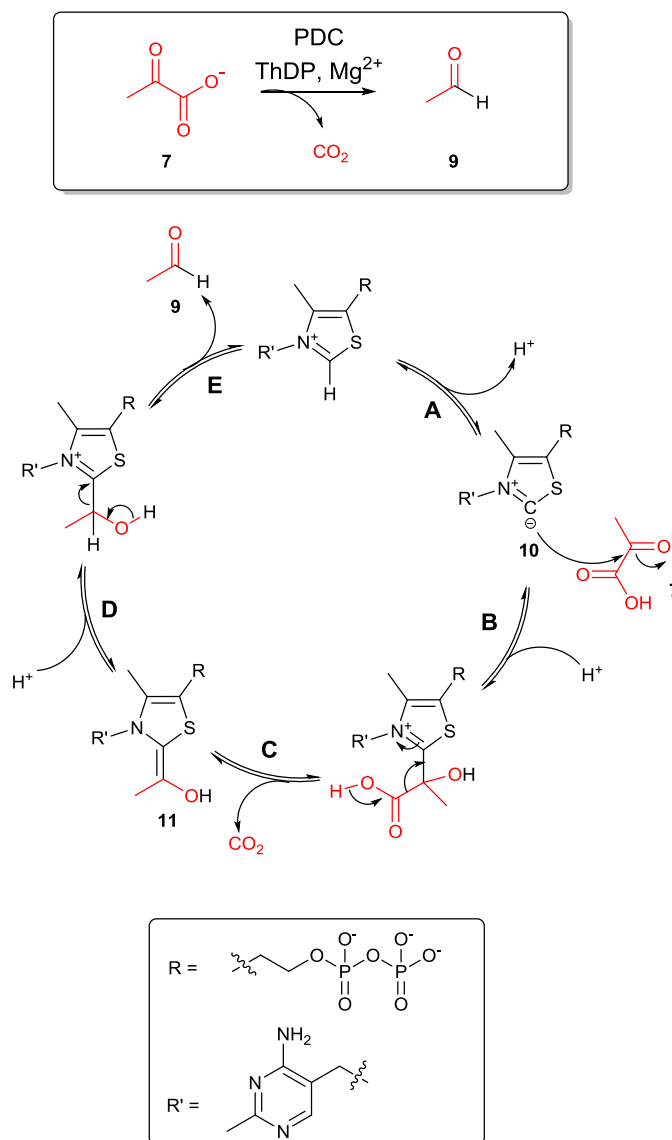
### 1.2.1 Pyruvate decarboxylase (PDC) (EC 4.1.1.1)

The first industrial scale, modern biotechnological process was developed in 1921, and utilized a whole cell Baker's yeast biotransformation to produce (*R*)-phenylacetylcarbinol ((*R*)-PAC, **5**),<sup>[13]</sup> a precursor to the alkaloid (-) ephedrine (**6**). It is now known that the enzyme responsible for this transformation is pyruvate decarboxylase (PDC). In this reaction, PDC transfers an activated ethanal unit from pyruvate (**7**) to benzaldehyde (**8**), to form (*R*)-PAC (**5**) (Scheme 1.2).



**Scheme 1.2. PDC catalysed formation of (*R*)-PAC (**5**)**

(*R*)-PAC (**5**) formation occurs as part of a competing side reaction to the non-oxidative decarboxylation of pyruvate (**7**), which is the main reaction catalysed by PDC, where ethanal (**9**) is released rather than acting as a reactive species in carbon-carbon bond formation (Scheme 1.3).<sup>[15, 16]</sup>



**Scheme 1.3.** Overall reaction scheme and mechanism for the *in vivo* decarboxylation of pyruvate (**7**) by PDC

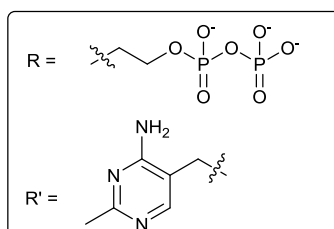
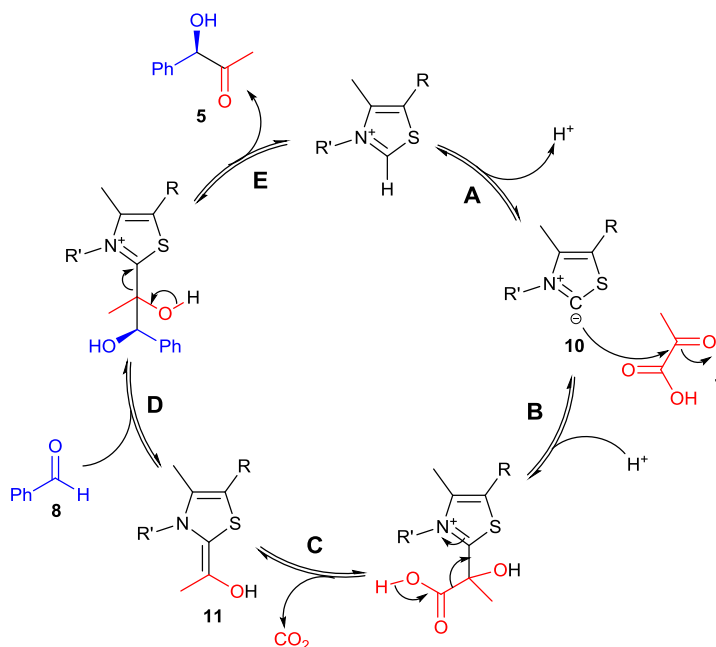
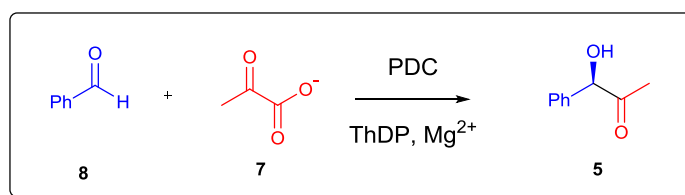
The first step (step A) is deprotonation of the thiazolium ring to form carbanion **10**, which then adds to the  $\alpha$ -keto acid, pyruvate (**7**). This is followed by subsequent protonation, decarboxylation (step C) and formation of the active enamine intermediate (**11**) which can then be protonated (step D) by a conserved glutamic

acid residue (E473). Subsequent deprotonation and reformation of the thiazolium ring releases ethanal (**9**) as a product.

PDC has been shown to accept a range of linear and branched  $\alpha$ -keto acids, and can be used to form ketols, such as in the formation of (*R*)-PAC (**5**) (Scheme 1.2).<sup>[14]</sup>

PDC is available from variety of sources, however PDCs from *Saccharomyces cerevisiae* and *Zymomonas mobilis* have been the most widely studied and so are frequently used in organic synthesis. The crystal structure of PDC from *Z. mobilis* was solved in 1998 and shown to be comprised of 4 subunits.<sup>[17]</sup> The mechanism of PDC catalysed ketol formation is similar to that of other ThDP dependent enzymes (Scheme 1.4) but differs from the main decarboxylation reaction (Scheme 1.3) at step D, where the enamine intermediate goes on to attack an acceptor aldehyde substrate, such as benzaldehyde (**8**), instead of being protonated (Scheme 1.4).<sup>[15]</sup>

Studies aimed at increasing the activity of PDC from *Z. mobilis* toward benzaldehyde, to improve production of (*R*)-PAC (**5**), focussed on the mutation of a conserved E473 residue.<sup>[15]</sup> This residue was chosen as it had been shown to be important for orienting the donor substrate carboxylate to aid decarboxylation and also to act as an acid to protonate active ThDP-enamine intermediate **11**. In the reaction mechanism of the PDC catalysed decarboxylation of pyruvate (Scheme 1.3) E473 aids decarboxylation in step C and protonates the enamine intermediate (**11**) in step D. Hence, mutation of this residue to glutamine would prevent protonation of the enamine intermediate (**11**), stalling the reaction at this stage, preventing the enzyme from releasing the decarboxylated product (**9**) and favouring attack of the enamine (**11**) on the acceptor aldehyde substrate (**8**) (Scheme 1.4). Indeed, E473Q exhibited a 20-fold higher reaction rate for (*R*)-PAC (**5**) production and 2-4 fold increased yields compared to the wild-type enzyme (up to 98% yield) with no negative effect on the stereoselectivity of the new enzyme (>98% ee).<sup>[15]</sup>



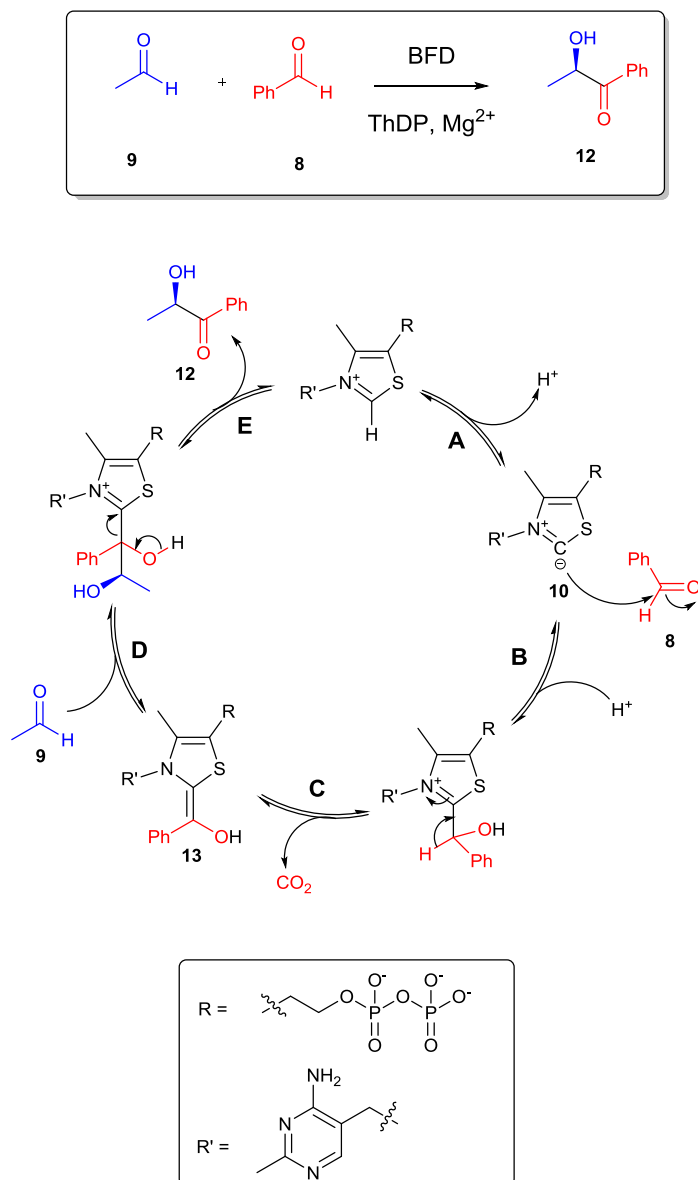
**Scheme 1.4. Overall reaction scheme and mechanism of pyruvate decarboxylase catalysed ketol formation**

### 1.2.2 Benzoylformate decarboxylase (BFD) (EC 4.1.1.7)

Benzoylformate decarboxylase (BFD) is another ThDP dependent enzyme that has been investigated for use in biocatalysis. It is available from several sources, but only BFD from *Pseudomonas putida* has been studied for its potential use in biocatalysis.<sup>[18]</sup> The crystal structure was solved in 1998, and BFD was shown to be tetrameric,<sup>[19]</sup> having a similar structure to PDC from *Z. mobilis*.<sup>[17]</sup> Indeed, BFD decarboxylates benzoylformate using an analogous mechanism to that by which PDC decarboxylates pyruvate. BFD is synthetically useful for its ability to form



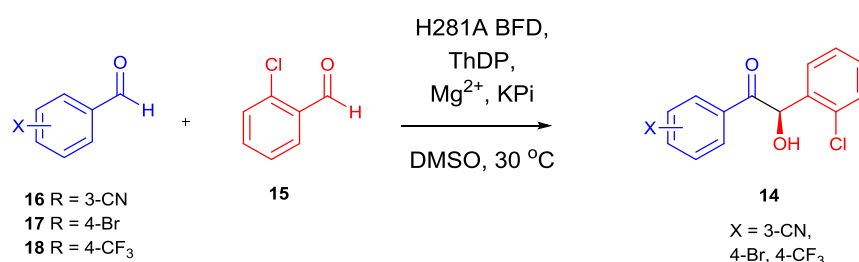
asymmetric carbon-carbon bonds (Scheme 1.5), and it accepts a range of donor substrates including benzaldehyde (**8**). When ethanal (**9**) is used as the acceptor substrate, chiral ketols such as **12** can be accessed.<sup>[20]</sup>



**Scheme 1.5. Overall reaction scheme and mechanism of BFD catalysed ketol formation**

Step A proceeds in a similar fashion as for the PDC mechanism (Scheme 1.3), but the active enamine intermediate (**13**) is formed by addition of carbanion **10** to an aldehyde substrate (**8**) as opposed to a ketoacid. Attack of the resulting enamine intermediate (**13**) on an acceptor aldehyde (**8**), followed by deprotonation and subsequent reformation of the thiazolium ring releases the ketol product **12**. A wide range of acceptor substrates have been reported to be accepted by BFD including;

benzaldehydes (1, 2, and 3-substituted, and 3, 5-disubstituted), heteroaromatic aldehydes, aliphatic and cyclic aldehydes.<sup>[20]</sup> Using ethanal (**9**) as an acyl acceptor, BFD has been shown to form the (*S*)-2-hydroxyketone product in each case, in variable conversion yields (up to 100%) and stereoselectivities (up to 99% *ee*).<sup>[20]</sup> BFD can also accept benzaldehyde (**8**) as the acyl acceptor, and in a condensation reaction with another benzaldehyde molecule, was shown to form the benzoin product with excellent stereoselectivity (>99% (*R*)), albeit with very low conversion (0.4%).<sup>[20]</sup> By creating a mutant of BFD, H281A, it was possible to access crossed benzoin products (**14**). Using 2-chlorobenzaldehyde (**15**) as the acceptor molecule (Scheme 1.6),<sup>[21]</sup> 3-formylbenzonitrile (**16**) (>99% conversion, 90% *ee*), 4-bromobenzaldehyde (**17**) (90% conversion, 95% *ee*) and 4-(trifluoromethyl)benzaldehyde (**18**) (75% conversion, 93% *ee*) were all transformed with high degrees of selectivity for the (*R*)-enantiomer.



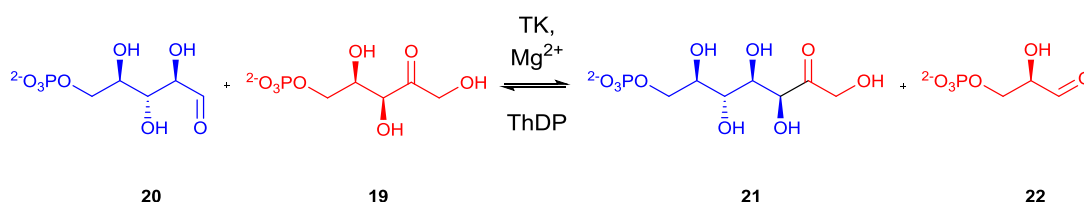
**Scheme 1.6. Crossed benzoin formation catalysed by BFD mutant, H281A**

### 1.2.3 Transketolase (EC 2.2.1.1)

The enzyme transketolase (TK) was first identified in 1953<sup>[22]</sup> in the yeast *Saccharomyces cerevisiae*. Since then, TK been characterised, from a variety of sources, as a dimer composed of two identical subunits, each with a mass of 74 kDa, with the active site located at the interface of these two subunits.<sup>[23]</sup> TK has been shown to have a crucial role in metabolic regulation in animals, catalysing ketol transfer in the non-oxidative branch of the pentose phosphate pathway (Scheme 1.7), while in plants and photosynthetic bacteria the reverse reactions are catalysed as part of carbon dioxide fixation in the Calvin cycle.<sup>[24]</sup> In organic chemistry, the synthetic application of transketolase has been widely studied due to its value in stereoselective carbon-carbon bond formation.<sup>[25]</sup>

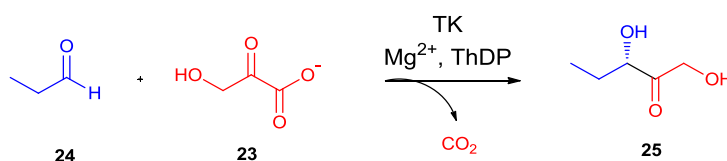
## 1.2.4 TK Function *in vivo*

*In vivo*, TK catalyses the reversible transfer of a two carbon ketol unit (also known as “activated glycolaldehyde”) from D-xylulose-5-phosphate (**19**) to D-ribose-5-phosphate (**20**), in the presence of the co-factors  $Mg^{2+}$  and thiamine diphosphate (ThDP), to form D-sedoheptulose-7-phosphate (**21**) and glyceraldehyde-3-phosphate (**22**) (Scheme 1.7), in a key step of the pentose phosphate pathway.<sup>[23]</sup>



Scheme 1.7. TK-catalysed reaction *in vivo*

These reactions are fully reversible; the products of the reaction can also act as donor and acceptor substrates for the reverse reaction. Transketolase can be made more synthetically useful if hydroxypyruvate (HPA) (**23**) is employed as the ketol donor (Scheme 1.8), as the concomitant generation of carbon dioxide renders the reaction irreversible. A range of aldehydes, such as propanal (**24**), have been shown to be accepted by *E.coli* TK with HPA (**23**) as the donor substrate, giving access to ketodiol products, such as **25**.<sup>[25, 26]</sup>

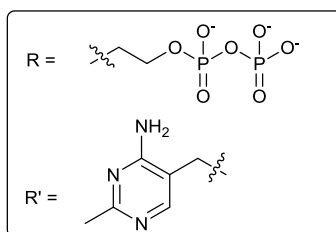
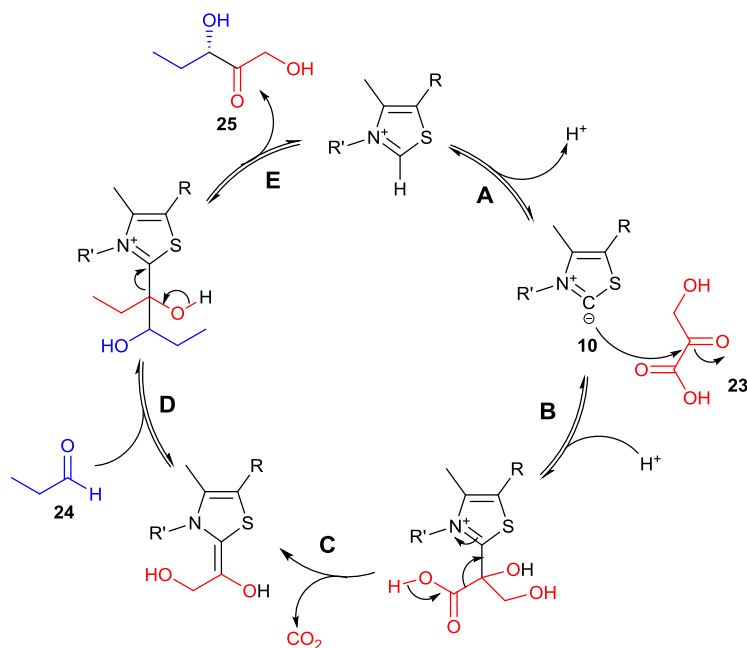
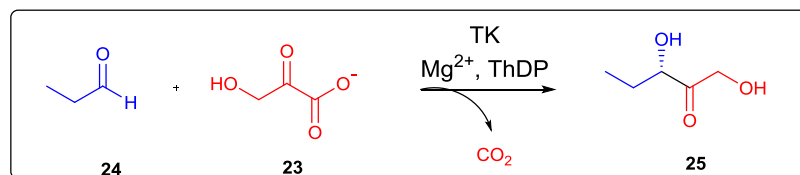


Scheme 1.8. TK-catalysed reaction *in vitro* with HPA as ketol donor

## 1.2.5 Mechanism of TK catalysis

TK catalyses the transfer of ketol groups from donor ketoses, such as HPA (**23**), to acceptor aldehyde substrates, usually an aldehyde, such as propanal (**24**) (Scheme 1.9).<sup>[24]</sup>

The first step of catalysis (step A) is deprotonation of the C-2 atom of the thiazolium ring of ThDP leading to the formation of ylid **10**. This is followed by nucleophilic attack of the carbanion on the ketose donor substrate (**23**). After nucleophilic attack, protonation of the carbonyl oxygen occurs followed by proton abstraction at the C-3 hydroxyl group of the substrate leading to elimination of carbon dioxide and the formation of an enamine (step C), which then attacks the aldose acceptor substrate (**24**) (step D). This is followed by deprotonation from the enol unit of the “active glycoaldehyde” reforming the thiazolium ring and releasing the ketodiol product (**25**) (step E).<sup>[24]</sup> The use of HPA (**23**) as a ketose donor in the *in vitro* reaction (Scheme 1.8) renders the reaction irreversible, as the generation of carbon dioxide in the step before enamine formation (step C) is irreversible, driving the equilibrium towards the formation of products. The main drawback with using HPA (**23**), however, is that since the reaction is irreversible a proton will be consumed for each reaction cycle, raising the pH beyond the optimum of 7.5. This must be taken into account either by using buffering medium or by the addition of acid throughout the reaction.<sup>[25]</sup>



**Scheme 1.9. Overall reaction scheme and mechanism for the *in vitro* TK reaction with HPA (23) as the ketol donor**

### 1.2.6 Sources of transketolase

Transketolase has been isolated from a wide range of sources including: pig liver,<sup>[27]</sup> rat liver,<sup>[28]</sup> rabbit liver,<sup>[29]</sup> *Candida utilis*,<sup>[30]</sup> mouse brain<sup>[31]</sup> and human leukocytes<sup>[32]</sup> and erythrocytes,<sup>[33]</sup> though commonly for synthetic purposes it has been isolated from Baker's yeast and spinach.<sup>[34]</sup> It can also be isolated from *E. coli*, where it has been over-expressed, giving access to substantial quantities of the enzyme which has proven to be useful for integration into industrial processes.<sup>[35]</sup>

### 1.2.7 Mutation and study of yeast transketolase

TK from *Saccharomyces cerevisiae* was the first ThDP dependent enzyme for which a crystal structure was solved<sup>[36]</sup> and the crystal structure of the enzyme with the acceptor substrate erythrose-4-phosphate bound allowed the molecular basis for catalytic activity to be studied in detail (Figure 1.2).<sup>[37]</sup>

**Figure 1.2 Representation of ThDP adduct in the active-site of yeast TK with the function of conserved residues indicated (adapted from<sup>[37]</sup>)**

Site directed mutagenesis of the E162 amino acid residue allowed subunit-subunit interactions to be probed, and showed that this residue was crucial for formation and stabilization of the transketolase dimer.<sup>[38]</sup> Replacement, by mutagenesis, of the E418 residue with glutamine and alanine gave an insight into ThDP activation. Both E418Q and E418A mutants showed a marked decrease in catalytic activity even though ThDP affinities were comparable to wild-type TK, showing that hydrogen bonding between ThDP and E418 was not required for ThDP binding but was essential for catalytic activity.<sup>[39]</sup> The molecular basis for substrate binding and recognition was investigated by the substitution of H69<sup>[40]</sup> (not shown) and H103 with alanine residues, resulting in a substantial decrease in catalytic activity.<sup>[41]</sup> This showed that these residues were crucial for substrate recognition and binding by the formation of hydrogen bonds with the C-1 hydroxyl group of the sugar phosphate.<sup>[41],[40]</sup> The stereospecificity of the enzyme was attributed to the D477

residue which forms a hydrogen bond with the C-2-hydroxyl group of the acceptor substrate.<sup>[41]</sup> Substitution of this residue for alanine gave a greatly reduced activity towards natural substrates as the hydrogen bonding which was present between the substrate and alanine was now disrupted, with no hydrogen bonding between the substrate and the new residue (Figure 1.2).<sup>[42]</sup>

Since writing this thesis, the Hanefeld group has created a library of double mutant yeast TKs, using an *in silico* modelling approach, focused on the natural phosphate binding region.<sup>[43]</sup> Five double mutants were found which increased the activity of yeast TK towards a non-phosphorylated substrate, glycolaldehyde, by up to 4-fold.<sup>[43]</sup> These libraries were screened using a novel GC-based assay which involved making trimethylsilyl derivatives of biotransformation products. This assay was shown to be very sensitive, and was able to detect bioconversions down to levels of 1%.<sup>[44]</sup>

### 1.2.8 Mutation and study of *E. coli* TK

*E. coli* TK is of great interest synthetically as it has been shown to have a 30-fold higher specific activity towards the non-natural ketol donor, lithium-HPA (Li-**23**), and a broad tolerance for hydroxylated aliphatic aldehyde substrates, compared with yeast or spinach TK.<sup>[45]</sup> However, its acceptance of non  $\alpha$ -hydroxylated substrates, such as propanal, is poor with activities typically 5-35% less than for hydroxylated substrates.<sup>[35]</sup> Mutants of *E. coli* TK have been created by various methods to increase substrate tolerance towards non-natural substrates, improving yields and stereoselectivities.<sup>[46, 47]</sup>

Using directed evolution, two complementary methods were adopted to select *E. coli* TK active-site residues for modification to increase activity towards the non-natural substrate, glycolaldehyde (**26**, Scheme 1.10).<sup>[46]</sup> The first approach was based simply on nearby residues in the active site, selecting all residues within 4 Å of the bound substrates (first shell mutants). The other set of residues was chosen on a phylogenetic basis, using residues within 10 Å of the bound substrates which have varied across bacterial and yeast TK evolution (second shell) (Figure 1.3).

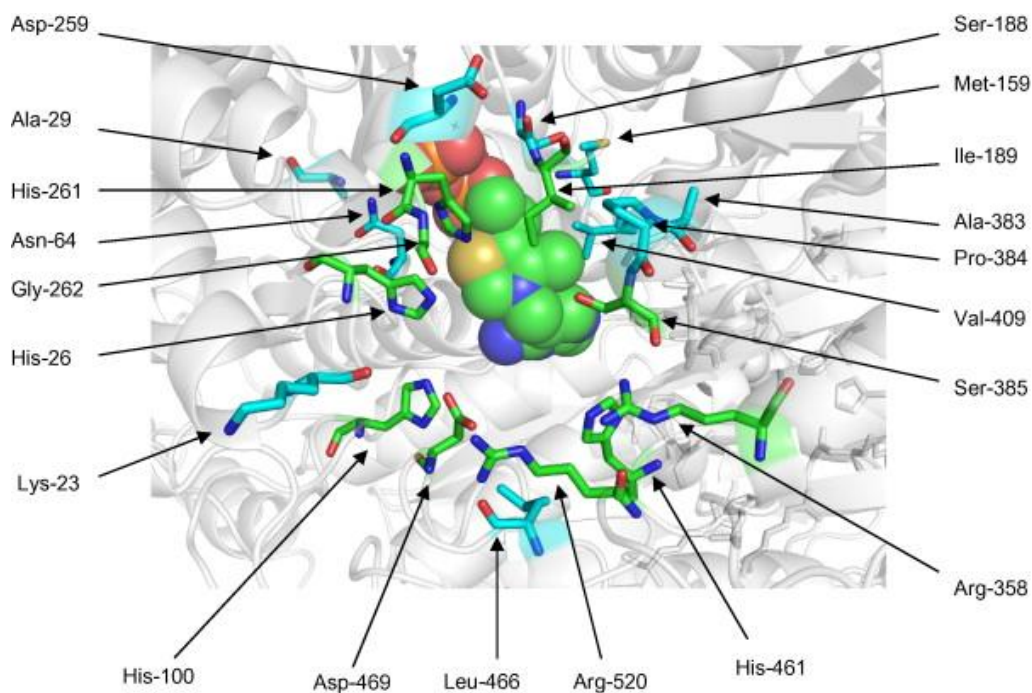
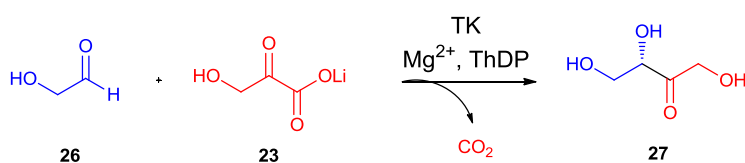


**Figure 1.3.** Structure of ThDP in the active site of *E. coli* TK, with 1st shell (green) and 2nd shell (cyan) amino acid residues. (Used with permission from Elsevier).<sup>[46]</sup>

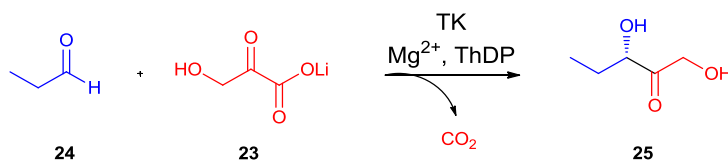
By screening these mutants for the conversion of HPA (**23**) and glycolaldehyde (**26**) to erythrulose (**27**) (Scheme 1.10), several mutant TKs (both first and second shell) were identified with higher activities than wild-type. These were: H461S, R520V, A29E and A29D. The high activities for H461S and R520V with this non-natural substrate were attributed to their position in the phosphate-binding region at the entrance to the active-site, allowing non-phosphorylated substrates to enter.<sup>[46]</sup> A29 is a second shell mutant with a methyl side-chain which is in direct contact with the ThDP terminal phosphate; mutation of this residue appeared to directly affect the catalytic mechanism of TK. Indeed, A29E gave a 3-fold increase in activity relative to WT with the acceptor glycolaldehyde (**26**).<sup>[46]</sup>



**Scheme 1.10** TK biotransformation of glycolaldehyde (**26**) to erythrulose (**27**) using HPA (**23**) as the donor substrate



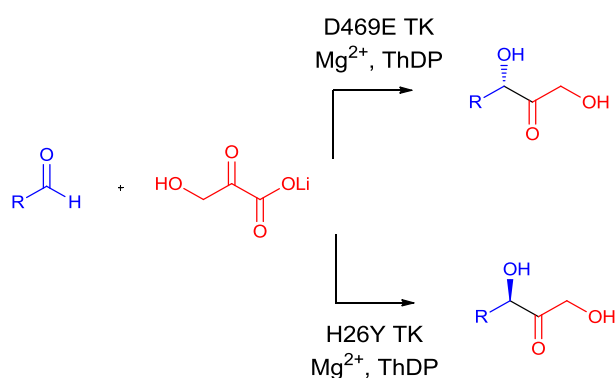
Further work has been carried out to tune the specificity of TK towards non-hydroxylated aldehyde substrates in order to improve the industrial viability of TK bioconversions with lipophilic substrates. By following the reaction of propanal (**24**) and Li-HPA (Li-**23**) to form ketodiol **25** (Scheme 1.11), five mutants were found with increased activity relative to wild-type; D469E, D469A, D469Y, D469T and R520V.<sup>[47]</sup>



**Scheme 1.11 TK biotransformation of propanal (**24**) to ketodiol (**25**) using HPA (**23**) as the donor substrate**

The D469 mutants were not previously identified as increasing the activity of the enzyme towards  $\alpha$ -hydroxylated substrates,<sup>[46]</sup> but the analogous residue in yeast TK, D477, had been shown to be crucial for the binding of hydroxylated substrates.<sup>[42]</sup> In *E. coli* TK, D469 interacts with the C-2 hydroxyl group of the natural substrates, but when propanal is used as the substrate, this hydroxyl group is now a methyl group. Therefore, high activity mutants were expected to have hydrogen bonding side-chain moieties replaced with non-polar groups to improve interactions with the new substrate. This is most likely to be why the D469 mutants, D469Y and D469T, showed increased specificity towards propanal compared to glycolaldehyde.<sup>[47]</sup> These studies clearly showed that active-site mutants could increase the activity and substrate specificity of the enzyme. However, stereoselectivities had not been considered. Since wild-type TK was shown to convert propanal with only 58% *ee* (3*S*-major isomer),<sup>[48]</sup> mutations of active site residues were considered which could also improve the stereoselectivity of carbon-carbon bond formation (Scheme 1.11). D477 in yeast TK had previously been shown to be important in determining the stereoselectivity of the TK reaction.<sup>[42]</sup> The importance of the analogous residue in *E. coli* TK, D469, in accepting hydroxylated substrates had been demonstrated, since mutation of this residue improved selectivity towards non-hydroxylated substrates such as propanal.<sup>[46]</sup> Also, from studies of analogous residues in yeast TK, D469, H26 and H100 were shown to form a pocket and interact with the C-2 hydroxy group

of natural  $\alpha$ -hydroxylated aldehyde substrates, affecting the stereoselectivity at this position and making them obvious choices for mutations to affect changes in stereoselectivities. The D469 mutants showed some good activities, as already discussed. When the stereoselectivities were assessed, D469E was shown to convert propanal with 90% *ee* for the 3*S*- product (**25**). Interestingly, several mutations of H26 were shown to reverse the stereoselectivity compared to wild-type, the best result being with H26Y which gave 88% *ee* for the 3*R*-product.<sup>[48]</sup> A similar trend was shown in biotransformations of other longer-chain aliphatic aldehydes,<sup>[26]</sup> with D469E favouring the formation of 3*S*-products and H26Y favouring 3*R*-product formation (Scheme 1.12).



**Scheme 1.12 Biotransformation of aliphatic aldehydes by D469E and H26Y TK**

For  $\text{C}_3$  to  $\text{C}_9$  aliphatic aldehydes (Scheme 1.12,  $\text{R} = \text{C}_2\text{H}_5 - \text{C}_8\text{H}_{17}$ ), D469E showed improved stereoselectivities and activities compared to wild-type TK, while H26Y showed reversed stereoselectivities for  $\text{C}_3$  and  $\text{C}_8$ . Interestingly, D469E gave greater than 99% *ee* when using the  $\text{C}_3$  and  $\text{C}_5$  cyclic aldehydes (Scheme 1.12,  $\text{R} = \text{C}_3\text{H}_5$  and  $\text{R} = \text{C}_5\text{H}_9$ ) and 97% *ee* for the  $\text{C}_6$  cyclic aldehyde (Scheme 1.12,  $\text{R} = \text{C}_6\text{H}_{11}$ ). All isolated yields were comparable to, or better than, those obtained from wild-type TK.<sup>[26]</sup>

Since writing this thesis, Yi *et al.*, have published a pH-based high-throughput assay for TK.<sup>[49]</sup> This assay was based on using phenol red as an indicator to measure the increase of pH which occurs when HPA is used in the TK reaction. The observed colour change was followed spectrophotometrically to allow specific activities to be calculated. WT, D469E and H26Y *E. coli* TKs, and WT yeast TK, were tested with this assay against a range of hydroxylated and non-hydroxylated non-natural

aldehyde substrates. This study confirmed that D469E was indeed more active towards non-hydroxylated aliphatic aldehydes, such as propanal, than either *E.coli* or yeast WT TKs, and was also more stereoselective.<sup>[49]</sup>

The low yields but high stereoselectivities obtained for D469E with cyclic aldehydes suggested the possibility of transforming aromatic aldehydes (although the reactivity of aromatic aldehydes would be expected to be different). The only previous work with aromatic aldehydes and TK was performed with yeast and spinach TKs, where the enzymatic reactions were followed by HPLC and the consumption of HPA was monitored as evidence of reaction progress. No products were isolated from the reactions; yields and optical purities were not established, and since HPA has been shown to degrade during the TK reaction, it was unclear whether any ketodiol products were actually generated.<sup>[34]</sup> Thus, if D469 mutants which accepted cyclic aldehydes could be used to transform aromatic aldehydes, this would represent the first example of aromatic ketodiol formation by mutant TKs.

### 1.2.9 Biomimetic transketolase reaction

A biomimetic TK reaction (Scheme 1.13) has been reported in which the tertiary amine *N*-methylmorpholine (NMM) (**28**) mediated carbon-carbon bond formation, using Li-HPA (Li-**23**) as a ketol donor group.<sup>[50]</sup>

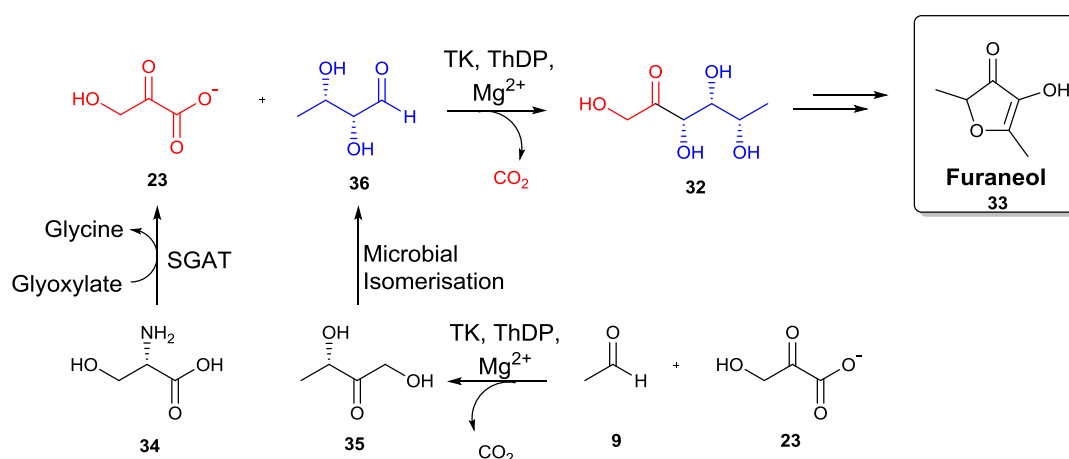
**Scheme 1.13. Overall reaction scheme and initial postulated mechanism for the NMM-catalysed biomimetic TK reaction<sup>[50]</sup>**

Aliphatic,  $\alpha$ -hydroxylated and aromatic aldehydes were all tolerated in this reaction, showing its value for the preparation of racemic substrates (**25**).<sup>[50]</sup> A postulated reaction mechanism (Scheme 1.13) included the conjugate addition of the tertiary amine to the enol (**29**) form of **23** or by direct addition to the tartronic semialdehyde (**30**) to generate enolate **31**. Addition of the aldehyde (**24**) followed by proton transfer, decarboxylation and amine elimination would give the dihydroxyketone product (**25**). This reaction has proved to be useful in the preparation of racemic dihydroxyketone products which can be used as standards in the development of chiral assays to establish the optical purity of subsequent biotransformations.<sup>[48]</sup>

## 1.3 Use of TK in organic synthesis

### 1.3.1 Spinach transketolase in synthesis

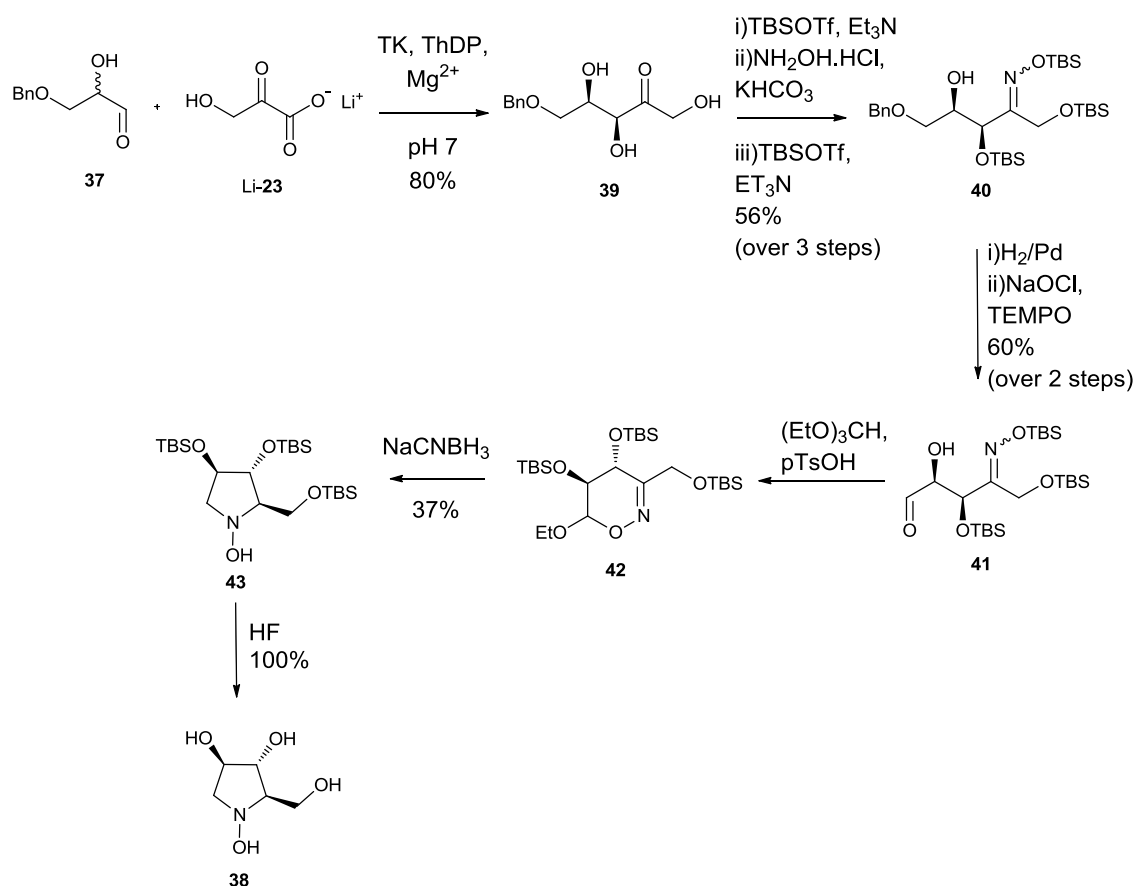
Spinach TK has been used to prepare “naturally-labelled” molecules for use in the food and flavour industry.<sup>[3]</sup> As opposed to synthetic products, nature identical alternatives are produced entirely by enzymatic “natural” processes and are therefore more desirable to consumers and of higher commercial value.<sup>[51]</sup> “Naturally-labelled” molecules are typically made either by extraction from appropriate sources, or by biocatalytic processes.<sup>[3]</sup> Spinach TK has been employed in the preparation of “natural-labelled” 6-deoxy-L-sorbose (**32**), a precursor of furaneol (**33**) which is an aromatic compound used industrially for its caramel-like flavour.<sup>[51]</sup> Several different techniques were used in this synthesis (Scheme 1.14), including the enzymatic generation of HPA (**23**) from L-serine (**34**) using glyoxylate aminotransferase (SGAT) from spinach, and the microbial isomerisation of 4-deoxy-L-erythrulose (**35**) to 4-deoxy-L-threose (**36**) using intact cells of *Corynebacterium equi* or *Sratiia liquefaciens*. Spinach TK was used in the final step to couple 4-deoxy-L-threose to HPA to yield 6-deoxy-L-sorbose (**32**) in 35% total yield. Transketolase was also used to prepare the “natural” 4-deoxy-L-erythrulose (**35**) from the coupling of HPA (**23**) with naturally available ethanal (**9**).



Scheme 1.14. Synthesis of "natural-labelled" 6-deoxy-L-sorbose (**32**) using spinach transketolase

### 1.3.2 *E. coli* transketolase in synthesis

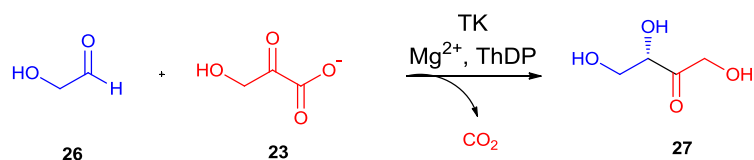
The use of *E. coli* TK in multigram synthesis has been previously demonstrated in the coupling of 3-*O*-benzylglyceraldehyde (**37**) with Li-HPA (Li-**23**) in unbuffered medium (Scheme 1.15).<sup>[52]</sup> The reaction was performed in an auto-titrator which maintained the pH of the reaction at 7 through the controlled addition of HCl. This product was then used in the subsequent synthesis of a potential glycosidase inhibitor (**38**),<sup>[53]</sup> where the starting material was the triol (**39**) obtained from the initial TK reaction step (Scheme 1.15). After the TK mediated synthesis of 5-*O*-benzyl-D-xylulose (**39**) in 80% yield, the next step was conversion to the silylated oxime (**40**), firstly by silylation (TBSOTf, triethylamine, 83% yield), then oxime formation (hydroxylamine hydrochloride, KHCO<sub>3</sub>, 71% yield, 2:1 mixture of (*E*)- and (*Z*)-geometric isomers) and finally further treatment with TBSOTf and triethylamine with 95% yield. Debenzylation was achieved using a 10% Pd-C catalyst under hydrogen, to yield the alcohol quantitatively. This was then oxidised to aldehyde **41** using NaOCl and catalytic TEMPO in 60% yield. Treatment of **41** with triethyl orthoformate and catalytic *p*-toluenesulfonic acid formed the oxazine (**42**) (no reported yield), which was reduced with sodium cyanoborohydride in acetic acid to give **43** as a single diastereoisomer (*R*) in 37% yield. Finally, desilylation was achieved using HF in 1:1 acetonitrile:THF which gave **38** in quantitative yield.<sup>[53]</sup>



**Scheme 1.15. Synthetic route towards a novel *N*-hydroxypyrrolidine (38) using TK mediated carbon-carbon bond formation in the first step**

### 1.3.3 Large scale process development

While the use of transketolase on a preparative scale has been shown to be useful in an organic laboratory environment,<sup>[3], [52],[53]</sup> the use of transketolase for organic synthesis on an industrial scale will depend on its suitability for integration into novel and existing industrial processes. As a model large scale reaction, the *E. coli* TK-mediated coupling of Li-HPA (Li-23) and glycolaldehyde (26) to produce L-erythrulose (27) (Scheme 1.16) has been studied and the important characteristics of the reaction evaluated from an industrial perspective.<sup>[54]</sup>



**Scheme 1.16. Model TK catalysed carbon-carbon bond formation reaction of Li-HPA (Li-23) and glycolaldehyde (26) to generate L-erythrulose (27)**

The parameters investigated were; substrate solubility, pH, and the concentration of substrates. This investigation showed that both the substrates and products were sensitive to alkaline environments, with degradation observed for pH >8. This is most important with respect to the expense of using HPA as a ketol donor. The lower pH limit was due to enzyme stability, as below pH 6.5 TK was shown to be irreversibly denatured. The optimum pH range for TK activity was therefore shown to be 7.0-7.5 in the absence of buffer solution. Glycolaldehyde (**26**) was shown to deactivate the enzyme at a rate proportional to its concentration, decreasing the half-life of the enzyme from ~65 hours at 50 mmol to ~3.5 hours at 500 mmol.<sup>[54]</sup> This will clearly be an important factor in large scale reactions, depending on the concentration and type of aldehyde used, necessitating either the removal of excess aldehyde or use of a repetitive batch process to avoid toxic levels of substrate.<sup>[55]</sup> The product, L-erythrulose (**27**), is itself a ketol donor and has been shown to have a deactivating effect on the enzyme, albeit to a lesser extent than glycolaldehyde.<sup>[55]</sup> The use of *in-situ* product removal (ISPR) techniques exploiting phenylboronate-diol interactions has been investigated. However, removal of L-erythrulose by this method was not effective, and free phenylboronic acid was shown to be toxic to the enzyme.<sup>[56]</sup> Immobilized boronates showed the greatest potential but exhibited high levels of non-specific binding to substrates. To overcome the low selectivity of binding, substrate feeding of glycolaldehyde and immobilisation of TK was employed and ISPR using immobilised phenylboronate resin allowed the reaction to reach completion.<sup>[56]</sup>

Enzyme immobilisation is a potential technique to increase the activity and stability of transketolase.<sup>[57]</sup> Enzymes can lose catalytic activity in many different ways during a reaction. This can be due to substrate/product inhibition or denaturation due to reaction conditions such as temperature, pH or high concentrations of reactants.<sup>[57]</sup> By immobilisation onto two commercial supports, Eupergit-C and Amberlite XAD-7, TK stability and activity was reported to increase.<sup>[57]</sup> Immobilised enzyme was



shown to lose only 50% of its activity after two months of storage under nitrogen. It was thought the nitrogen environment prevented the oxidation of C159 in the ThDP-binding site, which had been shown to promote enzyme deactivation.<sup>[56]</sup> The stability of the enzyme with regards to glycolaldehyde concentration was also improved. The immobilised enzyme lost no activity after six hours of operation at 500 mM concentration of glycolaldehyde, while the free enzyme exhibited a half-life of less than an hour under the same conditions.

In the end, the suitability of TK for use in large scale industrial processes will depend on the specific reaction environment (substrates, reagents, temperature, pH, etc.). Different techniques will need to be combined and altered, to ensure the enzymatic reaction is viable, as well as employing enzyme mutagenesis to improve enzyme stabilities.

## **1.4 Transaminase**

### **1.4.1 Function *in vivo***

Transaminases (TAMs), or aminotransferases, are a class of metabolic enzymes which catalyse the reversible transfer of an amino group from an amine donor to an acceptor aldehyde or ketone. TAMs are ubiquitous in nature as they play an important role in nitrogen metabolism in cells, indeed, most organisms will have several different TAMs with differing substrate specificities. The sheer number of TAMs makes them attractive candidates for use in biocatalysis, along with the potential for good enantio- and regio-selectivities, broad substrate tolerance, high reaction rates and good enzyme stabilities.<sup>[58]</sup>

### **1.4.2 Mechanism of catalysis**

The co-factor for all transaminases is pyridoxal 5'-phosphate (PLP, **44**, Figure 1.4), a form of vitamin B6 which acts as a co-factor for various amino acid metabolising enzymes.<sup>[59]</sup>

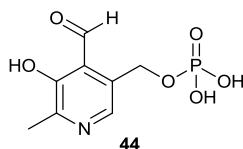
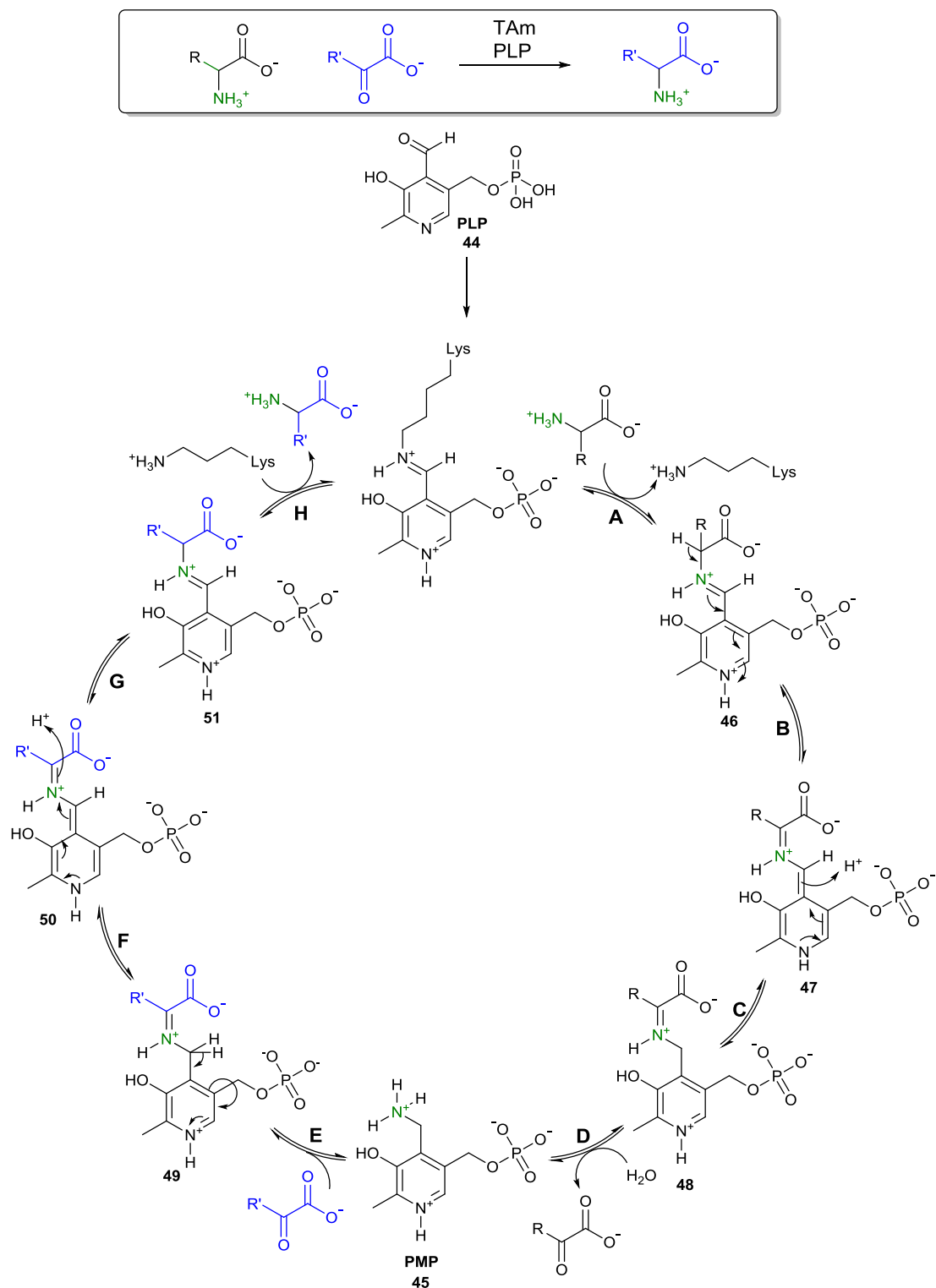


**Figure 1.4. Structure of PLP (44)**

The mechanism by which TAmS catalyse amine transfer consists of two half reactions (Scheme 1.17). The first half reaction involves the transfer of an amino group from the amino donor to PLP (**44**) to form pyridoxamine phosphate (PMP) (**45**). The second half reaction involves the transfer of the amino group from PMP (**45**) to an acceptor aldehyde or ketone moiety.<sup>[60]</sup> PLP (**44**) is secured in the enzyme active site via an imine bond formed between the aldehyde group of PLP and a conserved lysine residue. In the first catalytic step this lysine residue is displaced by the introduction of an amine donor, forming an external aldimine (**46**) (step A). A quinoid (**47**) is then formed by abstraction of a proton from the  $\alpha$ -carbon (step B), which is then protonated to form a ketimine intermediate (**48**) (step C). Subsequent hydrolysis releases the  $\alpha$ -ketoacid derived from the amine donor, forming PMP (**45**) and completing the first half reaction (step D). The second half reaction begins with the formation of a Schiff base (**49**) between PMP and the acceptor  $\alpha$ -ketoacid (step E), which upon proton abstraction (step F) and protonation of the resulting imine (**50**) (step G), gives another external aldimine (**51**). The newly formed amino acid is then displaced (step H) either by the conserved lysine residue, directly by another amine donor or by water to reform PLP (**44**).



**Scheme 1.17 Overall reaction scheme and the combined half-reactions of the *in vivo* transaminase reaction**

### 1.4.3 Classes of transaminase enzymes

There is a diverse range of transaminases, as all organisms have numerous transaminase enzymes covering a range of functions in nitrogen metabolism. The first attempt to classify these enzymes was based on sequence homology of the available amino acid sequences. This approach allowed TAMs to be divided into four groups based on their primary structure similarity.<sup>[61]</sup> A more recent classification attempt using a larger database of newly identified TAM sequences allowed further diversification in classes of TAMs to be made, with class I subdivided into two classes (class I and II) and class VI containing sugar aminotransferases.<sup>[58]</sup> However, only classes I, II, IV and V actually catalyse amino group transfer to keto acids.<sup>[62]</sup> Class III TAMs appear to be more useful as biocatalysts, as they have a broader substrate tolerance and can transfer amino groups to many different aldehyde and ketone containing substrates.<sup>[62]</sup> As well as being divided into six classes, TAMs can be identified as being  $\alpha$ ,  $\beta$ ,  $\gamma$ ,  $\delta$ ,  $\epsilon$  or  $\omega$ . This nomenclature refers to the position of the amino group in the donor substrate. It is possible for enzymes from the same class of TAM to exhibit different positional specificity, since they are classified by their total sequence similarity, not substrate acceptance.<sup>[62]</sup>

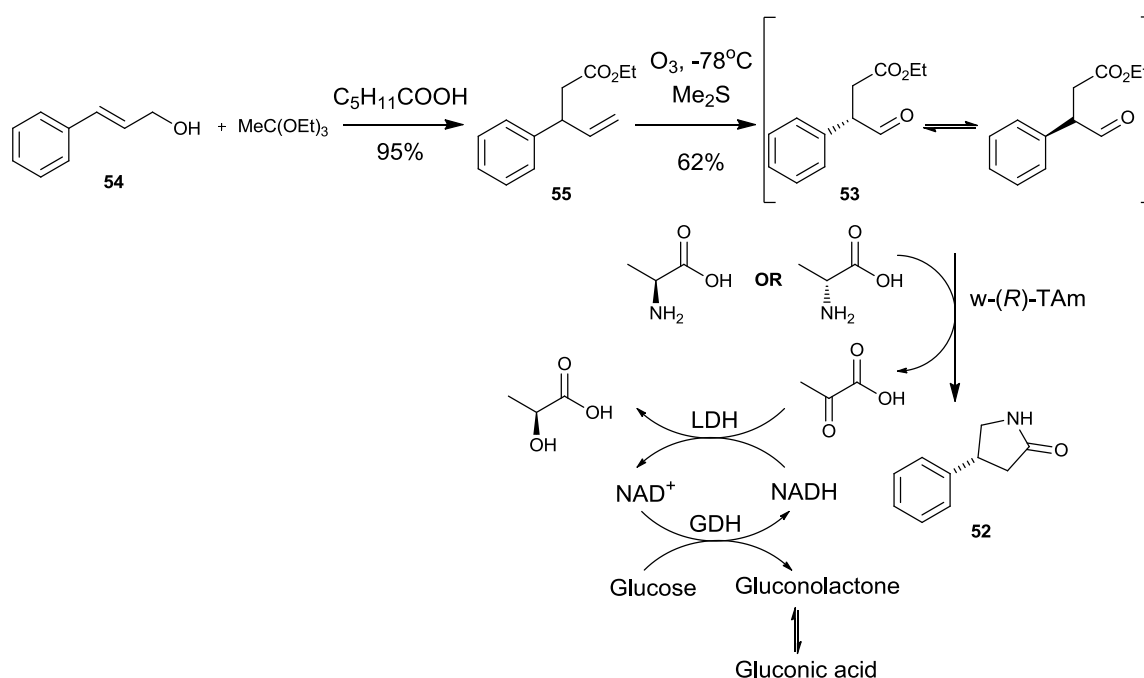
### 1.4.4 Omega transaminases ( $\omega$ -transaminases)

Omega transaminases are class III transaminase enzymes and are interesting from a biocatalysis perspective due to their broad substrate tolerance. The omega nomenclature refers to their acceptance of the amine group in any position of the amino donor molecule. The first  $\omega$ -transaminase to be studied was  $\omega$ -amino acid-pyruvate-aminotransferase from *Pseudomonas sp.* F-126.<sup>[63]</sup> This enzyme was shown to have good activity for a host of amino donors, including a range of amino acids, amines and diamines. Interestingly, despite this broad donor tolerance, the enzyme was specific for pyruvate as an acceptor molecule, and was inactive with a range of other acceptors.<sup>[64]</sup> However, for biocatalytic applications it is important to have a biocatalyst which accepts a range of acceptors as well as donors. To that end, the  $\omega$ -transaminase from *Vibrio fluvialis* (*V. fluvialis*) was studied and shown to have activity not only towards the expected  $\alpha$ -keto acids, but also aldehydes such as

propanal and interestingly, benzaldehyde.<sup>[65]</sup> Improved substrate tolerance was demonstrated by a TAM cloned from *Chromobacterium violaceum* DSM30191 which showed 38% sequence similarity to the *V. fluvialis* enzyme. This TAM, referred to as CV2025, showed increased activity towards a range of aliphatic and aromatic aldehydes, suggesting that the enzyme might be useful for use in amination in biotechnological applications.<sup>[66]</sup>

## 1.5 TAMs in organic synthesis

Chiral amines and amino acids are valuable pharmaceutical synthons, and are also useful in industry, nutrition and health care. Transaminases are increasingly being used to address the problems inherent in preparing compounds of this nature.<sup>[67]</sup> For example, a range of commercially available  $\omega$ -transaminases have been used in the preparation of an analogue of 3-aryl- $\gamma$ -aminobutyric acid (**52**) (Scheme 1.18).<sup>[68]</sup>

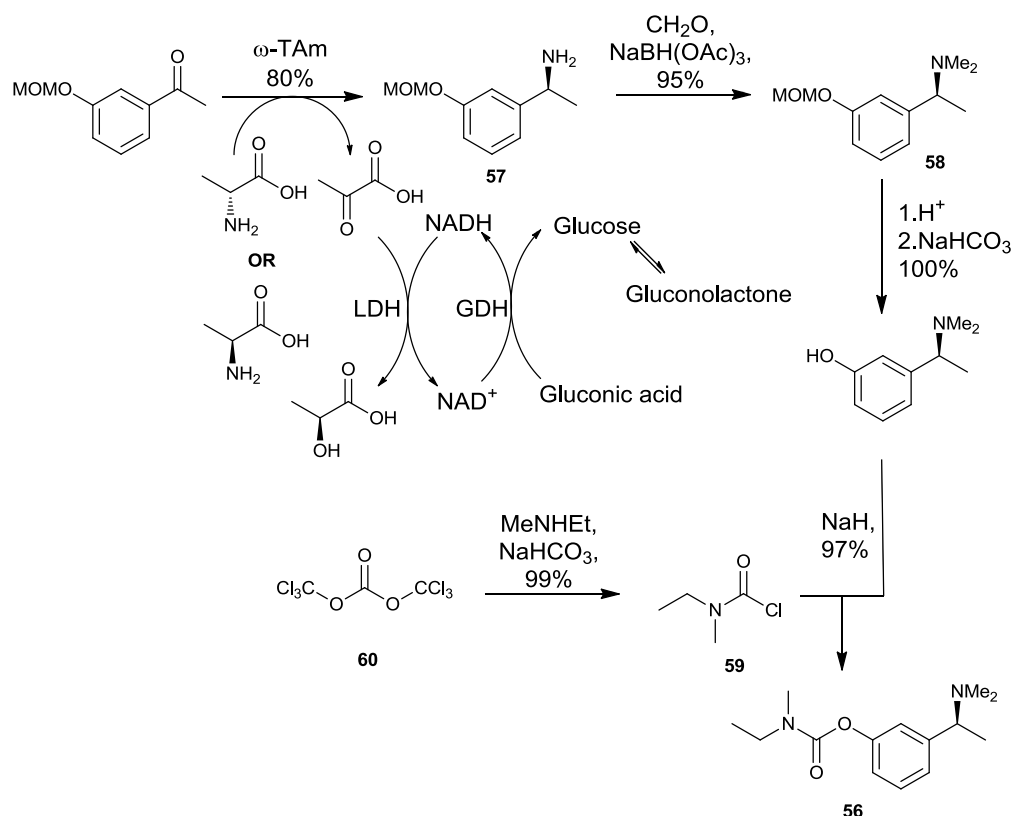


**Scheme 1.18. Synthesis of (R)-4-phenylpyrrolidin-2-one (**52**) via dynamic kinetic resolution catalysed by TAM**

Preparation of the racemic intermediate (**53**) proceeded by reacting cinnamyl alcohol (**54**) with triethyl orthoacetate and hexanoic acid catalyst to give **55** in 95% yield.

This was followed by ozonolysis of the double bond to give racemic aldehyde **53** in 62% yield. Various TAMs were tested in the final dynamic kinetic resolution step, using L or D- alanine as an amine donor and removal of the resulting pyruvate by reduction using lactate dehydrogenase combined with a glucose dehydrogenase/glucose recycling system. This shifted the equilibrium of the reaction towards the amine product. All of the TAMs tested gave good conversions (>90%) to the final 4-phenylpyrrolidin-2-one (**52**), three gave access to the (*S*)-enantiomer (< 46% *ee*), while the remaining nine gave the (*R*)-enantiomer (< 69% *ee*).<sup>[68]</sup>

(*S*)-Rivastigmine (**56**) is a drug which has been used to treat the early stages of Parkinson's disease. Previously, it has been synthesised via various resolution methods which require complex multi-step procedures. A concise chemoenzymatic strategy (Scheme 1.19) has been described which utilizes an  $\omega$ -transaminase to install the necessary stereochemistry.<sup>[69]</sup>

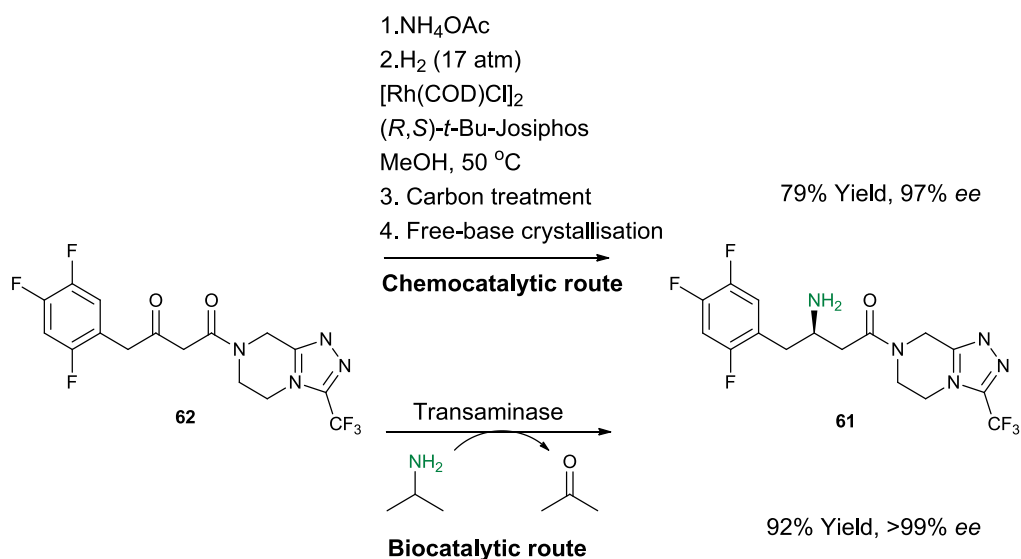


Scheme 1.19. Chemoenzymatic synthesis of (*S*)-Rivastigmine (**56**)

The initial biotransformation step was investigated using a variety of different protecting groups, solvent systems and  $\omega$ -transaminase enzymes. L- or D- alanine was used as the amine donor and the co-product, pyruvate, was once again removed

using lactate dehydrogenase combined with a glucose dehydrogenase/glucose recycling system. Initial testing without a hydroxyl protecting group gave good stereoselectivities (>99% *ee*) but low conversions (15-64%) and attempts at improving reaction rates using co-solvents were unsuccessful. However, protection of the hydroxyl group resulted in increased conversions without affecting the stereochemical outcome, the best of which was the methoxymethyl (MOM) ether which gave an isolated yield of **57** of 80% and >99% *ee*. The MOM protecting group was also useful from a synthetic perspective as it could easily be cleaved using mildly acidic conditions. The rest of the synthesis proceeded by *N*-methylation of the biotransformation product (**57**) in the presence of formaldehyde and triacetoxyborohydride to give **58** in 95% yield. Removal of the methoxymethyl ether was achieved quantitatively at room temperature using 5 M HCl. Carbamoylation by reaction with *N*-ethyl-*N*-methylcarbamoyl chloride (**59**), which had been prepared from triphosgene (**60**), gave (*S*)-Rivastigmine (**56**) in its enantiopure form in 97% yield.<sup>[69]</sup>

One of the most powerful examples of the use of transaminase in organic synthesis is in the production of the anti-diabetic compound, sitagliptin (**61**). The final step in the synthesis of this compound relied upon a rhodium catalysed stereoselective hydrogenation of an enamine of pro-sitagliptin ketone at 50 °C and pressure of 17 atmospheres (Scheme 1.20). While good yields and stereoselectivities were obtained, the process was far from ideal from an environmental perspective, as high pressure hydrogen and non-sustainable rhodium catalyst were required. In this work, a transaminase which had previously been shown to generate (*R*)-amines, ATA-117, a homologue of an enzyme from *Arthrobacter*., was used as a starting point to develop an (*R*)-specific TAM which could accept pro-sitagliptin ketone (**62**) as a substrate, giving access to sitagliptin (**61**) in a sustainable fashion and at a low cost.<sup>[7]</sup>



**Scheme 1.20.** Two catalytic routes to the synthesis of sitagliptin (**61**)

In order to develop an active biocatalyst, a substrate walking approach was used wherein a truncated model of the substrate was docked into the active-site of the enzyme in order to design the enzyme active-site in such a way that a larger substrate would be accepted. A larger analogue was then docked into the active-site of the enzyme designed in the first step, in order to identify active-site residues which would need to be mutated in order for the active-site to accommodate the desired substrate. Finally, the residues identified from the docking studies were altered by saturation mutagenesis and mutants were tested for activity against the pro-sitagliptin ketone (**62**). In the first round of mutation, residues were targeted to relieve steric hindrance within the active site. These mutations were combined to give a mutant which, for the first time, showed activity towards the pro-sitagliptin ketone (**62**). This mutant, Y26H/V65A/V69G/F122I/A284G was then used as the basis for a second round of mutation, again aimed at reducing steric hindrance within the active site. This second library was screened, and the most active mutant showed a 75-fold increase in activity over the parent enzyme. In order for the biocatalyst to be industrially useful however, it needed to be active in >25% DMSO which was required to solubilise the pro-sitagliptin ketone (**62**), and also active in 1 M concentration of amine donor, required to drive the equilibrium of the reaction toward product formation. Hence, more rounds of iterative mutagenesis were carried out, screening the mutants at these conditions, until a mutant containing 27 mutations was identified which produced 200 g/L of sitagliptin with 99.95% ee. This



final catalyst contained 4 structure aided mutations and 1 site saturation mutation in the small binding pocket, 5 site saturated mutations in the large binding pocket, 2 site saturation mutations of positions outside both binding pockets, 10 mutations based on homology libraries and 5 mutations from random mutagenesis. The final biocatalytic process was performed in 50% DMSO and gave a 13% increase in overall yield, a 53% increase in overall productivity and a 19% reduction in waste including total elimination of heavy metal waste compared to the previous rhodium catalysed process.<sup>[7]</sup>

## 1.6 Aminodiols synthesis by TK and TAM

Many chiral aminodiols have been reported which exhibit useful biological activities (Figure 1.5). *N*-butyl-deoxynojirimycin (**63**) is an iminosugar which has been reported as an inhibitor of glucosylceramide synthase and can be used as a treatment for lysosomal storage disease. It has also been shown to prevent HIV replication *in vitro*.<sup>[70]</sup> Swainsonine (**64**) is an  $\alpha$ -mannosidase inhibitor, and has been shown to possess anti-cancer properties.<sup>[71]</sup> Sphingosine (**65**) is an important sphingolipid which accounts for a large proportion of the cell membranes of eukaryotic cells,<sup>[72]</sup> while chloramphenicol (**66**) is a broad spectrum antibiotic which is active against many bacterial infections.<sup>[73]</sup>

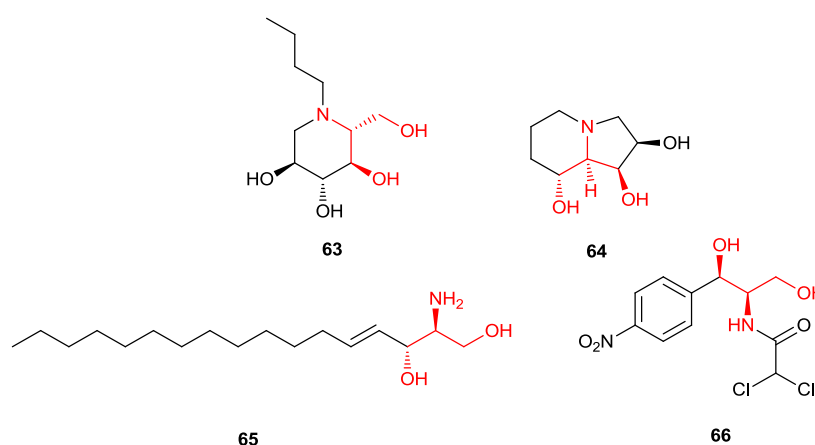


Figure 1.5. Structures of some biologically active aminodiols

Each of these compounds exhibit specific stereochemistries required for their biological activities which can be difficult to introduce using standard synthetic

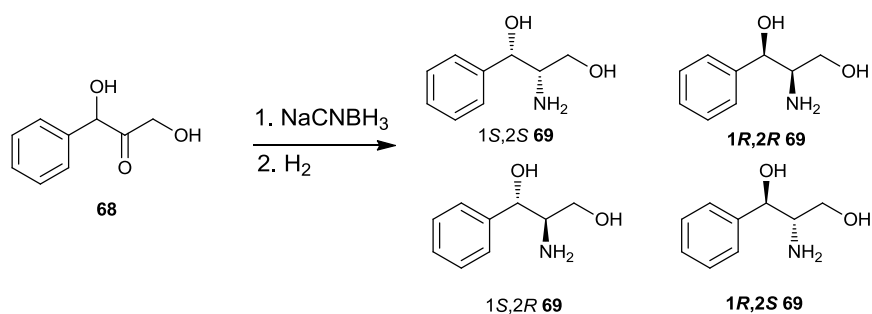
manipulations. The production of chiral aminodiols using enzymatic catalysis, however can offer a synthetically useful alternative to incorporate specific stereocentres.

A one-pot synthesis of 2-amino-1,3,4-butanetriol (ABT, **67**) (Scheme 1.21) has been reported using a single *E. coli* host containing two plasmids for the overexpression of TK (from plasmid pQR411) and a  $\beta$ -alanine:pyruvate aminotransaminase (overexpressed from plasmid pQR428).<sup>[74]</sup> This created a novel biocatalyst capable of the synthesis of chiral amino-alcohols via a one-pot, two-step synthetic pathway.

**Scheme 1.21. ABT (**67**) synthesis via a TK/TAm mediated synthetic pathway<sup>[74]</sup>**

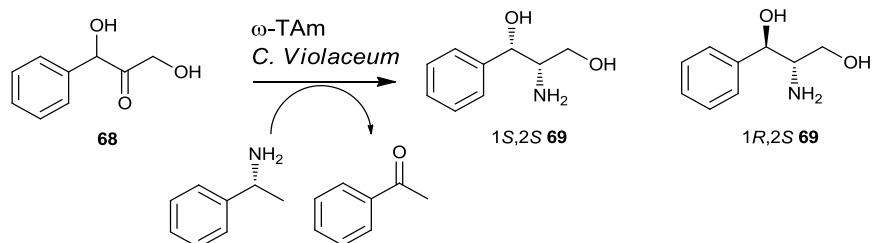
The TAm step required (*S*)- $\alpha$ -methylbenzylamine as an amine donor and the co-factor pyridoxal phosphate to transform the ketone moiety (**27**) to an amine (**67**). As a proof of concept the synthesis worked well, yielding a single diastereoisomer in 21% mol/mol yield. The TK catalysed condensation of Li-HPA (Li-**23**) and glycolaldehyde (**26**) was shown to proceed much faster than the TAm step, indicating that further work would be needed to identify a more active TAm enzyme, possibly by mutagenesis, to develop a more efficient process.<sup>[74]</sup>

The chemoenzymatic synthesis of aromatic aminodiols has been studied to establish the substrate tolerance and stereoselectivity of an  $\omega$ -transaminase from *Chromobacterium violaceum*.<sup>[75]</sup> The amino donor for the reaction was (*S*)- $\alpha$ -methylbenzylamine, and the acceptor was racemic 1,3-dihydroxy-1-phenylpropan-2-one (**68**) synthesised using the biomimetic transketolase reaction with benzaldehyde as the acceptor substrate. Chemical reductive amination of this racemic compound resulted in a mixture of four stereoisomers (**69**) (Scheme 1.22).<sup>[75]</sup>



**Scheme 1.22.** Four possible stereoisomers of **69** resulting from chemical reductive amination of ketodiol **68**

However, using CV2025 TAm, it was shown that only two stereoisomers were produced (Scheme 1.23). Asymmetric synthesis of three of the four stereoisomers, followed by chiral HPLC analysis of the acetylated products showed that the TAm accepted both (*R*) and (*S*)-isomers of ketodiol **68** but formed the new stereocentre (**69**) with (*2S*)-orientation exclusively.



**Scheme 1.23.** TAm reaction using ketodiol **68** as a substrate exclusively forming a new (*S*) stereocentre

In the future, and of particular importance to this PhD project, if new TK enzymes can be found which exclusively produce (*R*) or (*S*) aromatic ketodiols, optically pure aromatic aminodiols of *syn* and *anti* configuration should be accessible using a suitable TAm in the second step. This strategy could then be used to synthesise antibiotic molecules such as chloramphenicol (**66**).

## 1.7 Syntheses of chloramphenicol and thiamphenicol

Chloramphenicol (Figure 1.6, **66**) and thiamphenicol (Figure 1.6, **70**) are both broad spectrum antibiotics with a wide range of antimicrobial applications and both contain

an aminodiol moiety. Their potent biological activities have made them attractive targets for organic synthesis. Indeed, chloramphenicol was one of the first antibiotics to be produced in its optically active *D-threo* (*2R,3R*) form by chemical synthesis rather than by fermentation techniques.<sup>[76]</sup>

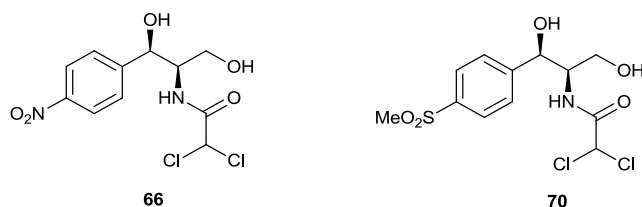


**Figure 1.6. Structures of chloramphenicol (66) and thiamphenicol (70)**

Several different syntheses to these molecules exist, with most relying on a Sharpless asymmetric epoxidation step to introduce the chiral alcohol.<sup>[76]</sup> A method used by Bhaskar *et al* (Scheme 1.24) started with the reaction of commercially available 4-nitrobenzaldehyde (**71**) with divinyl zinc to give the allylic alcohol (**72**) which was then subjected to Sharpless asymmetric epoxidation conditions to give the chiral epoxyalcohol (**73**) in 95% *ee*. Treatment with dichloroacetonitrile in the presence of sodium hydride was followed by an *in situ* epoxide opening of the dichloroamidate (**74**) using  $\text{BF}_3 \cdot \text{OEt}_2$ . Excess  $\text{BF}_3 \cdot \text{OEt}_2$  complexed with the oxazoline (**75**) and hydrolysed the resulting ring, which gave **66** in 23% overall yield.

**Scheme 1.24. Three- step synthesis of chloramphenicol (66)<sup>[76]</sup>**

Thiamphenicol (**70**) has been produced using a similar epoxidation strategy (Scheme 1.25). 4-(Methylthio)benzaldehyde (**76**) was converted to the allylic alcohol (**77**) using vinyl magnesium bromide and then selectively oxidised to the sulfone (**78**) using oxone. Sharpless asymmetric epoxidation was then carried out to give the chiral epoxyalcohol (**79**) in 95% *ee*. The rest of the synthesis proceeded as before, involving treatment with dichloroacetonitrile and sodium hydride to give **80**, which upon epoxide opening gave **81**. Hydrolysis using excess  $\text{BF}_3 \cdot \text{OEt}_2$  gave **70** in 21% overall yield.

**Scheme 1.25. Four step synthesis of thiamphenicol (70)**<sup>[76]</sup>

An alternate reaction has been proposed which uses the naturally available and cheaper reagent [(+)-DIPT], under kinetic resolution conditions, to install the chiral alcohol (*S*-**72**).<sup>[77]</sup> The second chiral centre was induced by a tethered aminohydroxylation (Scheme 1.26).<sup>[77]</sup> Here, the synthesis of chloramphenicol begins as shown previously (Scheme 1.24) using divinyl zinc to prepare the same allylic alcohol (**72**) from 4-nitrobenzaldehyde (**71**), followed by asymmetric epoxidation, this time using [(+)-DIPT], to give the chiral allylic alcohol (*S*-**72**) in 98% *ee*. Reduction with trichloroacetyl isocyanate, then treatment with potassium carbonate and methanol in water gave the carbamate (**82**). This was then subjected to

a tethered aminohydroxylation protocol using a *tert*-butyl hypochlorite oxidant, potassium osmate, NaOH, DIPEA, and propan-1-ol as the solvent. This gave the protected aminoalcohol **83** as a single isomer which upon treatment with NaOH in methanol and heating in methyl dichloroacetate gave **66** in an overall 29% yield and 98% *ee*.

**Scheme 1.26. 5 step Synthesis of chloramphenicol (66) using a tethered aminohydroxylation approach<sup>[77]</sup>**

This strategy was also used for thiamphenicol synthesis with the allylic alcohol and sulfone preparation achieved as previously described.<sup>[76]</sup>

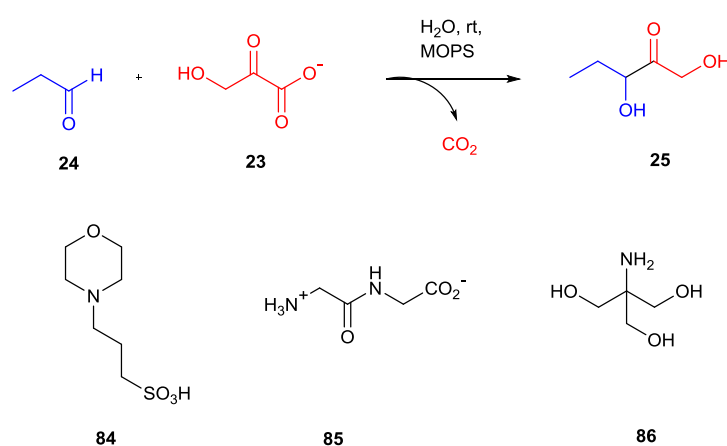
## **1.8 Project aims and objectives**

The aims of this project are 4-fold; firstly, to investigate the substrate scope of the biomimetic TK reaction and its potential for the asymmetric synthesis of aromatic ketodiols; secondly, to investigate the synthesis of ketodiols by TK and to develop and study mutants with increased activities and stereoselectivities for the production of aromatic ketodiols; thirdly, to investigate a two-step TK/TAm strategy towards aromatic aminodiol synthesis using the best TK mutants and CV2025 TAm; and finally to increase the synthetic utility of TK by investigating the tolerance of mutant TKs towards novel donor substrates other than HPA, to allow the stereoselective preparation of ketol compounds.

## **2 The Biomimetic Transketolase Reaction**

## 2.1 Previous work carried out by the group before starting the PhD

The first biomimetic transketolase reaction was reported in 2006.<sup>[50]</sup> While screening suitable buffers for the transketolase reaction it was found that 3-morpholinopropane-1-sulfonic acid (MOPS) (Scheme 2.1, **84**) catalysed ketodiol (**25**) formation between Li-HPA (Li-**23**) and propanal (**24**) without the addition of TK. However, no reaction was observed under comparable conditions when using glycylglycine (**85**) or tris(hydroxymethyl)aminomethane, (TRIS) (**86**), buffers.



Scheme 2.1 Reaction scheme of buffer catalysed ketodiol formation

The co-factor ThDP was not required for this reaction, indicating that some structural feature in MOPS (**84**) was required for the reaction to occur. A range of sulfonic acids and secondary and tertiary amines were therefore screened for the conversion of propanal (**24**) to ketodiol **25**, in order to determine which functional motif was responsible for mediating the reaction (Figure 2.1, Table 2.1).<sup>[50]</sup>

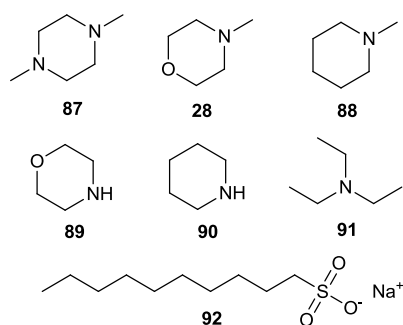


Figure 2.1 Tertiary amines and sulfonate screened with propanal for ketodiol formation



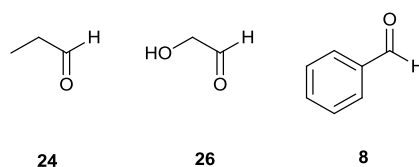
**Table 2.1 Tertiary amine catalysts screened for ketodiol formation with propanal<sup>[50]</sup>**

Putative catalyst	Product (25) yield %
<i>N,N'</i> -dimethylpiperazine (87)	26
<i>N</i> -methylmorpholine (28)	27
<i>N</i> -methylpiperidine (88)	8
morpholine (89)	0
piperidine (90)	0
triethylamine (91)	0
sodium 1-decanesulfonate (92)	0

Reactions were carried out in water at room temperature with 3 equivalents of aldehyde (24), 1 equivalent of LiHPA (Li-23) and 1 equivalent of catalyst (28, 87-92). Only the use of *N,N'*-dimethylpiperazine (87), *N*-methylmorpholine (NMM, 28) and *N*-methylpiperidine (88) as catalysts led to formation of the desired product (25) (Table 2.1). None of the other putative catalysts (89-92) gave any product, indicating that the cyclic tertiary amine motif was critical for catalytic activity. Upon optimisation of the reaction conditions using NMM (28), isolated yields of up to 35% of ketodiol 25 were obtained in only five hours at room temperature.<sup>[50]</sup>

## 2.2 Substrate scope of the racemic biomimetic reaction

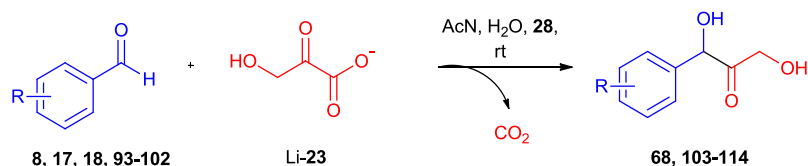
In the initial report of the biomimetic transketolase reaction only propanal (24), glycolaldehyde (26) and benzaldehyde (8) were screened with MOPS buffer (84) (Figure 2.2).<sup>[50]</sup>

**Figure 2.2 Aldehydes screened in initial investigation into the biomimetic TK reaction**

Clearly this reaction was useful for creating racemic substrates which could be used to develop chiral assays for analysing optically-active ketodiol formed from transketolase biotransformations. Therefore at the start of this PhD the substrate

scope of the biomimetic transketolase reaction was explored with aromatic aldehydes (**8**, **17**, **18**, **93-102**) to prepare racemic ketodiols (**68**, **103-114**) (Table 2.2). Some slight variations were made to the initial reaction conditions of the biomimetic reaction;<sup>[50]</sup> a 1:1 mixture of acetonitrile (AcN):water (total volume of 10 mL) was used to increase the solubility of the various aromatic aldehydes, and equimolar amounts of catalyst, Li-HPA (Li-**23**) and aldehyde were used, to ease purification. Since NMM (**28**) had been shown to be the best catalyst in the initial studies of the biomimetic TK reaction,<sup>[50]</sup> the conversion of these aromatic aldehydes were also studied with this catalyst.

**Table 2.2 Yields obtained for benzaldehydes screened in biomimetic TK reaction\***



Entry	Aldehyde (R=)	Product yield (%)
1	H ( <b>8</b> )	15 ( <b>68</b> )
2	3-OH ( <b>93</b> )	6 ( <b>103</b> )
3	3-Br ( <b>17</b> )	20 ( <b>104</b> )
4	3-F ( <b>94</b> )	23 ( <b>105</b> )
5	3-CO <sub>2</sub> Me ( <b>95</b> )	29 ( <b>106</b> )
6	3-vinyl ( <b>96</b> )	6 ( <b>107</b> )
7	3-CO <sub>2</sub> H ( <b>97</b> )	20 ( <b>108</b> ) (Conversion yield)
8	3-NO <sub>2</sub> ( <b>98</b> )	22 ( <b>109</b> )
9	3-CN ( <b>18</b> )	10 ( <b>110</b> )
10	4-Cl ( <b>99</b> )	2 ( <b>111</b> )
11	4-F ( <b>100</b> )	2 ( <b>112</b> )
12	4-Br ( <b>101</b> )	1 ( <b>113</b> )
13	4-I ( <b>102</b> )	3 ( <b>114</b> )

\*Reaction conditions; 1.0 mmol aldehyde, 1.0 mmol LiHPA, 1.0 mmol NMM, 1:1 AcN:H<sub>2</sub>O (10 mL total volume), pH 7, 24 hour reaction time.

The reaction showed a fairly wide substrate tolerance, accepting both *meta*- and *para*-substituted benzaldehydes. Benzaldehyde (**8**) (entry 1) gave ketodiol **68** (Table 2.2, R=H) in 15% isolated yield, which was slightly lower than the previously

reported 25% yield achieved using MOPS (**84**) as a catalyst,<sup>[50]</sup> presumably due to the 3-fold lower aldehyde concentration used to simplify product purification. *Meta*-substituted benzaldehydes were generally well tolerated in this reaction, 3-hydroxybenzaldehyde (**93**) gave a 6% yield of ketodiol **103** and halogenated derivatives **17** and **94** (entries 3 and 4), and aldehydes **95**, **97**, **98** and **18** (entries 5, 7, 8 and 9) gave isolated yields of ketodiol products of >20%. Interestingly, the *para*-substituted benzaldehydes **99-102** were less well tolerated in the reaction (entries 10-13), with no yields above 3% observed for ketodials **111-114**. Some benzaldehydes (**115-119**) were not accepted in the reaction at all, with no product formation observed by TLC analysis (Figure 2.3).

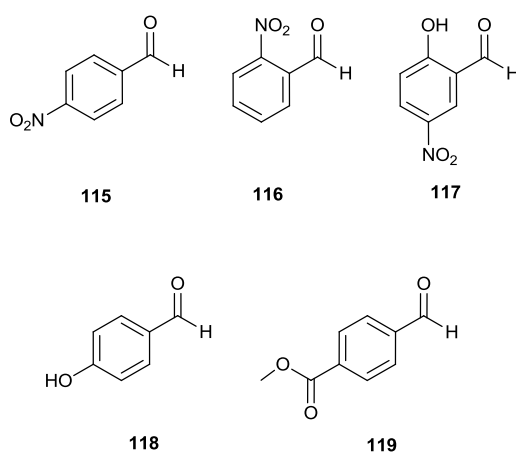
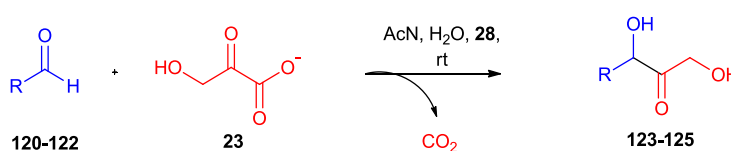


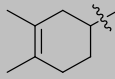
**Figure 2.3 Benzaldehydes 115-119 not accepted in biomimetic TK reaction**

No product formation was observed for 4-nitrobenzaldehyde (**115**), 2-nitrobenzaldehyde (**116**), 2-hydroxy-5-nitrobenzaldehyde (**117**), 4-hydroxybenzaldehyde (**118**) or methyl-4-formylbenzoate (**119**). Substitution at the *ortho* position did not seem favourable, as none of the *ortho*-substituted benzaldehydes were tolerated in the biomimetic reaction, possibly due to steric crowding of the aldehyde functionality. Also, substitution at the *para* position seemed to be poorly tolerated with only the *para* halogen benzaldehydes, **99-102**, transformed with low yields.

Some non-aromatic aldehydes (**120-122**) were also studied for conversion to the corresponding ketodials (**123-125**) with Li-HPA (Li-**23**) and NMM (**28**), under the same reaction conditions (Table 2.3)

**Table 2.3 Yields obtained for aliphatic aldehydes screened in biomimetic TK reaction\***

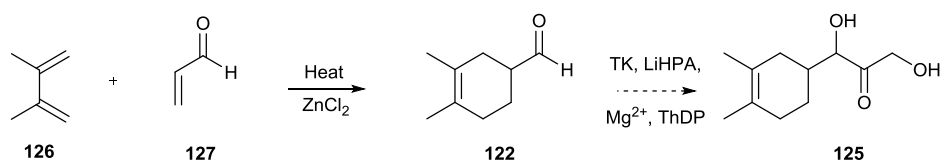


Aldehyde (R=)	Product yield %
C <sub>4</sub> H <sub>9</sub> ( <b>120</b> )	56 ( <b>123</b> )
C <sub>5</sub> H <sub>11</sub> ( <b>121</b> )	48 ( <b>124</b> )
 ( <b>122</b> )	4 ( <b>125</b> )

\*Reaction conditions; 1.0 mmol aldehyde, 1.0 mmol LiHPA, 1.0 mmol NMM, 1:1 AcN:H<sub>2</sub>O (10 mL total volume), pH 7, 24 hour reaction time.

The longer chain aliphatic aldehydes were well tolerated in the biomimetic reaction with similar isolated yields of ketodiols **123** and **124** obtained as reported for the biomimetic reaction with propanal (**23**).<sup>[26, 50]</sup> Butanal (**120**) and pentanal (**121**) had been previously investigated with the biomimetic reaction, though on a larger-scale, and lower isolated yields of ketodiols **123** and **124** of 12 % and 35%, respectively, had been obtained.<sup>[26]</sup>

The cyclic aldehyde, 3,4-dimethylcyclohex-3-enecarbaldehyde (**122**), was prepared by the Diels-Alder reaction of acrolein (**126**) and 2,3-dimethylbutadiene (**127**) (Scheme 2.2). This aldehyde (**122**) was of particular interest, as its synthesis is being investigated in a biocatalytic flowcell, which could then be combined with a second TK step, giving a two-step microfluidic reaction toward a complex, chiral substrate (**125**) (Scheme 2.2).<sup>[78]</sup> 3,4-Dimethylcyclohex-3-enecarbaldehyde (**122**) was prepared by reacting 2,3-dimethylbutadiene (**127**) with acrolein (**126**) in a sealed tube, with a catalytic amount of zinc chloride at 60 °C. After 18 hours the product was purified by flash silica chromatography to give 3,4-dimethylcyclohex-3-enecarbaldehyde (**122**) in 56% yield.

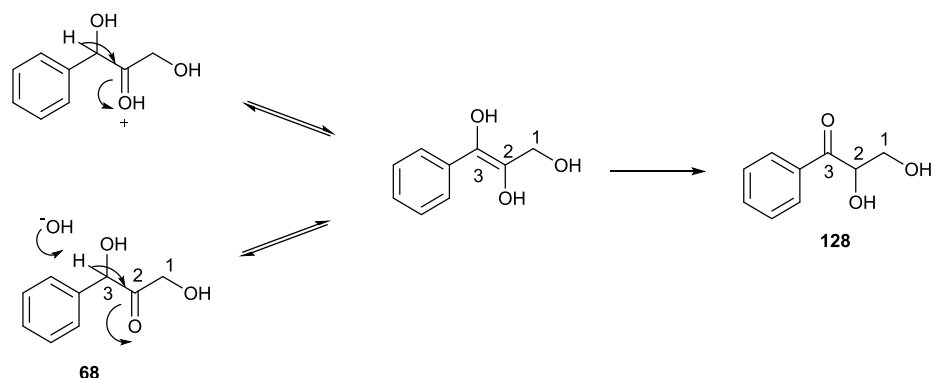


**Scheme 2.2 Synthesis of 3,4-dimethylcyclohex-3-enecarbaldehyde (**122**) and its potential use as a substrate in TK biotransformations**

Using this cyclic aldehyde (**122**) as a substrate in the biomimetic reaction gave a 4% isolated yield of ketodiol (**125**), much lower than the isolated yields of ketodiol **123** and **124** from butanal and pentanal (Table 2.3). Indeed this aldehyde (**122**) was less well tolerated than most of the aromatic aldehydes tested (Table 2.2).

Comparing the isolated yields obtained for all of the different aldehydes used it is interesting to note that the highest yields observed were for aliphatic aldehydes. It would therefore appear that steric factors are important in determining reactivity in the biomimetic TK reaction, which would also explain why no *ortho*-substituted benzaldehydes were tolerated as substrates.

While studying the biomimetic reaction with aromatic substrates it became clear that it was very important to keep the reaction as close to neutral pH as possible. When the reaction was performed at acidic or basic pH, or if the reaction was left for extended periods, one major side-product was isolated. This was identified as the 1,2-ketodiol (**128**) formed from the isomerisation of the desired 1,3-ketodiol product (**68**) (Scheme 2.3).



**Scheme 2.3** Possible mechanisms of formation of rearranged ketodiol (**128**)

Formation of this product was also observed during TK biotransformations and will be discussed later (Chapter 3).

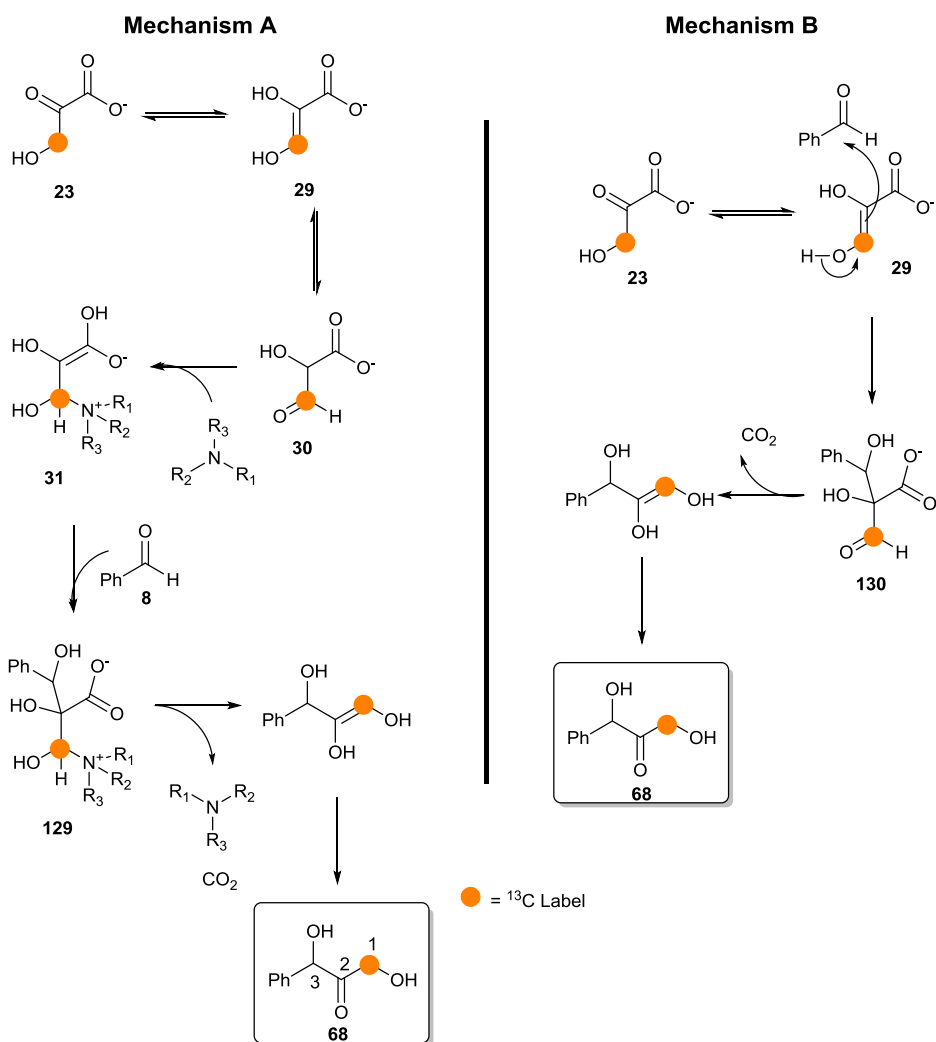
## 2.3 Mechanistic study of the biomimetic transketolase reaction<sup>[79]\*</sup>

After establishing that the biomimetic reaction could be used to transform a more extensive range of aliphatic and aromatic aldehydes (Table 2.2, Table 2.3), it was decided to elucidate the mechanism further to fully understand the differences in reactivity observed for different aldehydes and to see if an asymmetric variant of the reaction could be developed.

Four different reaction mechanisms were postulated for the biomimetic TK reaction. To distinguish between these mechanisms a <sup>13</sup>C labelling approach was used, utilising <sup>13</sup>C labelled HPA as the ketol donor and benzaldehyde (**8**) as the acceptor. The first mechanism, mechanism A (Scheme 2.4), proceeded by the addition of the tertiary amine either directly to the *ene*-diol (**29**) or tartronic acid semialdehyde (**30**) to give the quarternary amine enolate (**31**). This would then undergo an aldol addition to the acceptor aldehyde (**8**), which, followed by proton transfer would give (**129**). Elimination of CO<sub>2</sub> and the tertiary amine catalyst would furnish the *ene*-diol which could subsequently tautomerise to the 1,3-ketodiol (**68**).<sup>[79]</sup>

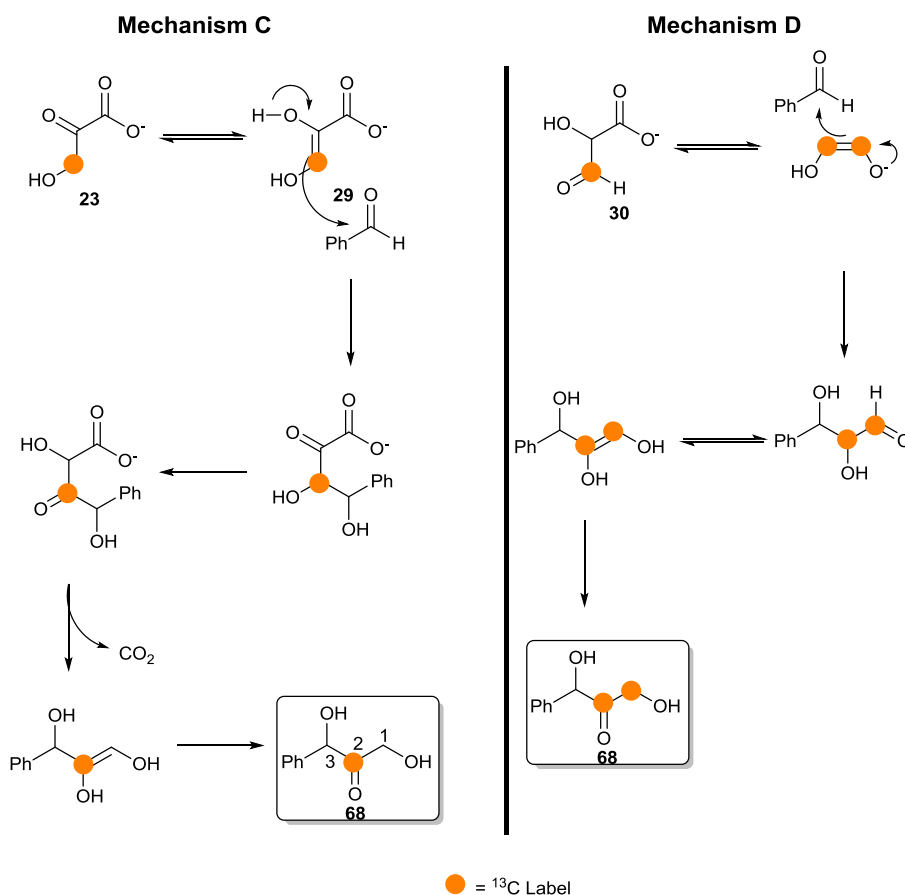
---

\* All isotopic labelling and MS studies were carried out by James Galman



**Scheme 2.4 Possible mechanism of the biomimetic TK reaction - Mechanisms A and B**

An aldol-based mechanism was also envisaged, as in mechanism B (Scheme 2.4), where the direct aldol addition of **29** to **8** would give **130**, which upon elimination of carbon dioxide, proton transfer and subsequent tautomerisation would give the 1,3-ketodiols (**68**).<sup>[79]</sup> Here the role of tertiary amine would be to act as a base, promoting the aldol reaction. An alternative mechanism could occur from an aldol addition to the less hindered carbon of *ene*-diol **29**, as in mechanism C (Scheme 2.5). This would be followed by tautomerisation, decarboxylation, and further tautomerisation to give the 1,3-ketodiols (**68**).<sup>[79]</sup> Here the role of tertiary amine would once again be to act as a base, promoting the aldol reaction, however in this case the label would be incorporated at C-2. A fourth possible mechanism, mechanism D (Scheme 2.5), would involve the decarboxylation of (**30**) to give a symmetrical enediolate intermediate which could then undergo aldol addition to the acceptor aldehyde. Subsequent tautomerisation would then give the 1,3-ketodiols product (**68**).<sup>[79]</sup>

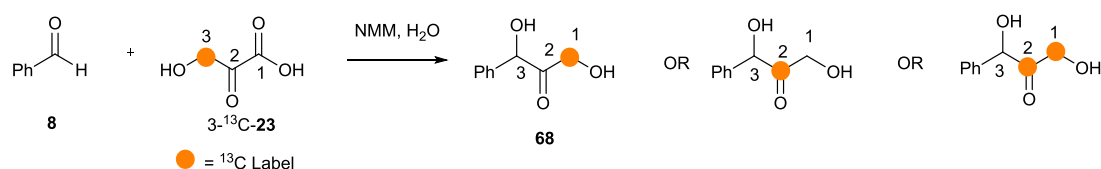


**Scheme 2.5 Possible mechanisms of the biomimetic TK reaction – Mechanisms C and D**

The position of the <sup>13</sup>C label could be established by <sup>13</sup>C-NMR and hence allow the correct mechanism to be established, since mechanisms A and B would result in incorporation of the <sup>13</sup>C label at C-1 (Scheme 2.4), mechanism C would lead to labelling at C-2 (Scheme 2.5) and mechanism D would lead to scrambling of the <sup>13</sup>C label at positions C-1 and C-2 (Scheme 2.5).<sup>[79]</sup>

3-<sup>13</sup>C labelled HPA was prepared by James Galman via the bromination of <sup>13</sup>C sodium pyruvate, and subsequent reaction with lithium hydroxide following a standard procedure.<sup>[50]</sup> The standard biomimetic reaction was then performed with benzaldehyde (**8**) as the acceptor substrate and 3-<sup>13</sup>C-LiHPA (3-<sup>13</sup>C Li-**23**) as the ketol donor to give the <sup>13</sup>C labelled ketodiol (**68**) in 10% isolated yield (Scheme 2.6). The position of the <sup>13</sup>C label was then established.<sup>[79]</sup>





**Scheme 2.6. Biomimetic TK reaction with  $^{13}\text{C}$ -labelled HPA and benzaldehyde**

$^{13}\text{C}$ -NMR analysis confirmed the incorporation of  $^{13}\text{C}$  at C-1, shown by the intensity of the C-1 signal compared to the unlabelled natural abundance spectra previously observed. The  $^1\text{H}$ -NMR spectra also confirmed the incorporation of  $^{13}\text{C}$  at C-1 by the observed coupling,  $^1J_{\text{CH}}$  of 145 Hz. Since incorporation of  $^{13}\text{C}$  at C-1 was observed exclusively, and no scrambling of the label was seen, this approach showed that only mechanisms A and B (Scheme 2.4) could be operating and mechanisms C and D (Scheme 2.5) were not involved.<sup>[79]</sup>

This labelling study could not distinguish between mechanisms A and B, so another approach was needed to further elucidate the mechanism. Electrospray ionisation mass spectrometry (ESI-MS) and tandem ESI-MS/MS have previously been successfully used to detect reaction intermediates and minor reaction products.<sup>[80, 81]</sup> With mechanisms A and B both implicated in the biomimetic TK reaction, ESI-MS and ESI-MS/MS were used to intercept and identify ions formed from reaction intermediates.<sup>[79]</sup> The reaction was continuously monitored by direct infusion of the reaction mixture into the ESI probe and highly charged covalent species were detected which corresponded to intermediates from both mechanisms A and B.<sup>[79]</sup> Tandem MS was then used to produce fragments of these intermediates to confirm their structures. While fragments were isolated and identified using this method, it was still not possible to determine whether mechanism A or B was operating as the identified fragments could have been formed from either mechanism,<sup>[79]</sup> though work by Rohr *et al* has shown that direct aldol additions can occur between suitable ketoacids and aldehydes in the presence of a tertiary amine catalyst,<sup>[82]</sup> supporting the existence of mechanism B.

## 2.4 The asymmetric biomimetic TK reaction\*

If mechanism A (Scheme 2.4) was indeed operating it was proposed that by using a chiral tertiary amine catalyst the addition of the aldehyde could be directed to its re- or si-face and hence some asymmetry induced in the final product. To investigate whether the biomimetic TK reaction could be made asymmetric, a range of chiral tertiary amine catalysts were tested using LiHPA (Li-**23**) as the ketol donor and benzaldehyde (**8**) as the acceptor.<sup>[79]</sup> The best catalyst was found to be quinine ether **131** (Figure 2.4), so this was screened against a larger range of benzaldehydes (**8**, **94**, **99-101**, **132-136**) (Table 2.4) and isolated yields of ketodiol products (**68**, **105**, **106**, **111-113**, **137-140**) obtained to establish whether more functionalised compounds would be tolerated in the reaction.<sup>[79]</sup>

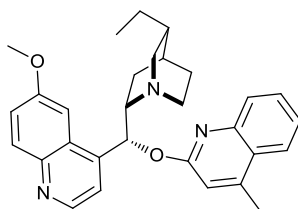


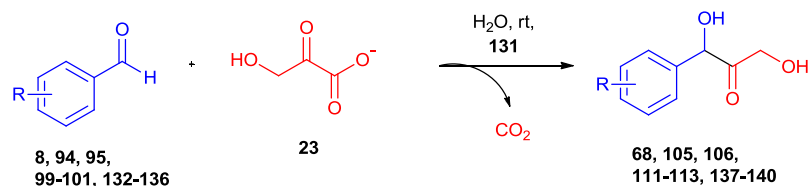
Figure 2.4 Structure of hydroquinine 4-methyl-2-quinolyl ether (**131**)

Low yields were consistently observed for all substrates tested; lower even than when using NMM (**28**) as the catalyst (Section 2.2), suggesting that the increased steric bulk of **131** may have been responsible for the reduced yields. However, the stereoselectivities observed were promising.

---

\* Some of the transformations carried out in Table 2.4 were carried out by James Galman

**Table 2.4 Yield and stereoselectivity data for substituted benzaldehydes screened in asymmetric biomimetic TK reaction\***



Entry	Aldehyde (R=)	Time (h)	Product yield %	ee (%)
1	H ( <b>8</b> )	12	4 ( <b>68</b> )	22
2	4-Me ( <b>132</b> )	12	2 ( <b>137</b> )	21
3	4-F ( <b>100</b> )	48	3 ( <b>112</b> )	36
4	4-Cl ( <b>99</b> )	24	2 ( <b>111</b> )	50
5	4-OMe ( <b>133</b> )	72	3 ( <b>138</b> )	0
6	4-Br ( <b>101</b> )	12	2 ( <b>113</b> )	0
7	3-F ( <b>94</b> )	48	2 ( <b>105</b> )	38
8	3-OMe ( <b>134</b> )	24	3 ( <b>139</b> )	36
9	3-CO <sub>2</sub> Me ( <b>95</b> )	24	4 ( <b>106</b> )	25
10	2-F ( <b>135</b> )	48	3 ( <b>140</b> )	0
11	2,4-Cl ( <b>136</b> )	48	0	ND

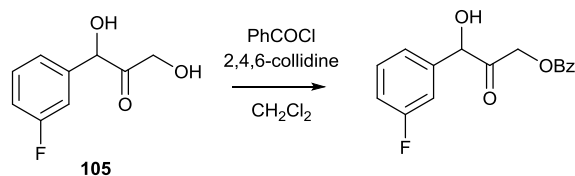
\* Reaction conditions: Entries 1,2 and 6,7, 1.0 mmol aldehyde, 1.0 mmol LiHPA, 5 mol% **131**, 1:1 THF:H<sub>2</sub>O (2 mL total volume). Entries 3-5 1.0 mmol aldehyde, 1.0 mmol LiHPA, 20 mol% **131**, 1:2 THF:H<sub>2</sub>O (2 mL total volume). Entries 8-9 1.0 mmol aldehyde, 1.0 mmol LiHPA, 10 mol% **131**, 1:1 THF:H<sub>2</sub>O (2 mL total volume).

*Para*-substituted fluorobenzaldehyde (**100**) and 4-Cl benzaldehyde (**99**) (entries 3 and 4) gave moderate *ees* (36% and 50% respectively), whereas substrates with larger *para*-substituents such as 4-methoxy (**133**) (entry 5) and 4-Br (**101**) (entry 6) showed no stereoselectivity whatsoever, suggesting that increasing the size of the *para*-substituent had a detrimental effect on the stereoselectivity of the reaction. *Meta*-substituents were fairly well tolerated, with both electron withdrawing (**94**, **95**) (entries 7 and 9) and donating groups (**134**) (entry 8) giving moderate *ees*, suggesting that *meta*-substituents were not as critical for stereochemical induction. Substitution at the *ortho*-position was not well tolerated, however. 2-Fluorobenzaldehyde (**135**) (entry 10) was accepted in the reaction but no stereoselectivity was observed, whereas 2,4-dichlorobenzaldehyde (**136**) was not transformed to the corresponding ketodiol, and so *ortho*-substituted benzaldehydes were not investigated further.

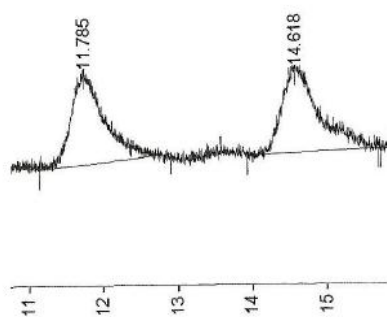
Higher yields (15-20%) were observed for some aliphatic aldehydes but no stereoselectivity was observed for any aliphatic substrates.<sup>[79]</sup>

#### **2.4.1 Chiral analysis of ketodiol products from asymmetric biomimetic TK reaction**

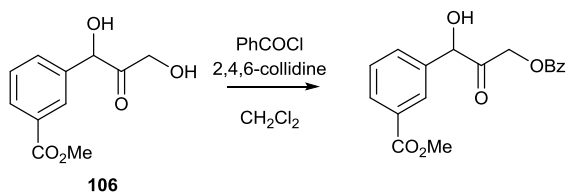
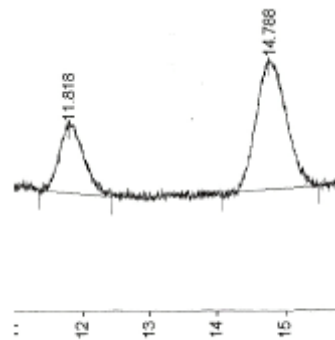
The stereoselectivities for these products were assigned by a combination of chiral HPLC analysis (of mono- or di-benzoylated derivatives) and the analysis of Mosher's ester derivatives.<sup>[83]</sup> Racemic standards were prepared using the NMM-catalysed biomimetic reaction and used to develop chiral HPLC assays which could then be used to analyse products from the asymmetric reaction. A hindered 2,4,6-collidine base was used to avoid racemisation of the products, as discussed further in Chapter 3. Good separation was achieved for all derivatives using a 90:10 *n*-hexane:isopropanol solvent system, a Chiralcel OD column at 1.0 mL/min and detection at 214 nm (Figure 2.5). Mosher's ester derivatives of ketodiol products were prepared and isolated to allow the absolute stereochemistry to be tentatively assigned as *R* by comparing the integrations of the diastereotopic protons as previously described,<sup>[26, 83]</sup> and as further discussed in Chapters 3 and 6.



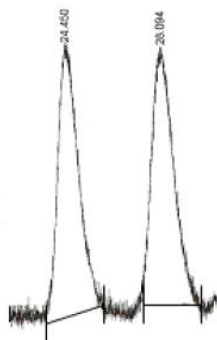
**Racemic Standard**



**Asymmetric Reaction Sample  
38% ee**



**Racemic Standard**



**Asymmetric Reaction Sample  
25% ee**

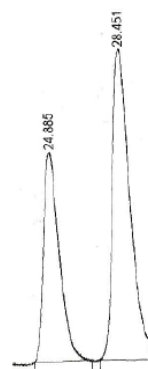


**Figure 2.5 Chiral HPLC traces of mono-benzoylated derivatives of (105) and (106). Elution times shown in minutes.**

The tentatively assigned *R*-selectivity was rationalised by considering reaction intermediate (**129**). In this intermediate the lower face of the enolate would not be accessible to the aldehyde, and so addition of the enolate would occur to the *si*-face of the aldehyde (Figure 2.6, underside as drawn) to give the *R*-product.

**Figure 2.6 Possible rationale for the formation of the assigned *R*-stereocentre (reproduced from<sup>[79]</sup>)**

As previously mentioned, the two reactions mechanisms, A and B (Scheme 2.4), had been proposed for the biomimetic TK reaction. That any stereoselectivity was observed at all suggests that mechanism A operates to some extent, since the intermediate formed from the addition of the chiral amine catalyst to HPA would allow facial stereodifferentiation of the approaching aldehyde, with only one face of the enolate exposed for attack. Mechanism B could also be expected to have an influence on facial stereodifferentiation, with the tertiary amine catalyst non-covalently interacting with the enolate, directing addition of the aldehyde. However, the required electrostatics would have to be very strong, and in water this seems unlikely. For substituents where lower or negligible *ees* were observed, this suggests the predominance of mechanism B, though the actual mechanism in operation still remains uncertain and is likely to depend on the catalyst, the aldehyde or a combination of both. The suitability of using the Mosher's ester analysis method to assign the absolute stereochemistry for these aromatic compounds has subsequently been studied, and will be discussed further in chapter 6.

## **2.5 Summary of chapter 2**

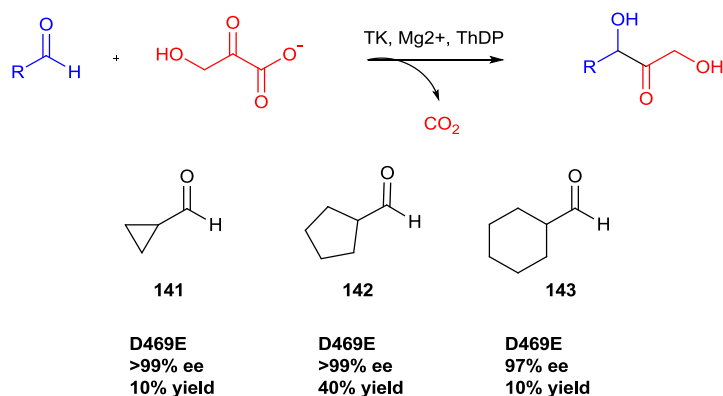
In conclusion, the biomimetic TK reaction has been studied in detail. The substrate scope of the NMM-catalysed biomimetic reaction has been investigated with a range of functionalised benzaldehydes and several aliphatic aldehydes. The mechanism of the reaction has been probed by isotopic labelling studies and mass spectrometry and

an asymmetric variant of the reaction has been established using a chiral tertiary amine catalyst. Chiral analysis methods for aromatic ketodiols have been developed and the asymmetric biomimetic reaction has been used to access aromatic ketodiols in water in up to 50% *ee*.<sup>[79]</sup> These are useful preliminary asymmetric results that can be used as a foundation for further studies with other chiral catalysts and a wider range of substrates.

### **3 Aromatic aldehydes with single point mutant TKs**



Single point mutant TKs had previously been shown to accept a range of aliphatic aldehydes, with good yields (up to 70%) and excellent stereoselectivities (>99% *ee*). Interestingly, the cyclic aldehydes cyclopropanecarboxaldehyde (**141**), cyclopentanecarboxaldehyde (**142**) and cyclohexanecarboxaldehyde (**143**), which were barely tolerated by WT-TK (<3% yield), were accepted by several D469 mutants, especially D469E (Scheme 3.1).<sup>[26]</sup>

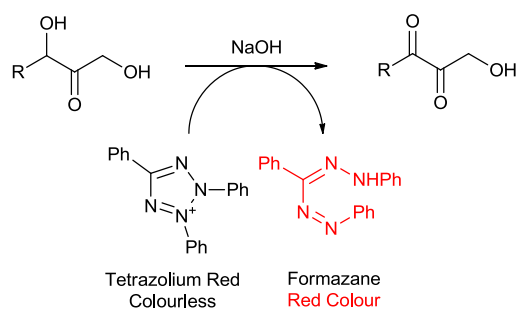


**Scheme 3.1** Transketolase catalysed ketodiol formation with cyclic aldehydes and D469E TK

D469E was generally the most active mutant towards these cyclic aliphatics, though D469T and D469K also showed activity, but lower yields and stereoselectivities were observed.<sup>[26]</sup>

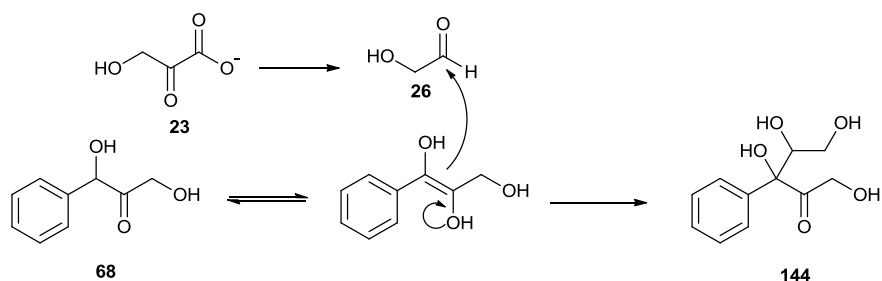
### **3.1 Previous work done by the group to identify active mutant TKs using a colorimetric assay**

The TK mutants studied with aliphatic aldehydes<sup>[26]</sup> were identified using a previously established high-throughput colorimetric assay.<sup>[84]</sup> In this assay, the ketodiol product was oxidised, reducing 2,3,5-triphenyltetrazolium chloride to 1,3,5-triphenylformazan in the process. 2,3,5-Triphenyltetrazolium chloride is colourless, but 1,3,5-triphenylformazan is red coloured and the optical density at 485nm was measured to quantify the amount of ketodiol produced in work previously carried out by the group. (Scheme 3.2).<sup>[84]</sup>



**Scheme 3.2** Colorimetric assay used to identify active TK mutants

To establish whether TK mutants could accept aromatic aldehydes, the colorimetric assay had been performed using benzaldehyde (**8**) (Scheme 3.1, R = Ph) and LiHPA (Li-**23**) to identify active mutants.<sup>[85]</sup> The assay gave several positive hits and subsequent sequencing revealed they were; D469E, D469K, D469S and D469T. Interestingly, 3 of these mutants; D469E, D469K, and D469T had previously shown activity toward cyclic aldehydes (Scheme 3.1).<sup>[26]</sup> Another mutant, F434A that had been previously prepared by site-directed mutagenesis was investigated as it was thought that this mutant would remove some unfavourable steric and electronic interactions in the active site to allow larger aromatic substrates to enter. From the colorimetric assay, D469S had appeared to give significant amounts of product and was investigated further. Upon scale-up and isolation of product however, only trace amounts of the desired ketodiol product (**68**) were observed. The main product from this reaction was **144**, the formation of which was postulated to be from the aldol addition of the ketodiol product (**68**) to glycolaldehyde (**26**) (Scheme 3.3) (presumably formed *in situ* from the decarboxylation of HPA) (**23**) to give a “double addition” product (**144**).



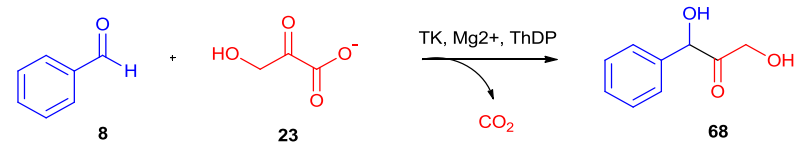
**Scheme 3.3** Proposed mechanism for the formation of the observed double addition product **144**

No double addition product was observed when the biomimetic TK reaction was performed with the same substrate concentrations, suggesting that the aldol addition of the ketodiol product to glycolaldehyde may occur in the TK active-site, either when the product is still attached to the ThDP-enamine, or after it has been displaced by another HPA molecule. The observation of this double addition product (**144**) made clear a serious limitation with the colorimetric assay, as it could not distinguish between the desired product and the double addition product, as both could be oxidised, thus reducing 2,3,5-triphenyltetrazolium chloride, forming the red colour associated with a “positive” hit. However, formation of the desired product (**68**), even as an intermediate, was a promising start, and the assay allowed identification of several mutants (D469E, D469T, D469K) which could be investigated further, along with F434A.<sup>[85]</sup>

### 3.2 Biotransformations of aromatic aldehydes with active single mutant TKs

Benzaldehyde (**8**) was the first aromatic substrate screened in scaled-up reactions with F434A and the D469 mutants which had given positive hits in the colorimetric screen (Table 3.1). Li-HPA (Li-**23**) was used as the ketol donor, and isolated yields and stereoselectivities of ketodiol **68** were established, where possible.

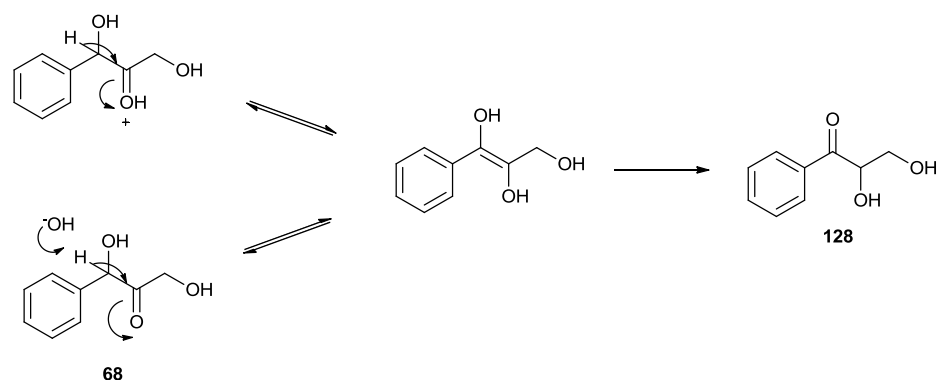
**Table 3.1 Biotransformations of benzaldehyde by single mutant TKs\***



WT-TK	D469E	D469T	D469K	F434A
Yield % (ee)	Yield % (ee)	Yield % (ee)	Yield % (ee)	Yield % (ee)
0	2 (0%)	2 (70%, 3R)	2 (82%, 3R)	10 (82%, 3R)

\*Biotransformation of benzaldehyde by D469K was carried out by James Galman. Reaction conditions: 1.0 mmol aldehyde, 1.0 mmol LiHPA, 2 mL TK cell-free lysate, 20 mL total volume, 48 hour reaction time.

WT-TK showed no activity, as expected, but isolated yields of 2-10% were observed for the mutant TKs. One major problem observed during the purification of **68** was the formation of the rearranged product **128** (Scheme 3.4), which was promoted by acidic or basic conditions or by extended reaction times,<sup>[85]</sup> as previously observed for the biomimetic reaction (Chapter 2).



**Scheme 3.4 Proposed mechanism for the formation of undesired rearranged ketodiol (**128**) in the TK reaction**

Formation of the rearranged ketodiol (**128**) was prevented by keeping the pH of the reaction as close to neutral as possible by performing the biotransformations in an autotitrator programmed to add 1 M HCl in a controlled fashion, to prevent an increase in pH as the reaction progressed.<sup>[26, 85]</sup>

F434A gave the highest isolated yield of ketodiol **68** (10%), with no double addition product observed. The D469 mutants however, each gave 5% of double addition product **144** and consequently lower yields of desired ketodiol **68**. The lack of double addition product (**144**) observed for F434A could be due to the increased accessibility to the active-site that the alanine mutation confers, allowing the ketodiol product to exit the enzyme active-site more readily, preventing formation of any double addition product in the active-site region. Interestingly, analysis of 382 ThDP-dependent enzyme sequences previously described,<sup>[86]</sup> showed that the position equivalent to F434 was always phenylalanine or tyrosine, except for benzoyl formate decarboxylase and benzaldehyde lyase enzymes where this residue was found to be alanine. This seemed to suggest that the F434A mutation was indeed important for the acceptance of aromatic rings in the active site of TK.<sup>[85]</sup> The stereoselectivities of the transformations were interesting, with both D469K and F434A forming the product (**68**) in 82% *ee*, D469T in 70% *ee* and D469E a

racemate, which is in contrast to the consistently high stereoselectivities observed for the linear and cyclic aliphatic aldehydes.<sup>[26]</sup> It also appeared that the aromatic ketodiols were formed with the opposite stereocentre to the aliphatic series, with the absolute stereochemistry tentatively assigned as (3*R*), using the same Mosher's ester analysis method as previously described.<sup>[26, 83, 85]</sup>

With enzymes in hand that could accept benzaldehyde, attention was then turned to the heteroaromatic aldehydes, furfural (**145**) (Table 3.2, R = C<sub>4</sub>H<sub>3</sub>O) and thiophenecarboxaldehyde (**146**) (Table 3.2, R = C<sub>4</sub>H<sub>3</sub>S), which were screened for their conversion to the corresponding ketodiols **147** (Table 3.2, R = C<sub>4</sub>H<sub>3</sub>O) and **148** (Table 3.2, R = C<sub>4</sub>H<sub>3</sub>S).

**Table 3.2 Biotransformation of heteroaromatic aldehydes by single mutant TKs\***

$\text{R-CHO} + \text{HO-CH}_2\text{-CO}_2^- \xrightarrow{\text{TK, Mg}^{2+}, \text{ThDP}} \text{R-CH(OH)-CO-CH}_2\text{OH} + \text{CO}_2$

**145, 146**                      **23**                      **147, 148**  
145 R = C<sub>4</sub>H<sub>3</sub>O  
146 R = C<sub>4</sub>H<sub>3</sub>S                      147 R = C<sub>4</sub>H<sub>3</sub>O  
148 R = C<sub>4</sub>H<sub>3</sub>S

Aldehyde	WT-TK	D469E	D469T	D469K	F434A
	Yield %	Yield %	Yield %	Yield %	Yield %
	( <i>ee</i> )	( <i>ee</i> )	( <i>ee</i> )	( <i>ee</i> )	( <i>ee</i> )
 <b>145</b>	0	5 ( <b>147</b> ) (ND)	3 ( <b>147</b> ) (ND)	3 ( <b>147</b> ) (ND)	1 ( <b>147</b> ) (ND)
 <b>146</b>	0	2 ( <b>148</b> ) (ND)	3 ( <b>148</b> ) (ND)	2 ( <b>148</b> ) (ND)	1 ( <b>148</b> ) (ND)

\*Biotransformations of these substrates were carried out by James Galman. Reaction conditions: 1.0 mmol aldehyde, 1.0 mmol LiHPA, 2 mL TK cell-free lysate, 20 mL total volume, 24 hour reaction time.

As observed for benzaldehyde, WT-TK showed no activity with these substrates. F434A and the D469 series of mutants gave low yields (<5%) of the desired ketodiol products **147** and **148** with small amounts (<2%) of rearranged product observed. No double addition product was observed for either substrate. Efforts to determine the stereoselectivities of these transformations failed, however, as rearrangement to the corresponding rearranged ketodiols occurred upon attempts to derivatise the ketodiol



phenylpropanal, stereoselectively forming the (3*S*)-isomer in both cases, as previously observed for other aliphatic aldehydes.<sup>[26]</sup> 2-Hydroxy-2-phenylacetaldehyde has previously been used as a substrate for *E.coli* WT-TK, and was also observed to form the (3*S*,4*R*)-isomer selectively.<sup>[87]</sup>

To further probe possible hydrogen bonding interactions in the active site, initial studies at the beginning of this PhD were carried out with 3-hydroxybenzaldehyde (**93**) (Table 3.4, R = 3-OHC<sub>6</sub>H<sub>4</sub>), 4-hydroxybenzaldehyde (**118**) (Table 3.4, R = 4-OHC<sub>6</sub>H<sub>4</sub>) and 4-chlorobenzaldehyde (**99**) (Table 3.4, R = 4-ClC<sub>6</sub>H<sub>4</sub>) and the TK single mutants (Table 3.4). These substrates were also chosen to establish whether the yields of the TK biotransformations could be affected by the addition of electron withdrawing or donating groups onto the aromatic ring, hence activating or deactivating the aldehyde to nucleophilic attack by the ThDP-enamine intermediate in the enzyme active site.

**Table 3.4 Biotransformations of 3-hydroxybenzaldehyde (99), 4-hydroxybenzaldehyde (118) and 4-chlorobenzaldehyde (99)\***

Aldehyde	WT-TK Yield % (ee)	D469E Yield % (ee)	D469T Yield % (ee)	D469K Yield % (ee)	F434A Yield % (ee)
 <b>93</b>	0	0	4 ( <b>103</b> ) (0%)	0	6 ( <b>103</b> ) (53%, 3 <i>R</i> )
 <b>118</b>	0	0	0	0	0
 <b>99</b>	0	0	0	0	0

\*Reaction conditions: 1.0 mmol aldehyde, 1.0 mmol LiHPA, 2 mL TK cell-free lysate, 20 mL total volume, 48 hour reaction time.

Again, none of these substrates were accepted by WT-TK. Disappointingly, 4-hydroxybenzaldehyde (**118**) and 4-chlorobenzaldehyde (**99**) were not accepted by any of the mutants tested. 3-Hydroxybenzaldehyde (**93**), however, was accepted by two of the single mutants forming ketodiol **103**. D469T gave a 4% isolated yield of the ketodiol product (**103**), which was formed as a racemate. F434A gave a similar isolated yield of **103** of 6%, but some stereoselectivity was observed for this mutant, forming the ketodiol product in 53% *ee*. It is interesting that D469T and F434A accept 3-hydroxybenzaldehyde (**93**), but not 4-hydroxybenzaldehyde (**118**). This suggests that either the active site is not large enough to accommodate *para*-substituted benzaldehydes, or there is a hydrogen bonding interaction which orients 3-hydroxybenzaldehyde into an active conformation, allowing it to react with the ThDP enamine in the active site, forming the ketodiol product.

### **3.3 Chiral analytical methods for determining the stereoselectivities of aromatic ketodials**

Two complementary methods were used to determine the stereoselectivities and absolute stereochemistries of the aromatic ketodiol products formed by single mutant TKs. Firstly, a chiral HPLC method was developed. Unfortunately, despite containing a chromophore the aromatic ketodials themselves could not be analysed directly using chiral HPLC, as the two enantiomers could not be separated. Previous work with ketodials had relied upon making either acetate or benzoate ester derivatives,<sup>[26, 75]</sup> so these methods were investigated. It quickly became clear that the derivatisation procedure would have to be altered due to the increased acidity of the  $\alpha$ -proton adjacent to the aromatic ring, which was easily removed under existing protocols, giving rise to rearranged (Scheme 3.4) and racemised products. By using a hindered 2,4,6-collidine base it was possible to derivatise the aromatic ketodials as either the mono- or di-benzoate esters without racemisation of the ketodiol product. Firstly, the racemic products were prepared by the NMM-catalysed biomimetic reaction (as in Chapter 2) and di-benzoylated, then used to develop an appropriate HPLC method (Figure 3.1, blue). Stereoselective products were then prepared using the TK mutants, purified, derivatised and analysed by chiral HPLC (Figure 3.1,



black). The traces of the racemic derivatives could then be compared to the stereoselective derivatives to determine the *ee* of the TK reaction (Figure 3.1).

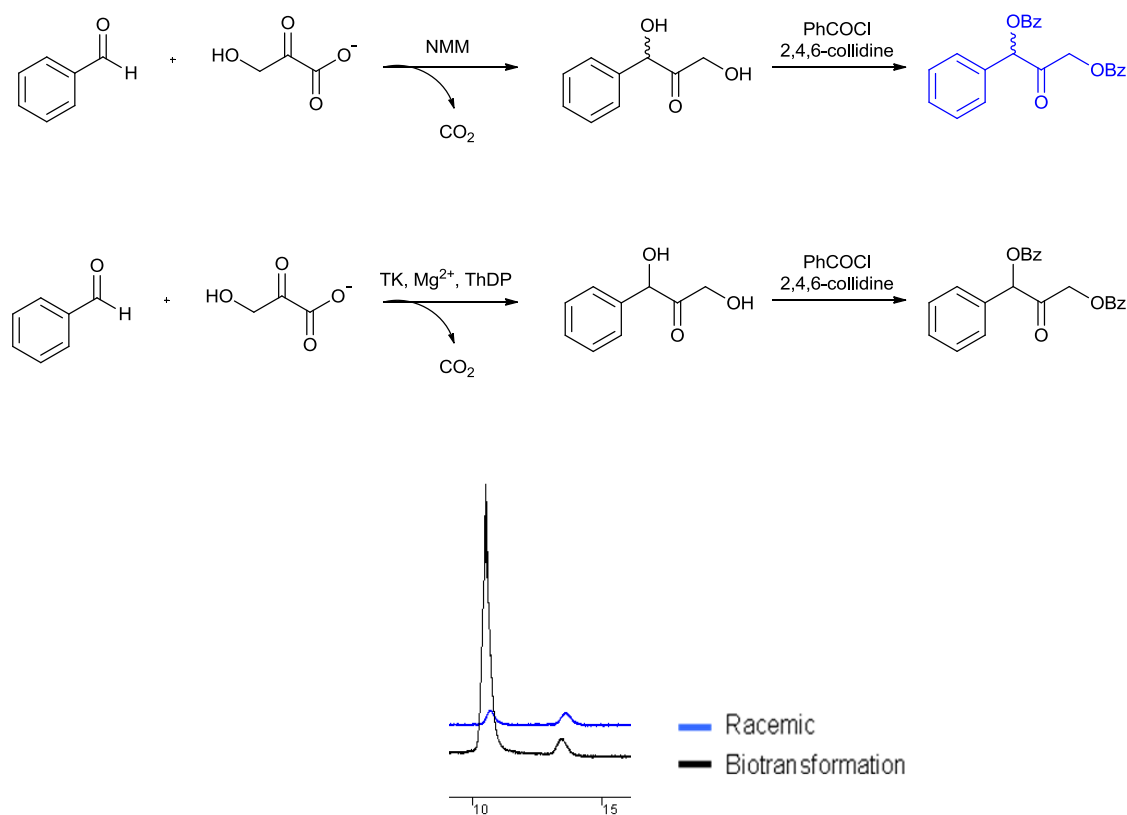


**Figure 3.1 Overlaid chiral HPLC traces of dibenzoylated (68) from the biomimetic reaction (blue) and F434A (black)**

The absolute stereochemistry was then tentatively assigned by preparing Mosher's ester derivatives of the biotransformation products as previously described.<sup>[26, 83]</sup> The observed difference in chemical shifts between the diastereotopic protons was used to assign the absolute stereochemistry, with the *syn*-isomer demonstrating a large chemical shift difference and the *anti*-isomer demonstrating a small chemical shift difference (Figure 3.2). The integrations for each isomer were then used to determine the major isomer, confirm the approximate *ee* and indicate the absolute configuration (Figure 3.2).

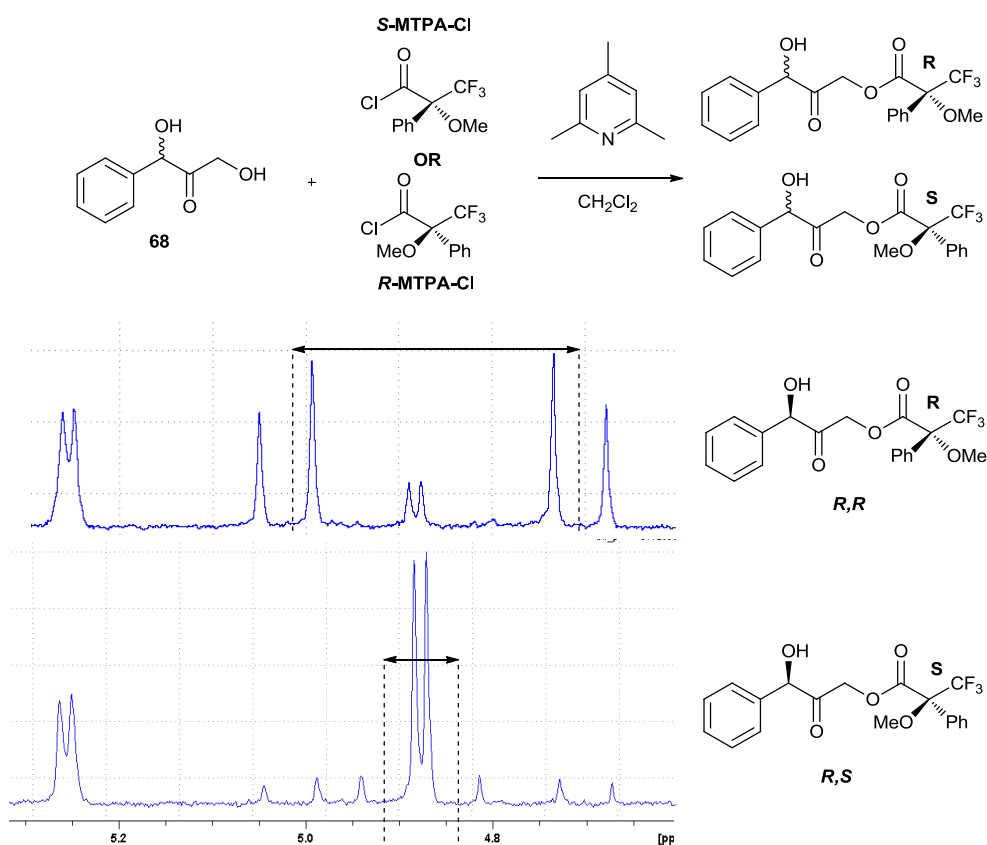


Figure 3.2  $^1\text{H}$  NMR Mosher's ester analysis for identification of the unknown absolute stereocentre in (68)\*

For example, if the ketodiol was derivatised with the (*S*)-Mosher's acid chloride, the new centre formed would be the (*R*)-isomer, and by looking at the chemical shift difference between the diastereotopic protons the absolute configuration of the unknown centre could then be elucidated. This method also used the hindered 2,4,6-collidine base to avoid rearrangement and racemisation of the ketodiol. Mosher's ester analysis had previously been validated using aliphatic substrates of known stereochemistry and used to determine the absolute stereochemistry of products from aliphatic aldehydes. The Mosher's method was further validated for ketodiols **150** and **152** from aliphatic aldehydes which contained aromatic groups (phenylacetaldehyde (**149**) and 2-hydroxy-2-phenylacetaldehyde (**151**))<sup>†</sup> where the (*S*)-isomer was shown to be formed preferentially, in agreement with previous reports.<sup>[87]</sup> However no standards with known stereocentres were available for

\* Data shown for (*S*)-Mosher's acid chloride was obtained by James Galman

† Chiral analysis of these compounds was carried out by James Galman

testing the method when applied to aromatic ketodiols.<sup>[83]</sup> Since these compounds were novel the absolute stereochemistries were only tentatively assigned.<sup>[87]</sup> For the ketodiols **68** and **103** from benzaldehyde (**8**) and 3-hydroxybenzaldehyde (**99**) Mosher's ester analysis suggested that the (3*R*)-centre was formed. If correct, this would mean that the aromatic TK products were formed with the opposite stereochemistry to all of the aliphatic series<sup>[26]</sup> possibly indicating that the aromatic aldehydes bound in a different fashion to the aliphatic aldehydes, resulting in formation of the opposite stereocentre. However, subsequent work has suggested that the Mosher's method may not be applicable to aromatic ketodiols and will be discussed further in Chapter 5.

### 3.4 Docking of benzaldehyde into D469T

In an attempt to gain more understanding into the biotransformation of benzaldehyde (**8**) by D469T TK, computational docking was performed using Autodock 4 modelling software. Since a crystal structure for D469T has not been solved, the crystal structure of WT TK from *E. coli* was mutated *in silico* and the structure minimised using the CHARMM force field to give a D469T structure which could be used for docking.\* To gain a more complete picture of the interactions between benzaldehyde and the TK active site, the ThDP-enamine intermediate was included in the structure of the protein used for docking. To do this, a structure of the ThDP-enamine was drawn in Chemdraw 10.0, subjected to an MM2 energy minimisation in Chem3D 10.0 and then docked into the D469T structure which had been generated *in silico*. The ThDP conformation obtained within the active-site of D469T (Figure 3.3, orange) very closely matched that found in the crystal structure of WT-TK co-crystallised with the ThDP-enamine intermediate (1QGD) (Figure 3.3, green), validating this modelling approach.

---

\* *In silico* mutation was carried out by Panwajee Payongsri

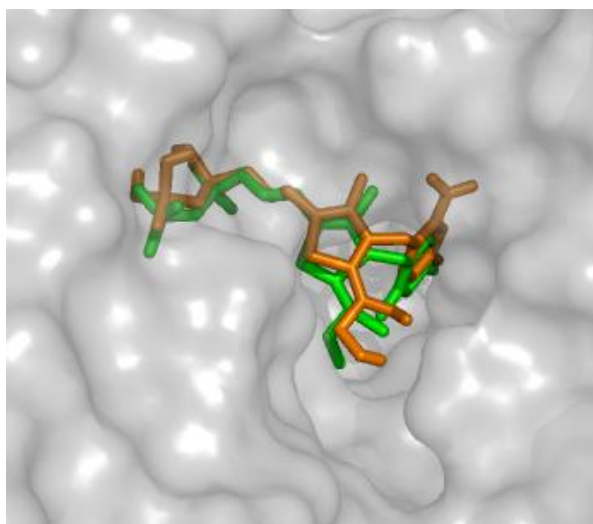


**Figure 3.3. Active site of D469T TK with the ThDP enamine from the crystal structure of WT-TK (1QGD) (green) and the ThDP-enamine configuration obtained from docking into D469T (orange) overlaid.**

The conformation obtained for the ThDP-enamine intermediate was then added to the D469T structure and this complex used as the protein input file for docking with benzaldehyde. This allowed interactions between benzaldehyde and the ThDP-enamine to be considered by the docking program. Benzaldehyde was prepared for the docking run in a similar fashion to the ThDP-intermediate; it was drawn in Chemdraw 10.0, the energy was then minimised and this was used as the ligand input file for Autodock 4. Three main clusters were obtained from the docking (Figure 3.4).

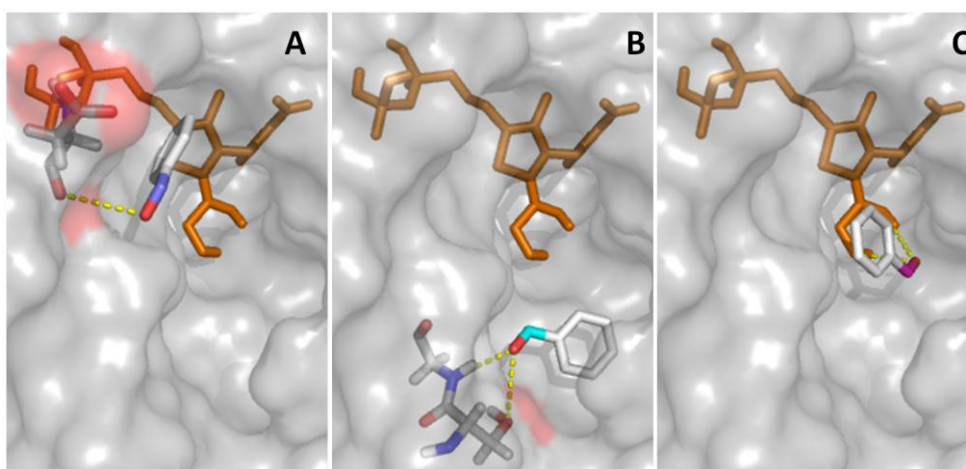


**Figure 3.4 Three binding clusters obtained from docking benzaldehyde into D469T TK with the ThDP-enamine intermediate (orange)**

The first cluster (Figure 3.4, A) was the lowest in energy, containing 21 conformations. Each of these conformations was bound as shown, with a hydrogen bonding interaction between the carbonyl oxygen of benzaldehyde and the D259 residue. This interaction held the benzaldehyde molecule at the entrance to the active site, orienting the aldehyde away from the ThDP-enamine intermediate, at a distance of 12.2 Å, too far away for nucleophilic attack by the ThDP-enamine to occur. This conformation was therefore considered to be unproductive. The second cluster obtained (Figure 3.4, B) was the most highly populated cluster, and again showed the benzaldehyde molecule being held at the entrance to the active site, this time by hydrogen bonding with S24 and G25. This kept the aldehyde away from the ThDP-enamine intermediate at a distance of 7.8 Å, which was closer than in the previous cluster, but still too far away to be considered productive. The final cluster (Figure 3.4, C) was the least populated of the three, and the highest in energy. The conformations in this cluster demonstrated hydrogen bonding not with the enzyme itself, but with the ThDP-enamine intermediate. Here, the carbonyl oxygen hydrogen bonded to the two hydroxyl groups of the ThDP-enamine, at a distance of 4.6 Å making it the only potentially productive conformation.

While these docking results only gave limited insights into the binding of benzaldehyde in the TK active site, they still provided some useful information. It was clear that the ThDP-enamine should be included in the enzyme structure for all future docking experiments, to allow interactions between the substrates and the active ThDP-enamine intermediate to be considered. They showed that benzaldehyde exhibits low affinity for the active-site of TK and does not display any specific binding to the active site, but instead seems to get ‘trapped’ by acidic residues on the entrance to the active site, or indeed by interactions with the protein backbone. This could account for the low yields observed for the single mutant TKs tested. The higher conversions previously observed for aliphatic aldehydes with single mutant TKs had been rationalised by hydrogen bonding interactions between the aldehyde oxygen atom and two histidine residues (H26 and H261) which held the aldehydes above the ThDP-enamine intermediate, allowing nucleophilic attack to occur.<sup>[26]</sup> Such interactions were not observed in the docking with benzaldehyde. This could be due to the increased steric bulk of the aromatic ring, or the reduced conformational flexibility of the aldehyde. Hence, to increase the activity of TK with aromatic aldehydes, such as benzaldehyde, a new binding mode would need to be

introduced, either by adding functionality to the aromatic ring to increase affinity of the substrate to the active site of TK, or by modifying the active site itself. For example, by introducing  $\pi$ -stacking interactions, or mutating residues on the entrance to the active site, such as D259, to prevent ‘trapping’ of the aldehyde before entering the active-site.

### **3.5 Summary of chapter 3**

In conclusion, the transformation of aromatic aldehydes, and aliphatic aldehydes containing aromatic groups, by single mutant TKs has been studied. Mutants were identified using a colorimetric assay, the utility of which was shown to be limited due its inability to distinguish between the desired ketodiol product and the double addition side-product. Chiral analysis methods were developed and showed that the single mutant TKs were capable of forming ketodiol with high degrees of stereoselectivity.<sup>[85]</sup> Computational docking studies were performed which suggested that the low yields observed for the transformation of benzaldehyde could be due to low affinity for the TK active-site, resulting in extensive non-specific binding of the substrate to residues outside the active-site.

## **4 Aliphatic aldehydes with single and combination mutant TKs**

Aliphatic aldehydes had previously been studied with single mutant TKs and a library of D469 mutations were identified, *via* a colorimetric assay, which accepted a range of cyclic and linear aldehydes.<sup>[26]</sup> The same colorimetric assay was then used to identify mutants with activity towards aromatic aldehydes (Chapter 3).<sup>[85]</sup> The yields obtained for the transformations of aromatic aldehydes by these mutants were around 10-fold lower than the yields obtained for aliphatic aldehydes.<sup>[26, 85]</sup> This was due in part to competing side reactions, but computational docking also suggested that low substrate affinity could be a factor (Chapter 3). Therefore, to successfully transform aromatic aldehydes a new library of mutants was needed. Unfortunately, the previously used colorimetric assay had already been shown to be misleading in screening for activity against aromatic aldehydes as it could not distinguish between the desired ketodiol (**68**) and the “double addition” side-product (**144**) (Figure 4.1).<sup>[85]</sup>

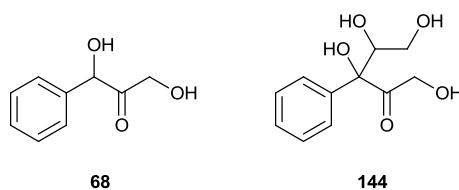


**Figure 4.1 Structures of desired aromatic ketodiol product (68) and undesired double addition product (144)**

Therefore, in an attempt to create a new generation of TK mutants with improved activities toward both aliphatic and aromatic aldehydes, combination mutants were created by selecting and combining existing active single mutations in an effort to create mutants with further improved activities, stereoselectivities and stabilities.<sup>[88]</sup>

#### **4.1 Creation of combination mutant libraries<sup>[88]\*</sup>**

The first library of double mutants was created by recombining single mutations which had shown increased activity towards propanal (**24**) compared to WT. A29E,

---

\* All of the mutants in this section were created and studied by John Strafford, Panwajee Payongsri, Edward Hibbert, Phattaraporn Morris and Sukhjeet Bath from the UCL Department of Biochemical Engineering.



H461S and R520V had all previously been shown to improve activity towards glycolaldehyde (**26**) and propanal (**24**),<sup>[46, 47]</sup> and so were recombined, by colleagues in the Department of Biochemical Engineering, as combinations of double mutants. D469T and D469A had also been shown to improve activity with propanal and so were recombined with D259A, D259G, D259S and D259Y which had been shown to improve activities with both propanal and glycolaldehyde.<sup>[46, 47]</sup> The double mutants were expressed and the soluble TK expression levels and activities with propanal were determined from their clarified lysates after sonication (Figure 4.2, white squares),<sup>[88]</sup> on a 225  $\mu\text{L}$  scale using a previously published HPLC method to detect product formation.<sup>[47]</sup>

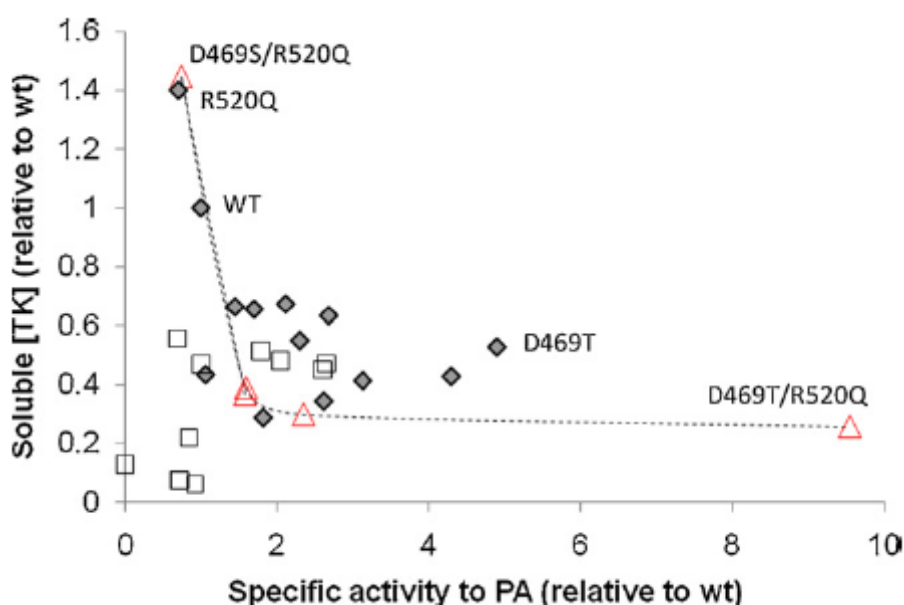


**Figure 4.2** Observed trade-off between specific activity and soluble TK concentration for a range of mutants with propanal. Diamonds-previously identified single mutants, squares-combination mutants made from active single mutants, triangles-combination mutants created after guidance by statistical coupling analysis.<sup>[88]</sup> (Used with permission from Elsevier).

All of the double mutants (Figure 4.2, white squares) showed marked decreases in specific activity and expression levels compared to the single mutants (Figure 4.2, black diamonds).<sup>[88]</sup> Indeed a dramatic loss of either soluble protein expression, specific activity, or both was observed for these double mutants. This indicated that simply combining active single mutations would not be an effective strategy to create active combination mutants, since all of the mutants created in this fashion gave enzymes with severely impaired function, due to decreased protein stability.<sup>[88]</sup>

TK protein stability and function is maintained through highly conserved residues in the active-site which have evolved over time to create synergistic networks responsible for maintaining correct folding, cofactor binding and efficient catalysis.<sup>[89]</sup> Introducing random mutations into such regions can disrupt these synergistic networks and give enzymes with severely impaired stability and function, as was observed (Figure 4.2, white squares).<sup>[88]</sup> To avoid disruption of these networks, statistical coupling analysis (SCA)<sup>\*</sup> was applied to 382 sequences of 17 different ThDP dependent enzymes types to identify co-evolved sites that may have been disrupted in the combination mutants for which severely impaired protein stability and function had been observed.<sup>[88]</sup>

The SCA method identified a cluster of nine residues (R520, G467, D469, G470, T472, P486, P493, E498 and D495) which formed a co-evolved network within the active-site (Figure 4.3). Within this cluster there were two major spatial groups, D495, E498 and P493, that were found to cap the N-terminus of an  $\alpha$ -helix which was 9 Å from R520 in the second group which packed against an active-site loop containing G467, D469, G470 and T472. The remaining residue, P486, was not observed to directly interact with either of these two groups, but formed part of a hairpin turn which brought the two groups in close proximity to each other.<sup>[88]</sup>

---

<sup>\*</sup> SCA was carried out by John Trafford

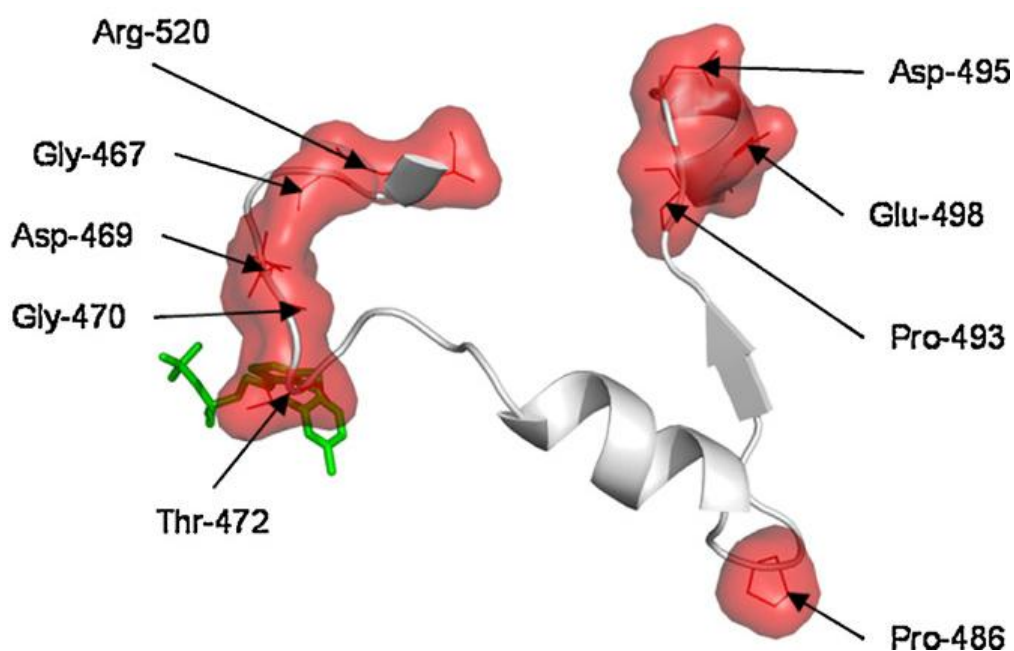


**Figure 4.3** The nine residues forming a co-evolved network within the active-site of TK.<sup>[88]</sup> (Used with permission from Elsevier).

Further analysis of the protein structure gave insights into why these residues may have co-evolved with each other. D469, for example, was observed to form an electrostatic interaction with R520, which in turn formed a salt bridge with E468 (not shown) which was adjacent to D469 and G467.

The inactive double mutants which had been created contained at least one residue found in this co-evolved cluster. Also, in every case the networked residues were mutated to amino acids not naturally found at that position, based on the 382 sequences analysed. With these results in mind, it seemed important that in order to create active double mutants, one position could be maintained as any beneficial single mutation (whether naturally found at that position or not), for example D469T, while the other residue could only be mutated to an alternative natural variation, based on the 382 ThDP-dependent enzyme sequences studied. To test this theory, and to probe potential synergies between groups of residues, four double mutant libraries (G467X/D495X, D469X/R520X, D469X/E498X, E498X/R520X) and one triple mutant library (D469X/E498X/R520X) were created and screened against propanal (Table 4.1, mutants with >70% of WT activity shown in bold), using the same HPLC assay as for the previous set of double mutants.<sup>[47, 88]</sup>

**Table 4.1 Library of combination mutants made to residues with the co-evolved network in TK. Variants with >70% activity of WT shown in bold.**

<b>Residues mutated</b>	<b>Library of variants</b>	<b>Best variants (activity &gt;70% WT)</b>
G467/D495	DVSA/NQEL	V/L, D/E
D469/R520	LTSA/GKQA	<b>T/Q, A/G, S/Q, S/G</b>
D469/E498	LTSA/DAVI	None
E498/R520	DAVI/GKQA	V/Q, D/K

Only the D469/R520 library gave variants with activities greater than WT. The initial set of double mutants, created by combination of active single mutants without considering co-evolution of residues, had demonstrated a severe loss of activity due to protein instability (Figure 4.2, white squares). This new library of double mutants, however, showed no such trend (Figure 4.2, red triangles). The total amount of soluble protein for the double mutants was shown to trade-off in a similar fashion to the initial active single mutants, indicating that these combination mutants no longer lost both stability and function. Therefore, despite all of the mutations causing protein instability to a certain extent, the positive synergy between the networked residues was enough to ensure that severe disruption of stability and function did not occur.

R520Q was shown to increase the expression level of TK when combined with D469S, so other D469 mutations were then recombined with R520Q to see whether more active combination mutants could be created. D469T/R520Q had been identified as an active mutant in the previous screen (Table 4.1), and so was investigated further. D469Y had previously been shown to reverse the stereochemistry of the biotransformation of propanal (**24**),<sup>[48]</sup> so this double mutant was also investigated (Figure 4.4). D469Y/R520Q demonstrated no synergy, but D469T/R520Q showed positive synergy, with the experimentally determined specific activity for propanal exceeding that expected from the additive accumulation of improvements for the single mutants (Figure 4.4).

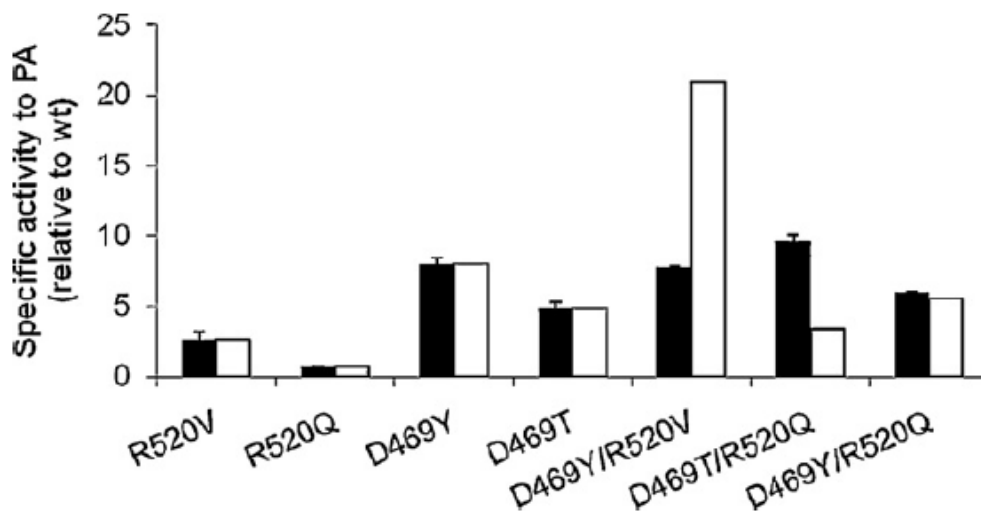


**Figure 4.4** Effect of recombining R520V and R520Q with D469 mutants. Experimental specific activities shown in black, expected specific activities from additive effects of single mutants shown in white.<sup>[88]</sup> (Used with permission from Elsevier).

Indeed, D469T/R520Q gave the highest specific activity that had been obtained for any TK mutant to date under the same conditions.<sup>[88]</sup>

## **4.2 Biotransformations of aliphatic aldehydes with single and combination mutant TKs**

All of the combination mutants which had been created in the SCA study had only been investigated for their use as biocatalysts in terms of specific activities, which had been studied using HPLC analysis of 225  $\mu$ L scale reactions by colleagues from the Department of Biochemical Engineering.<sup>[88]</sup> No isolated yields or stereoselectivity data from scaled-up reactions had been established. Hence, a range of these combination mutants and their representative single mutants were used in scaled-up (20 mL) biotransformations with a range of aliphatic aldehydes, firstly with propanal (**24**) and LiHPA (Li-**23**) to form ketodiol **25** (Table 4.2). Products were isolated, purified and stereoselectivities determined using the previously described chiral HPLC analysis of mono-benzoate ester derivatives.<sup>[26]</sup>

**Table 4.2 Isolated yield and stereoselectivity data obtained for the biotransformation of propanal by single, double and triple mutant TKs\***

Reaction scheme: Propanal (24) + LiHPA (23)  $\xrightarrow{\text{TK, ThDP, Mg}^{2+}}$  Ketodiol (25) + CO<sub>2</sub>

Entry	Mutant	Yield	<i>ee</i>
1	WT <sup>[26]</sup>	36%	58% (3 <i>S</i> )
2	F434A	18%	63% (3 <i>S</i> )
3	D469E	70%	95% (3 <i>S</i> )
4	D469T <sup>[26]</sup>	68%	64% (3 <i>S</i> )
5	D469Y	11%	68% (3 <i>R</i> )
6	H461S	13%	64% (3 <i>S</i> )
7	A29E	7%	50% (3 <i>S</i> )
8	H26Y <sup>[26]</sup>	63%	88% (3 <i>R</i> )
9	A29E/H461S	3%	33% (3 <i>S</i> )
10	A29E/R520V	4%	40% (3 <i>S</i> )
11	A29E/H461S/R520V	4%	21% (3 <i>S</i> )
12	H26Y/D469Y	4%	38% (3 <i>S</i> )
13	D469Y/R520V	51%	85% (3 <i>R</i> )
14	F434A/R520Q	43%	63% (3 <i>S</i> )
15	D469Y/R520Q	42%	65% (3 <i>R</i> )
16	D469T/R520Q	32%	68% (3 <i>S</i> )

\*All mutants in this section were created by Panwajee Payongsri. WT and single mutant data previously recorded is indicated. Reaction conditions: 50 mM aldehyde, 50 mM LiHPA, 2 mL TK cell-free lysate, 20 mL reaction volume, 24 hour reaction time.

F434A (entry 2) was a mutant which had been previously engineered to be active towards aromatics,<sup>[85]</sup> so the lower yield of ketodiol (**25**) formed compared to the best performing D469E and D469T mutants was not surprising. Interestingly though, the 18% yield of **25** produced by F434A was still higher than the yields observed for this mutant with aromatic aldehydes,<sup>[85]</sup> indicating the general preference of TK for aliphatic aldehydes over aromatics, as reflected by the *in vivo* WT substrates. D469E (entry 3) was the best performing single mutant with propanal, giving a 70% yield of **25** and comparable stereoselectivity to the 90% *ee* previously reported for this mutant.<sup>[26]</sup> D469Y (entry 5) had been previously identified as a mutation which reversed the stereoselectivity of ketodiol **25**.<sup>[48]</sup> The biotransformation of propanal (**24**) by D469Y had not been scaled-up previously however, so an 11% isolated yield was slightly disappointing, however a reversal of stereochemistry was once again observed, with 68% *ee* for the 3*R*-isomer, compared to the 53% *ee* previously reported in the small-scale reaction for this mutant.<sup>[48]</sup> This increase in *ee* could have been due to the pH of the reaction being carefully controlled throughout the reaction,

preventing racemisation of the ketodiol product (**25**). H461S and A29E were mutations which had previously been identified as increasing the specific activity of TK toward propanal on a 250  $\mu$ L scale,<sup>[47]</sup> but the scaled-up reactions had not been investigated. An isolated yield of 13% of **25** was observed for H461S (entry 6), with an *ee* of 64% for 3*S*-(**25**). A29E (entry 7) gave a lower isolated yield of **25** of 7% with an *ee* of 50% also for the 3*S*-product. Combining these two mutations to make A29E/H461S (entry 9) gave an enzyme with severely reduced activity. Only a 3% isolated yield of **25** was obtained, and an *ee* lower than both of the individual single mutations of 33% (3*S*) was observed. This is consistent with the impaired stability and function demonstrated by the soluble enzyme expression level and specific activity data obtained for A29E/H461S (Section 4.1, Figure 4.2).<sup>[88]</sup> A mutant, R520V, had previously been shown to increase the activity of TK towards propanal,<sup>[47]</sup> but combination of this mutant with A29E, in A29E/R520V (entry 10), did not improve the yields or stereoselectivities with propanal, with only a 4% yield and 40% *ee* of 3*S*-**25** observed. Addition of R520V to A29E/H461S did not restore the function of this mutant either, with only a 4% yield of **25** obtained in 21% *ee* (3*S*) produced by A29E/H461S/R520V (entry 11). H26Y had previously been shown to be an effective reverser of stereochemistry in the formation of **25**,<sup>[26]</sup> and so was combined with D469Y to establish whether a more active double mutant could be made which further reversed the stereochemistry of **25**. Interestingly though, this double mutant, H26Y/D469Y (entry 12), not only gave a lower isolated yield than both of the individual single mutants, but the observed stereochemistry was also opposite to what was expected, with 3*S*-(**25**) formed in 4% yield with 38% *ee*. This suggested that the structure of the enzyme must have been severely altered by the introduction of these two mutations, affecting not only the activity of the enzyme, giving greatly reduced yields, but changing the shape of the active-site such that the opposite enantiomer was formed compared to the individual single mutants.

The combination mutants; A29E/H461S (entry 9), A29E/R520V (entry 10), A29E/H461S/R520V (entry 11) and H26Y/D469Y (entry 12) were all examples of combining two, or more, active single mutations in an attempt to create a more active double mutant, but obtaining an enzyme with drastically reduced function (Section 4.1). This was demonstrated by the lower yields and *ees* observed for the combination mutants when compared to their parent single mutants. These results supported the hypothesis that blindly combining active single mutants was not an

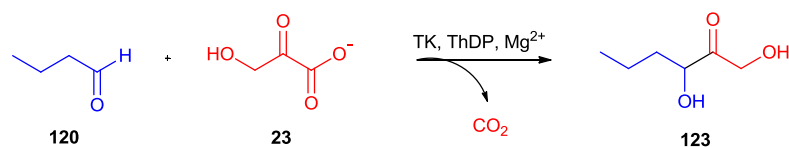
effective strategy to develop new biocatalysts due to the disruption of the co-evolved network found in the TK active-site (Section 4.1).<sup>[88]</sup>

Four mutants were tested which had been created to prevent disruption of the co-evolved network of residues in the TK active site. D469Y/R520V was a mutant which had been shown to exhibit negative synergy, with a specific activity lower than expected from the accumulative effects of the two single mutants.<sup>[88]</sup> However, the scaled-up biotransformation of propanal (**24**) by D469Y/R520V (entry 13) gave an almost 5-fold increase in isolated yield over D469Y and an excellent *ee* of 85% for the 3*R*-isomer. F434A/R520Q (entry 14) also gave an increased yield (43%) of ketodiol **25** over the parent mutant F434A, whilst not affecting the stereochemical outcome as both mutants formed the 3*S*-isomer in 63% *ee*. The increase in isolated yield for F434A/R520Q can be explained by R520Q stabilising the double mutant and increasing the expression level of TK, as previously observed for R520Q in combination with other mutations.<sup>[88]</sup> The same can be said for D469Y/R520Q (entry 15), where the yield of **25** was increased to 42%, nearly a 4-fold increase over the parent D469Y enzyme. However, D469T/R520Q gave a lower yield of ketodiol **25** than the individual single mutant, D469T, despite D469T/R520Q exhibiting the highest specific activity toward propanal reported to date. The low yield could be explained by a decreased expression of soluble protein compared with D469T.<sup>[88]</sup>

With several combination mutants identified which improved the biotransformation of propanal compared to WT,<sup>[88]</sup> longer chain aliphatic aldehydes were investigated with the best combination mutants to establish the substrate scope of these new TK mutants. Firstly, the TK reaction of butanal (**120**) with LiHPA (Li-**23**) was investigated with D469Y (which had not been previously studied with this substrate), and the D469Y double mutants (Table 4.3). Stereoselectivities of ketodiol **123** were once again assessed by chiral HPLC of mono-benzoate ester derivatives, using previously described methods.<sup>[26]</sup>



**Table 4.3 Isolated yield and stereoselectivity data for single and double mutant TKs with butanal\***



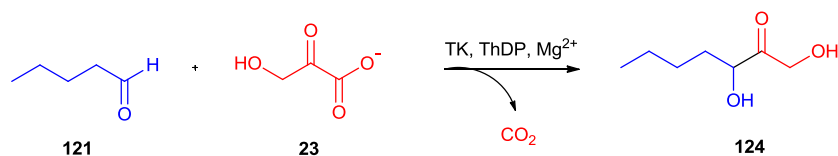
Mutant	Yield	<i>ee</i>
<b>D469Y</b>	9%	45% (3 <i>S</i> )
<b>D469Y R520V</b>	8%	ND
<b>D469Y R520Q</b>	10%	17% (3 <i>R</i> )

\*Reaction conditions: 50 mM aldehyde, 50 mM LiHPA, 2 mL TK cell-free lysate, 20 mL reaction volume, 24 hour reaction time.

The D469Y mutant gave only 9% isolated yield of ketodiol **123**, formed with an *ee* of 45% in favour of the 3*S*-isomer. This was a similar yield as observed for the biotransformation of propanal (**24**) by D469Y, but with a lower *ee* in favour of the opposite stereoisomer. The best performing mutant with butanal was previously found to be D469E where a 44% yield and an *ee* of 98% was observed,<sup>[26]</sup> D469Y compares unfavourably to this. Indeed, the combination mutants performed just as unfavourably, with 8% and 10% isolated yields observed for D469Y/R520V and D469Y/R520Q respectively.

It seemed as if these combination mutants were less tolerant to longer chain aliphatic aldehydes, giving lower yields and stereoselectivities than for propanal (**24**). To further investigate this, pentanal (**121**) was then used as a substrate (Table 4.4) in the TK reaction with LiHPA (Li-**23**) to assess yields and stereoselectivities of resulting ketodiol **124**.

**Table 4.4 Isolated yield and stereoselectivity data for single and double mutant TKs with pentanal\***



Mutant	Yield	<i>ee</i>
<b>D469Y</b>	8%	50% (3 <i>S</i> )
<b>D469Y R520V</b>	10%	ND
<b>D469Y R520Q</b>	10%	44% (3 <i>S</i> )

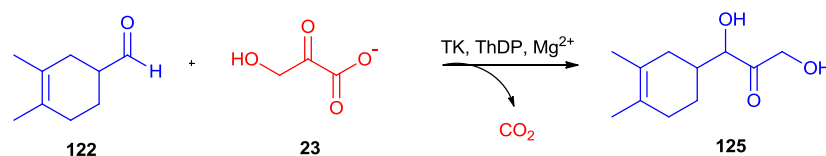
\*Reaction conditions: 50 mM aldehyde, 50 mM LiHPA, 2 mL TK cell-free lysate, 20 mL reaction volume, 24 hour reaction time.

A similar trend was observed for the transformation of pentanal (**121**) by these double mutants as for the transformation of butanal. A negligible increase in yield of **124** was observed for D469Y/R520V and D469Y/R520Q, both giving 10% isolated yields of **124** compared to D469Y (8% yield), but the *ee* was not improved. Interestingly, while D469Y was shown to reverse the stereochemistry of the propanal transformation forming ketodiol (**25**) in 68% *ee* (3*R*), the transformation of the longer chain aldehydes, butanal (**120**) and pentanal (**121**), by D469Y gave the 3*S*-isomer in both cases. This suggested that longer chain aliphatics were oriented differently within the active site, binding in a different conformation to propanal (**24**) and favouring formation of the opposite stereoisomer. Indeed, previous docking studies have suggested the presence of an alternative binding mode for propanal compared with longer chain aliphatics.<sup>[26]</sup>

The fact that the combination mutants did not perform as well with the longer chain aliphatic aldehydes, butanal (**120**) and pentanal (**121**), compared to propanal (**24**) is perhaps not surprising, given that the screening of the combination mutant libraries was performed using propanal, and so only mutants that performed well with this substrate were selected. Also if the longer chain aliphatic aldehydes are indeed oriented differently within the TK active site, as previously suggested,<sup>[26]</sup> then it is not surprising that mutants active towards propanal would not necessarily be active with longer chain aliphatic aldehydes.

To further investigate the substrate scope of these combination mutants and to ascertain whether they would possibly be able to accommodate larger cyclic or aromatic substrates, a bulky cyclic aliphatic, 3,4-dimethylcyclohex-3-enecarbaldehyde (**122**), was used as a substrate in the TK reaction with LiHPA (Li-**23**) to form **125** (Table 4.5). This substrate had been previously investigated in the biomimetic reaction, and was prepared in the same fashion (Chapter 2).

**Table 4.5 Isolated yield data for single, double and triple mutants with 3,4-dimethylcyclohex-3-enecarbaldehyde\***



Mutant	Yield
<b>F434A</b>	11%
<b>D469T</b>	10% (98% 1S,1'R) <sup>†</sup>
<b>D469Y</b>	0%
<b>H461S</b>	Trace
<b>A29E</b>	0%
<b>H26Y</b>	0%
<b>A29E H461S</b>	0%
<b>A29E R520V</b>	0%
<b>A29E H461S R520V</b>	0%
<b>H26Y D469Y</b>	0%
<b>D469Y R520V</b>	0%
<b>F434A R520Q</b>	Trace
<b>D469Y R520Q</b>	Trace

\*Reaction conditions: 50 mM aldehyde, 50 mM LiHPA, 2 mL TK cell-free lysate, 20 mL reaction volume, 24 hour reaction time.

<sup>†</sup>Transformation of this substrate with D469T was performed previously by James Galman

None of the combination mutant TKs formed isolable quantities of product with this substrate (**122**), which is not necessarily surprising given the complexity of the substrate compared to propanal (**24**), which the mutants had been screened against. Interestingly though, two of the single mutants, F434A and D469T, did accept the substrate with 11% and 10% isolated yields of **125** obtained, respectively. Both of these mutants had previously been shown to accept aromatic substrates,<sup>[85]</sup> so their acceptance of the sterically-demanding 3,4-dimethylcyclohex-3-enecarbaldehyde (**122**) was pleasing. Given that R520Q had previously been shown to improve the specific activity of D469T/R520Q towards propanal (**24**) it is interesting to note that in combination with F434A in F434A/R520Q it did not increase the activity of this mutant towards 3,4-dimethylcyclohex-3-enecarbaldehyde (**122**) with only trace amounts of product observed (**125**).

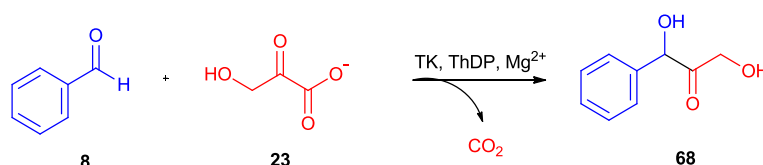
### **4.3 Summary of chapter 4**

In conclusion, the transformation of aliphatic aldehydes by combination mutant TKs has been studied in detail. TK mutants made through the combination of active-single mutant TKs showed dramatically impaired structure and function. Further investigation showed that only certain combinations of mutations could be made to avoid the disruption of a co-evolved network of residues within the TK active-site. Combination mutants made on this basis were shown to maintain structure and function. Isolated yield and stereoselectivity data supported these studies, with drastically reduced yields and stereoselectivities observed for combination mutants made from combinations of active single mutants. Combination mutants made considering the co-evolution of residues in the active-site showed greatly increased yields and stereoselectivities over the previous set of combination mutants, and indeed over WT and some existing single mutants. These combination mutants did not seem to exhibit a broad substrate scope however, with low yields and stereoselectivities observed for the transformation of other aliphatic aldehydes. The knowledge gained from the study of these combination mutants would prove invaluable in the creation of combination mutant TK libraries for the transformation of aromatic aldehydes (Chapter 5).

## **5 Aromatic aldehydes with combination mutant TKs**

A range of combination mutant TKs had been created guided by a statistical coupling analysis method (Chapter 4).<sup>[88]</sup> This involved taking into account the co-evolution of certain active-site residues when creating combination mutants, to prevent the disturbance of a co-evolved network of residues crucial for enzyme structure and function.<sup>[88]</sup> This method led to the generation of a mutant, D469T/R520Q, which had the highest specific activity reported for any mutant with propanal (Chapter 4).<sup>[88]</sup> Since previous single mutant TKs had given low yields and variable stereoselectivities with aromatic aldehydes, it was hoped that combination mutant TKs might have increased activities with aromatic substrates. As a starting point, the previously prepared library of combination mutants, identified from screening propanal as a substrate, was tested with benzaldehyde (**8**) (Table 5.1) and LiHPA (Li-**23**) and isolated yields and stereoselectivities of the ketodiols **68** were determined (Table 5.1). Selected single mutants that were previously generated and incorporated into combination mutants were also tested.

**Table 5.1 Isolated yields and stereoselectivities for the transformation of benzaldehyde (**8**) by mutant TKs\***



Entry	Mutant	Yield	<i>ee</i>
1	F434A <sup>[85]</sup>	10%	82% ( <i>R</i> )
2	D469E <sup>[85]</sup>	2%	0 %
3	D469T <sup>[85]</sup>	2%	70% ( <i>R</i> )
4	D469K <sup>[85]</sup>	2%	82% ( <i>R</i> )
5	D469Y	4%	0%
6	H461S	4%	0%
7	A29E	3%	0%
8	A29E H461S	3%	0%
9	H26Y D469Y	5%	0%
10	A29E R520V	4%	0%
11	D469Y R520V	3%	0%
12	A29E H461S R520V	7%	0%
13	F434A R520Q	3%	18% ( <i>R</i> )
14	D469Y R520Q	2%	0%
15	D469T R520Q	3%	54% ( <i>R</i> )

\*Mutant TKs were created by Panwajee Payongsri. Reaction conditions: 50 mM benzaldehyde, 50 mM Li-HPA, 2 mL TK cell-free lysate, 20 mL total reaction volume, 48 hour reaction time.

Stereoselectivities were assessed by chiral HPLC analysis of the mono-benzoate ester derivatives of ketodiol products, and absolute stereochemistries were assigned based on previous chiral HPLC retention time data<sup>[85]</sup>, for which absolute stereochemistries had been tentatively assigned by a Mosher's ester analysis.<sup>[85]</sup>

No significant improvements were witnessed for any of the single or combination mutants. D469Y (entry 5), a mutation observed to reverse the stereoselectivity of the propanal reaction,<sup>[48]</sup> gave rise to no stereoselectivity in the transformation of benzaldehyde and no improvements in the yield of ketodiol **68** over previous mutants. This is perhaps not surprising given that adding a tyrosine residue into the active-site of TK would restrict the access of benzaldehyde into the TK active-site because of increased steric hindrance. H461S (entry 6) and A29E (entry 7) had both been previously observed to increase the specific activity of TK towards propanal,<sup>[47]</sup> but did not increase the isolated yield or *ee* of **68**, either as single mutants or double mutants (entry 8). H26Y, along with D469Y, had been shown to reverse the stereoselectivity of the TK reaction with propanal,<sup>[26]</sup> but combining these mutants in H26Y/D469Y (entry 9) gave no stereoselectivity in the transformation of benzaldehyde. Combinations of these mutants, A29E, H461S and D469Y, with another mutant which had been shown to increase the activity of TK towards propanal, R520V (entries 10-12),<sup>[47]</sup> gave no improvements in yield over the best performing single mutant, F434A. Interestingly, the yields observed for these mutants with benzaldehyde were similar to those for the reaction of the combination mutants with propanal (Chapter 4), again suggesting loss of enzyme stability and/or function. Since F434A was still the most active single mutant with benzaldehyde,<sup>[85]</sup> it was thought that by combining this mutant with R520Q, which had been shown to increase the expression level of soluble TK,<sup>[88]</sup> that F434A/R520Q (entry 13) might increase the yields of ketodiol **68**. Disappointingly however, this mutant only gave a 3% isolated yield of **68** with only marginal stereoselectivity observed, forming ketodiol (**68**) in an 18% *ee*. It seemed that in this case adding the R520Q mutation was not beneficial, leading to a 7% lower yield of **68** and a major decrease in stereoselectivity from 82% to 18% *ee* when compared to F434A. In fact, adding R520Q to both D469T and D469Y gave no improvement in yield or stereoselectivity over the parent mutants either. D469Y/R520Q (entry 14) gave a comparable yield of **68** as for D469Y, with both mutants forming racemic ketodiol **68**. D469T/R520Q

(entry 15) gave a similar yield of **68** as D469T, but a lower *ee* of 54% was observed compared to 70% with D469T.

By investigating these combination mutants in the transformation of benzaldehyde to **68** it was clear, from the low yields and poor stereoselectivities observed, that these mutants gave no improvement over previously identified single mutants.<sup>[85]</sup> The addition of mutations, such as R520Q, which had been proven to improve TK expression, stability and activity toward propanal (chapter 4),<sup>[88]</sup> showed no improvement in the transformation of benzaldehyde. Therefore, a different approach was needed in order to identify combination mutants that would transform aromatic aldehydes in good yields and stereoselectivities.

### 5.1 Probing TK active-site with formylbenzoic acid

Previous docking studies with benzaldehyde (**8**) and the *in silico* generated variant D469T (Chapter 2) had shown only one productive conformation, where the aldehyde oxygen atom formed hydrogen bonding interactions with the ThDP intermediate in the active-site (Figure 5.1, C). The only other conformations identified from the docking experiment involved non-specific binding of the benzaldehyde molecule to acidic residues at the entrance to the active-site (Figure 5.1, A), and to the protein backbone preventing entrance to the active-site (Figure 5.1, B).

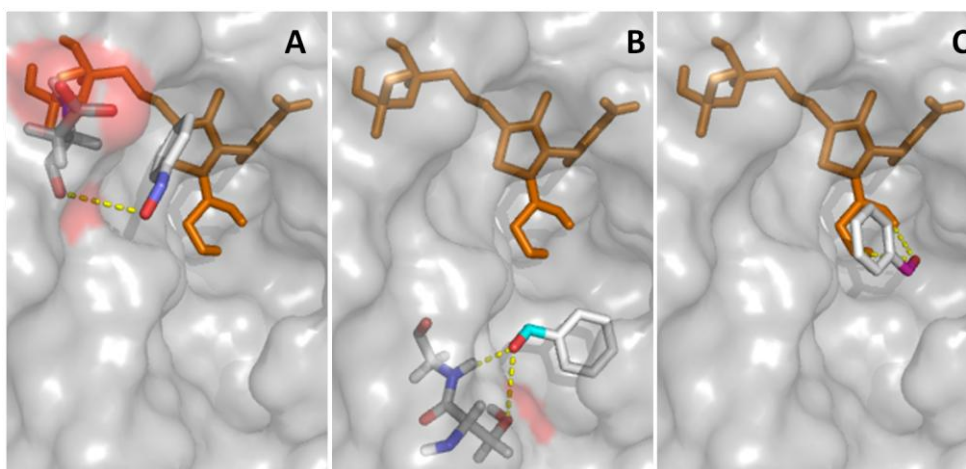


**Figure 5.1** Conformations obtained from the computational docking of benzaldehyde (**8**) into D469T. (ThDP-enamine intermediated shown in orange).



These docking results suggested that specific interactions between benzaldehyde and the TK active-site would have to be introduced in order to increase the activity of TK with aromatic substrates. It was therefore necessary to probe the active-site interactions with the natural substrate, ribose-5-phosphate further, to determine if any structural features could be exploited to improve the acceptance of aromatic substrates by TK. With this in mind, the X-ray crystal structure of TK with ThDP and the natural substrate, ribose-5-phosphate (R5P) (**20**), bound (2R5N)<sup>[90]</sup> was analysed (Figure 5.2).

**Figure 5.2 Structure of R5P (**20**) and crystal structure of *E. coli* WT TK with R5P bound (2R5N)<sup>[90]</sup>**

Analysis of this structure showed two main binding regions, one region (H26, H261, S385, D469) responsible for binding the hydroxyl groups of R5P, and the other region (S385, R358, H461, R520) involved in binding of the phosphate group. Previous work directing TK activity towards hydroxylated aliphatic aldehydes has shown that D469, along with H26 and H261, is crucial for the binding of hydroxylated substrates,<sup>[47]</sup> as observed in this crystal structure (Figure 5.2). Also, mutation of the phosphate binding region has been carried out to effectively improve the acceptance of non-phosphorylated substrates by TK.<sup>[46]</sup> Since docking studies had suggested that the acceptance of aromatic aldehydes by mutant TKs was poor potentially due to a lack of specific interactions between the substrate and the active-

site, it was envisaged that the natural phosphate binding region could be exploited to increase specific interactions. If aromatic aldehyde substrates bearing a phosphate, or phosphate mimic, were used as substrates for TK, this moiety could interact with the phosphate binding region, potentially increasing the affinity of TK towards aromatic aldehydes.

Since D469T had already been shown to be a useful mutation for increasing the acceptance of non- $\alpha$ -hydroxylated aldehydes, particularly cyclic aldehydes,<sup>[26, 47]</sup> this mutant was used as a starting point for computational docking studies. Formylbenzoic acids, such as 3-formylbenzoic acid (3-FBA) (**97**) (Figure 5.3) and 4-formylbenzoic acid (4-FBA), bearing carboxylic acid functionalities at the *meta* and *para*-positions respectively, were considered useful probes for studying active-site interactions with the phosphate binding region. 2-Formylbenzoic acid was considered to be too sterically hindered, and so was not investigated. 3-FBA was initially used as the substrate in docking studies with D469T.<sup>[91]</sup>

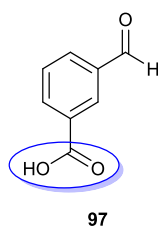


**Figure 5.3 3-Formylbenzoic acid (3-FBA) (**97**) with the phosphate mimic carboxylate group highlighted**

D469T was prepared *in silico* by mutation of the WT-TK crystal structure 2R5N.\* The active enamine intermediate of ThDP and HPA was created *in silico* and docked separately into D469T. This complex was then used as the protein structure for 3-FBA to be docked into, allowing the interactions between the substrate and the ThDP-enamine intermediate to be considered by the docking program, as described in Chapter 3.<sup>[91]</sup>

The docking results were very encouraging. Whereas previous docking experiments with benzaldehyde had demonstrated the non-specific binding of benzaldehyde with the enzyme (Figure 5.1), with most conformations found at the entrance to the active

---

\* *In silico* mutation was carried out by Panwajee Payongsri

site (Figure 5.1 A and B), the results with 3-FBA were very different. The most populated cluster of conformations showed **97** bound by the phosphate binding region of S385, H461, R358 and R520 (Figure 5.4), in a similar docking conformation as observed for the natural substrate, R5P (**20**), in WT TK. (Figure 5.2).<sup>[90]</sup>

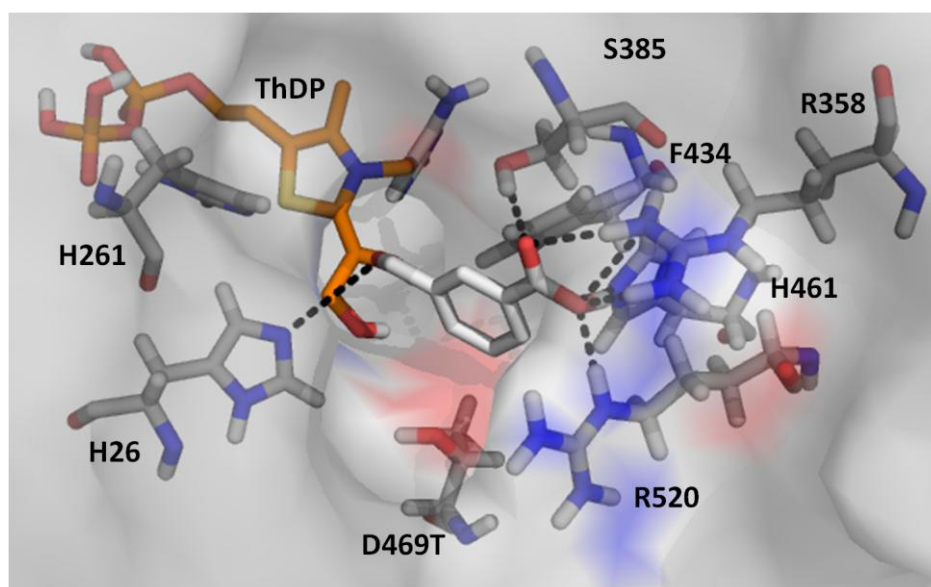


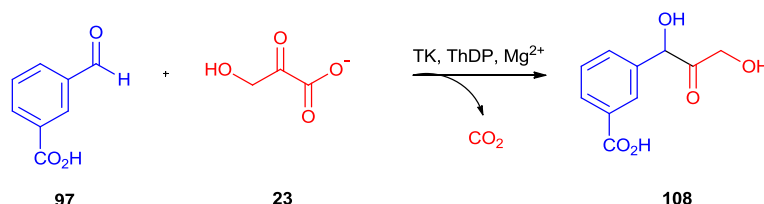
**Figure 5.4 Most populated cluster obtained by docking of 3-FBA (**97**) into D469T. (ThDP-enamine shown in orange)**

In addition to the carboxylate interactions with the phosphate binding region, the docking also showed a hydrogen bond between H26 and the aldehyde oxygen atom, holding it in an active conformation at a distance of 4.9 Å from the active ThDP-enamine intermediate. While D469T has been shown to be an important mutation for the acceptance of non- $\alpha$ -hydroxylated substrates, as it prevents the burial of a positive charge upon substrate binding and removes a hydrogen bond,<sup>[26]</sup> it also appeared that for aromatic aldehydes the D469T mutation was important on steric grounds to allow the entrance of bulky substrates into the active site. Alignment of the WT structure and D469T structure showed that D469 would be only 2.9 Å away from the aromatic ring of 3-FBA compared to 4.1 Å in D469T.<sup>[91]</sup>

## 5.2 Screening of 3-formylbenzoic acid with TK mutants

Encouraged by these docking results, 3-FBA (**97**) was screened against WT-TK, D469T, D469Y and F434A in small-scale biotransformations with LiHPA (Li-**23**) to form ketodiol (**108**) (Table 5.2). Aldehyde consumption was followed by HPLC analysis to allow preliminary conversion yields to be rapidly established without a pure product standard (Table 5.2).<sup>[91]</sup>

**Table 5.2** Conversions obtained for the transformation of 3-formylbenzoic acid (**97**) by mutant TKs\*



The reaction scheme shows 3-formylbenzoic acid (**97**) reacting with LiHPA (**23**) in the presence of TK, ThDP, and Mg<sup>2+</sup> to produce ketodiol (**108**) and CO<sub>2</sub>.

Mutant	Isolated yield with benzaldehyde	Conversion of <b>97</b>
WT	0% <sup>[85]</sup>	0%
D469T	2% <sup>[85]</sup>	65%
D469Y	4%	0%
F434A	10% <sup>[85]</sup>	0%

\*Screening carried out by Panwajee Payongsri. Reaction conditions; 50 mM 3-FBA, 50 mM Li-HPA, 30  $\mu$ L TK cell-free lysate, 50 mM tris buffer (300  $\mu$ L total volume). Conversion yields were determined after 24 hours.

HPLC analysis showed that of all the mutants only D469T gave any observable product formation with a 65% conversion yield to ketodiol (**108**), representing a potential 30-fold increase in yield over the conversion of benzaldehyde by D469T.<sup>[85]</sup> Further HPLC analysis of the progression of the reaction showed that the reaction of **97** with D469T reached its peak conversion of 65% after only 2 hours, compared to the 17 hours required to reach a 2% yield for the reaction of benzaldehyde with D469T, representing a 250-fold increase in specific activity for 3-FBA over benzaldehyde for D469T.<sup>[91]</sup>

Interestingly, while D469T gave a 65% conversion yield of **108**, D469Y showed no conversion whatsoever, suggesting steric hindrance was a key factor for the acceptance of **97** by D469T compared to D469Y. The tyrosine side chain would have a much greater steric bulk than aspartic acid or threonine, and could completely

restrict access of 3-FBA into the active site.<sup>[91]</sup> Interestingly, F434A, which had been shown to be the most active mutant toward benzaldehyde,<sup>[85]</sup> did not accept 3-FBA. This suggested that while the mutation of phenylalanine for alanine gave a hydrophobic pocket large enough to accommodate the steric bulk of the aromatic ring of benzaldehyde, it did not accept 3-FBA in a productive orientation to allow catalysis to occur.<sup>[91]</sup>

In an effort to further understand the influence of the phosphate binding residues, R358, H461 and R520, on the conversion of **97**, a series of mutations were made at these positions. These were based on previously identified functional mutations which had been shown to lower the affinity of TK for phosphorylated substrates,<sup>[37]</sup> and increase activity toward non-phosphorylated substrates.<sup>[46]</sup> The influence of these residues on phosphorylated substrates made them ideal candidates for studying the binding of a phosphate mimic, such as a carboxylate group, in this case. These combination mutants were first screened with 3-FBA, in the same fashion as for the single mutants (Table 5.2). Conversions to **108** were again assessed by HPLC, based on the consumption of aldehyde **97** in the reaction after 24 hours.<sup>[91]</sup>

**Table 5.3 Conversions obtained for the transformation of 3-FBA (**97**) by TKs with mutations at phosphate binding residues\***

<b>Mutant</b>	<b>Conversion of 97</b> <sup>[91]</sup>
<b>WT</b>	0%
<b>D469T</b>	65%
<b>H461S/D469T</b>	65%
<b>D469T/R520Q</b>	65%
<b>H461S/D469T/R520Q</b>	65%
<b>R358P/D469T</b>	65%
<b>R358L/D469T</b>	<10%
<b>R358P/D469T/R520Q</b>	14%

\*Screening carried out by Panwajee Payongsri after collaborative discussions. Reaction conditions; 50 mM 3-FBA, 50 mM Li-HPA, 30  $\mu$ L TK cell-free lysate, 50 mM tris buffer (300  $\mu$ L total volume). Conversion yields were determined after 24 hours.

All of the mutants, except for R358L/D469T and R358P/D469T/R520Q, gave approximately 65% conversion yields of **108**, even after multiple experimental repeats, suggesting product inhibition to the same extent for all mutants.

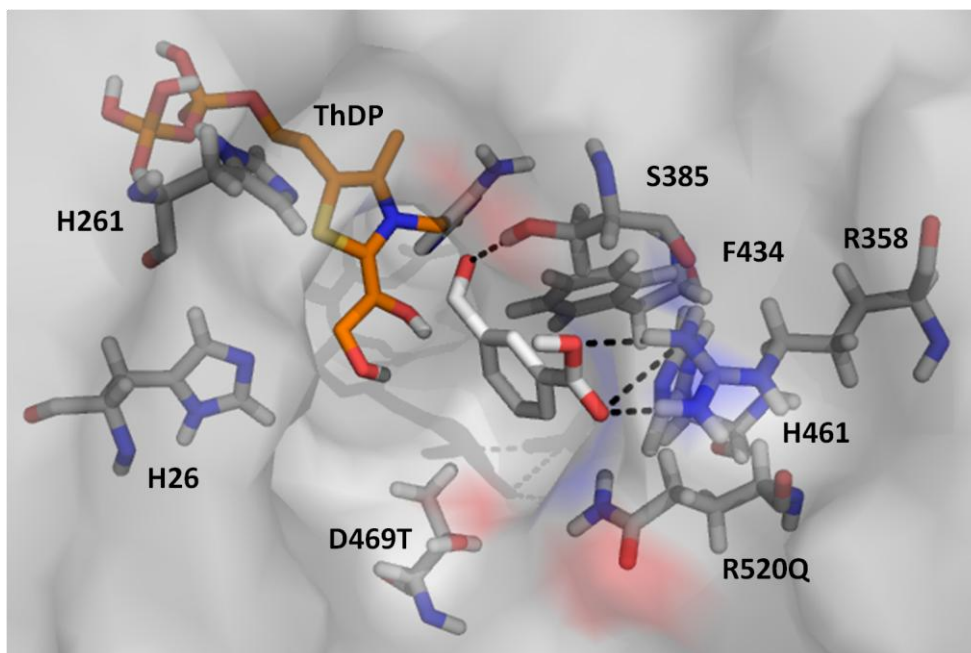
The kinetic parameters for all of these mutants were obtained, to further investigate the effects of these mutations.<sup>[91]\*</sup> The results showed that affinity for 3-FBA (**97**) was increased by the removal of a positive charge from the phosphate-binding region in the TK active-site. This is plausible, given that the TK active-site has evolved to bind phosphate groups in the natural TK substrates such as, R5P, which has a charge of -2 (pKa<sub>1</sub> 1.2, pKa<sub>2</sub> 6.6) and the carboxylate functionality of 3-FBA has a charge of -1 (pKa 3.85). Since removal of a positive charge from the active-site increased its affinity for 3-FBA, it seemed that the close proximity of the two positively charged arginine residues, R358 and R520, interacting with the positively charged H461, might be destabilising when interacting with 3-FBA which has a single negative charge. Charge neutralising mutations such as R358P, H461S or R520Q would remove this destabilisation, caused by the burial of an additional positive charge, and hence increase the affinity of TK for 3-FBA. When both positive charges were removed the affinity increased again, potentially due to repositioning of 3-FBA in the active-site stabilised by an interaction with other positively charged active-site residues. Despite all of the charge-neutralising mutations increasing the affinity of TK for 3-FBA, the kinetics showed that the turnover for all combination mutants was decreased compared to D469T suggesting that removal of a positive charge from the active site, by mutation of R358, H461 or R520, resulted in unfavourable repositioning of the aldehyde relative to the ThDP-enamine intermediate.

In order to understand the active-site interactions responsible for the increase in affinity but decrease in turnover for 3-FBA with the combination mutant TKs, computational docking was carried out with D469T/R520Q (Figure 5.5).<sup>†</sup> This mutant had shown a 4-fold decrease in affinity and a corresponding 2-fold decrease in turnover compared to D469T.<sup>[91]</sup>

---

\* Kinetic studies were performed by Panwajee Payongsri

† *In silico* mutation was carried out by Panwajee Payongsri after collaborative discussions

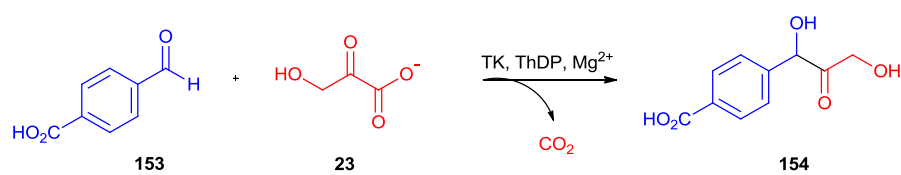


**Figure 5.5** Results obtained for docking 3-FBA (97) into D469T/R520Q (ThDP-enamine shown in orange).

Compared to the docking results obtained for 3-FBA with D469T (Figure 5.4), the binding with D469T/R520Q was slightly different. A small shift of 3-FBA towards R358 was observed, resulting in the removal of a hydrogen bond between the carboxylate group and S385 and the introduction of a new hydrogen bond between the aldehyde oxygen atom and S385. This interaction moved the aldehyde further away from the ThDP-enamine intermediate, to a distance of 6.6 Å, compared to a 4.9 Å distance observed for 3-FBA and D469T. This increase in distance between the aldehyde moiety and the ThDP-enamine intermediate could help to explain the 2-fold lower turnover observed for D469T/R520Q compared to D469T.<sup>[91]</sup>

### **5.3 Screening of 4-formylbenzoic acid with TK mutants**

With the encouraging activities observed for TK mutants and 3-FBA, a related substrate, 4-formylbenzoic acid (**153**) (4-FBA), was investigated in the TK reaction with LiHPA (Li-**23**). The same range of mutants was screened as with 3-FBA, using the same conditions. The conversion yields to ketodiol **154** were assessed by HPLC analysis which was used to determine the consumption of 4-FBA (**153**) in the reactions after 24 hours (Table 5.4).<sup>[91]</sup>

**Table 5.4 Conversions obtained for the transformation of 4-FBA (153) by mutant TKs\***

Mutant	Conversion of 153 to 154
WT	0%
D469T	30%
D469Y	0%
D469K	ND
D469E	ND
F434A	0%

\*Screening carried out by Panwajee Payongsri. Reaction conditions; 50 mM 4-FBA, 50 mM Li-HPA, 30  $\mu$ L TK cell-free lysate, 50 mM tris buffer (300  $\mu$ L total volume). Conversion yields were determined after 24 hours.

The results with 4-FBA (**153**) as a substrate followed a similar trend to those for 3-FBA (**97**). Only D469T gave any observable product, with a conversion yield to **154** of 30%. D469Y still gave no product (**154**), again possibly due to the extra steric bulk introduced to the active-site by the mutation of aspartic acid to tyrosine. While the conversion yield observed for D469T with 4-FBA (**153**) still represented a large increase in activity compared to D469T with benzaldehyde,<sup>[85]</sup> the 30% conversion yield was less than half that observed for D469T with 3-FBA as the substrate. To investigate this 4-FBA was docked into the D469T structure containing the active ThDP-enamine intermediate (Figure 5.6), as carried out previously for 3-FBA (Figure 5.4).



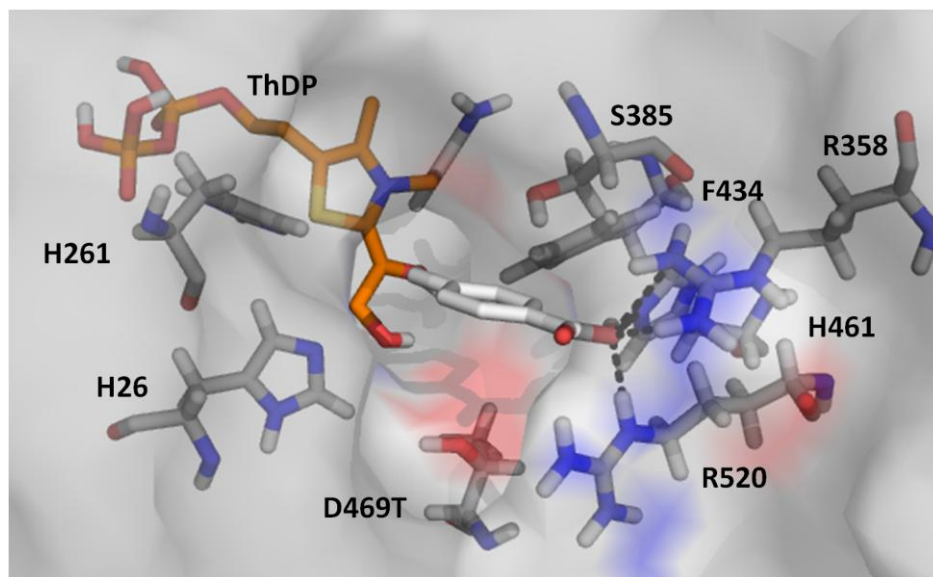


**Figure 5.6 Results obtained for docking 4-FBA (153) into D469T**

The docking results obtained were similar to those for the docking of 3-FBA (**97**) into D469T (Figure 5.4). The carboxylate group was bound by the phosphate binding region of R358, H461 and R520, orienting the aldehyde into an active conformation at a distance of 5.1 Å from the ThDP-enamine active intermediate, only 0.2 Å further away than found for 3-FBA when docked into D469T. Perhaps the most important result from this docking, however, was the loss of several hydrogen bonds to the carboxylate group compared to 3-FBA, notably between the carboxylic acid and S385. This, coupled with the slightly increased distance of the aldehyde from the ThDP enamine could help to explain the observed decrease in conversion from 65% for 3-FBA (**97**) to 30% for 4-FBA (**153**) with D469T.<sup>[91]</sup>

Since many of the combination mutants had given good conversions with 3-FBA, a selection of these were also screened with 4-FBA (Table 5.5).<sup>[91]\*</sup>

\* Mutants were created by Panwajee Payongsri

**Table 5.5 Conversions obtained for the transformation of 4-FBA by TKs with mutations at phosphate binding residues<sup>†</sup>**

<b>Mutant</b>	<b>Conversion of 153 to 154</b>
<b>WT</b>	0%
<b>D469T</b>	30%
<b>D469T/R520Q</b>	13%
<b>R358P/D469T</b>	1%
<b>R358L/D469T</b>	5%
<b>R358P/D469T/R520Q</b>	<1%

<sup>†</sup>Screening carried out by Panwajee Payongsri. Reaction conditions; 50 mM 4-FBA, 50 mM Li-HPA, 30  $\mu$ L TK cell-free lysate, 50 mM tris buffer (300  $\mu$ L total volume). Conversion yields were determined after 24 hours.

The conversion yields for all of the combination mutants with 4-FBA were lower than those observed for D469T. This is in contrast with the results obtained when 3-FBA was used as a substrate, where the majority of the combination mutants gave similar conversion yields compared to D469T (Table 5.3).

Kinetic parameters for the combination mutants with 4-FBA were obtained where possible to investigate why lower conversion yields were observed for 4-FBA compared to 3-FBA.\* Only the kinetic parameters for the two best performing mutants, D469T and D469T/R520Q, could be obtained. Interestingly, although D469T/R520Q gave a 2-fold lower conversion yield for 4-FBA than D469T, this was not due to impaired affinity. In fact, D469T/R520Q had a 10-fold higher affinity for 4-FBA than D469T.<sup>[91]</sup> This is consistent with the hypothesis that there is an increase in stability when a positive charge is removed from the active site, bringing the active-site closer to neutral when binding these single negatively charged substrates.<sup>[91]</sup> While affinity was shown to increase 10-fold for 4-FBA with D469T/R520Q, a 20-fold decrease in turnover was observed suggesting that this increase in affinity resulted in a repositioning of the substrate to a less-productive conformation. Computational docking of 4-FBA with D469T/R520Q supported this hypothesis. 4-FBA was docked into D469T/R520Q with the ThDP-enamine

\* Kinetic parameters were obtained by Panwajee Payongsri

intermediate already bound. No single productive conformations were obtained, in contrast to the docking of 3-FBA with D469T/R520Q, which showed specific interactions between the substrate carboxylate group and H461, R358 and R520Q (Figure 5.5). These results are consistent with the 30-fold lower turnover observed for 4-FBA compared to 3-FBA with D469T/R520Q.<sup>[91]</sup>

#### 5.4 Creation of a new mutant library to improve the bioconversions with aromatic aldehydes

To further investigate the importance of the key electrostatic interactions between the phosphate binding region and carboxylate substituents of 3-FBA and 4-FBA, a range of other *meta* and *para*-substituted benzaldehydes were screened with D469T (Figure 5.7) to determine whether neutral substituents would be accepted. 3-Methylbenzaldehyde (**155**), 4-methylbenzaldehyde (**132**), 3-methoxybenzaldehyde (**134**), 4-methoxybenzaldehyde (**133**), 3-isopropylbenzaldehyde (**156**), 4-isopropylbenzaldehyde (**157**) were all individually screened at a 50 mM concentration in scaled-up (20 mL) biotransformations with Li-HPA (50 mM) and D469T. Product formation was followed by TLC analysis.

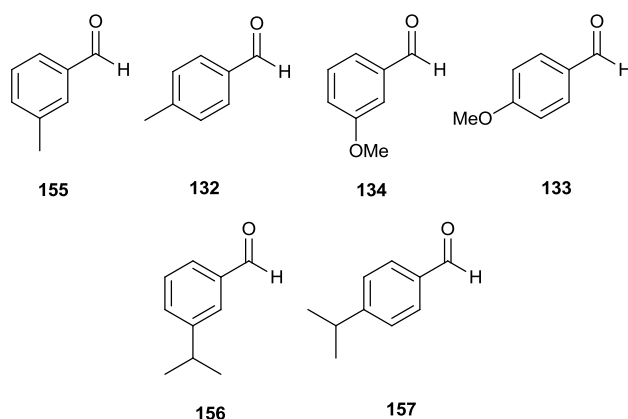


Figure 5.7 Additional substituted benzaldehydes screened with D469T

No product formation was observed for any of these substrates even after extended (48 hour) reaction times. This was in stark contrast to the 65% conversion yield observed for D469T with 3-FBA (**97**),<sup>[91]</sup> suggesting that the binding of the carboxylate groups in 3-FBA and 4-FBA was indeed responsible for the high

activities observed for these substrates with D469T.<sup>[91]</sup> Considering that the removal of a positive charge from the TK active-site in D469T/R520Q might potentially provide a better microenvironment for benzaldehyde, the conversion of benzaldehyde by D469T/R520Q was also investigated. Disappointingly, only a 3% isolated yield of ketodiol product was obtained, in 55% *ee*, representing no improvement over D469T.<sup>[85]</sup> These studies confirmed the importance of the charged carboxylate functionality on 3-FBA and 4-FBA for efficient binding and catalysis, and showed that hydrophobic interactions alone were not sufficient to obtain high turnover for benzaldehyde and other functionalised derivatives.<sup>[91]</sup> With this in mind, it was clear that while rational design targeted toward the phosphate binding site was effective at increasing the activity of TK toward certain aromatic aldehydes, further work focused on the TK active-site was needed to improve the biotransformations of benzaldehyde and other aromatic aldehydes in general.

Previous work had shown that saturation mutagenesis at residues close to the active-site had more potential to improve enzyme activities and stereospecificities than mutation of residues at positions further from the enzyme active-site.<sup>[92]</sup> Therefore, to develop a strategy to improve activities of TK with aromatic aldehydes, first shell residues within 4 Å of the active-site, which had been previously identified as targets for mutation,<sup>[46]</sup> were targeted, and mutants created based on the knowledge gained from studying the co-evolution of certain active-site residues<sup>[88]</sup> and the subsequent acceptance of formylbenzoic acids by certain TK mutants.<sup>[91]</sup>

D469T had been shown to be the most active mutant towards 3 and 4-formylbenzoic acids,<sup>[91]</sup> while the combination mutant D469T/R520Q was also active to both of these substrates, albeit to a lesser extent.<sup>[91]</sup> However, the R520Q mutation had previously been shown to stabilise the combination mutants containing D469T and other D469 mutations,<sup>[88]</sup> so D469T/R520Q was used as the initial TK template for saturation mutagenesis. The other residues were chosen for mutation based on their position in the active-site and the knowledge gained from previous protein engineering studies.<sup>[88, 91]</sup>

F434A had previously been shown to be the most active single mutant for the transformation of benzaldehyde.<sup>[85]</sup> This activity was rationalised by the removal of steric bulk within the active site, allowing benzaldehyde to enter.<sup>[85]</sup> However, the activities observed for D469T with the more sterically-demanding 3 and 4-formylbenzoic acids showed that sterics were not a limiting factor for the acceptance

of aromatic aldehydes, and that the low affinity of benzaldehyde for the active-site of TK seemed more likely a reason for the low yields observed for this substrate. This hypothesis was supported by docking experiments where non-specific binding of benzaldehyde had been observed (Figure 5.1). Also, since F434A is more than 4 Å from the TK active-site, it was not chosen for further study.

To increase affinity for aromatic substrates the natural phosphate binding region seemed a logical area to target for mutation. H461, a positively charged residue responsible for phosphate binding of the TK natural substrates, was considered as a target for mutagenesis to potentially improve the affinity of the TK active-site towards neutral substrates, such as benzaldehyde. However, previous mutation of this residue, for example to H461S, had shown that the stability and function of the resulting mutant was severely affected and only partially restored by the addition of the stabilising R520Q mutation.<sup>[88]</sup> H461 was therefore considered integral to the structure and function of TK, and so not targeted for mutagenesis.

R358 had previously been successfully targeted for mutation to remove a positive charge from the phosphate binding region of TK, and as such had only been mutated to neutral residues.<sup>[91]</sup> Therefore, this residue was targeted for saturation mutagenesis, using the D469T/R250Q template, to obtain R358X/D469T/R520Q.

The remaining residue in the phosphate binding region, S385, had previously been identified as a residue suitable for mutation to improve activity toward non-phosphorylated substrates.<sup>[46]</sup> Though no active single mutations of this residue were reported,<sup>[46]</sup> the resulting mutants maintained structure and function, unlike H461 mutants.<sup>[88]</sup> This residue was therefore also chosen for saturation mutagenesis in combination with D469T/R520Q to obtain a library of S385X/D469T/R520Q mutants.\*

Mutant libraries were screened with 3-FBA (**97**), 4-FBA (**153**) and 3-hydroxybenzaldehyde (**93**) (3-HBA) (Figure 5.8). 3-FBA and 4-FBA were chosen since they had already been shown to be well tolerated by D469T,<sup>[91]</sup> whereas 3-HBA was chosen as it had been previously shown to be poorly accepted by D469T.<sup>[85]</sup> Screening the mutants with these substrates would therefore give an indication of whether the mutant libraries were merely binding the carboxylate

---

\* All TK mutant libraries were created by Panwajee Payongsri after collaborative discussions

functionality of 3-FBA and 4-FBA in a more productive conformation, or whether mutants were being created which were generally more active towards aromatic aldehydes. Screening was carried out using an HPLC assay to assess aldehyde consumption and hence rapidly identify active mutants.\*

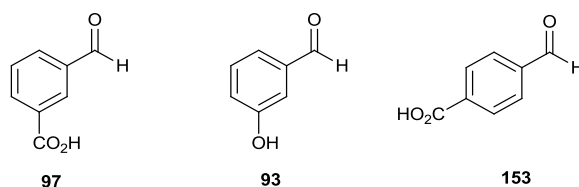


**Figure 5.8 Substrates used for screening of R358X/D469T/R520Q and S385X/D469T/R520Q mutant libraries**

The initial screening of the R358X/D469T/R520Q library showed that half of the library maintained activity toward 3-HBA, but variations in activity with 3-FBA and 4-FBA were observed. All of the mutants were less active towards 4-FBA, and only one mutant, R358T/D469T/R520Q maintained activity towards 3-FBA. However, none of these mutants increased activity towards any of the substrates compared to D469T and more than a third of the colonies lost activities towards all three substrates, indicating a complete loss of catalytic function or enzyme stability. The R358X/D469T/R520Q library was therefore not considered to be useful for the conversion of aromatic aldehydes and not investigated further.

In contrast to the R358X/D469T/R520Q library, the S385X/D469T/R520Q library was much more interesting. The majority of the mutants showed a marked increase in activity for 3-HBA compared to D469T, whilst maintaining activity towards 3-FBA. Some of the mutants also showed increased activities towards 4-FBA. Only one fifth of the mutants showed no activity toward any of the substrates, far fewer than the number of inactive mutants found for the R358X/D469T/R520Q library, indicating that while S385 is a highly conserved residue, it may be more stable towards mutation than R358. Of all of the mutations in the S385X/D469T/R520Q library, S385T/D469T/R520Q, S385Y/D469T/R520Q and S385E/D469T/R520Q were the most active mutants identified by the initial screening. S385T/D469T/R520Q showed a 2.5-fold increase in 4-FBA conversion yield, a 5.5-

\* Screening was carried out by Panwajee Payongsri

fold increase in 3-HBA conversion yield whilst only halving the activity with 3-FBA compared to D469T. S385Y/D469T/R520Q showed a similar trend, halving activity with 3-FBA while giving a 1.5-fold increase in conversion yield for 4-FBA and a 5-fold increase in conversion yield for 3-HBA compared to D469T. Finally, S385E/D469T/R520Q maintained the conversion yield for 4-FBA, but gave a 1.5-fold increase in activity with 3-FBA and a 2.5-fold increase in conversion yield for 3-HBA.

As S385T/D469T/R520Q, S385Y/D469T/R520Q and S385E/D469T/R520Q were the best performing mutants, they were chosen for detailed kinetic analysis.\* The most interesting results were found for S385E/D469T/R520Q with 3-FBA, S385Y/D469T/R520Q with 4-FBA and S385Y/D469T/R520Q with 3-HBA.

S385E/D469T/R520Q showed a 2.5-fold increase in turnover and a 3-fold increase in affinity for 3-FBA, and showed no substrate inhibition even at high substrate concentrations (up to 90 mM). This suggested a different binding mode compared to D469T, so docking studies with the *in silico* generated mutant were carried out with 3-FBA as the substrate.†

The docking experiment gave two different clusters. The first cluster was the lowest in energy but had a small population, while the second cluster was higher in energy but had a large population. The first cluster (Figure 5.9) showed two different conformations, both considered to be unproductive due to the distance of the aldehyde functionalities from the ThDP-enamine intermediate. One conformation (Figure 5.9, red) brought the aldehyde to 7.1 Å away from the ThDP-enamine, and the other conformation (Figure 5.9, green) showed the aldehyde at a greater distance of 9.0 Å. In both cases the carboxylate group was bound by the phosphate binding residues of R358 and H461, and in the conformation where the aldehyde was 9.0 Å from the ThDP-enamine (Figure 5.9, green), the position of the aldehyde was stabilised by hydrogen bonding interactions with D469T.

---

\* Kinetic parameters obtained by Panwajee Payongsri

† *In silico* mutagenesis was carried out by Panwajee Payongsri

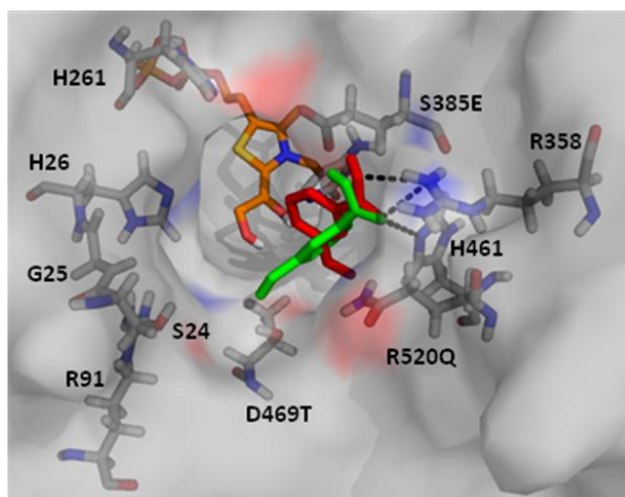


**Figure 5.9** Lowest energy, non-productive cluster found for docking 3-FBA (97) into S385E/D469T/R520Q. (Two non-productive conformations shown in red and green, ThDP-enamine shown in orange).

The second cluster (Figure 5.10) found by the docking program had a higher population, and demonstrated a more productive conformation.

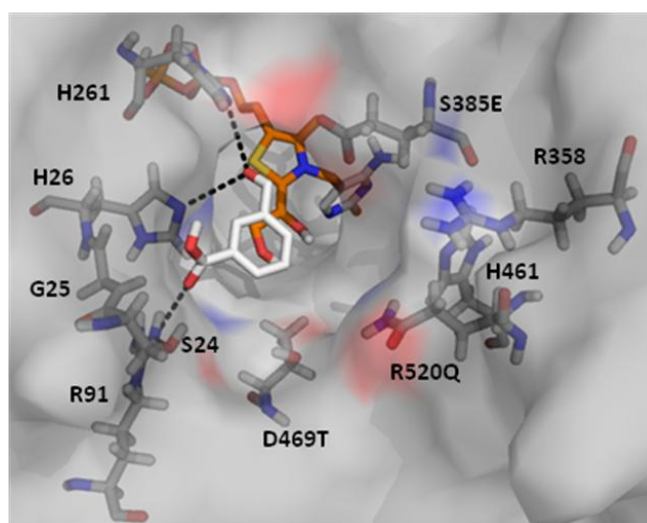


**Figure 5.10** Productive cluster found for docking 3-FBA (97) into S385E/D469T/R520Q. (ThDP-enamine shown in orange).

In this second cluster (Figure 5.10) the aldehyde was positioned at a closer distance of 4.6 Å from the ThDP-enamine intermediate. This is a similar distance as found in the docking of 3-FBA with D469T (4.9 Å), however this cluster showed a different binding mode than that found for D469T (Figure 5.4) or D469T/R520Q (Figure 5.5), as the carboxylate group was not bound by the phosphate binding residues of R358



or H461 but rather by S24, G25, H26 and R91. Also, in this case, the aldehyde moiety was held in a productive conformation directly above the ThDP-enamine stabilised by hydrogen bonding interactions with H26 and H261. The increased number of hydrogen bonding interactions and shorter distance between the 3-FBA aldehyde moiety and ThDP-enamine found for S385E/D469T/R520Q could help to explain the increased affinity and turnover observed for this mutant compared to D469T.

Compared to D469T, S385Y/D469T/R520Q showed a 17-fold increase in affinity and only a 2.5-fold decrease in turnover for 4-FBA, making it the most active mutant towards this substrate. S385Y/D469T/R520Q was also the most active mutant for 3-HBA showing a similar turnover as for 4-FBA but demonstrating a much lower affinity. To try and understand these results, both 4-FBA and 3-HBA were used as substrates for computational docking with S385Y/D469T/R520Q.\*

Docking of 4-FBA with S385Y/D469T/R520Q gave only one cluster (Figure 5.11), in which the carboxylate group was bound by the phosphate binding residues of R358 and H461. This brought the aldehyde to a distance of 5.1 Å from the ThDP-enamine, the same distance as docking had predicted for 4-FBA with D469T (Figure 5.6). The docking also suggested possible  $\pi$ -stacking interactions of the aromatic ring with S385Y, which would further stabilise this binding conformation. However, it was not clear from the docking results why such an increase in affinity (>16-fold) was observed for 4-FBA with S385Y/D469T/R520Q compared to D469T.

---

\* *In silico* mutation was carried out by Panwajee Payongsri

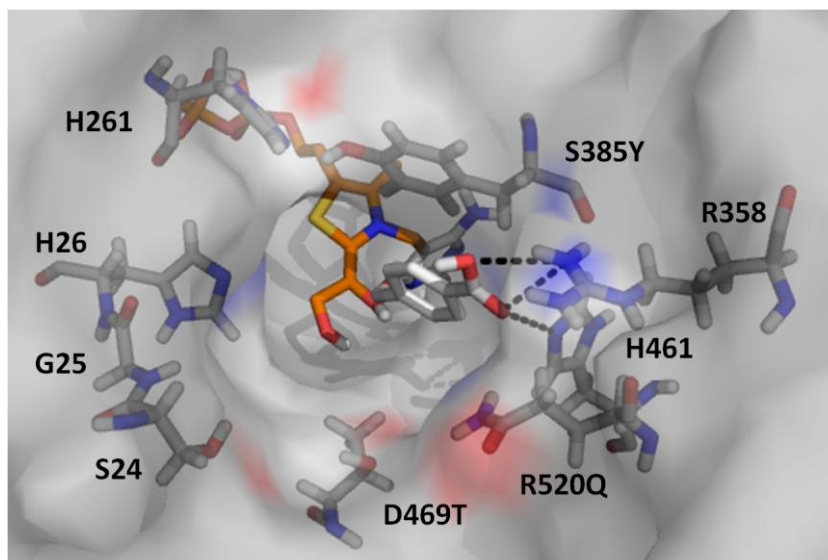


**Figure 5.11 Results found for docking 4-FBA (153) into S385Y/D469T/R520Q. (ThDP enamine shown in orange).**

The docking of 3-HBA into S385Y/D469T/R520Q predicted four major clusters, again demonstrating the difficulty in obtaining clear docking results for substrates where low affinities are observed, as non-specific binding around the TK active-site is favoured. Of these four clusters only one was considered to be productive (Figure 5.12). In this cluster the hydroxyl group of the substrate formed hydrogen bonding interactions with both H261 and S385Y and the aldehyde moiety was bound by the ThDP-enamine at a distance of 4.6 Å. The number of different binding clusters predicted by Autodock suggests the prevalence of non-specific binding in and around the TK active-site, which helps to explain the low affinities observed for S385Y/D469T/R520Q with 3-HBA.

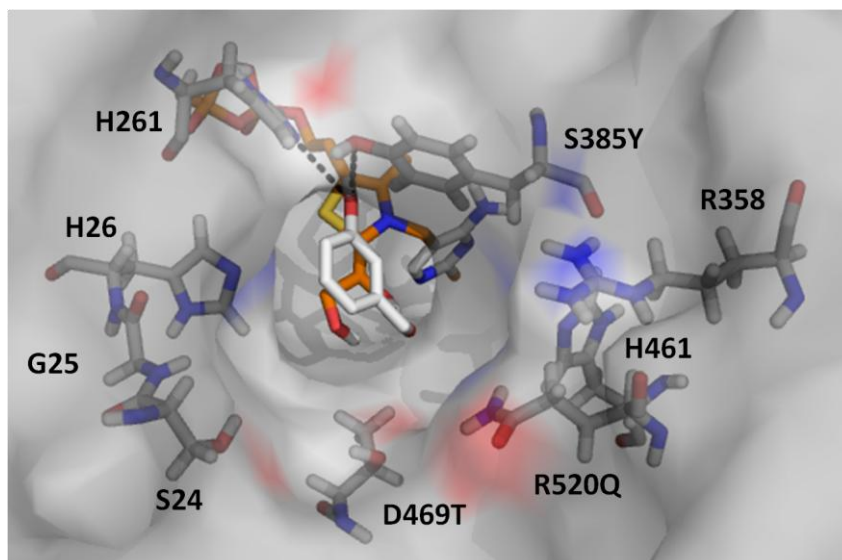


**Figure 5.12 Productive cluster found for docking 3-HBA (93) into S385Y/D469T/R520Q. (ThDP-enamine shown in orange).**

Through knowledge gained from previous investigation into the co-evolution of active-site residues,<sup>[88]</sup> and mutation of the phosphate binding residues H461, R520, and R358,<sup>[91]</sup> three mutants were identified which showed increased activity towards an aromatic aldehyde not bearing a phosphate mimic, with up to 13-fold increased specific activities for 3-HBA observed compared to D469T (0.0071  $\mu\text{mol}/\text{mg}/\text{min}$ )\*. These mutants, S385E/D469T/R520Q (0.0426  $\mu\text{mol}/\text{mg}/\text{min}$ )\*, S385Y/D469T/R520Q (0.0884  $\mu\text{mol}/\text{mg}/\text{min}$ )\* and S385T/D469T/R520Q (0.0902  $\mu\text{mol}/\text{mg}/\text{min}$ )\* could now be tested with other aromatic aldehydes in scaled-up biotransformations, to allow stereoselectivities and isolated yields to be obtained and to assess the value of these mutants as biocatalysts in a two-step pathway towards aromatic aminodiols.

## **5.5 Biotransformation of aromatic aldehydes with combination mutant TKs**

In previous work with TK and aromatic aldehydes, the concentration of aldehyde substrate used was 50 mM.<sup>[85]</sup> While assessing the activities of newly created triple

\* Specific activities for TK mutants towards 15 mM 3-HBA/50 mM HPA, as determined by Panwajee Payongsri.

mutants with 3- and 4-FBA, it was noted that most of the mutants were inhibited by substrate concentrations over 40 mM.<sup>[91]</sup> With this in mind, when scaling-up the biotransformation of aromatic aldehydes, a lower concentration of 25 mM was used to avoid inhibition of TK. Biotransformations were carried out using 4 mL of TK cell-free lysate, with a protein concentration of approximately 1 mg/mL.\*

Benzaldehyde (**8**) was tested with the S385X/D469T/R520Q combination mutants and the isolated yields and stereochemistry of ketodiol **68** were assessed (Table 5.6). The previous highest yielding mutant with benzaldehyde was F434A, which gave an isolated yield of ketodiol **68** of 10% and an *ee* of 70%,<sup>[85]</sup> at 50 mM concentration of benzaldehyde. D469T previously gave a yield of 2% at 50 mM concentration of benzaldehyde.<sup>[85]</sup> Testing D469T at a lower substrate concentration of benzaldehyde of 25 mM, but maintaining the concentration of HPA at 50 mM, gave an isolated yield of 12% of **68** without affecting the stereoselectivity. Stereoselectivities were assessed by chiral HPLC analysis of mono-benzoate ester derivatives.

**Table 5.6 Isolated yields and stereoselectivities obtained for the transformation of benzaldehyde by S385X/D469T/R520Q†**

c1ccc(cc1)C=O (8) + OC(CC(=O)[O-])O (23)  $\xrightarrow[\text{CO}_2]{\text{TK, ThDP, Mg}^{2+}}$  c1ccc(cc1)C(O)C(=O)CO (68)

F434A <sup>[85]</sup>	D469T	D469T R520Q	S385T D469T/R520Q	S385Y D469T/R520Q	S385E D469T/R520Q
Yield ( <i>ee</i> )	Yield ( <i>ee</i> )	Yield ( <i>ee</i> )	Yield ( <i>ee</i> )	Yield ( <i>ee</i> )	Yield ( <i>ee</i> )
‡10%	12%	7%	34%	30%	33%
(70%)	(70%)	(54%)	(98%)	(97%)	(37%)
	‡2% <sup>[85]</sup>				

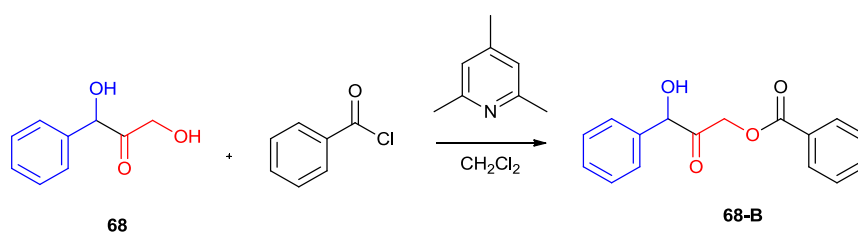
†Reactions were performed in duplicate and consistent yields and *ees* were observed. Reaction conditions: 25 mM benzaldehyde, 50 mM Li-HPA, 4 mL TK cell-free lysate, 20 mL total reaction volume, 18 hour reaction time. ‡50 mM concentration of aldehyde.

D469T/R520Q had not previously been studied with benzaldehyde as a substrate, and gave a 7% isolated yield of **68** formed with an *ee* of 54%, both values lower than for D469T. Interestingly, D469Y/R520Q had only given a 2% yield of the racemic

\* Protein concentrations were determined by Panwajee Payongsri who also created all of the TK mutants used in this chapter.

ketodiol **68** (Table 5.1), so some stereoselectivity with D469T/R520Q was encouraging. S385T/D469T/R520Q, which was shown to be the most active mutant when screened with 3-HBA, gave a dramatically increased isolated yield of **68** of 34%, representing a 3-fold increase in yield over D469T. This triple mutant also gave an unprecedented level of stereoselectivity, forming ketodiol **68** in an excellent 98% *ee*. S385Y/D469T/R520Q had displayed a similar activity as S385E/D469T/R520Q for 3-HBA, and indeed performed similarly with benzaldehyde, with an isolated yield of **68** of 30%. This mutant was also highly stereoselective forming the product (**68**) in an excellent 97% *ee*. The final triple mutant, S385E/D469T/R520Q had shown half the specific activity of the other two triple mutants for 3-HBA, however with benzaldehyde this mutant gave a comparable isolated yield of ketodiol **68** of 33%. Disappointingly, however, this mutant lost the high degree of stereoselectivity shown by the other two triple mutants, forming the product (**68**) in only 37% *ee*.

The stereoselectivity of these reactions was assessed by chiral HPLC analysis of the mono-benzoate ester derivatives (**68-B**) (Scheme 5.1) of the reaction product. A racemic standard was prepared using the previously reported biomimetic reaction, and then mono-benzoylated in the same fashion as previously described (Scheme 5.1).<sup>[79, 85]</sup>



**Scheme 5.1** Monobenzoylation of ketodiol (**68**) for chiral HPLC analysis

Good separation of both enantiomers was achieved using a Chiralpak AD column with a solvent system of 90:10 (*n*-hexane:isopropanol, 1 mL/min) and detection at 214 nm. The purified biotransformation products (**68**) from all mutants were then derivatised in the same fashion and analysed using the chiral HPLC method developed for the racemic sample. HPLC traces of **68-B** derived from the racemic reaction (Figure 5.13. A), and the two best performing mutants, are shown (Figure 5.13, B and C).

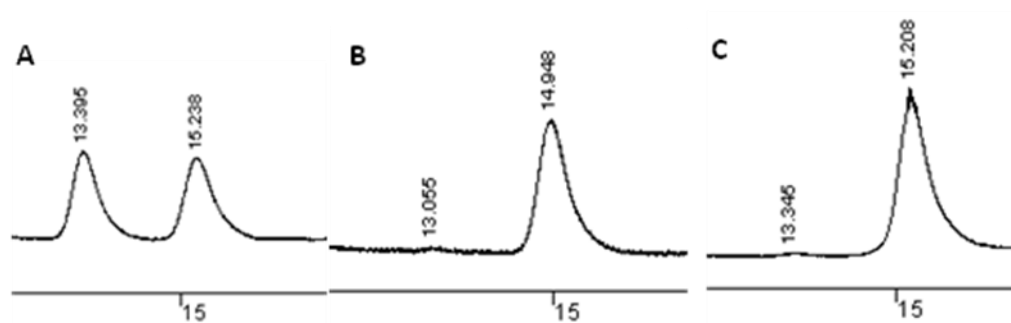


**Figure 5.13** Chiral HPLC traces for mono-benzoate derivatives (**68-B**) of ; **A** - racemic product, **B** - S385T/D469T/R520Q product, **C** - S385Y/D469T/R520Q product. (Elution time shown in minutes).

The exquisite stereoselectivities demonstrated by S385T/D469T/R520Q and S385Y/D469T/R520Q for the formation of ketodiol (**68**) from benzaldehyde were very pleasing, especially since these triple mutants had been engineered and selected solely to improve the activity of TK toward aromatic substrates, and not to improve stereoselectivity.

In an attempt to rationalise the dramatic increases in yield and stereoselectivity observed for these mutants with benzaldehyde, computational docking of benzaldehyde was carried out with S385T/D469T/R520Q, which was created by *in silico* mutagenesis.\* Unfortunately, the docking results were similar to previous results obtained from docking with benzaldehyde. Extensive non-specific binding was observed, with 12 different clusters found by Autodock, the most populated of which showed benzaldehyde docked in a non-productive conformation (Figure 5.14).

\* *In silico* mutagenesis was performed by Panwajee Payongsri

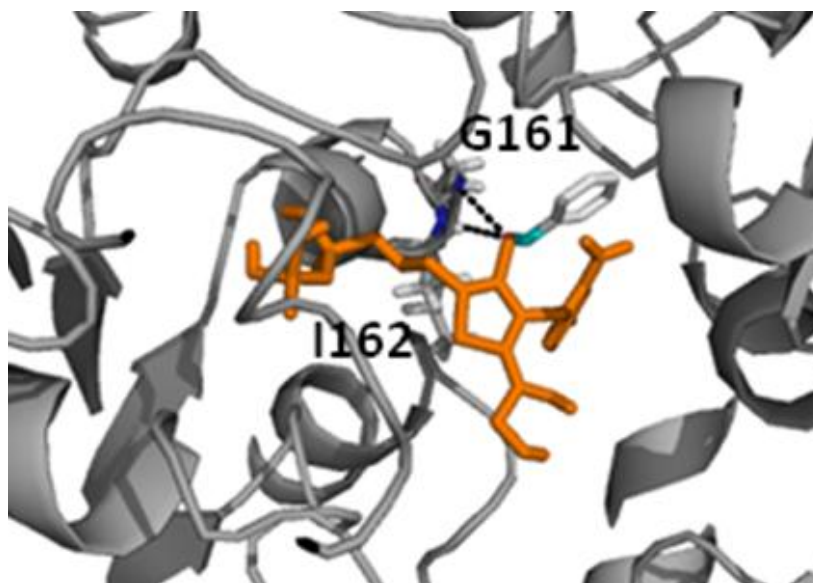
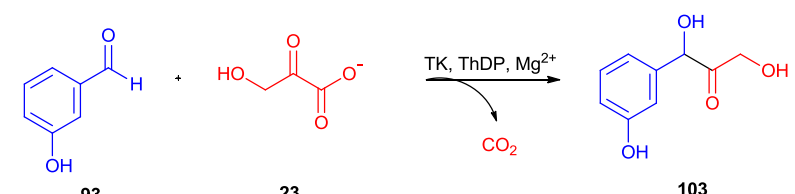


**Figure 5.14** Most populated conformation found for docking of benzaldehyde into S385T/D469T/R520Q. (Non-productive conformation shown in white, ThDP-enamine shown in orange).

This cluster showed non-specific binding of the benzaldehyde molecule with the protein backbone at residues G161 and I162, approximately 12 Å behind the ThDP-enamine, far from the active-site. This again demonstrated the limitations of using computational docking when studying molecules which exhibit low affinity for the TK active-site. The increased activity of these triple mutants with benzaldehyde might therefore be due to more efficient catalysis, and faster turnover rather than increased affinity, although this cannot be concluded definitively without further kinetic data.

The next substrate tested in scaled-up biotransformations with these triple mutants was 3-HBA (**93**, Table 5.7). This substrate had been used to screen this mutant library, and largely increased specific activities were noticed compared to D469T. Previous work had identified F434A as the most active single mutant towards 3-HBA with a yield of 6% forming the ketodiol product (**103**) in 53% *ee*.<sup>[85]</sup> D469T had given 4% yield of racemic **103**.<sup>[85]</sup> Both of these reactions had been performed at 50 mM concentration of 3-HBA. Performing the reaction with D469T at 25 mM concentration of 3-HBA gave no product whatsoever, so all the other mutants were tested at the higher concentration of 50 mM of 3-HBA and isolated yields and stereoselectivities obtained (Table 5.7).

**Table 5.7 Isolated yields and stereoselectivities obtained for the transformation of 3-HBA (93) by S385X/D469T/R520Q mutants\***



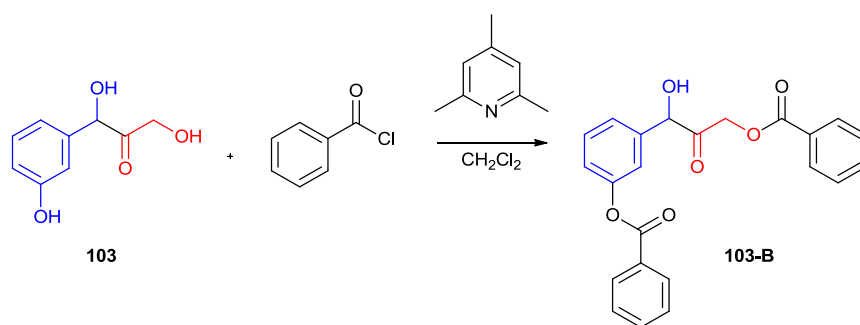
F434A <sup>[85]</sup>	D469T	D469T R520Q	S385T D469T/R520Q	S385Y D469T/R520Q	S385E D469T/R520Q
Yield ( <i>ee</i> )	Yield ( <i>ee</i> )	Yield ( <i>ee</i> )	Yield ( <i>ee</i> )	Yield ( <i>ee</i> )	Yield ( <i>ee</i> )
6% (53%)	3% (0%) 4% <sup>[85]</sup>	5% (0%)	7% (50%)	3% (55%)	2% (60%)

\*Reactions were performed in duplicate and consistent yields and *ees* were observed. Reaction conditions: 50 mM aldehyde, 50 mM Li-HPA, 4 mL TK cell-free lysate, 20 mL total reaction volume, 18 hour reaction time.

S385T/D469T/R520Q had been shown to give a 12-fold increase in specific activity with 3-HBA compared to D469T. However, only a slightly increased isolated yield was observed of 7% compared to 3% for D469T. However, whereas D469T formed the product as a racemic mixture, S385T/D469T/R520Q formed the ketodiol product (**103**) in 50% *ee*. The other triple mutants behaved similarly to S385T/D469T/R520Q, albeit with slightly lower yields. S385Y/D469T/R520Q had been shown to increase the specific activity with 3-HBA 12-fold compared to D469T, but gave ketodiol **103** in an isolated yield of only 3%. However, this mutant showed some stereoselectivity forming the product (**103**) in 55% *ee*, slightly increased from S385T/D469T/R520Q. S385E/D469T/R520Q showed the lowest specific activity of the triple mutants, with only a 6-fold increase compared to D469T, however it gave a comparable isolated yield of 2%. This triple mutant was the most stereoselective for 3-HBA, forming the product in 60% *ee*.

The stereoselectivity of these transformations was once again assessed by chiral HPLC analysis of benzoate ester derivatives. In this case since the phenolic proton was more acidic than the primary alcohol so the dibenzoate ester was prepared (**103-B**), (Scheme 5.2). The racemic standard was prepared using the biomimetic TK reaction, and dibenzoate ester prepared as previously described.<sup>[85]</sup>





**Scheme 5.2** Di-benzoylation of ketodiol (103) for chiral HPLC analysis.

Good separation of both enantiomers was achieved with a Chiralpak AD column, with a solvent system of 20:80 (*n*-hexane:isopropanol, 1 mL/min). HPLC traces of the racemic product and the product from S385T/D469T/R520Q are shown (Figure 5.15).

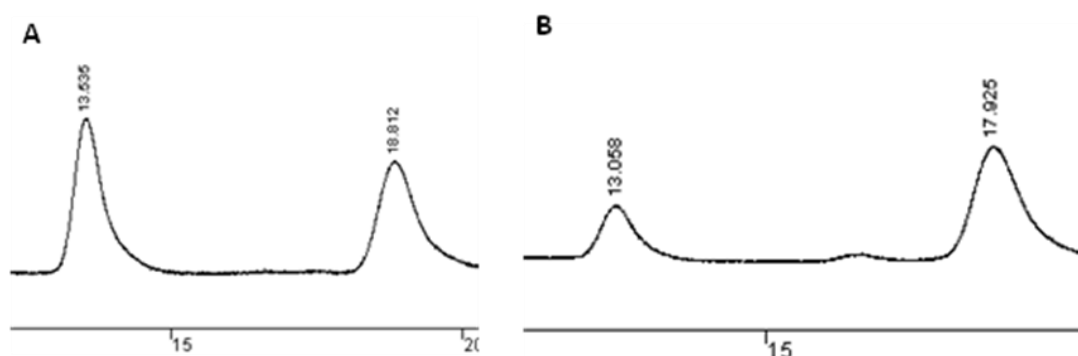


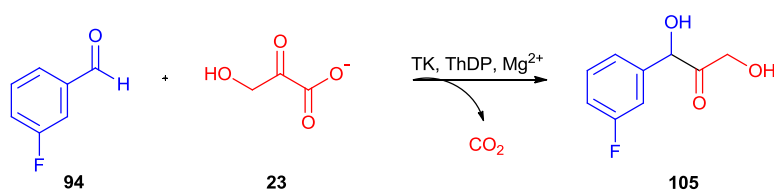
**Figure 5.15** Chiral HPLC traces of di-benzoylated derivatives (103-B) of; **A** - racemic product, **B** - S385T/D469T/R520Q product. Elution times are shown in minutes.

Previous docking of 3-HBA into S385Y/D469T/R520Q had not been productive, with non-specific binding of the substrate to the protein backbone, and to residues outside of the enzyme active-site extensively demonstrated. Hence, this substrate was not investigated in any further computational docking.

Whilst these triple mutants did not increase the isolated yields with 3-HBA, it should be noted that initial studies with 3-HBA and single mutants required 48 hour reaction times,<sup>[85]</sup> whereas the triple mutant reactions were run for only 18 hours. Also, while not increasing isolated yields the triple mutants were far more stereoselective than previous single mutants,<sup>[85]</sup> giving products with *ees* >50%. This was very encouraging, so a further range of functionalised benzaldehydes were assessed in scaled-up biotransformations.

3-Fluorobenzaldehyde (**94**) (Table 5.8) had not been previously investigated with transketolase, but had been investigated in the asymmetric biomimetic reaction where low yields (<5%) were observed (Chapter 2).<sup>[79]</sup> The yields and stereoselectivities of ketodiol **105** from a range of single and combination mutant TKs were obtained (Table 5.8). Since the use of 25 mM concentration of benzaldehyde had been shown to reduce substrate inhibition for the S385X/D469T/R520Q mutants a 25 mM concentration of 3-fluorobenzaldehyde was used for all of the biotransformations.

**Table 5.8 Isolated yields and stereoselectivities obtained for the transformation of 3-fluorobenzaldehyde (**93**) by S385X/D469T/R520Q mutants\***



F434A	D469T	D469T	S385T	S385Y	S385E
Yield	Yield	R520Q	D469T/R520Q	D469T/R520Q	D469T/R520Q
( <i>ee</i> )	( <i>ee</i> )	Yield ( <i>ee</i> )	Yield ( <i>ee</i> )	Yield ( <i>ee</i> )	Yield ( <i>ee</i> )
ND	12%	8%	12%	10%	11%
	(20%)	(78%)	(70%)	(64%)	(90%)

\*Reactions were performed in duplicate and consistent yields and *ees* were observed. Reaction conditions: 25 mM aldehyde, 50 mM Li-HPA, 4 mL TK cell-free lysate, 20 mL total reaction volume, 18 hour reaction time.

D469T gave a 12% isolated yield of ketodiol (**105**), the same yield as obtained for the transformation of benzaldehyde by this mutant (Table 5.6). However, a much lower stereoselectivity of 20% *ee* was observed compared to the transformation with benzaldehyde. D469T/R520Q gave a slightly reduced yield of **105** of 8%, but gave a large increase in stereoselectivity to 78% *ee*. This was greater than when the same mutant was used to transform both benzaldehyde (Table 5.6) and 3-hydroxybenzaldehyde (Table 5.7). S385T/D469T/R520Q gave the same isolated yield of **105** as for D469T, but again gave a large increase in stereoselectivity compared to D469T, with a product *ee* of 70%, though this was slightly disappointing given the 98% *ee* for this mutant when benzaldehyde was used as the substrate (Table 5.6). S385Y/D469T/R520Q performed similarly to

S385T/D469T/R520Q, with a slightly reduced product (**105**) yield of 10%, and slightly reduced stereoselectivity of 64% *ee*. S385E/D469T/R520Q gave a similar yield as the other two triple mutants, with an isolated yield of ketodiol (**105**) of 11%. Interestingly, although this mutant was not highly stereoselective with benzaldehyde, forming ketodiol **68** with an *ee* of only 37%, with 3-fluorobenzaldehyde S385E/D469T/R520Q was highly stereoselective, forming **105** with an *ee* of 90%. This suggests that 3-fluorobenzaldehyde could adopt a different binding mode to benzaldehyde with S385E/D469T/R520Q, giving rise to a much higher degree of stereoselectivity. It is also possible that the electron withdrawing effects of the 3-fluoro substituent could be responsible for tighter binding, increasing the stereoselectivity of the transformation.

Stereoselectivities were determined by chiral HPLC analysis of mono-benzoate ester derivatives (**105-B**) of biotransformation product (**105**) and racemic **105** as carried out as for benzaldehyde, and as previously described (Chapter 2).<sup>[79]</sup> Benzoylated derivatives (**105-B**) from the biomimetic reaction (Figure 5.16, A) and S385Y/D469T/R520Q and S385E/D469T/R520Q reaction products (Figure 5.16, B and C) are shown below.

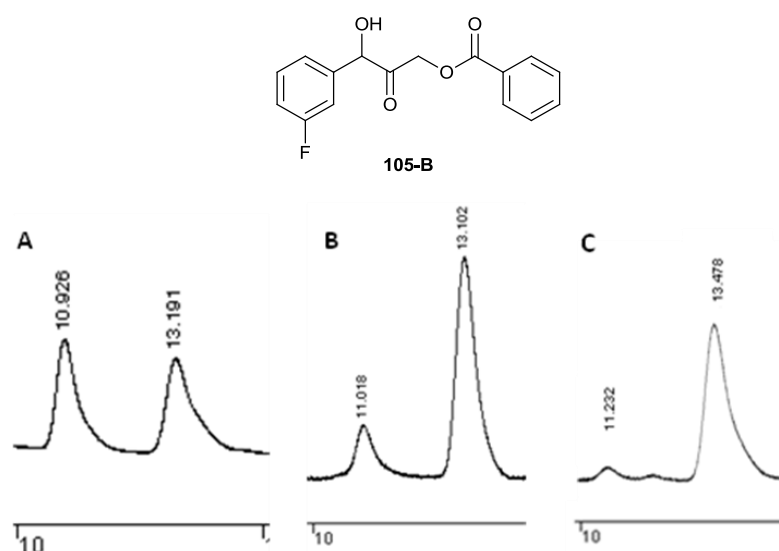
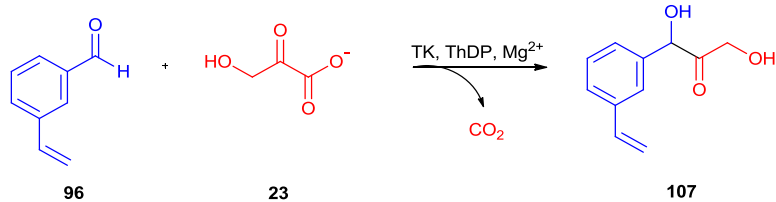


**Figure 5.16** Chiral HPLC traces of mono-benzoylated derivatives (**105-B**) of; **A** - Racemic product, **B** - S385Y/D469T/R520Q product, **C** - S385E/D469T/R520Q product. Elution times are shown in minutes.

A more lipophilic substrate was then tested with these combination mutants. 3-Vinylbenzaldehyde (**96**) (Table 5.9) had not been previously reported as substrate for

the TK reaction. It is an interesting substrate as it contains a vinyl group which can act as a synthetic handle, for example, in cross metathesis reactions. This substrate was at a concentration of 25 mM and isolated yields and stereoselectivities of ketodiol **107** were obtained where possible (Table 5.9).

**Table 5.9 Isolated yields and stereoselectivities obtained for the transformation of 3-vinylbenzaldehyde (96) by S385X/D469T/R520Q mutants\***



	96	23	107			
	F434A	D469T	D469T	S385T	S385Y	S385E
	Yield	Yield	R520Q	D469T/R520Q	D469T/R520Q	D469T/R520Q
	( <i>ee</i> )	( <i>ee</i> )	Yield ( <i>ee</i> )	Yield ( <i>ee</i> )	Yield ( <i>ee</i> )	Yield ( <i>ee</i> )
	ND	2%	4%	4%	5%	Trace
		(0%)	(0%)	(84%)	(90%)	

\*Reactions were performed in duplicate and consistent yields and *ees* were observed. Reaction conditions: 25 mM aldehyde, 50 mM Li-HPA, 4 mL TK cell-free lysate, 20 mL total reaction volume, 18 hour reaction time.

All of the mutants gave comparable yields of product (**107**) of <5%. D469T showed least activity toward the substrate, with only a 2% yield of racemic **107** isolated. D469T/R520Q showed a similar activity with a 4% yield of racemic product (**107**) isolated. However, S385T/D469T/R520Q and S385Y/D469T/R520Q both exhibited some stereoselectivity giving isolated yields of 4% and 5% of ketodiol **107** respectively, with product *ees* of 84% and 90%. S385E/D469T/R520Q only showed traces of **107** by TLC analysis, and no product could be isolated. The low isolated yields observed for all mutants are perhaps not surprising, given that this substrate was poorly soluble in water even at 25 mM concentration. However, the stereoselectivities exhibited by S385T/D469T/R520Q and S385Y/D469T/R520Q were once again very encouraging.

Since ketodiol **107** was a new analogue, chiral HPLC analysis methods had to be established. The same HPLC method as used for both the benzaldehyde and 3-fluorobenzaldehyde mono-benzoylated products (**68-B**, **105-B**) gave good separation of both enantiomers of the mono-benzoylated derivative (**107-B**) of ketodiol **107**.

The chiral HPLC traces of both the racemic mono-benzoylated biomimetic product (Figure 5.17, A) and S385Y/D469T/R520Q product (Figure 5.17, B) are shown.

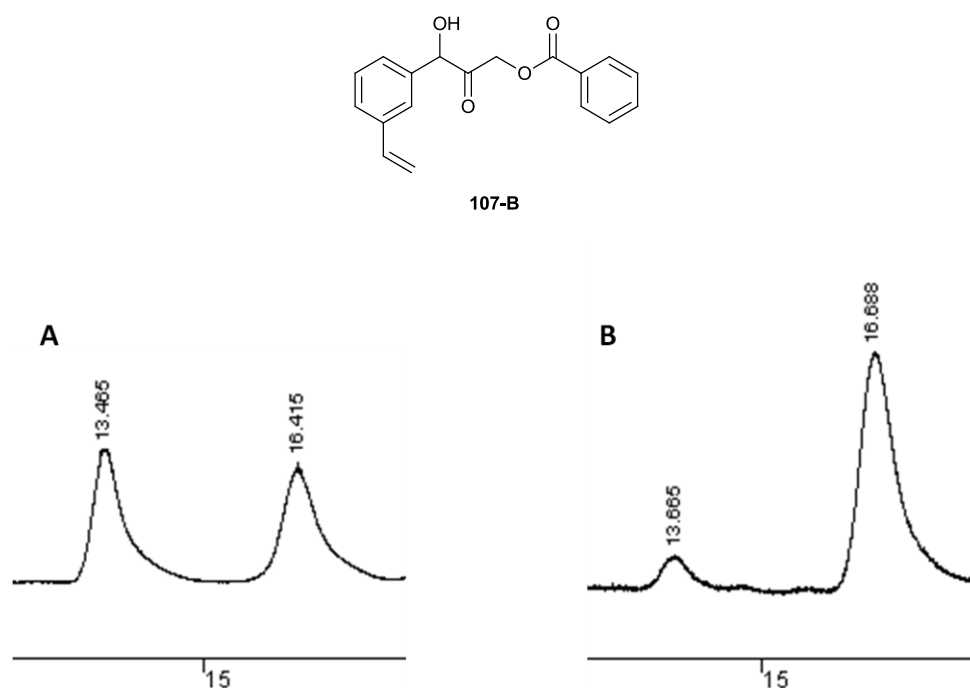


**Figure 5.17** Chiral HPLC traces of mono-benzoylated derivatives (107-B) of; A - Racemic product, B - S385Y/D469T/R520Q product.

It appeared that meta-substituted benzaldehydes were well tolerated by this family of S385X/D469T/R520 mutant enzymes, whether in terms of isolated yields, stereoselectivities, or both. To probe this tolerance further, a more bulky substrate, methyl-3-formylbenzoate (**95**), which had been investigated in the asymmetric biomimetic TK reaction,<sup>[79]</sup> was tested as a substrate (Table 5.10). Since these mutants were developed based on phosphate binding interactions with 3-formylbenzoic acid, it was thought that the methyl ester variant of this substrate should be tolerated, albeit to a lesser extent due to the absence of an acid group. Isolated yields and stereoselectivities were established at 25 mM concentration to avoid substrate inhibition (Table 5.10).

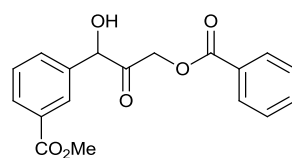
**Table 5.10 Isolated yields and stereoselectivities obtained for the transformation of methyl-3-formylbenzoate (**95**) by S385X/D469T/R520Q mutants\***

95		23		106	
F434A	D469T	D469T	S385T	S385Y	S385E
Yield	Yield	R520Q	D469T/R520Q	D469T/R520Q	D469T/R520Q
( <i>ee</i> )	( <i>ee</i> )	Yield ( <i>ee</i> )	Yield ( <i>ee</i> )	Yield ( <i>ee</i> )	Yield ( <i>ee</i> )
ND	Trace	Trace	34%	9%	Trace
			(96%)	(72%)	

\*Reactions were performed in duplicate and consistent yields and *ees* were observed. Reaction conditions: 25 mM aldehyde, 50 mM Li-HPA, 4 mL TK cell-free lysate, 20 mL total reaction volume, 18 hour reaction time.

D469T and D469T/R520Q gave only trace amounts of **106**, observed by TLC analysis, and no product could be isolated for either mutant. This was disappointing, given that D469T had one of the highest observed specific activities towards the related substrate, 3-FBA,<sup>[91]</sup> suggesting that in this case the methyl ester did not interact productively with the phosphate binding region. Interestingly, S385T/D469T/R520Q gave a large increase in isolated yield, giving a 34% yield of ketodiol product (**106**). This mutant was also highly stereoselective, forming **106** in 96% *ee*. S385Y/D469T/R520Q on the other hand only gave a 9% isolated yield of **106**, and showed a decrease in stereoselectivity, with a product *ee* of 72%. Once again, as for 3-vinylbenzaldehyde (**96**), S385E/D469T/R520Q formed only trace amounts of product, indicating that this mutant was not as tolerant to meta-substituents as the other triple mutants.

The chiral analysis of these compounds was carried out as previously described (Chapter 2).<sup>[79]</sup> Good separation of enantiomers was achieved using a chiralpak AD column with a solvent system of 90:10 (*n*-hexane:isopropanol, 1 mL/min) with detection at 214 nm. Racemic **106** was prepared using the biomimetic reaction. HPLC traces of the mono-benzoate esters (**106-B**) of racemic **106** (Figure 5.18, A) and **106** from the S385T/D469T/R520Q reaction (Figure 5.18, B) are shown.



106-B

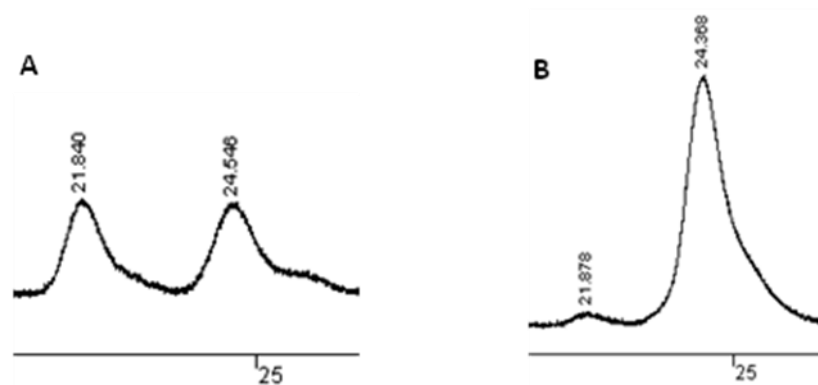


**Figure 5.18** Chiral HPLC traces of mono-benzoylated derivatives (106-B) of; **A** - racemic product, **B** - S385T/D469T/R520Q product

The increases in yield and stereoselectivity observed for methyl-3-formylbenzoate with S385T/D469T/R520Q compared to all of the other mutants was very interesting and so further investigation with computational docking was carried out. Firstly, methyl-3-formylbenzoate was docked into the structure of D469T with the ThDP-enamine intermediate already in place. D469T had only formed trace amounts of product with this substrate, and four main clusters were observed, with the lowest in energy being the most populated. This cluster contained the only productive conformations, where the ester group formed hydrogen bonding interactions with R358, S385 and R520 (Figure 5.19, A). These interactions held the aldehyde in a productive conformation pointing toward the ThDP enamine at a distance of 4.1 Å from the ThDP enamine, which was closer than computationally predicted for this mutant and 3-FBA, for which excellent conversions were observed.<sup>[91]</sup> The second cluster found by the docking program showed similar interactions as the first cluster, but in this case the aldehyde was flipped into a non-productive conformation where it was stabilised by L466 (Figure 5.19, B). The third cluster showed similar interactions to the previous two clusters, but the hydrogen bond between the substrate and S385 was lost, pointing the aldehyde away from the ThDP enamine at an increased distance of 8.1 Å (Figure 5.19, C). The final cluster showed the ester group of the methyl-3-formylbenzoate substrate forming hydrogen bond interactions

with H26 and one of the diols on the ThDP-enamine intermediate, pointing the aldehyde out of the active-site where it formed a hydrogen bond interaction with the protein backbone of G25 (Figure 5.19, D). The existence of so many non-productive binding modes could explain the low product yield observed for D469T.

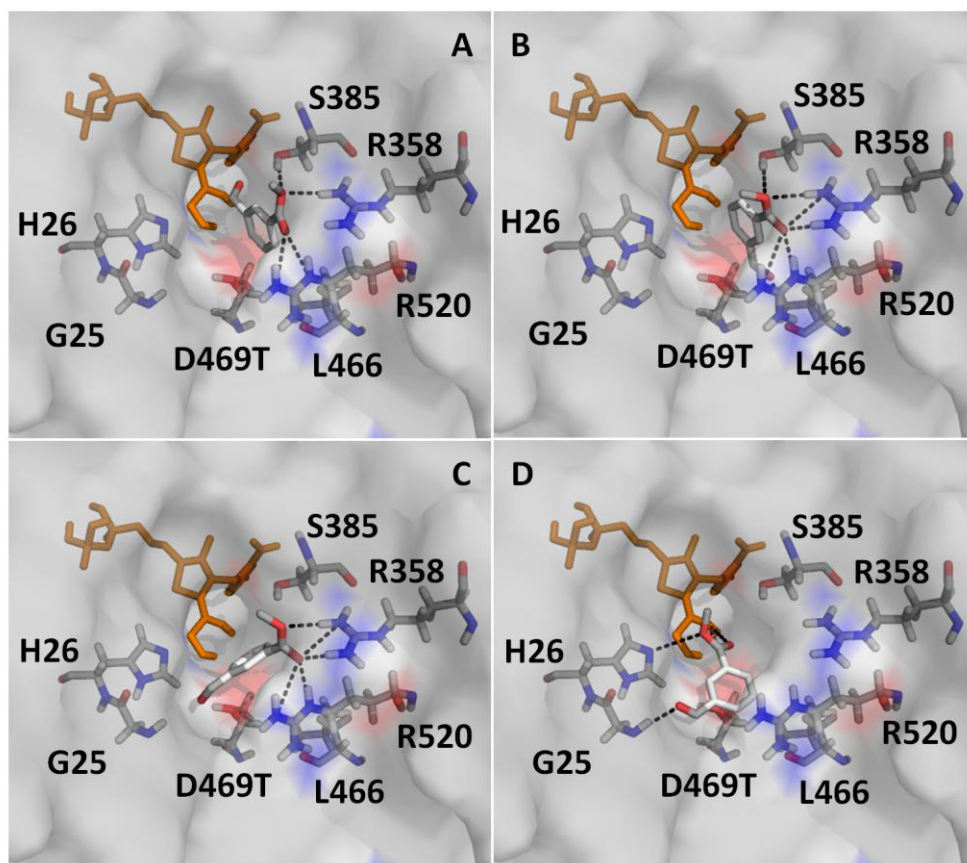


**Figure 5.19 Results obtained for docking of methyl-3-formylbenzoate (95) into D469T. A- Lowest energy, most highly populated cluster showing productive conformation, B-Second cluster showing non-productive conformation, C-Third cluster showing non-productive conformation, D-Fourth cluster showing non-productive conformation.**

Computational docking of methyl-3-formylbenzoate (**95**) into S385T/D469T/R520Q was then carried out, to try to rationalise such an improved tolerance with this mutant. The docking program gave two highly populated, low energy clusters, both of which showed productive conformations (Figure 5.20).



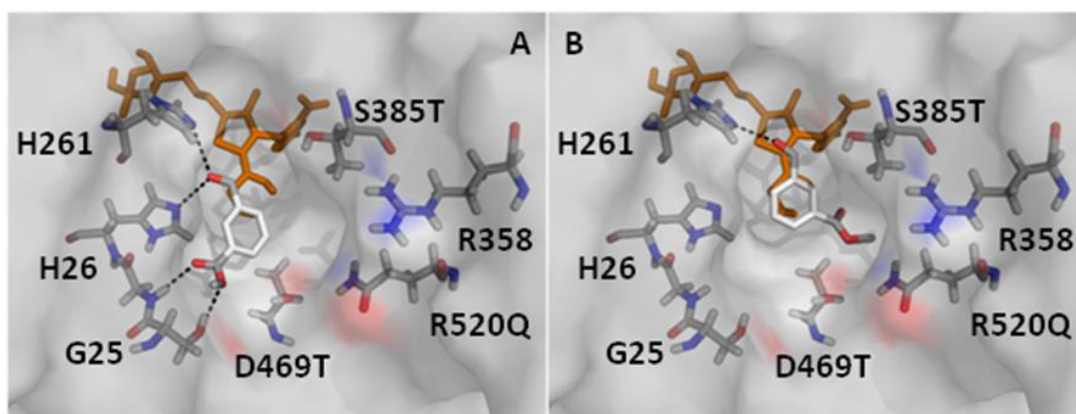


**Figure 5.20 Results obtained for docking of methyl-3-formylbenzoate into S385T/D469T/R520Q. A - First low-energy, highly populated cluster, showing productive conformation, B - Second low-energy, highly populated cluster showing productive conformation**

In contrast to the productive cluster found when docking methyl-3-formylbenzoate into D469T (Figure 5.19, A), in S385T/D469T/R520Q the first productive cluster showed hydrogen bonding interactions not between the ester group of the substrate and the phosphate binding region, but between the ester group and G25 (Figure 5.20, A). The aldehyde moiety also formed additional hydrogen bonds with H26 and H261, holding it in position directly above the ThDP-enamine at a distance of 4.8 Å. Interestingly, studies of WT-TK with aliphatic aldehydes had given similar yields as S385T/D469T/R520Q and methyl-3-formylbenzoate, and computational docking studies of aliphatic aldehydes with WT-TK had identified a similar binding mode, with the aldehyde oxygen atom held in position by H26 and H261.<sup>[26]</sup> This interaction could therefore be responsible for the increase in yield for methyl-3-formylbenzoate with S385E/D469T/R520Q. In the other productive cluster (Figure 5.20, B) the ester group was directed towards the phosphate binding region, but at too great a distance to form hydrogen bonding interactions. However, the aldehyde was again held directly above the ThDP-enamine intermediate, stabilised by a hydrogen bond with H261, at a slightly reduced distance of 4.7 Å. It is possible that the existence of these two productive binding modes for S385T/D469T/R520Q could explain the increased isolated yields for methyl-3-formylbenzoate compared to D469T, where only 1 productive cluster was found. Also, the interactions of the aldehyde with H26 and H261, as found for aliphatic aldehydes, may activate the

aldehyde moiety for nucleophilic attack by the ThDP-enamine intermediate, increasing turnover of the substrate.

Both D469T and D469T/R520Q had been observed to have good activities with 3-FBA (**97**).<sup>[91]</sup> This substrate had then been used to screen the S385X/D469T/R520Q library (Section 5.4), and so was used as a substrate in scaled-up biotransformations (Table 5.11). Despite substrate inhibition being observed above 40 mM, good conversions were still observed at 50 mM, and so this concentration of substrate was used. It was observed that ketodiols **108** was difficult to isolate and prone to rearrangement. Hence, for ease of isolation, conversion yields were assessed by the <sup>1</sup>H-NMR spectroscopy analysis of peaks corresponding to **108** formation and the crude product was then subjected to the standard benzylation procedure. Here, the di-benzoate esters were formed and then isolated and analysed by chiral HPLC to determine stereoselectivities (Table 5.11).

**Table 5.11 Conversions and stereoselectivities obtained for the transformation of 3-FBA (**97**) by S385X/D469T/R520Q mutants\***

Reaction scheme: 3-FBA (**97**) + 3-hydroxybutyrate (**23**)  $\xrightarrow[\text{CO}_2]{\text{TK, ThDP, Mg}^{2+}}$  3-hydroxy-3-phenylbutanoic acid (**108**)

F434A	D469T	D469T R520Q	S385T D469T/R520Q	S385Y D469T/R520Q	S385E D469T/R520Q
Conv. ( <i>ee</i> )	Conv. ( <i>ee</i> )	Conv. ( <i>ee</i> )	Conv. ( <i>ee</i> )	Conv. ( <i>ee</i> )	Conv. ( <i>ee</i> )
ND	100% <sup>†</sup> (62%)	70% (56%)	78% (49%)	87% (45%)	73% (0%)

\*Reactions were performed in duplicate and consistent yields and *ees* were observed. Reaction conditions: 50 mM aldehyde, 50 mM Li-HPA, 4 mL TK cell-free lysate, 20 mL total reaction volume, 18 hour reaction time.<sup>†</sup> No aldehyde proton could be observed

The conversion yields obtained were excellent for all of the mutants (Table 5.11). After 18 hours no starting aldehyde could be observed when using D469T, which was consistent with the high activities for this mutant with 3-FBA (section 5.2). D469T/R520Q gave a conversion yield of **108** of 70%, consistent with the lower specific activity reported compared to D469T.<sup>[91]</sup> S385T/D469T/R520Q and S385Y/D469T/R520Q gave comparable conversion yields of **108** of 78% and 87%,

again consistent with their lower specific activities compared to D469T. S385E/D469T/R520Q had an almost 2-fold higher specific activity than D469T for 3-FBA, so was expected to perform well. Disappointingly, however, this mutant gave a lower conversion yield of **108** of 73%. This was not due to substrate inhibition, as S385E/D469T/R520Q had been screened with aldehyde concentrations up to 90 mM and no substrate inhibition had been observed (Section 5.4). Also, S385E/D469T/R520Q was shown to give a nearly 6-fold increase in turnover compared to D469T, so reaction time should not have been an issue. The limited yield could potentially have been caused by lower expression levels of S385E/D469T/R520Q. The stereoselectivities for all of the mutants were very disappointing, especially considering the excellent conversions. This could possibly be due to analytical methods and rearrangement of the product during derivatisation, as previously observed for several other aromatic ketodiols.<sup>[85]</sup> Indeed, the electron withdrawing effects of the carboxylate substituent would be expected to promote rearrangement of these products, causing racemisation. Rearranged products were indeed observed in <sup>1</sup>H-NMR spectra of crude biotransformation reactions, especially after extended reaction times. Dibenzoylated products (**108-B**) were used in chiral HPLC analyses, using a method developed by analysis of the dibenzoylated racemate generated from the biomimetic reaction. Good separation of isomers was achieved using a Chiralpak AD column and a solvent system of 77:23 (*n*-hexane:isopropanol, 1 mL/min, 214 nm). The chiral HPLC traces of the racemate (Figure 5.21, A) and S385Y/D469T/R520Q product are shown (Figure 5.21, B).

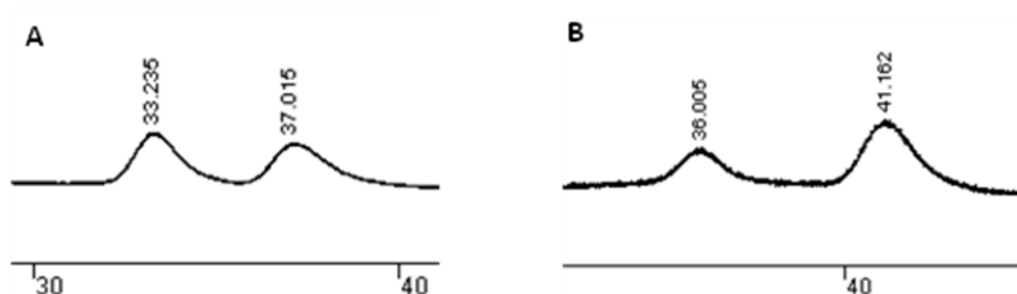
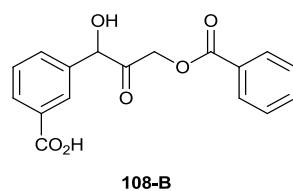


**Figure 5.21** Chiral HPLC traces of di-benzoylated derivatives (**108-B**) of; **A** - Racemic product, **B** - S385Y/D469T/R520Q product

3-Formylbenzonnitrile (**18**) (Table 5.12) had not been previously studied with TK and so was investigated with the new combination mutants and isolated yields and stereoselectivities of ketodiols (**110**) were determined (Table 5.12).

**Table 5.12** Isolated yields and stereoselectivities obtained for the transformation by S385X/D469T/R520Q mutants\*

	18	23	110			
Aldehyde	F434A	D469T	D469T	S385T	S385Y	S385E
	Yield	Yield	R520Q	D469T/R520Q	D469T/R520Q	D469T/R520Q
	( <i>ee</i> )	( <i>ee</i> )	Yield ( <i>ee</i> )	Yield ( <i>ee</i> )	Yield ( <i>ee</i> )	Yield ( <i>ee</i> )
<b>R=3-CN</b>	ND	Trace	Trace	10%	26%	Trace
				(90%)	(91%)	

\*Reactions were performed in duplicate and consistent yields and *ees* were observed. Reaction conditions: 25 mM aldehyde, 50 mM Li-HPA, 4 mL TK cell-free lysate, 20 mL total reaction volume, 18 hour reaction time.

Neither D469T, D469T/R520Q, or S385E/D469T/R520Q gave any isolable quantities of ketodiol product (**110**), with only trace amounts seen by TLC analysis. S385T/D469T/R520Q however, gave 10% yield of product (**110**), and demonstrated excellent stereoselectivity with an *ee* of 90%. S385Y/D469T/R520Q performed even

better, with an isolated yield of 26% of ketodiol **110** and again excellent stereoselectivity with a product *ee* of 91%. Racemic **110** was prepared using the biomimetic reaction, mono-benzoylated (**110-B**) and then used to develop a chiral HPLC method. Good separation of both enantiomers was achieved using a Chiralpak AD column and a solvent system of 90:10 (*n*-hexane:isopropanol, 1mL/min, 214 nm). The chiral HPLC traces of racemic product **110-B** (Figure 5.22, A) and **110-B** derived from S385T/D469T/R520Q and S385Y/D469T/R520Q products (Figure 5.22, B and C) are shown below.

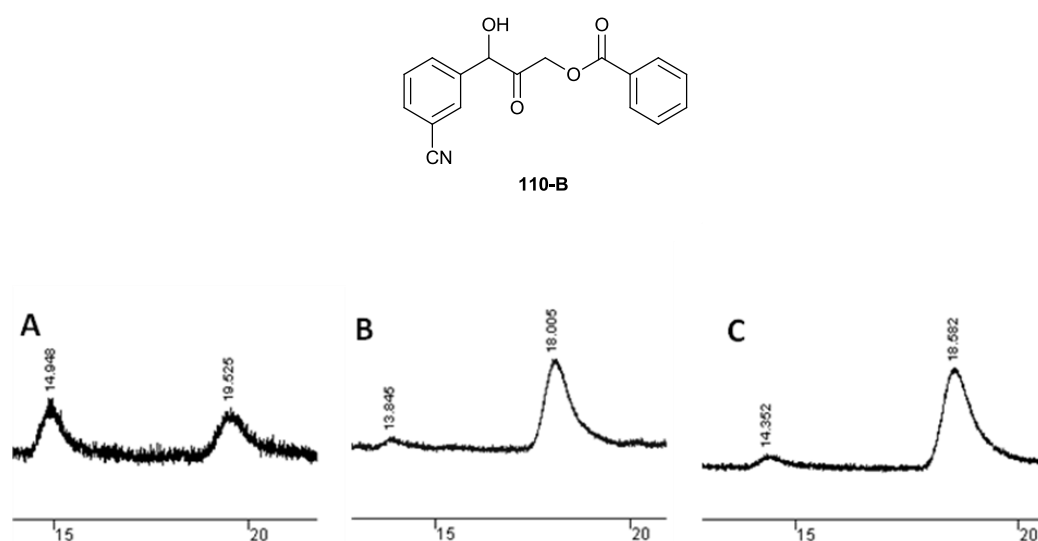


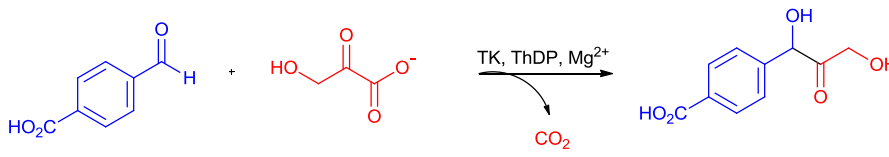
**Figure 5.22** Chiral HPLC traces of monobenzoylated derivatives (**110-B**) of; **A** - Racemic product, **B** - S385T/D469T/R520Q product, **C** - S385Y/D469T/R520Q product

The acceptance of this substrate was interesting, especially since the nitrile moiety could act as a synthetic handle to introduce more functionality to the ketodiol product (**110**).

A wide-range of *meta*-substituted benzaldehydes had been screened, so it was decided to also test some *para*-substituted benzaldehydes as substrates in the TK reaction with these combination mutants. 4-Formylbenzoic acid (**153**) (Table 5.13) had initially been screened with the library of triple mutants and >3 fold increases in specific activity were observed compared to D469T, so scaled-up biotransformations with 4-FBA to form ketodiol **154** were investigated (Table 5.13). The biotransformation product (**154**) was also found to be difficult to isolate due to its

high polarity, so conversion yields were calculated by  $^1\text{H-NMR}$  spectroscopy analysis.

**Table 5.13 Conversions obtained for the biotransformation of 4-FBA (**153**) by S385X/D469T/R520Q mutants\***



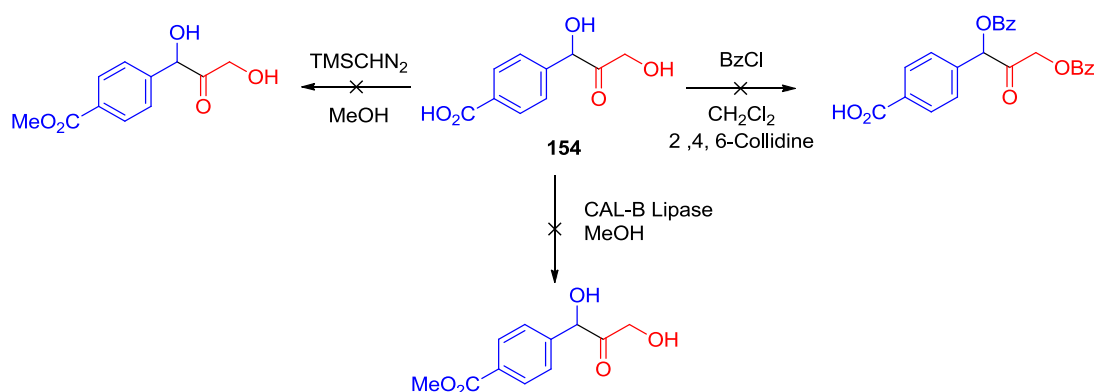
F434A	D469T	D469T R520Q	S385T D469T/R520Q	S385Y D469T/R520Q	S385E D469T/R520Q
Conversion	Conversion	Conversion	Conversion	Conversion	Conversion
ND	31%	42%	78%	56%	17%

\*Reactions were performed in duplicate and consistent yields and *ees* were observed. Reaction conditions: 50 mM aldehyde, 50 mM Li-HPA, 4 mL TK cell-free lysate, 20 mL total reaction volume, 18 hour reaction time.

D469T had already been reported to give a 30% conversion yield to **154** in small-scale biotransformations monitored by HPLC,<sup>[91]</sup> which was comparable to the 31% conversion yield of **153** observed for D469T upon scale-up. Interestingly, while D469T/R520Q was observed to decrease the conversion yield of **153** in the small-scale transformations, at a 20 mL scale an increased conversion yield to **154** of 42% was observed. S385T/D469T/R520Q was previously shown to give a 2-fold increase in specific activity with 4-FBA compared to D469T, and this was also represented by an increase in conversion yield of **153** to 78%, more than twice the conversion yield of D469T. S385Y/D469T/R520Q was shown to give the largest increase in specific activity for 4-FBA compared to D469T, but while the conversion yield observed was greater than that for D469T, at 56%, this was lower than that for S385T/D469T/R520Q. S385E/D469T/R520Q was previously shown to have severely impaired activity toward 4-FBA, with a 5-fold decrease in specific activity observed (Section 5.4). This decreased activity was also observed in a larger scale biotransformation, giving a conversion yield of 17%, lower than any of the other mutants.

Unfortunately, all attempts to derivatise the biotransformation product to allow purification and analysis of the stereoselectivities failed (Scheme 5.3). Standard acid catalysed ester formation was avoided to prevent the racemisation of the

stereocentre, which had been observed to be sensitive to acidic and basic conditions (Chapter 2). TMS-diazomethane has been shown to be an effective method to prepare methyl esters from carboxylic acids under mild conditions.<sup>[93, 94, 95]</sup> This method was attempted using crude biotransformation product but numerous attempts to protect the acid functionality of the ketodiol product (**154**) in this manner failed, despite using increasing amounts of reagent. Lipases have been identified as useful biocatalysts for the reversible formation of esters from carboxylic acids under mild conditions.<sup>[96]</sup> To assess the use of *Candida antarctica* lipase B (CAL-B) to protect the acid functionality of ketodiol **154**, it was first tested with 4-formylbenzoic acid. By stirring 50 mg of immobilized CAL-B in methanol with 20 mM concentration of 4-formylbenzoic acid, a quantitative conversion to methyl-4-formylbenzoate was observed. This was encouraging, and so the same procedure was used with crude biotransformation material. Unfortunately this was unsuccessful, and despite numerous repeats of the experiment with increased enzyme loadings no ester formation was observed, only formation of the rearranged ketodiol and methyl-4-formylbenzoate (formed from 4-FBA remaining in the crude biotransformation mixture) was observed. Attempts to derivatise the alcohol functionalities using standard benzylation methods were also unsuccessful (Scheme 5.3). Since writing this thesis a trimethylsilyl derivatisation method for polyol TK products has been published by the Hanefeld group, however the harsh conditions required would not be suitable for sensitive products such as **154**.<sup>[44]</sup>



**Scheme 5.3 Attempts to derivatise 4-FBA biotransformation product (**154**)**

The stereoselectivities in the 3-FBA biotransformation reaction had been observed to be fairly low (<65% *ee*), potentially due to the racemisation of product *in situ* or when derivatised, due to the electron withdrawing effects of the carboxylic acid functionality. The 4-FBA product (**154**) would be expected to racemise even more

readily, due to the position of the carboxylic acid functionality, increasing the acidity of the proton adjacent to the aromatic ring and making the product more susceptible to rearrangement. Thus, even if derivatisation had been possible, it is likely that the stereoselectivities that could be monitored would be even lower than those observed for the biotransformations of 3-FBA.

The final substrate investigated with these mutants was 4-(methylsulfonyl)benzaldehyde (**158**) (Table 5.14), a substrate which, if accepted by TK, would furnish a direct precursor to the antibiotic, thiamphenicol. Once again, the increased polarity of the ketodiol product (**159**) made it difficult to purify, so conversion yields were assessed by <sup>1</sup>H-NMR (Table 5.14) and crude material brought through to the benzylation reaction. Di-benzoate ester derivatives (**159-B**) were then isolated and analysed by chiral HPLC to determine the stereoselectivity of the ketodiol product (**159**).

**Table 5.14 Conversion yields and stereoselectivities obtained for the biotransformation of 4-methylsulfonylbenzaldehyde by S385X/D469T/R520Q mutants\***

	158	23			159
<b>F434A</b>	<b>D469T</b>	<b>D469T</b>	<b>S385T</b>	<b>S385Y</b>	<b>S385E</b>
<b>Yield</b>	<b>Yield</b>	<b>R520Q</b>	<b>D469T/R520Q</b>	<b>D469T/R520Q</b>	<b>D469T/R520Q</b>
<b>(ee)</b>	<b>(ee)</b>	<b>Yield (ee)</b>	<b>Yield (ee)</b>	<b>Yield (ee)</b>	<b>Yield (ee)</b>
ND	Trace	Trace	*49%	*20%	Trace
			(90%)	(70%)	

\*Reactions were performed in duplicate and consistent yields and *ees* were observed. Reaction conditions: 50 mM aldehyde, 50 mM Li-HPA, 4 mL TK cell-free lysate, 20 mL total reaction volume, 18 hour reaction time.

When both D469T and D469T/R520Q variants were used, only traces of **159** were observed by TLC analysis. S385T/D469T/R520Q had so far been the best performing mutant for benzaldehyde (34% yield of (**68**) in 98% *ee*), 3-hydroxybenzaldehyde (7% yield of (**103**) in 50% *ee*), 3-fluorobenzaldehyde (12% yield of (**105**) in 70% *ee*) and methyl-3-formylbenzoate (34% yield of (**106**) in 96% *ee*), and was also found to be the best performing mutant for 4-(methylsulfonyl)benzaldehyde with a 49% conversion yield and high degree of stereoselectivity



forming the product (**159**) in 90% *ee*. S385Y/D469T/R520Q had performed similarly to S358T/D469T/R520Q for most of the substrates, with similar yields and stereoselectivities observed, and this was also the case with 4-(methylsulfonyl)benzaldehyde where a slightly reduced conversion yield of 20% was observed along with a slightly reduced *ee* of (**159**) of 70%. S385E/D469T/R520Q had not been as tolerant as the other two triple mutants towards substituted benzaldehydes, and this was again observed with 4-methylsulfonylbenzaldehyde where only trace amounts of product were observed by TLC analysis.

In an attempt to rationalise the large variation in activity observed for these mutants with 4-methylsulfonyl benzaldehyde, computational docking was performed with this substrate and D469T, S385E/D469T/R520Q and S385T/D469T/R520Q with the ThDP-enamine already docked in all structures (Figure 5.23). D469T gave only trace amounts of product with 4-(methylsulfonyl)benzaldehyde and the computational docking results supported the experimental data, with one major binding cluster predicted by the docking program, which appeared to be non-productive. In this cluster (Figure 5.23, A) the sulfonyl functionality formed hydrogen bonding interactions with H258 and D259 at the entrance to the active-site, pointing the aldehyde away from the ThDP-enamine intermediate at a distance of 8.7 Å. S385E/D469T/R520Q demonstrated a low energy cluster (Figure 5.23, B) where the sulfonyl group was bound by R358, S385E and H461, pointing the aldehyde towards the ThDP-enamine, at a distance of 6.0 Å. It is possible that this distance is too far away for nucleophilic attack to occur, which could explain why only trace amounts of product were observed.

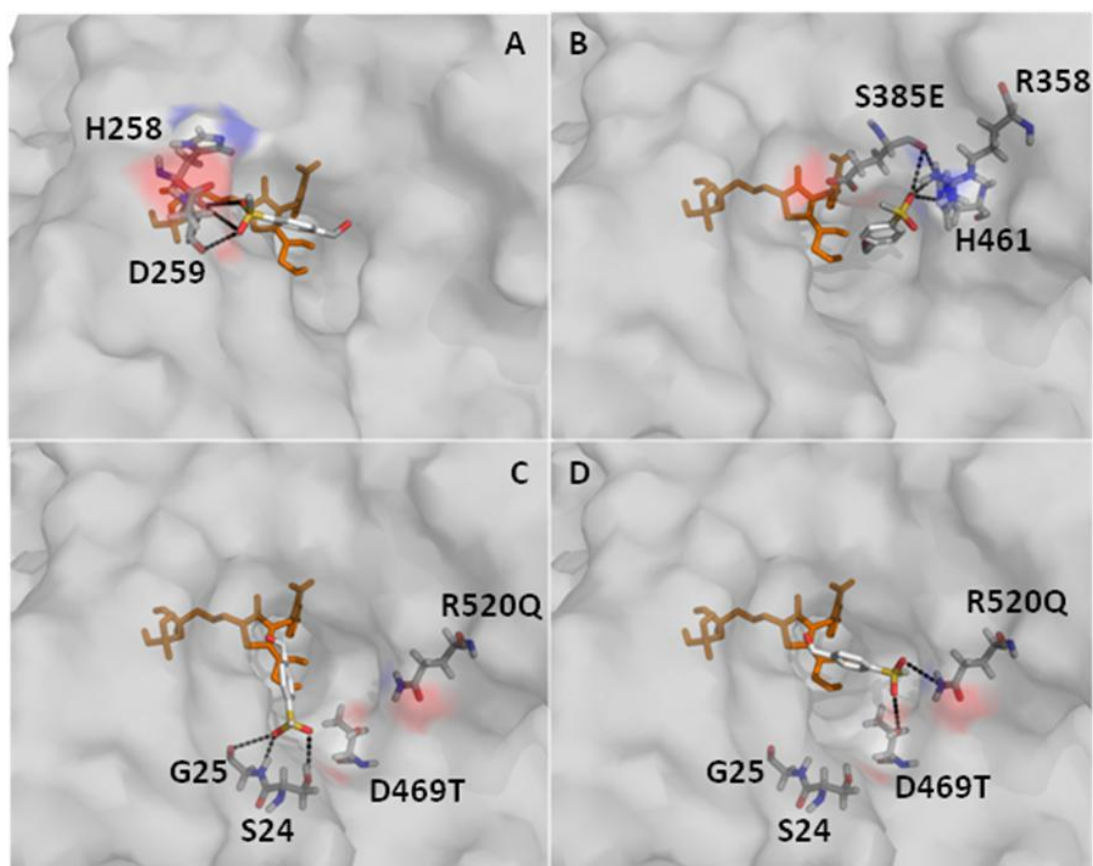


**Figure 5.23 Results obtained for the docking of 4-methylsulfonylbenzaldehyde. A – Non-productive cluster found for docking into D469T. B – Non-productive, lowest energy cluster found for docking into S385E/D469T/R520Q. C – Productive cluster found for docking into S385T/D469T/R520Q. D - Productive cluster found for docking into S385T/D469T/R520Q**

For S385T/D469T/R520Q two major binding clusters were predicted, with very similar populations and energies. The first cluster (Figure 5.23, C) showed the sulfonyl group bound by S24 and G25, holding the aldehyde directly above the ThDP-enamine at a distance of 3.9 Å. The other cluster (Figure 5.23, D) showed the sulfonyl group bound by D469T and R520Q, again holding the aldehyde above the ThDP-enamine intermediate at a slightly increased distance of 4.6 Å. The presence of two low energy binding clusters for S385T/D469T/R520Q with 4-(methylsulfonyl) benzaldehyde supports the high conversion yields observed for this mutant as both clusters show potentially productive orientation of the aldehyde in relation to the ThDP-enamine, at short distances (<5 Å).

## 5.6 Aromatic substrates not accepted by combination mutant TKs

Since these triple mutants, especially S385T/D469T/R520Q, showed good tolerances towards substituted aromatic aldehydes, a more sterically demanding substrate, 1,8-naphthalaldehydic acid (**160**) (Figure 5.24) was investigated. This substrate was chosen as it would investigate whether fused aromatic rings would be accepted by the mutant TKs, and also because it maintained the 1,3 relationship between the aldehyde and acid functionalities which had been observed to increase the activity of TKs with 3-FBA (Section 5.3), albeit in a different orientation.

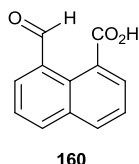


Figure 5.24 Structure of 1,8-naphthalaldehydic acid (**160**)

Unfortunately, no product was seen with this substrate for any of the mutants at either 25 mM or 50 mM concentrations, even with extended reaction times (up to 48 hours). This is perhaps not surprising given the size of the substrate, and indicated that while these mutants showed a good tolerance for several aromatic aldehydes, there was a steric limit to the aldehydes that they would accept.

A range of more functionalised benzaldehydes was also tested with these mutants, to see whether they would be tolerated. Vanillin (4-hydroxy-3-methoxybenzaldehyde, **161**, Figure 5.25), ortho-vanillin (2-hydroxy-3-methoxybenzaldehyde, **162**, Figure 5.25) and iso-vanillin (3-hydroxy-4-methoxybenzaldehyde, **163**, Figure 5.25) were all used at 25 mM concentrations. Reactions were followed by TLC analysis but no product formation was observed for any of the mutants even after extended reaction times (48 hours).

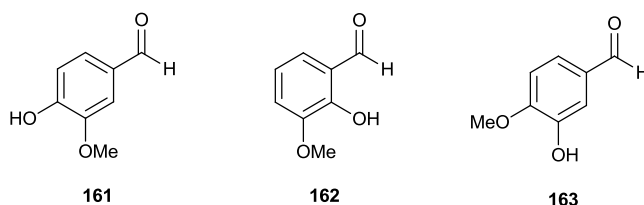
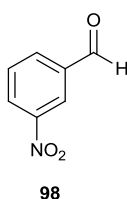


Figure 5.25 Range of Vanillin analogues tested with TK mutants.

Given that 3-hydroxybenzaldehyde (**93**) was accepted by all of the mutants, albeit with low yields and moderate stereoselectivities (Table 5.7), the lack of product formation observed for these vanillin derivatives (Figure 5.25) was disappointing. It is possible that the presence of two electron donating groups renders the aldehyde less reactive towards nucleophilic attack by the ThDP-enamine intermediate. It is also possible that the presence of additional substituents at either the 2- or 4-position of the aromatic ring create unfavourable steric hinderence which restrict access of these vanillin derivatives into the TK active-site.

Another substrate which was investigated with these mutants was 3-nitrobenzaldehyde (**98**, Figure 5.26).

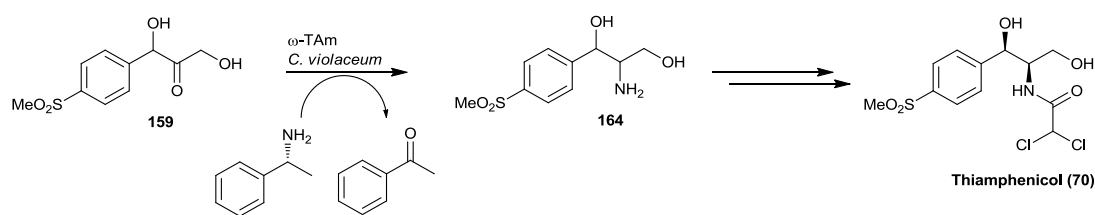


**Figure 5.26 Structure of 3-nitrobenzaldehyde (98)**

Unlike the vanillin derivatives where no products of any kind were formed, the formation of multiple products was observed by TLC analysis for all mutants, however no ketodiol product was observed in the  $^1\text{H-NMR}$  spectra of crude biotransformation reaction mixtures, so this substrate was not investigated further.

## **5.7 Aminodiol synthesis with TAm**

The acceptance of 4-methylsulfonyl benzaldehyde (**158**) in good yield and with excellent stereoselectivity by S385T/D469T/R520Q (Table 5.14), was very exciting, since this gave access to a direct precursor (**159**) of thiamphenicol (**70**) which could be used in a second-step with transaminase (Scheme 5.4) to give the aminodiol core (**164**) of thiamphenicol in a total of two enzymatic steps.



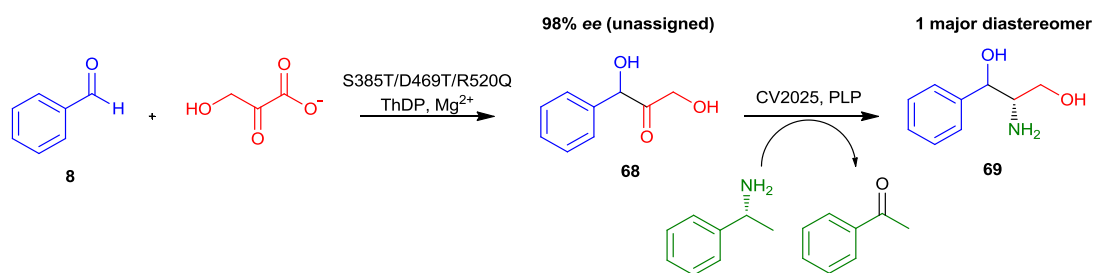
**Scheme 5.4 Approach to thiamphenicol using TAM**

A TAM from *Chromobacterium violaceum*, CV2025, had already been reported to accept the racemic product (**68**) of the biomimetic TK reaction with benzaldehyde. This TAM accepted both enantiomers of racemic **68**, but formed the new stereocentre (**69**) with *S*-configuration exclusively (Scheme 5.5).<sup>[75]</sup>

**Scheme 5.5 Stereoselectivity of aromatic aminodiols synthesis by CV2025<sup>[75]</sup>**

A number of substrates could now be transformed with high degrees of stereoselectivity (>90% *ee*) using mutant TKs, so it was possible to investigate the synthesis of optically pure aminodiols using a TK/TAM approach.

Since the ketodiols product (**68**) formed by the TK reaction with benzaldehyde had been shown to be accepted by TAM,<sup>[75]</sup> and this substrate could be prepared by S385T/D469T/R520Q with 98% *ee*, this was the first substrate tested with CV2025 (Scheme 5.6). The TK reaction with benzaldehyde (**8**) was performed with S385E/D469T/R520Q as previously described, and a portion of the product (**68**) was benzoylated, analysed by chiral HPLC and the *ee* confirmed to be >95%, in accordance with the data already gathered for this mutant. The remaining product was used as the acceptor substrate for TAM, using reaction conditions previously described, with *S*- $\alpha$ -methylbenzylamine as the amine donor. TAM cell-free lysate was prepared as previously described with a protein concentration of approximately 4 mg/mL.<sup>[75]</sup>



**Scheme 5.6 Combined TK and TAM strategy to an aromatic aminodiol (69) starting from benzaldehyde (8)**

The reaction was followed by TLC analysis, until no starting material could be observed after 24 hours. Difficulty isolating these aminodiols has been reported,<sup>[75]</sup> so the reaction was concentrated to dryness under reduced pressure, and the crude reaction mixture subjected to the acetylation conditions of acetic anhydride, DMAP and pyridine.<sup>[75]</sup> The <sup>1</sup>H-NMR spectrum of the crude material showed two products, which were identified as acetylated *S*- $\alpha$ -methylbenzylamine (**165**) (Figure 5.27), the amine donor which had been used in excess, and the desired acetylated aminodiol (**69-B**) (Figure 5.27).

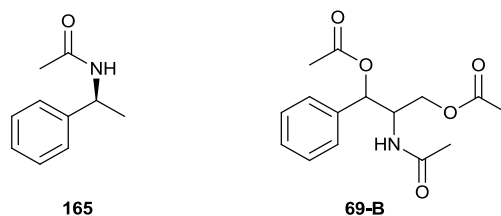


**Figure 5.27 Two major products isolated after acetylation of the crude TAM reaction**

These two compounds were separated by flash silica chromatography, and the pure acetylated aminodiol was isolated in low yield (<5% yield based on starting amount of ketodiol). However, the TLC analysis of the TAM reaction had shown no ketodiol remaining, so the low yield was not due to the inefficiency of the TAM reaction, but more likely loss of product during the acetylation and subsequent purification. This compound was then used to determine the absolute stereochemistry of the starting ketodiol, as discussed later (section 5.8).

The conversion to aminodiol **69** was encouraging, and so other ketodiols which had been generated in high yields and/or stereoselectivities by the combination mutant TKs were prepared and investigated as substrates for CV2025 (Figure 5.28). 3-Fluorobenzaldehyde had been converted by S385E/D469T/R520Q to ketodiol **105**

with 10% yield and 90% *ee* and so was used as a substrate. Methyl-3-formylbenzoate had been transformed by S385T/D469T/R520Q to **106** in 34% yield and 96% *ee*, the good yield and excellent stereoselectivity making this an interesting substrate to investigate with TAm. 3-Formylbenzoic acid was converted quantitatively to **108** by D469T, but with disappointing *ee*. Swift conversion of the ketodiol product (**108**) to the corresponding aminodiol would hopefully prevent racemisation, maintaining any stereoselectivity and so using this ketodiol as a substrate for TAm would hopefully give insights into the stereoselectivity of the initial TK step. This was also the case for the ketodiol product (**154**) from 4-formylbenzoic acid (**153**) for which stereoselectivity data could not be obtained, despite excellent conversion yields to **154** of 78% observed for S385T/D469T/R520Q. The final substrate of interest was the ketodiol (**159**) from 4-methylsulfonyl benzaldehyde which was transformed with 49% conversion yield and 90% *ee* by S385T/D469T/R520Q. This was possibly the most interesting substrate, since performing the transaminase reaction on this substrate would give access to the core structure (**164**, Scheme 5.4) of thiamphenicol (Scheme 5.4).

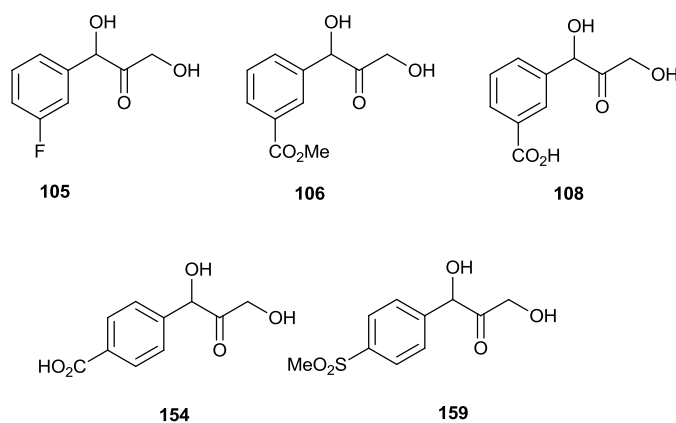


**Figure 5.28** Range of aromatic ketodiols investigated with CV2025

All ketodiols were isolated and purified for use in the transaminase reaction, except for ketodiol products **154** and **159** from 4-FBA and 4-methylsulfonyl benzaldehyde which were isolated as mixtures of the ketodiols and their respective aldehydes. In these cases conversion yields from the TK reaction were assessed by <sup>1</sup>H NMR analysis and found to be in accordance with previous data. TAm reactions were then performed as for the benzaldehyde ketodiol product (**68**), and as previously described.<sup>[75]</sup> Reactions were followed by TLC analysis to monitor the consumption

of ketodiol substrate, and also by reverse phase HPLC analysis to screen for acetophenone production, which is generated upon consumption of the amine donor, *S*- $\alpha$ -methylbenzylamine.<sup>[66]</sup>

After 24 hours, TLC analysis of the TAm reactions of all of the ketodiol substrates showed large amounts of starting ketodiol remaining. To each reaction more cell-free TAm lysate was added and reactions left for a further 24 hours at 37 °C. After this time TLC analysis once again showed large amounts of starting ketodiol for each case. However, HPLC analysis showed generation of acetophenone in each case, indicating the consumption of some amine donor, and thus potential turn-over of ketodiol. It was decided that even though reactions had not gone to completion, the generation of acetophenone was encouraging, and so reactions were concentrated to dryness and the crude reaction mixtures subjected to acetylation conditions to enable more facile product purification. Analysis of the <sup>1</sup>H-NMR spectra for all crude reaction mixtures revealed no acetylated aminodiols for any of the transaminase reactions with these substituted aromatic ketodiols. Only acetylated methylbenzylamine (**165**) was observed. This was very disappointing, especially given the good acceptance of the benzaldehyde TK product (**68**) by CV2025.

The non-acceptance of substituted aromatic ketodiols was interesting, especially since relatively small substituents such as fluorine, were not accepted. The active site of transaminases have been shown to have two binding pockets, a large pocket and a small pocket.<sup>[97]</sup> The aromatic ring of the aromatic ketodiols would be expected to occupy the large pocket of the enzyme, which seems to accept a non-substituted benzene ring, but will not accept any substituents on *meta* or *para*-positions. It seems possible that to increase the activity of CV2025 with these substrates mutations would need to be introduced into the large pocket to increase its size, thus increasing its acceptance of larger aromatic substrates. A library of CV2025 mutants has subsequently been generated by the Dalby group to address this problem, and can be explored with these substrates in future work.\*

---

\*CV2025 mutants have been created by Dawid Deszcz in UCL Dept. Of Biochemical Engineering



## 5.8 Assignment of absolute stereochemistry of aromatic ketodiols using transaminase

Previous work with aromatic ketodiols had tentatively assigned their absolute stereochemistry based on a modified Mosher's ester analysis method which had been developed using aliphatic ketodiols (Figure 5.29).<sup>[79, 83, 85]</sup> This method was particularly useful as only small amounts of material (<5 mg) were required for derivatisation.

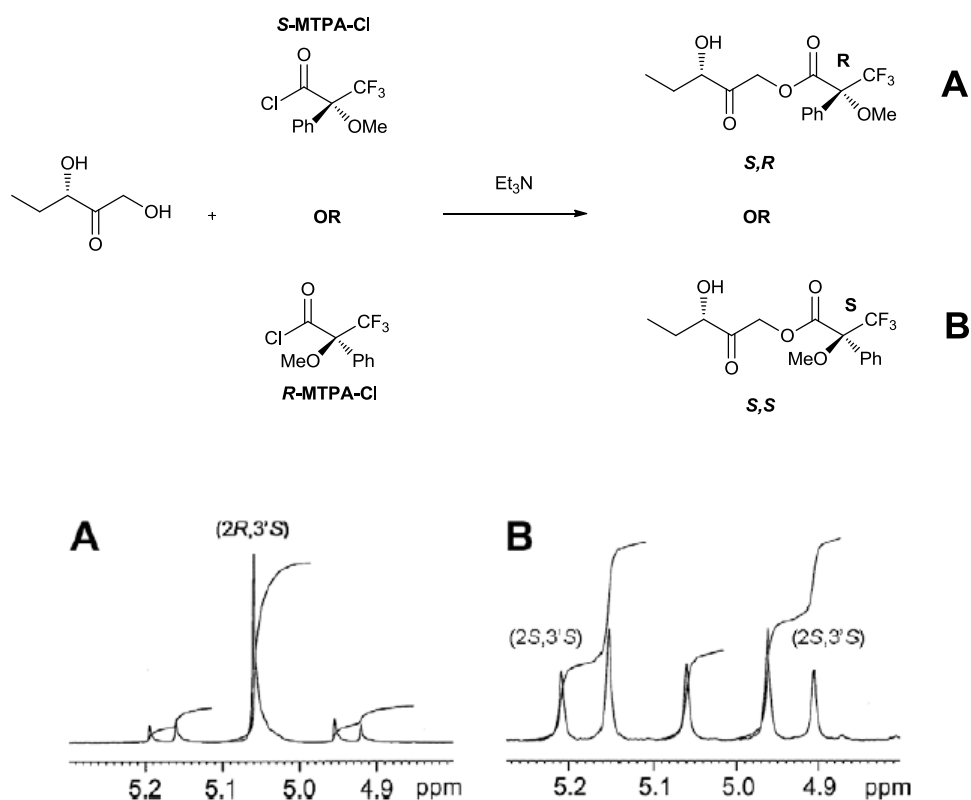
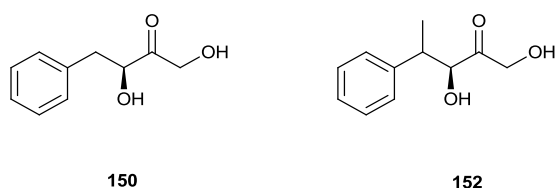


Figure 5.29 Assignment of absolute stereochemistry of aliphatic ketodiols based on a modified Mosher's analysis method. (Used with permission from Elsevier).<sup>[83]</sup>

The absolute stereochemistries of the ketodiols were assigned based on previously published absolute stereochemistries, either from synthesis of chiral standards, or established stereochemistries of, for example, L-erythrulose.<sup>[48, 83]</sup> When this Mosher's method was applied to ketodiols **150** and **152** formed from phenylacetaldehyde and 2-phenylpropanal, it indicated the formation of the (3*S*)-isomer, which was also in agreement with the absolute stereochemistry already reported for the transformation of the structurally related 2-hydroxy-2-

phenylacetaldehyde (Figure 5.30).<sup>[87]</sup> On this basis, application of the Mosher's method to aromatic compounds was a logical extension.



**Figure 5.30 Aliphatic ketodiols containing aromatic groups used to prove validity of modified Mosher's ester analysis method**

Crucially, however, an aromatic ketodiol standard of known stereochemistry was never tested with this method to confirm the assignment of absolute stereochemistry for aromatic ketodiols, because no synthetic methods exist to produce these compounds with known stereochemistry.<sup>[83]</sup>

While no chiral aromatic ketodiol standards are available, chiral aminodiols do exist. Both (1*S*,2*S*)-2-amino-1-phenyl-1,3-propanediol (1*S*,2*S*-**69**) (Figure 5.31) and (1*R*,2*R*)-2-amino-1-phenyl-1,3-propanediol (1*R*,2*R*-**69**) (Figure 5.31) are commercially available.

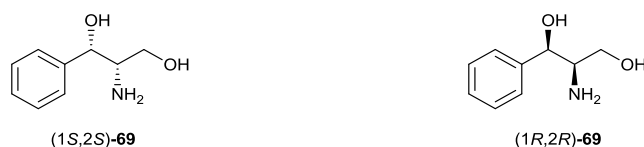
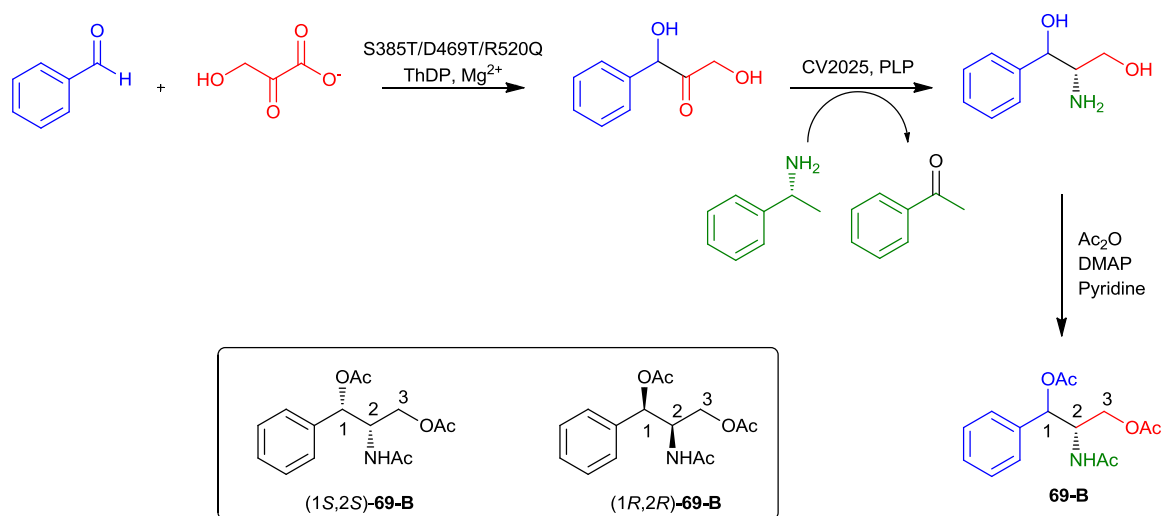


**Figure 5.31 Structures of both *syn*-diastereomers of **69****

In previous work examining the stereoselectivity of the transformation of the benzaldehyde TK product (**68**) by CV2025, these two commercially available *syn*-isomers were triacetylated and analysed by chiral HPLC. One of the two remaining *anti*-isomers, (1*R*,2*S*) was then synthesised, tri-acetylated and also studied by chiral HPLC.<sup>[75]</sup> Analysis of the racemic product gave the elution times of the four diastereoisomers, three of which could be directly correlated to available standards, and the remaining diastereoisomer was assigned as (1*S*,2*R*) (Table 5.15).<sup>[75]</sup>

Benzaldehyde was accepted by S385T/D469T/R520Q in 98% *ee* and CV2025 had been shown to exclusively form the (*S*)-isomer at the new stereocentre (**69**). This product had been triacetylated (**69-B**) to allow easy isolation of product from the

TAm reaction, so this gave the opportunity, for the first time, to assign the stereocentre from the TK reaction by direct correlation to known chiral standards (Scheme 5.7). Therefore, commercially available (1*S*,2*S*)-**69** and (1*R*,2*R*)-**69** were triacetylated, and chiral HPLC analysis was performed, using a Chiralpak AD column and a solvent system of 97:3 (*n*-hexane:isopropanol, 0.8 mL/min, detection at 214 nm),<sup>[75]</sup> on these two samples and the triacetylated biotransformation sample (**69-B**).



**Scheme 5.7** **69-B** of known stereochemistry, and formation of **69-B** derived from the two-step biotransformation procedure

**Table 5.15** Previously reported elution times for all four diastereoisomers of triacetylated aminodiols **69**<sup>[75]</sup>

Diastereoisomer of <b>69-B</b>	Elution time (min)
<b>1<i>R</i>,2<i>R</i></b>	74.4
<b>1<i>S</i>,2<i>S</i></b>	77.1
<b>1<i>R</i>,2<i>S</i></b>	99.8
<b>1<i>S</i>,2<i>R</i></b>	105.4

The chiral HPLC profile for the biotransformation product (**69-B**) showed a major peak at 77 minutes and a minor peak at 93 minutes. The major peak corresponded to (1*S*,2*S*)-**69** which was confirmed by analysis of acetylated (1*S*,2*S*)-**69-B** and comparison of the HPLC traces (Figure 5.32). This confirmed for the first time that the TK reaction was (*S*)-selective in the reaction with benzaldehyde to form ketodiols

**68**, with the minor diastereomer assigned as (1*R*,2*S*) based on the previously reported retention time for this isomer, and the highly *S*-selective nature of CV2025.<sup>[75]</sup> This confirmed that the combined TK and TAM strategy using benzaldehyde as the starting substrate gave an overall 95% selectivity in favour of (1*S*,2*S*)-**69-B** with the minor (1*R*,2*S*) isomer present at a level of 5%. The slight loss in *de* was probably due to a slight amount of racemisation during the TAM step with ketodiol **68**, as this reaction required elevated temperatures of 37 °C and a slightly elevated pH, conditions which have previously been shown to erode the optical purity of aromatic ketodiol.<sup>[85]</sup>

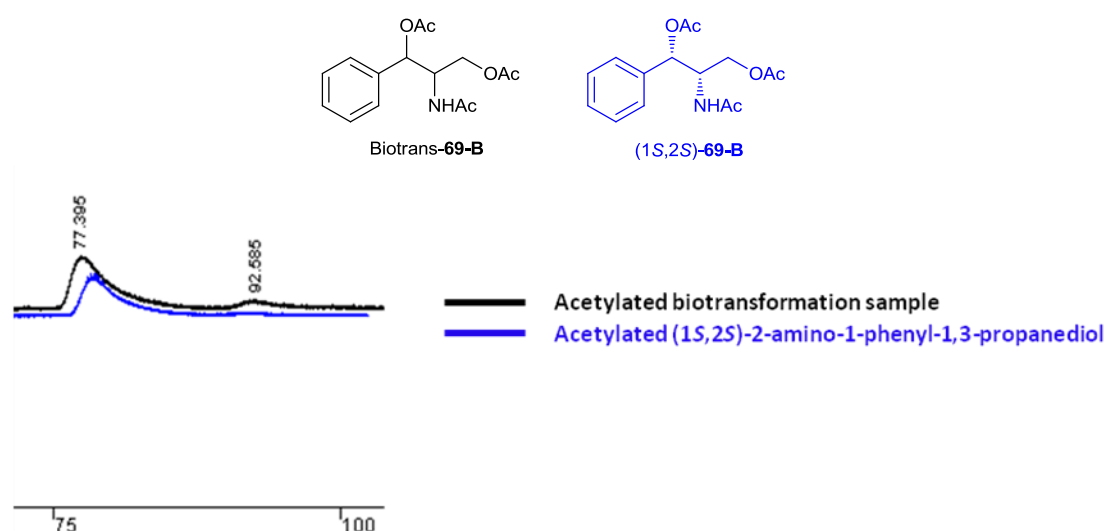
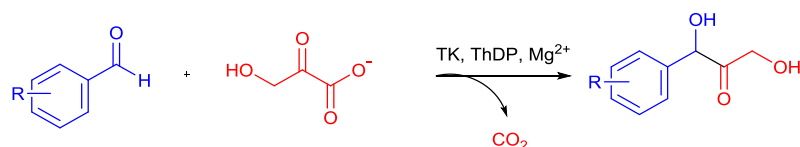


**Figure 5.32** Overlaid chiral HPLC profiles of **69-B** from the TK/TAM strategy and (1*S*,2*S*)-**69-B**. Elution times shown in minutes.

Previous work with aromatic ketodiol and TK had assigned absolute stereochemistries as 3(*R*) based on the extension of the modified Mosher's method (Figure 5.29).<sup>[79, 83, 85]</sup> However, the chiral HPLC data for aminodiol **69**, based on the correlation of stereochemistry to known standards, showed that TK was (*S*)-selective in the formation of ketodiol **68**, the same stereoselectivity as observed for aliphatic ketodiol formed by TK.<sup>[26]</sup> This indicates that the Mosher's method cannot be applied in the same way for aliphatic and aromatic ketodiol with stereocentres at the C-3 position. It is possible that ring current effects from the presence of the aromatic ring affect the shift patterns of the diastereotopic protons misleadingly indicating the formation of the opposite stereoisomer. Indeed, problems have previously been reported in assigning the absolute stereochemistry of some aromatic compounds

using this method.<sup>[98]</sup> To date, all available Mosher's and chiral HPLC data for aromatic ketodiols has consistently indicated the formation of the same stereocentre in all cases. Since the HPLC data for aminodiol **69-B** formed from the combined TK/TAm strategy definitively showed that the 3(*S*) isomer was formed by TK (Figure 5.32), the absolute stereochemistry of all aromatic ketodiols can now be assigned as 3(*S*) by analogy (Table 5.16).

**Table 5.16 Summary of stereoselectivities obtained for mutant TKs with aromatic aldehydes. Absolute stereochemistries based on the observed selectivity for TK with benzaldehyde, from study of acetylated aminodiol from combined TK/TAm approach**



Aldehyde (R=)	F434A	D469T	D469T R520Q	S385T D469T R520Q	S385Y D469T R520Q	S385E D469T R520Q
<b>H (8)</b>	82% <sup>[85]</sup> (3 <i>S</i> ) ( <b>68</b> )	70% (3 <i>S</i> ) ( <b>68</b> )	54% (3 <i>S</i> ) ( <b>68</b> )	98% (3 <i>S</i> ) ( <b>68</b> )	97% (3 <i>S</i> ) ( <b>68</b> )	37% (3 <i>S</i> ) ( <b>68</b> )
<b>3-OH (93)</b>	53% <sup>[85]</sup> (3 <i>S</i> ) ( <b>103</b> )	0% ( <b>103</b> )	0% ( <b>103</b> )	50% (3 <i>S</i> ) ( <b>103</b> )	55% (3 <i>S</i> ) ( <b>103</b> )	60% (3 <i>S</i> ) ( <b>103</b> )
<b>3-F (94)</b>	ND	20% (3 <i>S</i> ) ( <b>105</b> )	78% (3 <i>S</i> ) ( <b>105</b> )	70% (3 <i>S</i> ) ( <b>105</b> )	64% (3 <i>S</i> ) ( <b>105</b> )	90% (3 <i>S</i> ) ( <b>105</b> )
<b>3-vinyl (96)</b>	ND	0%	0%	84% (3 <i>S</i> ) ( <b>107</b> )	90% (3 <i>S</i> ) ( <b>107</b> )	ND
<b>3-CO<sub>2</sub>Me (95)</b>	ND	ND	ND%	96% (3 <i>S</i> ) ( <b>106</b> )	72% (3 <i>S</i> ) ( <b>106</b> )	ND
<b>3-CO<sub>2</sub>H (97)</b>	ND%	62% (3 <i>S</i> ) ( <b>108</b> )	56% (3 <i>S</i> ) ( <b>108</b> )	49% (3 <i>S</i> ) ( <b>108</b> )	45% (3 <i>S</i> ) ( <b>108</b> )	0%
<b>3-CN (18)</b>	ND	ND	ND	90% (3 <i>S</i> ) ( <b>110</b> )	91% (3 <i>S</i> ) ( <b>110</b> )	ND
<b>4-SO<sub>2</sub>Me (158)</b>	ND	ND	ND	90% (3 <i>S</i> ) ( <b>159</b> )	70% (3 <i>S</i> ) ( <b>159</b> )	ND

These results indicate that the predominant isomer formed in all cases is (*S*), as found for the aliphatic series of ketodiols.<sup>[26, 85]</sup> It should be noted that the initial absolute stereochemistries of aromatic ketodiols were only ever tentatively assigned by the Mosher's method,<sup>[79, 85]</sup> as at the time it was the only method available. Also, the absolute stereochemistries of the aromatic ketodiols prepared by the asymmetric biomimetic TK reaction were also assigned using the Mosher's method (Chapter 2), and so should be re-assigned as 3(*S*) by analogy to the formation of (1*S*,2*S*)-**69**.

### **5.9 Analysis of docking results to support assignment of absolute stereochemistry**

In an attempt to support the assignment of the stereocentre formed by the mutant TKs with aromatic aldehydes as 3*S*, the docking experiments performed with these mutants and some of the aromatic aldehydes were studied in more detail. The most productive docking experiments came from the docking of 3-FBA (**97**) into D469T, 4-(methylsulfonyl)benzaldehyde (**158**) into S385T/D469T/R520Q and methyl-3-formylbenzoate (**95**) into S385T/D469T/R520Q, so these docking experiments were chosen for further analysis.

The productive conformation obtained by docking 3-FBA into D469T showed the carboxylate group bound by the phosphate binding region, with hydrogen bonding interactions with R358, S385, H461 and R520. This held the aldehyde almost perpendicular to the ThDP-enamine intermediate, exposing neither face of the aldehyde preferentially to nucleophilic attack (Figure 5.33). This is in contrast to the 62% *ee* 3(*S*) which was experimentally determined for the ketodiol **108** from the reaction of 3-FBA with D469T (Table 5.16).

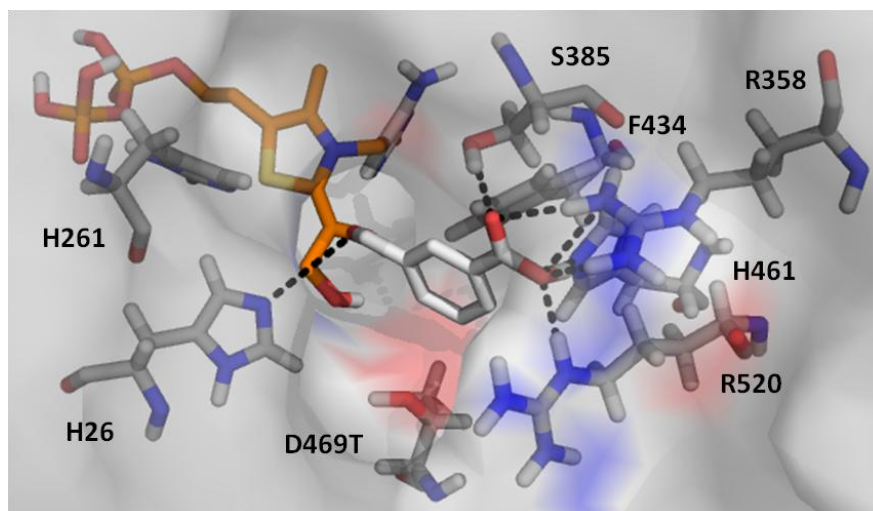


**Figure 5.33** Productive conformation found for docking 3-FBA (**97**) into D469T, where neither face of the substrate is preferentially exposed to the ThDP-enamine intermediate.

A very similar binding mode was observed for the docking of 4-(methylsulfonyl)benzaldehyde (**158**) into S385T/D469T/R520Q (Figure 5.34). The sulfonyl group was bound by D469T and R520Q, placing the aldehyde in a position perpendicular to the ThDP-enamine intermediate with neither face of the substrate preferentially exposed to nucleophilic attack. This was again in contrast to the 90% *ee* (3*S*) which was determined experimentally for ketodiol **159** (Table 5.16).

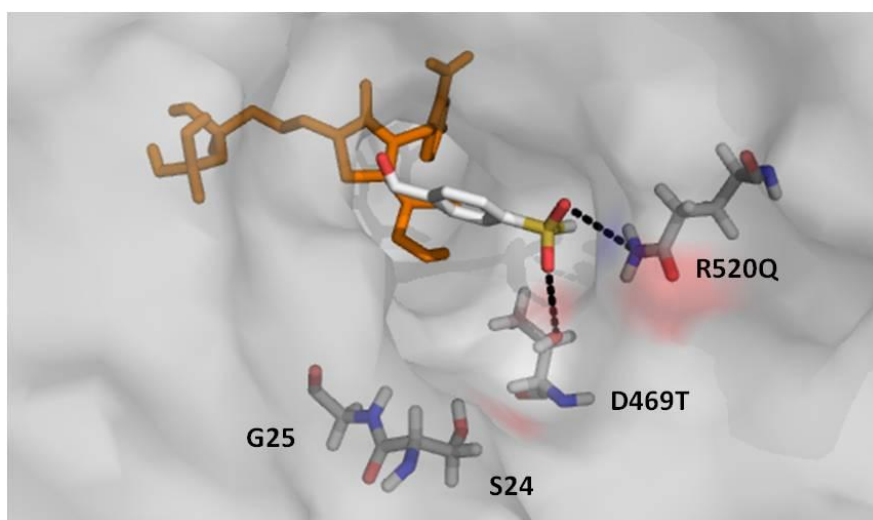


**Figure 5.34** Productive conformation found from docking of 4-(methylsulfonyl)benzaldehyde into S385T/D469T/R520Q, where neither face of the aldehyde is preferentially exposed to the ThDP-enamine intermediate.

The results obtained for the docking of methyl-3-formylbenzoate (**95**) into S385T/D469T/R520Q were very different. The ester group was bound by G25 and the aldehyde functionality held in place by interactions with H26 and H261. In this case the *re*-face of the substrate was preferentially exposed to attack by the ThDP-enamine intermediate (Figure 5.35), which would lead to formation of the 3*S*-ketodiol product. This result supports the experimentally determined formation of the 3*S*-**106** in 96% *ee*.

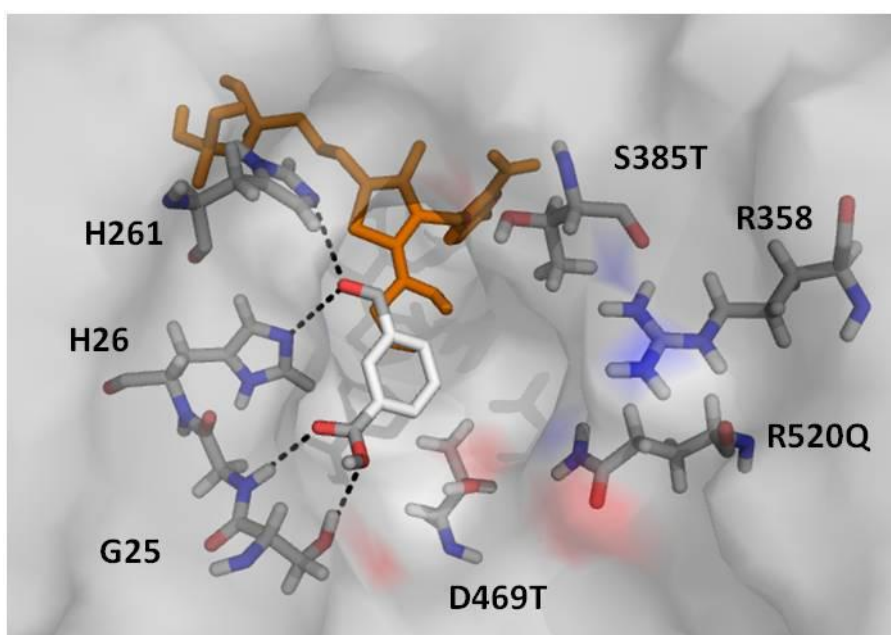


**Figure 5.35** Productive conformation found from docking of methyl-3-formylbenzoate into S385T/D469T/R520Q, with the *re*-face preferentially exposed to the ThDP-enamine intermediate attack.

These results show the difficulty in using computational docking to analyse the stereoselectivity of reactions, since two of the docking experiments showed conformations that would lead to no stereoselectivity in the products, despite stereoselectivity being observed experimentally. However, the result obtained from docking methyl-3-formylbenzoate into S385T/D469T/R520Q supported the experimentally determined absolute stereochemistry as 3*S*. It would seem that computational docking in this case is not a reliable method for assessing stereochemistry, but may be a useful tool for supporting some experimental observations.



## 5.10 Summary of chapter 5

In conclusion, the transformation of aromatic aldehydes by combination mutant TKs has been extensively studied. 3 And 4-formylbenzoic acids were used as molecular probes to investigate interactions between these substrates and the TK active-site. The natural phosphate binding region within the active-site was shown to be effective at binding the carboxylic acid groups of these substrates, leading to dramatically increased activities compared to previous work with mutant TKs and aromatic aldehydes. Mutant TK libraries were then created by focussing on this phosphate binding region and from knowledge gained from previous studies on the co-evolution of active-site residues in TK.<sup>[88]</sup> The most active combination mutants were then used to transform a range of aromatic aldehydes and dramatic increases in yield and stereoselectivity over previous single mutant TKs were observed, with aromatic ketodiols formed in up to 98% *ee*. A two enzyme strategy was then investigated using the best performing combination mutant TK, S385T/D469T/R520Q and CV2025 TAm, to access an aromatic aminodiol in 90% *de*. By correlation with optically pure reference standards this aminodiol was shown to be predominantly the (1*S*,2*S*) isomer. This conclusively showed that the Mosher's ester analysis method which had been used to tentatively assign the absolute stereochemistry of aromatic ketodiols as 3(*R*) was incorrect and as a result all compounds were re-assigned as 3(*S*). The molecular basis for the increased activities of these mutant TKs with aromatic aldehydes was extensively investigated using computational docking studies, which helped to explain the increases in isolated yield over previously studied single mutant TKs. While the docking results were not conclusive in rationalising observed stereoselectivities, some of the results helped to support the assignment of absolute stereochemistry and the conversions observed for aromatic aldehydes.

## **6 Novel donor substrates with transketolase**

Much of the work with transketolase has been focussed on increasing the substrate scope of the enzyme with respect to the acceptor substrate. As such, mutant enzymes have been developed which accept a broad range of aliphatic, cyclic, and aromatic aldehydes.<sup>[26, 85, 91]</sup> However, the substrate scope of the donor substrate has been poorly studied, presumably due to the high specificity that TK exhibits towards its natural phosphorylated substrates (Figure 6.1) and hydroxypyruvate.<sup>[99, 100, 101]</sup> Analysis of the active-site of WT *E.coli* TK with two of these natural phosphorylated substrates, xylulose-5-phosphate (**19**) and fructose-6-phosphate (**166**), bound shows the origin of this specificity (Figure 6.2).<sup>[90]</sup>

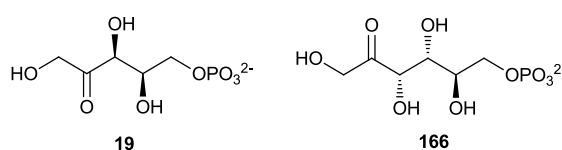


**Figure 6.1 Structures of two of the natural substrates for TK, xylulose-5-phosphate (**19**) and fructose-6-phosphate (**166**)**

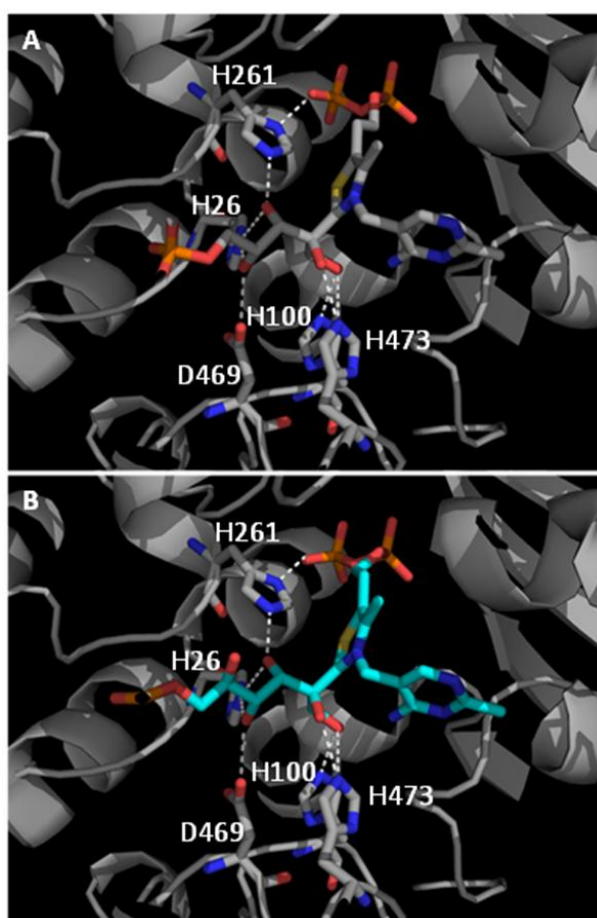


**Figure 6.2 Crystal structures of WT-TK (2R5N) with; A - xylulose-5-phosphate (**19**) and B - fructose-6-phosphate (**166**), bound.**

In both cases the same interactions are observed. The ketol moiety is stabilised by interactions with H473 and H100, while the 3-hydroxyl group interacts with H261 and H26, and the 4-hydroxyl group is bound by D469. It is reasonable to suppose that if the key interactions with the ketol group and H100 and H473 can be maintained, then other ketol donors could be accepted by TK.

Recently the use of halogenated pyruvate derivatives as donor substrates for yeast TK has been reported (**23**, **167-171**) (Figure 6.3).<sup>[102]</sup>

**Figure 6.3 Pyruvate derivatives studied as donor substrates for yeast TK**<sup>[102]</sup>

These substrates were studied by circular dichroism for their reaction with ThDP in the active site of TK to form the active ThDP-enamine intermediate. The further reaction of the enamine with an acceptor substrate was not studied. Nevertheless, some kinetic parameters for these donors were obtained (Table 6.1).<sup>[102]</sup>

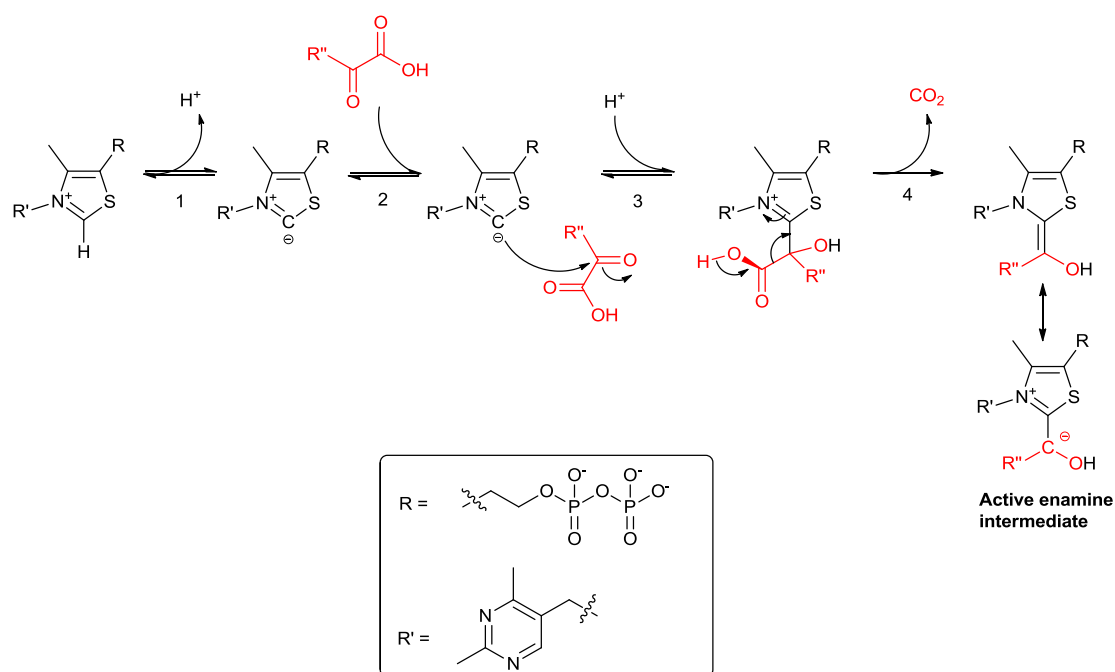
**Table 6.1 Kinetic parameters obtained for pyruvate derivatives and their reaction with ThDP in the active-site of yeast TK**<sup>[102]</sup>

Substrate	$k_{cat}$ (%)	$K_M$ (mM)
<b>Hydroxypyruvate (23)</b>	100	0.05
<b>Bromopyruvate (167)</b>	130	0.13
<b>Dibromopyruvate (170)</b>	90	2.0
<b>Chloropyruvate (168)</b>	80	0.4
<b>Dichloropyruvate (171)</b>	100	1.1
<b>Fluoropyruvate (169)</b>	30	2.5

Interestingly, while hydroxypyruvate (**23**) showed the highest affinity for yeast TK with the lowest  $K_M$  value of 0.05 mM, bromopyruvate (**167**) actually showed the

highest  $k_{\text{cat}}$ , with a  $k_{\text{cat}}$  value 1.3 fold higher than that obtained for hydroxypyruvate.<sup>[102]</sup>

This work was performed with yeast TK and no products were isolated or characterised,<sup>[102]</sup> as only the formation of the active ThDP-enamine was studied by circular dichroism. However, this suggested that transketolase could potentially accept different donor substrates, providing a suitable leaving group on the  $\alpha$ -position of the ketol donor was present. The leaving group is crucial for the formation of the active ThDP-enamine intermediate (Scheme 6.1), as this renders the reaction irreversible, driving the reaction to completion, as in the case of pyruvate derivatives where the leaving group is  $\text{CO}_2$ .<sup>[100]</sup>



**Scheme 6.1** Formation of the active ThDP-enamine intermediate in the active site of TK with pyruvate derivatives

Therefore, modifying the  $R''$  group (Scheme 6.1) of the  $\alpha$ -ketoacid should not affect the catalytic mechanism of TK, and if key active-site interactions are maintained, different groups should be tolerated. Novel ketol donors would be beneficial to investigate, especially in terms of increasing the synthetic use of transketolase in preparing a more diverse range of compounds. This is especially true given that the ketol products, which could be accessed by the TK reaction with pyruvate (**7**) and 2-ketobutyric acid (**172**) as donor substrates (Figure 6.4), have not been accessed

asymmetrically using standard synthetic techniques, and only lipase catalysed kinetic resolutions have previously been reported to prepare such compounds.<sup>[103]</sup>

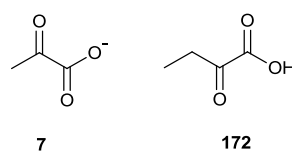
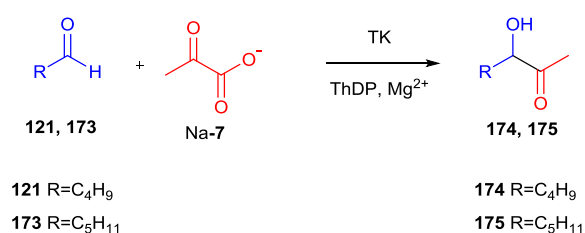


**Figure 6.4** Potential novel donor substrates for TK

## 6.1 Sodium pyruvate as a donor in the TK reaction

The investigation into novel donors was started by using pyruvate (**7**) as the ketol donor (Scheme 6.2) using the same conditions as previously reported for standard biotransformations.<sup>[26, 85]</sup> Sodium pyruvate (Na-**7**) was first used as a donor with WT TK and with aliphatic aldehydes that had been shown to be tolerated by the WT enzyme. Low boiling points had been reported for the corresponding ketol compounds,<sup>[104, 105]</sup> so longer chain aliphatics were used to enhance the ease of isolating any resulting products. Initially, sodium pyruvate was investigated with pentanal (**121**) (R = C<sub>4</sub>H<sub>9</sub>) and hexanal (**173**) (R = C<sub>5</sub>H<sub>11</sub>) as the acceptor substrates, to form ketols **174** (R = C<sub>4</sub>H<sub>9</sub>) and **175** (R = C<sub>5</sub>H<sub>11</sub>).



**Scheme 6.2** TK reaction using sodium pyruvate as the donor substrate

No product formation was observed for either of these substrates, in contrast to the 16% and 25% isolated yields previously reported for WT TK using HPA (**23**) as the ketol donor with **121** and **173** respectively.<sup>[26]</sup>

A mutant TK, D469E, had been shown to lead to increased yields with HPA (**23**) as the donor and pentanal and hexanal as acceptor substrates,<sup>[26]</sup> so this mutant was then investigated with sodium pyruvate (Scheme 6.2, Table 6.2) and a larger range of

acceptor aldehydes, including cyclohexanecarboxaldehyde (**143**, R = cyclohexyl) and benzaldehyde (**8**, R = Ph).

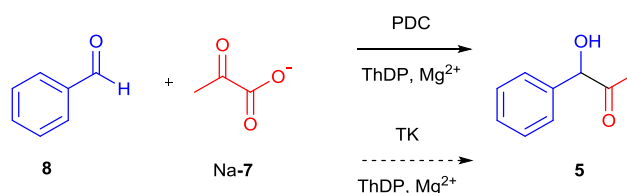
**Table 6.2 Yields obtained for D469E with sodium pyruvate (Na-7) as the donor substrate\***

Substrate	Yield
<b>Pentanal (121) (R = C<sub>4</sub>H<sub>9</sub>)</b>	5% ( <b>174</b> )
<b>Hexanal (173) (R = C<sub>5</sub>H<sub>11</sub>)</b>	4% ( <b>175</b> )
<b>Cyclohexanecarboxaldehyde (143) (R = cyclohexyl)</b>	No reaction
<b>Benzaldehyde (8) (R = Ph)</b>	No reaction

\*D469E TK was made by Panwajee Payongsri. Reaction conditions: 50 mM aldehyde. 50 mM sodium pyruvate, 2 mL TK cell-free lysate, 20 mL reaction volume, 24 hour reaction time.

Interestingly, after 18 hours, TLC analysis of the reactions with both pentanal and hexanal showed the formation of products with lower polarities than the corresponding ketodiols. To investigate these products further they were isolated and purified by flash silica chromatography. Column fractions were carefully concentrated *in vacuo* to prevent evaporation of any ketol products. <sup>1</sup>H-NMR analysis of both products showed that the corresponding ketols **174** and **175** had been formed in each case, with isolated yields of 5% for **174** and 4% for **175**.

The formation of ketol products, and the acceptance of pyruvate by TK, was completely unprecedented, so two other aldehydes, cyclohexanecarboxaldehyde (**143**) (Scheme 6.2, R = cyclohexyl) and benzaldehyde (**8**) (Scheme 6.2, R = Ph) were investigated. The potential for TK to form ketol **5** from benzaldehyde and sodium pyruvate was particularly interesting as this would represent transketolase acting in a similar fashion to pyruvate decarboxylase, forming the phenylacetylcarbinol **5** (Scheme 6.3).<sup>[15]</sup>



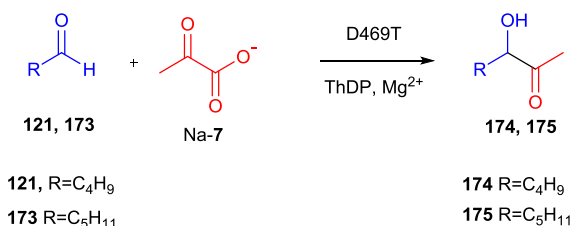
**Scheme 6.3 Phenylacetylcarbinol (5) formation by pyruvate decarboxylase and transketolase**

D469E had been reported to transform both cyclohexanecarboxaldehyde (**143**) and benzaldehyde (**8**) using HPA as the ketol donor, though <5% isolated yields were

reported in both cases.<sup>[26, 85]</sup> Disappointingly, no reaction was observed with sodium pyruvate as the donor substrate.

D469T was another TK mutant which had been shown to be useful in the transformation of aliphatic aldehydes with HPA (**23**),<sup>[26]</sup> and so this was also investigated for its acceptance of sodium pyruvate (Na-7), with the same range of acceptor substrates as D469E (Scheme 6.2, Table 6.3).

**Table 6.3 Yields obtained for D469T with sodium pyruvate (Na-7) as the donor substrate\***



Aldehyde	Yield
<b>Pentanal (121)</b>	5% ( <b>174</b> )
<b>Hexanal (173)</b>	4% ( <b>175</b> )
<b>Cyclohexanecarboxaldehyde (143)</b>	Trace
<b>Benzaldehyde (8)</b>	Trace

\*D469T TK was made by Panwajee Payongsri. Reaction conditions: 50 mM aldehyde, 50 mM sodium pyruvate, 2 mL TK cell-free lysate, 20 mL reaction volume, 24 hour reaction time.

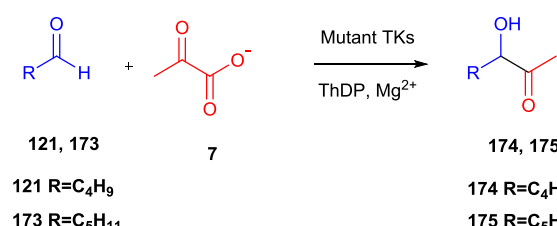
Interestingly, D469T performed similarly to D469E with pentanal and hexanal, with isolated yields of 5% of (**174**) and 4% of (**175**) obtained for these two substrates. Trace amounts of product with comparable R<sub>f</sub> values were observed by TLC analysis of the reactions with cyclohexanecarboxaldehyde and benzaldehyde, but not enough product was formed in either case to allow isolation of these products. Since cyclohexanecarboxaldehyde and benzaldehyde were poorly tolerated in the TK reaction with sodium pyruvate, they were not investigated further as acceptor substrates.

D469Y was a TK mutant which had been shown to be active towards aliphatic aldehydes, forming the opposite stereoisomer compared to other TK mutants,<sup>[47, 48]</sup> and so was investigated with sodium pyruvate as the ketol donor (Table 6.4). Combination mutant TKs had already been shown to increase the activity of TK toward a range of aliphatic and aromatic aldehydes,<sup>[88, 91]</sup> and so were also investigated with sodium pyruvate as the donor substrate in an attempt to increase the isolated yields of ketols **174** and **175** obtained. R520Q was a mutation which had



previously been shown to increase the activity of certain TK mutants towards propanal.<sup>[88]</sup> Since D469E had given the highest isolated yields with sodium pyruvate as the donor, these two mutants were recombined to give D469E/R520Q and tested with sodium pyruvate and pentanal and hexanal (Table 6.4). Another combination mutant, S385T/D469T/R520Q, had been shown to be the most active TK mutant towards a range of aromatic aldehydes (Chapter 5) and so was also used (Table 6.4).

**Table 6.4 Yields obtained for D469Y, D469E/R520Q and S385T/D469T/R520Q with sodium pyruvate (Na-7) as the donor substrate\***

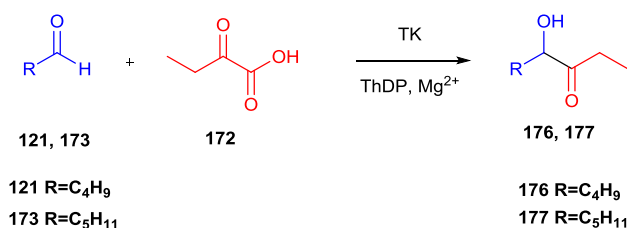
			
121, 173			174, 175
121 R=C <sub>4</sub> H <sub>9</sub>			174 R=C <sub>4</sub> H <sub>9</sub>
173 R=C <sub>5</sub> H <sub>11</sub>			175 R=C <sub>5</sub> H <sub>11</sub>
<b>Aldehyde</b>	<b>D469Y</b>	<b>D469E/R520Q</b>	<b>S385T/D469T/R520Q</b>
	<b>Yield</b>	<b>Yield</b>	<b>Yield</b>
<b>Pentanal (121)</b>	Trace	Trace	Trace
<b>Hexanal (173)</b>	Trace	Trace	Trace

\*D469Y, D469E/R520Q and S385T/D469T/R520Q TK mutants were made by Panwajee Payongsri. Reaction conditions: 50 mM aldehyde, 50 mM sodium pyruvate, 2 mL TK cell-free lysate, 20 mL reaction volume, 24 hour reaction time.

Despite D469E and D469T giving isolatable quantities of product with sodium pyruvate as the donor substrate, D469Y only formed trace amounts of ketols **174** and **175**. Disappointingly this was also the case for both of the combination mutants where only trace amounts of product were observed once again. Nevertheless, two TK mutants, D469E and D469T, accepted sodium pyruvate as the donor substrate with both pentanal and hexanal. With this in mind, a further novel donor substrate was investigated.

## 6.2 2-Ketobutyric acid as a donor in the TK reaction

2-Ketobutyric acid (**172**) (Scheme 6.4), is structurally similar to sodium pyruvate (Na-7), but with an extra methylene group. Given the structural similarity of these substrates it was hoped that the TK mutants might show similar activities with 2-ketobutyric acid as for sodium pyruvate.



**Scheme 6.4** TK reaction with 2-ketobutyric acid as the donor substrate

D469E had been the best performing mutant using sodium pyruvate as the donor, and so was the first mutant to be investigated with 2-ketobutyric acid (**172**) (Table 6.5).

**Table 6.5** Yields obtained for D469E with 2-ketobutyric acid as the donor substrate\*

Aldehyde	Yield
<b>Pentanal (121)</b>	Trace
<b>Hexanal (173)</b>	7% ( <b>177</b> )

\*D469E was made by Panwajee Payongsri. Reaction conditions: 50 mM aldehyde, 50 mM 2-ketobutyric acid, 2 mL TK cell-free lysate, 20 mL reaction volume, 24 hour reaction time.

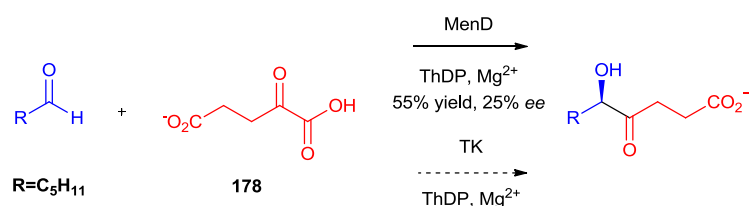
Only trace amounts of product were observed when pentanal was used as the acceptor substrate. When hexanal was used as the acceptor substrate, however, a 7% yield of ketol **177** was obtained. Despite bearing an extra methylene group compared to ketol **175**, **177** was still observed to be highly volatile and product isolation was once again difficult.

The acceptance of 2-ketobutyric acid (**172**) by D469E was encouraging, so a range of other TK mutants were tested with this donor (Table 6.6).



### 6.3 2-ketoglutaric acid as a donor in the TK reaction

One final donor substrate was briefly investigated with D469E.  $\alpha$ -Ketoglutaric acid (**178**) is a substrate for another ThDP-dependent enzyme, 2-succinyl-6-hydroxy-2,4-cyclohexadiene-1-carboxylate synthase (menD), which has been reported to accept a range of aromatic and aliphatic aldehydes with variable yields and stereoselectivities observed.<sup>[106]</sup> Thus, acceptance of  $\alpha$ -ketoglutarate by TK as an acceptor substrate would represent TK mimicking the function of menD (Scheme 6.5).



**Scheme 6.5 Potential use of  $\alpha$ -ketoglutaric acid as a donor substrate for TK**

D469E was one of the best performing mutants with the other two novel donors, sodium pyruvate and 2-ketobutyric acid, and so was chosen for investigation with  $\alpha$ -ketoglutaric acid (Scheme 6.5, Table 6.7).

**Table 6.7 Yields obtained for D469E with  $\alpha$ -ketoglutaric acid as the donor substrate\***

Aldehyde	Yield
<b>Pentanal (121)</b>	No reaction
<b>Hexanal (173)</b>	No reaction

\*Reaction conditions: 50 mM aldehyde, 50 mM  $\alpha$ -ketoglutaric acid, 2 mL TK cell-free lysate, 20 mL reaction volume, 24 hour reaction time.

Disappointingly, no product formation was observed for either of the acceptor aldehydes, not even trace amounts by TLC analysis. Since D469E had been one of the most tolerant mutants towards novel donors, this substrate was not investigated further.

## **6.4 Determination of stereoselectivity of TK with novel donors**

### **6.4.1 Determination of stereoselectivity of TK reaction with sodium pyruvate as donor substrate**

While the ketol products (**174-177**) from the TK reaction with sodium pyruvate and 2-ketobutyric acid had been isolated and fully characterised, the stereoselectivity of these reactions had not yet been established. Ketols **174** and **175** formed when using sodium pyruvate as a donor (Scheme 6.2) have been previously reported as compounds present in the pheromones of various longhorn beetle species.<sup>[104]</sup> Several chiral analytical methods have been reported for these compounds, mainly relying on chiral gas chromatography analysis.<sup>[105]</sup> However, facile isomerisation of these compounds has been observed upon heating, making GC methods unreliable.<sup>[105]</sup> A method has also been reported which involves the preparation of Mosher's ester derivatives of the ketol compounds.<sup>[104]</sup> The coupling of the chiral auxiliary affected the signal of the terminal methyl triplet in each enantiomer ( $\delta$  0.83 for (*S,S*) and  $\delta$  0.87 for (*S,R*)), which could be easily distinguished from each other. It also caused a shift in the signal of the singlet methyl peak ( $\delta$  2.22 for (*S,S*) and  $\delta$  2.12 for (*S,R*)) which were also easily distinguishable. The relative integrations of each signal would therefore give the enantiomeric excess and absolute stereochemistry of the starting ketol compound. As each peak had been unambiguously confirmed by the synthesis of chiral standards,<sup>[104]</sup> this method would allow assignment of the absolute stereochemistries and *ees* (Figure 6.5). Previous optical rotations had also been reported for each enantiomer, so the absolute stereochemistries assigned by the Mosher's method could be re-affirmed by measurement of the optical rotations for the ketol compounds.<sup>[105]</sup>

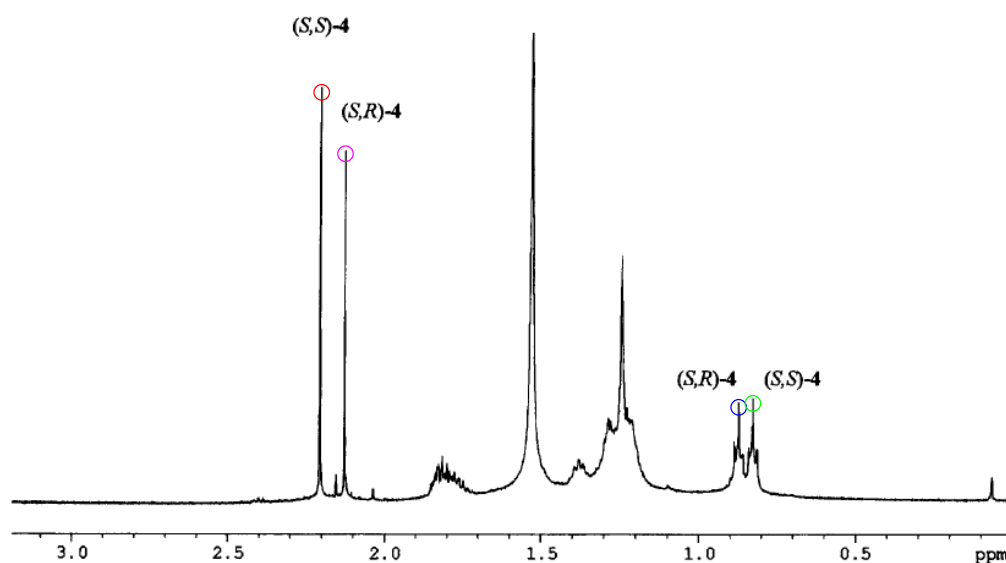
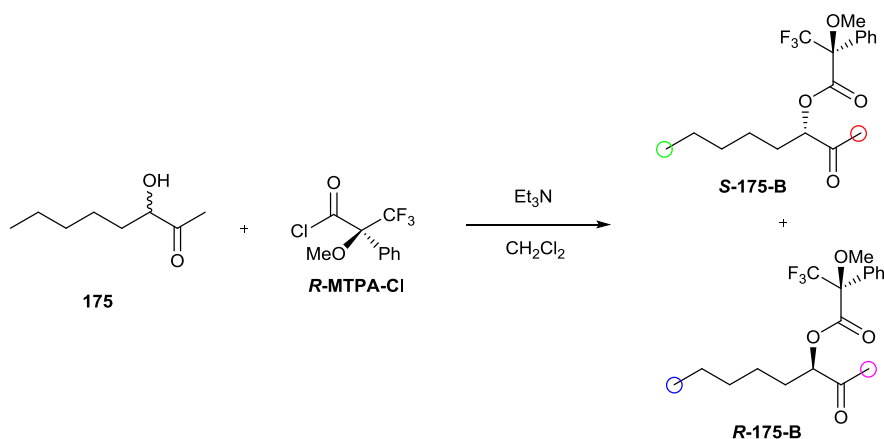


**Figure 6.5** Use of Mosher's ester analysis to determine the absolute stereochemistry of ketol products (**175**)<sup>[104]</sup> (Used with permission from Elsevier).

Of all the mutants tested with sodium pyruvate as a donor substrate, only D469E and D469T had given any isolatable products, with both enzymes producing ketols **174** and **175** from pentanal (**121**) and hexanal (**173**). Therefore, purified samples of ketols **174** and **175** from both enzymes were derivatised with *R*-Mosher's acid chloride, using an analogous procedure as previously described for ketodiols,<sup>[26, 85]</sup> to make the *S*-Mosher's esters (**174-B** and **175-B**). The peaks of the singlet methyl groups were then analysed to determine which enantiomers were being formed (Scheme 6.2). The resulting  $^1\text{H-NMR}$  spectrum of **175-B** is shown in Figure 6.6.

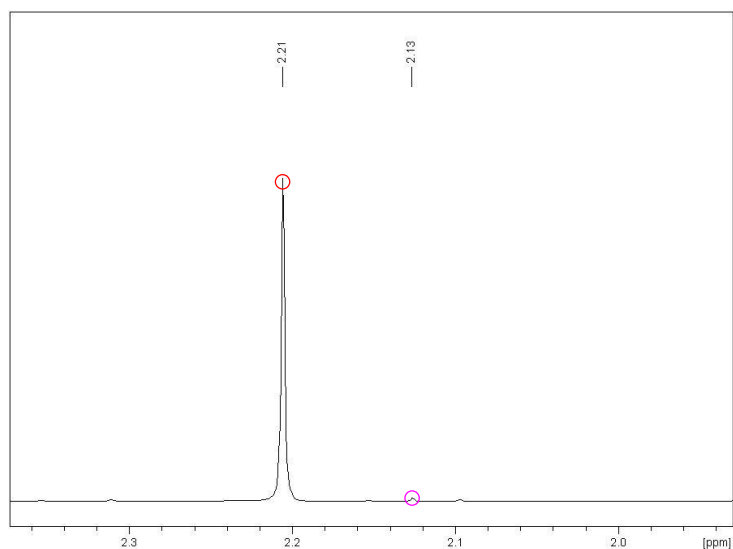
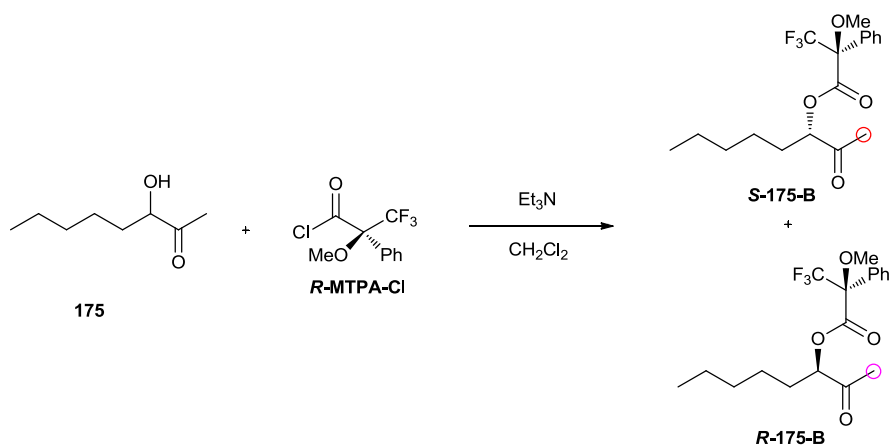


**Figure 6.6**  $^1\text{H-NMR}$  of *S*-Mosher's derivative (**175-B**) of ketol (**175**) from D469E reaction with hexanal and sodium pyruvate, with terminal methyl singlet region expanded

Pleasingly, comparison of the singlet methyl signals at  $\delta$  2.21 and  $\delta$  2.13 and the integrations for each signal showed that the *S*-enantiomer of **175** was formed almost exclusively by D469E in  $> 95\%$  *ee*. This method was then extended to ketol **174** from the D469E TK reaction of pentanal and sodium pyruvate (Figure 6.7).

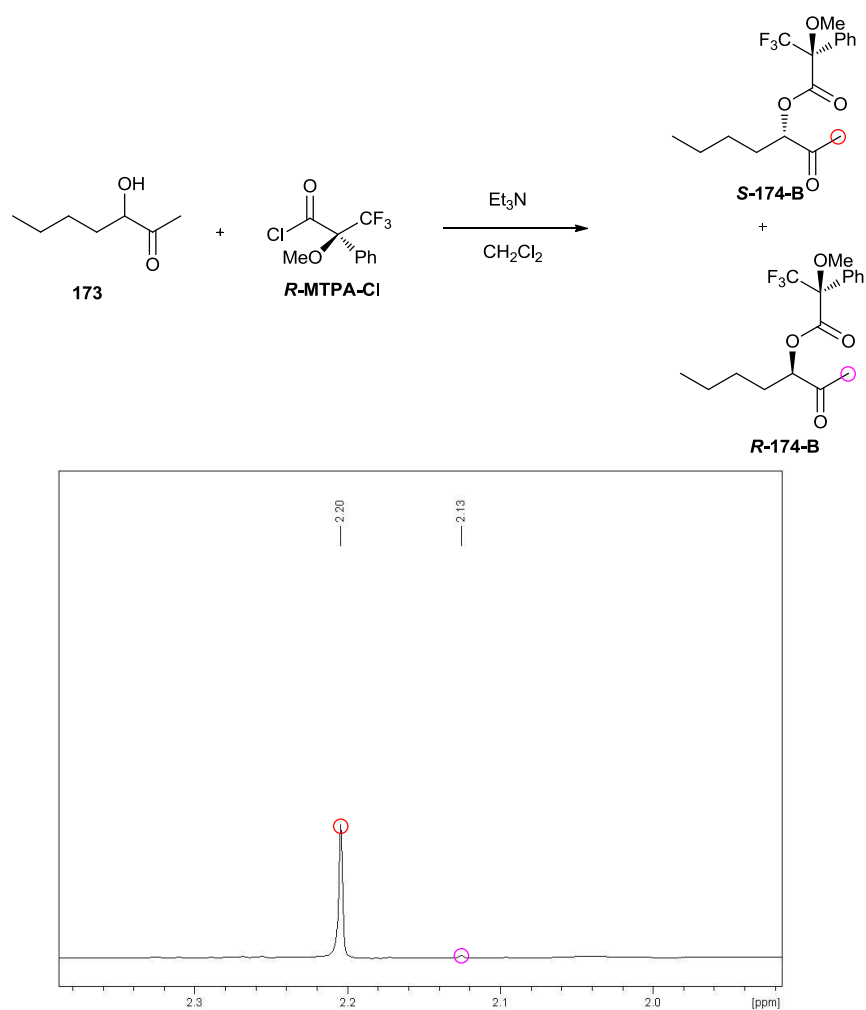


**Figure 6.7**  $^1\text{H-NMR}$  of *S*-Mosher's derivative (**174-B**) of ketol (**174**) from D469E reaction with pentanal and sodium pyruvate, with terminal methyl singlet region expanded

Once again, analysis of the singlet methyl signals at  $\delta$  2.20 and  $\delta$  2.13 showed that D469E formed the *S*-enantiomer almost exclusively with a product *ee* > 95%. The optical rotation values of both ketol compounds supported the  $^1\text{H-NMR}$  data in the assignment of the absolute stereochemistry, with both exhibiting positive optical rotations as previously reported for the *S*-enantiomers of these compounds.<sup>[104, 105]</sup>

Ketol products **174** and **175** from D469T were then subjected to the same Mosher's derivatisation method, and the singlet methyl regions in each  $^1\text{H-NMR}$  spectrum analysed as before. Once again, exquisite selectivity was observed with products formed with >95% *ee* for the (*S*)-enantiomer. The absolute stereochemistry was confirmed by the optical rotation values for all compounds.<sup>[104, 105]</sup> The results with sodium pyruvate as the donor substrate for both D469E and D469T are summarised below (Table 6.8).



**Table 6.8 Isolated yields and stereoselectivities obtained for D469E and D469T with sodium pyruvate as the donor substrate**

Substrate (R=)	D469E Yield (ee)	D469T Yield (ee)
<b>C<sub>4</sub>H<sub>9</sub> (121)</b>	5% (>95% 3 <i>S</i> ) ( <b>174</b> )	5% (>95% 3 <i>S</i> ) ( <b>174</b> )
<b>C<sub>5</sub>H<sub>11</sub> (173)</b>	6% (>95% 3 <i>S</i> ) ( <b>175</b> )	4% (>95% 3 <i>S</i> ) ( <b>175</b> )

#### 6.4.2 Determination of stereoselectivity of TK reaction with 2-ketobutyric acid as donor substrate

While the ketol products (**174**, **175**, Scheme 6.2) from the TK reaction with aliphatic aldehydes and sodium pyruvate had been previously reported, along with chiral analysis methods,<sup>[104, 105]</sup> no such methods had been reported for products **176** and **177** formed from 2-ketobutyric acid as the donor substrate. However, it was considered that the Mosher's ester analysis method could once again be applied using an analogous approach. The 2-ketobutyric acid products (**176** and **177**) contained an extra methylene group, changing both the shift and multiplicity of the singlet methyl signal used to assign the stereochemistry in **174-B** and **175-B**. However, as previously mentioned, the terminal triplet methyl signal can also be used to assign absolute stereochemistries.<sup>[104]</sup> The shift of this proton would be unaffected by using 2-ketobutyric acid as the donor substrate, so this signal could be used to assign the absolute stereochemistry.

To confirm that this approach was feasible, the <sup>1</sup>H-NMR spectrum of the Mosher's ester derivative of the D469E TK product of **175** was analysed again (Figure 6.8), focusing on the terminal methyl triplet signal (Figure 6.6).

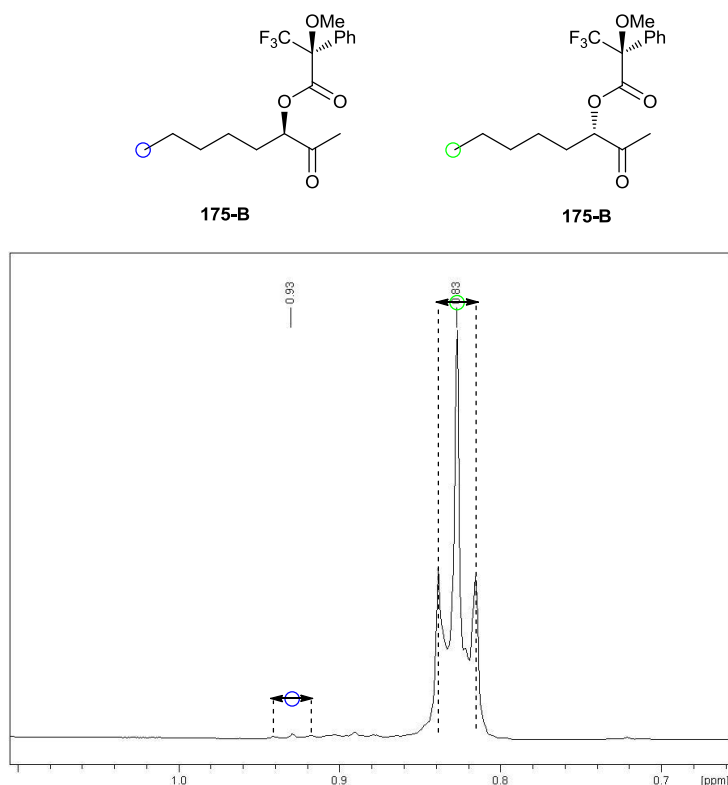


**Figure 6.8**  $^1\text{H-NMR}$  spectrum of *S*-Mosher's derivative (**175-B**) of ketol (**175**) from the D469E reaction of hexanal with sodium pyruvate, with terminal methyl triplet region expanded

The triplet methyl signals for each isomer at  $\delta$  0.83 and  $\delta$  0.93 were in good agreement with previously reported chemical shift data (Figure 6.5),<sup>[104]</sup> and confirmed the stereoselectivity as >95% (*3S*), the same as found by analysing the singlet methyl signal of this Mosher's ester derivative (Figure 6.6).

The Mosher's ester derivative of ketol **177** from the S385T/D469T/R520Q TK reaction product of hexanal and 2-ketobutyric acid was then prepared as previously described and studied by  $^1\text{H-NMR}$  spectroscopy, focusing on the triplet methyl signals (Figure 6.9).

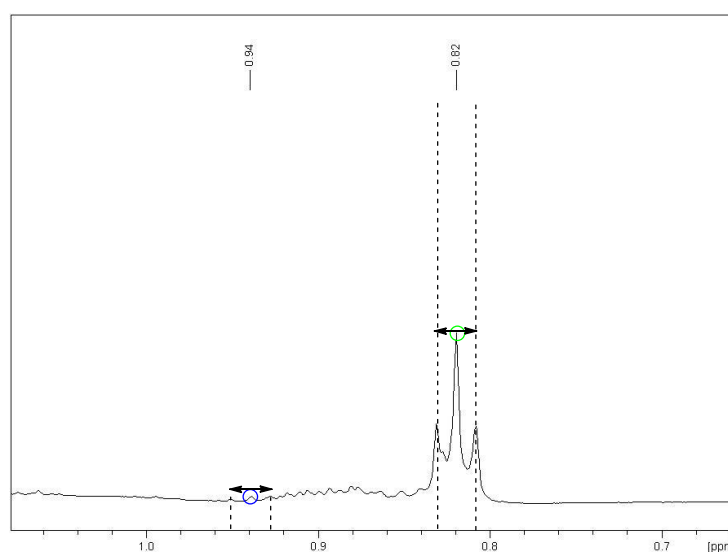
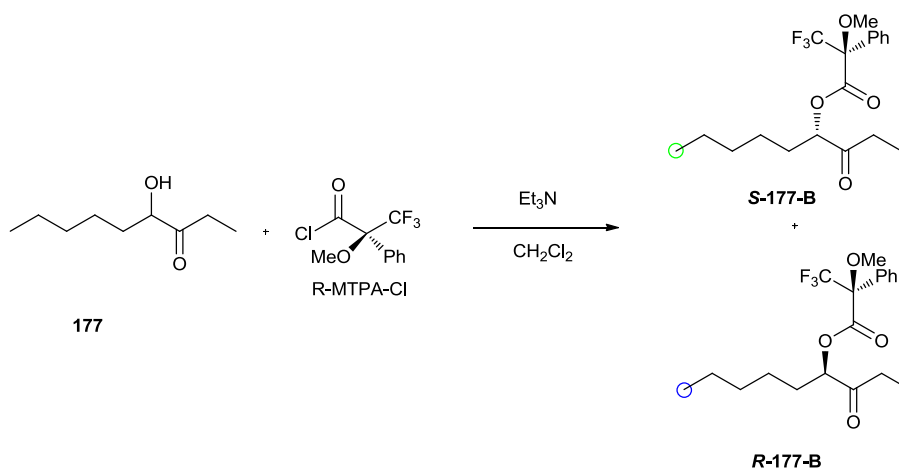


**Figure 6.9 Formation of S-Mosher's ester derivative (177-B) of ketol (177) from the S385T/D469T/R520Q TK reaction with hexanal and 2-ketoglutaric acid. The resulting <sup>1</sup>H-NMR is shown, with the terminal methyl triplet region expanded**

Integration of the triplet methyl signals at  $\delta$  0.82 and  $\delta$  0.94 indicated that S385T/D469T/R520Q gave the same selectivity with 2-ketobutyric acid as D469E and D469T did with sodium pyruvate, forming the 4(*S*)-enantiomer exclusively with >95% *ee*. In addition ketol **177** from S385T/D469T/R520Q gave a positive optical rotation, as did ketols **176** and **177** from the other mutants, which were therefore all assigned as 4(*S*), as summarised below (Table 6.9).

**Table 6.9 Isolated yields and stereoselectivities obtained for mutant TKs with 2-ketobutyric acid (172) as the donor substrate**

$\text{R-CHO} + \text{CH}_3\text{C(=O)CH}_2\text{C(=O)OH} \xrightarrow[\text{ThDP, Mg}^{2+}]{\text{Mutant TKs}} \text{R-CH(OH)CH}_2\text{C(=O)CH}_3$

121, 173                      172                      176, 177  
 121 R=C<sub>4</sub>H<sub>9</sub>                      176 R=C<sub>4</sub>H<sub>9</sub>  
 173 R=C<sub>5</sub>H<sub>11</sub>                      177 R=C<sub>5</sub>H<sub>11</sub>

Aldehyde (R=)	D469E Yield ( <i>ee</i> )	D469T Yield ( <i>ee</i> )	D469Y Yield ( <i>ee</i> )	D469E R520Q Yield ( <i>ee</i> )	S385T D469T R520Q Yield ( <i>ee</i> )
<b>C<sub>4</sub>H<sub>9</sub> (121)</b>	Trace (176)	4% (4 <i>S</i> ) (176)	Trace (176)	6% (4 <i>S</i> ) (176)	4% (>95% (4 <i>S</i> )) (176)
<b>C<sub>5</sub>H<sub>11</sub> (173)</b>	7% (4 <i>S</i> ) (177)	Trace (177)	8% (4 <i>S</i> ) (177)	3% (4 <i>S</i> ) (177)	Trace (177)

## 6.5 Summary of chapter 6

The unprecedented acceptance of novel donor substrates by mutant TKs has been investigated. Sodium pyruvate was accepted by a range of mutant TKs with aliphatic acceptor substrates, and low yields but excellent stereoselectivities were observed. 2-Ketobutyric acid was also accepted by a range of mutant TKs, forming ketol products with a similar degree of stereoselectivity. There have been no reports of *E. coli* TK accepting non-natural donor substrates (other than HPA), and only one report of yeast TK accepting non-natural substrates.<sup>[102]</sup> In this study, circular dichroism was used to prove that novel donor substrates bound to ThDP in the TK active-site, but did not indicate whether the donors were turned over to generate products. The work presented in this chapter therefore represents the first conclusive report of TK accepting novel donor substrates. Ketol products were isolated and fully characterised and chiral analysis methods were developed and used to prove that the products were formed with exquisite stereoselectivity in all cases.

## **7 Conclusions and future work**

This thesis has described detailed investigations into ketodiol synthesis using both organocatalytic (Chapter 2) and biocatalytic (Chapters 3-5) strategies. Initial investigations into the transformation of some aromatic ketodiol by CV2025 TAm have also been conducted (Chapter 5) and a proof-of-concept two-step TK/TAm pathway to aromatic aminodiol has been demonstrated using benzaldehyde as the starting substrate (Figure 7.1). The absolute stereochemistry of the TK-catalysed conversion of benzaldehyde was shown to be (*S*)-selective by correlation to optically pure aminodiol reference compounds, and all other ketodiol have been assigned as 3(*S*) by extension and based on previous chiral data. The acceptance of several novel donor substrates by TK has also been investigated (Chapter 6), and the reaction shown to be highly (*S*)-selective. While this thesis describes the first in-depth studies into the acceptance of aromatic acceptor substrates and novel donor substrates by TK, there is much future work still to be carried out.

Firstly, it would be beneficial to solve crystal structures of the mutant TKs, especially those which showed excellent activity towards aromatic aldehydes (Chapter 5). This would allow more detailed modelling experiments to be performed to account for enzyme activities, stereoselectivities and also to aid the design of more active biocatalysts.

Secondly, in order to fully recognise one of the main goals of this project, namely the enzymatic synthesis of antibiotic molecules such as thiamphenicol and chloramphenicol (Figure 7.1), the use of mutant TKs which reverse the stereoselectivity of the reaction with aromatic aldehydes needs to be investigated. Since both of the target compounds exhibit (1*R*,2*R*)-stereochemistry, these new TK mutants would have to be combined with an (*R*)-selective transaminase. Since *R*-selective transaminases which accept aromatic substrates have been reported in the literature,<sup>[107]</sup> if mutant TKs can be created which reverse the stereochemistry of aromatic ketodiol then the biocatalytic synthesis of molecules such as thiamphenicol and chloramphenicol should be possible (Figure 7.1).

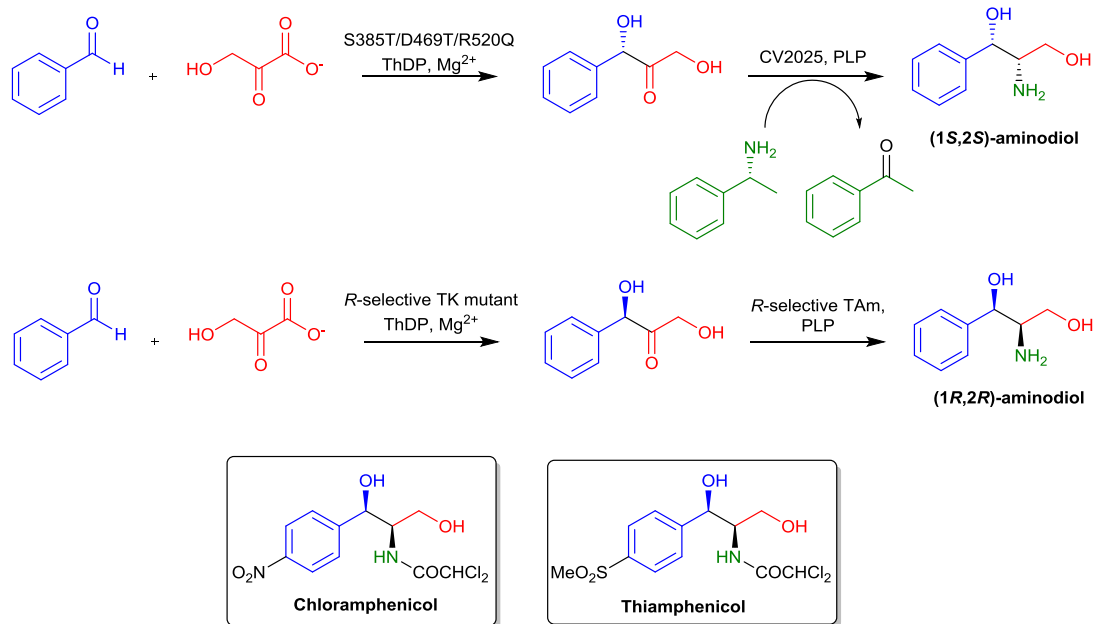


**Figure 7.1** Approach to biocatalytic aminodiol synthesis; above route using currently available enzymes, below ideal route using (*R*)-selective enzymes

Thirdly, CV2025 TAm was shown to be poorly tolerant of aromatic ketodiols, transforming only the TK product of benzaldehyde, and none of the other aromatic ketodiols tested (Chapter 5). It is clear that in order to prepare a diverse range of aromatic aminodiols more work is required to find a TAm which accepts substituted aromatic ketodiol substrates. A library of mutant CV2025 TAm has been created, by colleagues in biochemical engineering, which can now be studied in further detail.

Finally, three pyruvate derivatives were tested with a range of mutants, and two of these substrates were transformed with high stereoselectivities (>95% (*S*)). It would be of great interest to investigate this area more comprehensively with a wider range of both donor and acceptor substrates, to further assess the donor substrate scope of mutant TKs. Also, while the stereoselectivity of these reactions was shown to be excellent the isolated yields were rather low (<10%). This is perhaps due, in part, to the volatility of the ketol products, however there is plenty of scope to optimise the reaction conditions of these biotransformations to generate products in higher yields.

## 8 Experimental

### 8.1 General experimental

$^1\text{H}$  NMR and  $^{13}\text{C}$  NMR spectra were recorded using Bruker AMX 300 MHz, Avance 500 MHz and 600 MHz machines.  $^{19}\text{F}$  NMR spectra were recorded using a Bruker AMX 300 MHz machine. All NMR spectra were recorded at 298 K. Chemical shifts are given in ppm ( $\delta$ ), relative to tetramethylsilane as reference. IR spectra were recorded neat using Nicolet FT-IR and Shimadzu FTIR-8700 machines.  $\text{ES}^+$  mass spectra were recorded using Thermo Finnigan MAT 900XP and Micro Mass QC. CI spectra and HRMS were obtained using Fisons VG70-SE and LTQ orbitrap XL (EPSRC National Mass Spectrometry Service Centre, Swansea University). Chiral HPLC was performed with a Varian Prostar machine fitted with a UV detector prostar/dynamic system 24 (2 volts) absorbance at 214 nm. *Ees* were determined using Chiralcel OD and Chiralpak AD columns (Daicel; Chiral Technologies Europe, France) 25 cm x 0.46 cm. Polar mobile phase (isopropanol) and non-polar mobile phase (*n*-hexane) were used with the indicated methods. TLC was carried out on pre-coated aluminium backed silica plates (Merck 60 F254 normal phase) and examined under UV fluorescence at 254 nm and stained using phosphomolybdic acid. Chemicals were used as received from Aldrich Chemical Company or Fisher Chemical Company without further purification. Solvents used were of analytical and HPLC grade. Optical rotations were recorded on a Perkin Elmer 343 model polarimeter at 589 nm, at the indicated temperature, using the indicated solvent and quoted in  $\text{deg cm}^2 \text{g}^{-1}$  and concentration (*c*) in g/100 mL. Melting points (m.p) were established using a Gallenkamp apparatus and measured in  $^{\circ}\text{C}$ .

### 8.2 Preparation of TK cell-free lysate

Glycerol stocks of TK mutants were obtained from Panwajee Payongsri (25% v/v glycerol) and stored at  $-80^{\circ}\text{C}$  until needed. These were then used to inoculate 250 mL shake flasks containing 50 mL LB broth containing ampicillin (150  $\mu\text{g}/\text{mL}$ ) and incubated overnight at  $37^{\circ}\text{C}$  and 160 rpm using an SI 50 orbital shaker (Stuart Scientific, Redhill, UK.) This culture was then used to inoculate a 1 L shake flask

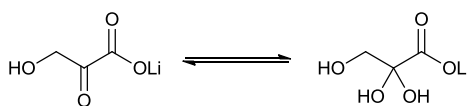


containing 200 mL LB-Amp media and incubated at 37 °C and 200 rpm. The culture was then centrifuged at 4400 rpm for 20 minutes at 4 °C and approximately 4 g of cell paste was obtained and subsequently re-suspended in cold sodium phosphate buffer (5 mM, pH 7) to a final concentration of 1 g of cell paste per 10 mL buffer. The cells were then lysed by sonication for 4 minutes (cycles of 10 seconds on, 10 seconds off) using a Soniprep 150 sonicator (MSE, Sanyo, Japan), and centrifuged at 4400 rpm for 20 minutes at 4 °C. Supernatant cell-free lysate (approximately 40 mL total) was stored in 2 mL eppendorf tubes and kept at -20 °C until needed. TK protein concentration was determined to be approximately 1 mg/mL.

### 8.3 Representative biotransformation procedure

MgCl<sub>2</sub> (0.390 mL of 0.10 g/mL solution, 0.40 mmol) was added to ThDP (0.022 g, 48 mmol) in water (10 mL) at pH 7. TK cell-free lysate (2 mL or 4 mL, as indicated) was added and the mixture incubated for 20 minutes. In a separate flask, Li-HPA (0.110 g, 1.0 mmol) was dissolved in water (10 mL) and the pH adjusted to 7 with NaOH (1 M), this was then added to the enzyme mixture along with the desired aldehyde (25 mM or 50 mM as indicated). Reactions were then stirred at room temperature for 24 hours or 48 hours, as indicated, in an autotitrator programmed to add 1 M HCl when the pH increased above 7.

#### **Lithium hydroxypyruvate (Li-23)<sup>[26]</sup>**



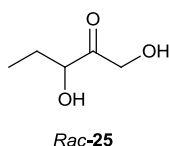
Li-23

Bromopyruvic acid (10.0 g, 60.0 mmol) was dissolved in water (100 mL) and LiOH solution (1 M) was added until the pH was 9.5. Then, glacial acetic acid was added until the pH reached 5. The solvent was then removed under reduced pressure to a final volume ~20 mL and the product was left to crystallise out of solution overnight at 4 °C. The crude off-white precipitate was then washed with ethanol and collected by suction filtration. The crude solid was then re-suspended in ethanol (50 mL) and

stirred at 40 °C for 30 min before being collected by suction filtration and washed with more ethanol (50 mL) to give Li-**23** (4.42 g, 70%) as a white powder.

mp (decomposed before melting);  $\nu_{\max}/\text{cm}^{-1}$  (neat): 3340, 1595, 1532, 1377;  $^1\text{H}$  NMR (300 MHz;  $\text{D}_2\text{O}$ )  $\delta$ : 4.61 (2H, s,  $\text{CH}_2$  gem diol), 3.60 (2H, s,  $\text{CH}_2$  ketone)  $^{13}\text{C}$  NMR (125 MHz;  $\text{CDCl}_3$ )  $\delta$ : 203.0 ( $\text{C}=\text{O}$ ), 177.0 ( $\text{C}=\text{O}$ ), 167.9 ( $\text{C}=\text{O}$ ), 94.7 ( $\text{C}(\text{OH})_2$ ), 66.5 ( $\text{CH}_2$ ), 65.8 ( $\text{CH}_2$ ).

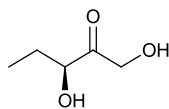
### ***Rac-1,3-dihydroxypentan-2-one (Rac-25)***<sup>[26]</sup>



Li-HPA (1.10 g, 10.0 mmol) was dissolved in water (300 mL) at room temperature. Propanal (0.72 mL, 10.0 mmol) and *N*-methylmorpholine (1.10 mL, 1.0 mmol) were added and the pH was adjusted to 8 with hydrochloric acid (1 M). The reaction mixture was stirred overnight at room temperature and monitored by TLC analysis. The crude reaction mixture was then dry-loaded onto silica and purified by flash silica chromatography (EtOAc:hexane, 3:7) to give *rac-25* as an orange oil (0.21 g, 17%),  $R_f = 0.20$  (EtOAc:hexane, 1:1).

$\nu_{\max}/\text{cm}^{-1}$  (neat): 3412, 2957, 2934, 2874, 1720;  $^1\text{H}$  NMR (300 MHz;  $\text{CDCl}_3$ )  $\delta$ : 4.40 (1H, d,  $J = 19.7$  Hz,  $\text{CHHCO}$ ), 4.38 (1H, d,  $J = 19.7$  Hz,  $\text{CHHCO}$ ), 4.20 (1H, m,  $\text{CH}_2\text{CHOH}$ ), 3.60 (2H, br s,  $\text{OH}$ ), 1.80-1.72 (1H, m,  $\text{CH}_3\text{CHH}$ ), 1.61-1.52 (1H, m,  $\text{CH}_3\text{CHH}$ ), 0.91 (3H, t,  $J = 7.2$  Hz,  $\text{CH}_3$ );  $^{13}\text{C}$  NMR (125 MHz;  $\text{CDCl}_3$ )  $\delta$ : 213.0 ( $\text{C}=\text{O}$ ), 76.0 ( $\text{CHOH}$ ), 65.8 ( $\text{CH}_2\text{OH}$ ), 27.4 ( $\text{CH}_2$ ), 9.4 ( $\text{CH}_3$ );  $m/z$  (HR ES+) found  $[\text{MH}]^+ 119.0703$ .  $\text{C}_5\text{H}_{11}\text{O}_3$  requires 119.0630.

**(3S)-1,3-Dihydroxypentane-2-one (S-25)<sup>[26]</sup>**

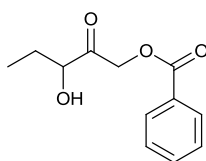


S-25

The standard biotransformation procedure was performed with D469Y TK cell-free lysate (2 mL) and propanal (50 mM) for 48 hours. The crude reaction mixture was then dry-loaded onto silica and purified by flash silica chromatography (EtOAc:hexane, 3:7) to give S-25 as a colourless oil (0.013 g, 11%),  $R_f = 0.20$  (EtOAc:hexane, 1:1).

Characterisation data was as found for the racemic product (*rac*-25).

**3-Hydroxy-2-oxopentyl benzoate (25-B)**



25-B

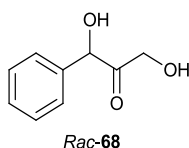
To a stirred solution of **25** (0.013 g, 0.11 mmol) in  $\text{CH}_2\text{Cl}_2$  (5 mL) was added 2,4,6-collidine (0.014 mL, 0.11 mmol) and benzoyl chloride (0.021 mL, 0.11 mmol). The reaction was followed by TLC analysis and stirred overnight at room temperature. The reaction was then washed with HCl (2 M, 25 mL) and extracted with  $\text{CH}_2\text{Cl}_2$  (20 mL), before being dry-loaded onto silica and purified by flash silica chromatography (EtOAc:hexane, 1:9) to give **25-B** as a colourless oil (0.022g, 91%),  $R_f = 0.17$  (EtOAc:hexane, 2:8).

$\nu_{\text{max}}/\text{cm}^{-1}$  (neat): 3482, 2930, 1720, 1273;  $^1\text{H}$  NMR (500 MHz;  $\text{CDCl}_3$ )  $\delta$ : 8.07 (2H, m, Ar H), 7.59 (1H, m, Ar H), 7.46 (2H, t,  $J = 7.8$  Hz, Ar H), 5.15 (1H, d,  $J = 17.2$  Hz, COCHH), 5.04 (1H, d,  $J = 17.2$  Hz, COCHH), 4.36 (1H, dd,  $J = 8.0$  Hz, 3.9 Hz, CHOH), 1.94 (1H, m,  $\text{CH}_3\text{CHH}$ ), 1.71 (1H, m,  $\text{CH}_3\text{CHH}$ ), 1.02 (3H, t,  $J = 7.4$  Hz,  $\text{CH}_3$ );  $^{13}\text{C}$  NMR (125 MHz;  $\text{CDCl}_3$ )  $\delta$ : 206.0 (C=O), 171.1 (C=O), 133.7, 129.8

(Signals overlapping), 128.5, 76.2 (CHOH), 66.3 (CH<sub>2</sub>), 27.1 (CH<sub>2</sub>), 9.0 (CH<sub>3</sub>); *m/z* (HR ES+) found [MH]<sup>+</sup> 223.0964. C<sub>12</sub>H<sub>15</sub>O<sub>4</sub> requires 223.0970.

HPLC analysis (Chiralpak AD column, isopropanol:hexane, 5:95, 0.8 mL/min) gave retention times of 22.0 minutes (*R*-isomer) and 24.5 minutes (*S*-isomer).

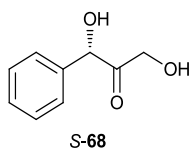
### ***Rac* 1,3-dihydroxy-1-phenylpropan-2-one (*Rac*-68)<sup>[85]</sup>**



Li-HPA (0.110 g, 1.0 mmol) was dissolved in water:acetonitrile, 3:2 (5 mL total), at room temperature. Benzaldehyde (0.102 mL, 1.0 mmol) and *N*-methylmorpholine (0.110 mL, 1.0 mmol) were added and the pH was adjusted to 7 with hydrochloric acid (1 M). The reaction was stirred overnight at room temperature and monitored by TLC analysis. The crude reaction mixture was then dry-loaded onto silica and purified by flash silica chromatography (EtOAc:hexane, 1:4) to give *rac*-68 as a colourless oil (0.025 g, 15%), *R<sub>f</sub>* = 0.34 (EtOAc:hexane, 1:1).

$\nu_{\max}/\text{cm}^{-1}$  (neat): 3400, 2925, 1724; <sup>1</sup>H NMR (300 MHz; CDCl<sub>3</sub>)  $\delta$ : 7.60-7.30 (5H, Ar *H*), 5.23 (1H, d, *J* = 3.9 Hz, CHOH), 4.35 (1H, dd, *J* = 19.1 Hz, 4.4 Hz, COCHH), 4.25 (1H, dd, *J* = 19.1 Hz, 4.4 Hz, COCHH), 3.88 (1H, d, *J* = 3.9 Hz, OH), 2.76 (1H, t, *J* = 4.4 Hz, OH); <sup>13</sup>C NMR (125 MHz; CDCl<sub>3</sub>)  $\delta$ : 209.0 (C=O), 137.4, 129.3, 128.7, 127.0, 77.8 (CHOH), 65.2 (CH<sub>2</sub>OH); *m/z* (HR ES+) found [MH]<sup>+</sup> 167.0712. C<sub>9</sub>H<sub>11</sub>O<sub>3</sub> requires 167.0630.

### (3S)-1,3-Dihydroxy-1-phenylpropan-2-one (S-68)

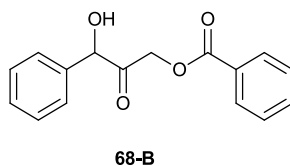


The standard biotransformation procedure was performed with F434A TK cell-free lysate and 50 mM benzaldehyde for 48 hours. Solvent was then removed and the crude product purified by flash silica chromatography (EtOAc:hexane, 1:4) to give **S-68** (0.016 g, 10%) as a colourless oil.

$[\alpha]_{\text{D}}^{20} = +74.0$  (*c* 0.5, CHCl<sub>3</sub>)

Characterisation data was as found for the racemic product (*rac*-**68**).

### 3-Hydroxy-2-oxo-3-phenylpropyl benzoate (68-B)

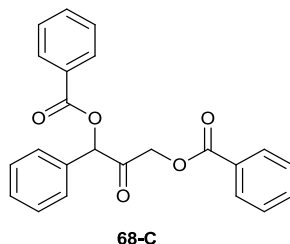


To a stirred solution of **68** (0.025 g, 0.15 mmol) in CH<sub>2</sub>Cl<sub>2</sub> (20 mL) was added benzoyl chloride (0.019 mL, 0.16 mmol) and 2,4,6-collidine (0.023 μL, 0.16 mmol). The reaction was stirred at room temperature overnight, then washed with HCl (50 mL, 2M) and extracted with CH<sub>2</sub>Cl<sub>2</sub> (100 mL). The organic layer was then dry-loaded onto silica and purified by flash silica chromatography (EtOAc:hexane, 5:95) to give **68-B** as a colourless oil (0.001 g, 2%), *R*<sub>f</sub> = 0.26 (EtOAc:hexane, 2:8).

$\nu_{\text{max}}/\text{cm}^{-1}$  (neat): 3020, 2836, 2676, 2565, 1685, 1326, 1292; <sup>1</sup>H NMR (300 MHz; CDCl<sub>3</sub>)  $\delta$ : 8.10-8.00 (2H, m, Ar H), 7.62-7.30 (8H, m, Ar H), 5.34 (1H, s, CHOH), 5.00 (1H, d, *J* = 16.9 Hz, COCHH), 4.25 (1H, d, *J* = 16.9 Hz, COCHH); <sup>13</sup>C NMR (125 MHz; CDCl<sub>3</sub>)  $\delta$ : 203.2 (C=O), 168.9 (C=O), 137.1, 133.8, 130.3, 130.0, 129.4, 128.9, 128.7, 127.5, 78.4 (CHOH), 65.7 (CH<sub>2</sub>OH); *m/z* (HR ES<sup>+</sup>) found [MH]<sup>+</sup> 271.0961. C<sub>16</sub>H<sub>15</sub>O<sub>4</sub> requires 271.0970.

HPLC analysis (Chiralpak AD column, isopropanol:hexane, 10:90, 1 mL/min) gave retention times of 13.4 minutes (*S*-isomer) and 15.2 minutes (*R*-isomer).

## 2-Oxo-1-phenylpropane-1,3-diyl dibenzoate (68-C)<sup>[85]</sup>

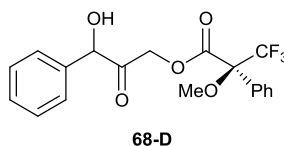


To a stirred solution of **68** (0.025 g, 0.15 mmol) in CH<sub>2</sub>Cl<sub>2</sub> (20 mL) was added 2,4,6-collidine (0.040 mL, 0.34 mmol) and benzoyl chloride (0.038 mL, 0.32 mmol). The reaction was stirred at room temperature overnight, then washed with HCl (50 mL, 2 M) and extracted with CH<sub>2</sub>Cl<sub>2</sub> (50 mL). The organic layer was dry-loaded onto silica and purified by flash silica chromatography (EtOAc:hexane, 1:9) to give **68-C** as a colourless oil (0.001 g, 1%), R<sub>f</sub> = 0.4 (EtOAc:hexane, 2:8).

$\nu_{\max}/\text{cm}^{-1}$  (neat): 2921, 2851, 1726, 1272; <sup>1</sup>H NMR (300 MHz; CDCl<sub>3</sub>)  $\delta$ : 8.10-8.05 (4H, m, Ar *H*) 7.63-7.41 (11H, m, Ar *H*), 6.43 (1H, s, CHO), 5.17 (1H, d, *J* = 16.9 Hz, COCHH), 4.25 (1H, d, *J* = 16.9 Hz, COCHH); <sup>13</sup>C NMR (125 MHz; CDCl<sub>3</sub>)  $\delta$ : 197.9 (C=O), 165.8 (C=O), 165.7 (C=O), 133.8, 133.6, 132.9, 130.6, 130.3, 130.1, 130.0, 129.9, 129.5, 128.7, 128.6, 128.3, 79.0 (CHOH), 66.3 (CH<sub>2</sub>OH); *m/z* (HR ES+) found [MH]<sup>+</sup> 375.1221. C<sub>23</sub>H<sub>19</sub>O<sub>5</sub> requires 375.1232.

HPLC analysis (Chiralcel OD column, isopropanol:hexane, 18:82, 1 mL/min) gave retention times of 10.5 minutes (*R*-isomer) and 13.4 minutes (*S*-isomer).

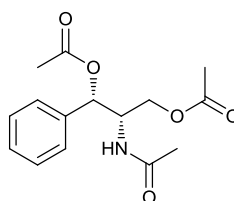
## (2*S*)-3,3,3-Trifluoro-2-methoxy-2-phenyl-propionic acid 3-hydroxy-2-oxo-3-phenyl-propyl ester (68-D)<sup>[85]</sup>



To a stirred solution of *rac*-**68** (0.005 g, 0.03 mmol) in CH<sub>2</sub>Cl<sub>2</sub> was added triethylamine (0.010 mL, 0.07 mmol) and (*R*)-MTPA-Cl (0.010 mL, 0.05 mmol) and the reaction stirred at room temperature overnight. The crude reaction mixture was dry-loaded onto silica and purified by flash silica chromatography (EtOAc:hexane, 1:9) to give **68-E** as a colourless oil (0.001 g, 9%), R<sub>f</sub> = 0.63 (EtOAc:hexane, 1:1).

$\nu_{\max}/\text{cm}^{-1}$  (neat): 3420, 2930, 2855, 1734;  $^1\text{H}$  NMR (300 MHz;  $\text{CD}_3\text{OD}$ )  $\delta$ : 7.80-7.30 (10H, m, Ar *H*), 5.26 (1H, s, *CHOH*), 5.01 (0.5H, d,  $J = 17.0$  Hz, *COCHH*), 4.91 (0.5H, d,  $J = 17.0$  Hz, *COCHH*), 4.86 (0.5H, d,  $J = 17.0$  Hz, *COCHH*), 4.70 (0.5 H, d,  $J = 17.0$  Hz, *COCHH*), 3.62 (3H, s,  $\text{COCH}_3$ );  $^{13}\text{C}$  NMR (150 MHz;  $\text{CDCl}_3$ )  $\delta$ : 201.7 (C=O), 166.3 (C=O), 133.8, 130.1, 129.6, 129.2, 128.7, 128.5, 127.6, 126.4, 77.1 (*CHOH*), 71.6 ( $\text{OCH}_3$ ), 66.5 ( $\text{CH}_2\text{OH}$ );  $^{19}\text{F}$  NMR (300 MHz;  $\text{CDCl}_3$ )  $\delta$ : -77.2 ( $\text{CF}_3$ );  $m/z$  (HR ES+) found  $[\text{MH}]^+$  383.1109.  $\text{C}_{19}\text{H}_{18}\text{F}_3\text{O}_3$  requires 383.1106.

**(1*S*,2*S*)-2-Acetamido-1-phenylpropane-1,3-diyl diacetate**  
**((1*S*,2*S*)-69-B)<sup>[75]</sup>**



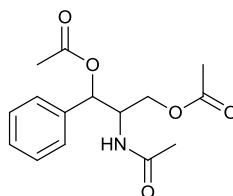
(1*S*,2*S*)-69-B

To a stirred solution of (1*S*,2*S*)-2-amino-1-phenyl-1,3-propanediol (0.050 mg, 0.30 mmol) in pyridine (1.0 mL, 12.0 mmol) was added acetic anhydride (1.0 mL, 13.0 mmol) and *N,N*-dimethylaminopyridine (0.025 g, 0.20 mmol). The reaction was stirred at room temperature for 18 hours and then concentrated under vacuum. The crude mixture was then redissolved in water and the product extracted with  $\text{CH}_2\text{Cl}_2$  (2 x 25 mL). The organic layer was dried over magnesium sulfate, filtered and concentrated under vacuum to give the title compound as a light yellow oil (0.085 g, 97%),  $R_f = 0.30$  (EtOAc:hexane, 1:1).

$\nu_{\max}/\text{cm}^{-1}$  (neat): 3289, 3065, 1739, 1659; 1540;  $^1\text{H}$  NMR (600 MHz;  $\text{CDCl}_3$ )  $\delta$ : 7.50-7.32 (5H, m, Ar *H*), 5.93 (1H, d,  $J = 7.2$  Hz, *CHOAc*), 5.89 (1H, d,  $J = 9.3$  Hz, *NHAc*), 4.63 (1H, m, *CHNHAc*); 4.05 (1H, dd,  $J = 11.6$  Hz, 5.0 Hz, *CHHOAc*), 3.84 (1H, dd,  $J = 11.6$  Hz, 4.8 Hz, *CHHOAc*), 2.09 (3H, s,  $\text{CH}_3$ ), 2.05 (3H, s,  $\text{CH}_3$ ), 1.94 (3H, s,  $\text{CH}_3$ )  $^{13}\text{C}$  NMR (150 MHz;  $\text{CDCl}_3$ )  $\delta$ : 170.7 (C=O), 170.5 (C=O), 170.0 (C=O), 136.6, 128.9 (signals overlapping), 126.9, 74.3 (*CHOAc*), 63.3 ( $\text{CH}_2\text{OAc}$ ), 52.3 (*CHNAc*), 23.3 ( $\text{CH}_3$ ), 21.2 ( $\text{CH}_3$ ), 20.9 ( $\text{CH}_3$ );  $m/z$  (HR CI+) found  $[\text{MH}]^+$  294.1324.  $\text{C}_{15}\text{H}_{19}\text{NO}_5$  requires 294.1336.

HPLC analysis (Chiralpak AD column, isopropanol:hexane, 3:97, 0.6 mL/min) gave a retention time of 77.9 minutes.

### ***Biotrans-2-acetamido-1-phenylpropane-1,3-diyl diacetate (69-B)***



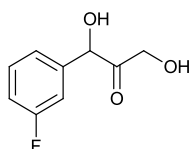
**Biotrans-69-B**

To a sample of **68** (0.016g, 0.10 mmol) dissolved in HEPES buffer (7.5 mL, 100 mM, pH 8, 0.2 mM PLP) was added CV2025 cell-free lysate (5 mL) and *S*- $\alpha$ -methylbenzylamine (0.026 mL, 0.20 mM). The reaction was adjusted to pH 8 and the mixture incubated at 37 °C and followed by TLC analysis until no starting material could be observed. The reaction was then concentrated to dryness and acetylation performed as for (1*S*,2*S*)-**69-B**.

Spectroscopic data was as found for (1*S*,2*S*)-**69-B**.

HPLC analysis (Chiralpak AD column, isopropanol:hexane, 3:97, 0.6 mL/min) gave retention times of 77.9 mins (1*S*,2*S*)-major isomer and 92.9 mins (1*R*,2*S*)-minor isomer.

### ***Rac-1-(3-fluorophenyl)-1,3-dihydroxypropan-2-one (Rac-94)<sup>[79]</sup>***



**Rac-94**

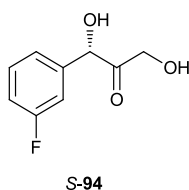
Li-HPA (0.110 g, 1.0 mmol) was dissolved in water:acetonitrile, 1:1 (10 mL total), at room temperature. 3-Fluorobenzaldehyde (0.106 mL, 1.0 mmol) and *N*-methylmorpholine (0.110 mL, 1.0 mmol) were added and the pH was adjusted to 7 with hydrochloric acid (1 M). The reaction mixture was stirred at room temperature



overnight and monitored by TLC analysis. The crude reaction mixture was then dry-loaded onto silica and purified by flash silica chromatography (EtOAc:hexane, 3:7) to give *rac*-**94** as a colourless oil (42 mg, 23%),  $R_f = 0.29$  (EtOAc:hexane, 1:1).

$\nu_{\max}/\text{cm}^{-1}$  (neat): 3440, 2938, 1721, 1272;  $^1\text{H NMR}$  (600 MHz;  $\text{CDCl}_3$ )  $\delta$ : 7.38-7.05 (4H, m, Ar *H*), 5.25 (1H, d,  $J = 4.2$  Hz, *CHOH*), 4.35 (1H, dd,  $J = 19.8$  Hz, 5.2 Hz, *COCHH*), 4.25 (1H, dd,  $J = 19.8$  Hz, 5.2 Hz, *COCHH*), 3.80 (1H, d,  $J = 4.2$  Hz, *OH*), 2.67 (1H, t,  $J = 5.2$  Hz, *OH*);  $^{13}\text{C NMR}$  (150 MHz;  $\text{CDCl}_3$ )  $\delta$ : 208.5 (*C=O*), 163.2 (*C-F*, d,  $^1J_{CF} = 248.7$  Hz), 139.7 (d,  $^3J_{CF} = 6.6$  Hz), 131.1 (d,  $^3J_{CF} = 8.8$  Hz), 122.7 (d,  $^4J_{CF} = 2.2$  Hz), 116.3 (d,  $^2J_{CF} = 20.9$  Hz), 114.0 (d,  $^2J_{CF} = 21.9$  Hz) 76.9 (*CHOH*), 65.2 (*CH}\_2\text{OH}*);  $^{19}\text{F NMR}$  (300 MHz;  $\text{CDCl}_3$ )  $\delta$ : - 111.6;  $m/z$  (HR ES+) found  $[\text{MH}]^+$  185.0610.  $\text{C}_9\text{H}_{10}\text{O}_3\text{F}$  requires 185.0614.

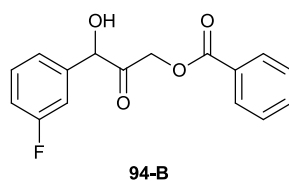
### **(3*S*)-1-(3-Fluorophenyl)-1,3-dihydroxypropan-2-one (S-94)**



The standard biotransformation procedure was performed with S385T/D469T/R520Q TK cell-free lysate (4 mL) and 3-fluorobenzaldehyde (25 mM) for 24 hours. The crude reaction mixture was then dry-loaded onto silica and purified by flash silica chromatography (EtOAc:hexane, 1:4) to give *S*-**94** as a colourless oil (0.011 g, 12 %).

Characterisation data was as found for the racemic product (*rac*-**94**).

### **3-(3-Fluorophenyl)-3-hydroxy-2-oxopropyl benzoate (94-B)<sup>[108]</sup>**



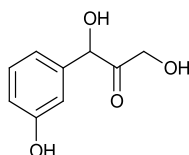
To a stirred solution of **94** (0.040 g, 0.20 mmol) in  $\text{CH}_2\text{Cl}_2$  (5 mL) was added 2,4,6-collidine (0.026 mL, 0.20 mmol) and benzoyl chloride (0.023 mL, 0.20 mmol). The

reaction was stirred overnight at room temperature and monitored by TLC analysis. The reaction was then washed with HCl (2 M, 25 mL) and extracted with CH<sub>2</sub>Cl<sub>2</sub> (20 mL), before being dry-loaded onto silica and purified by flash silica chromatography (EtOAc:hexane, 1:9) to give **94-B** as a colourless oil (0.020 g, 35%), R<sub>f</sub> = 0.21 (EtOAc:hexane, 2:8).

$\nu_{\max}/\text{cm}^{-1}$  (neat): 3440, 3073, 2938, 1721, 1272; <sup>1</sup>H NMR (600 MHz; CDCl<sub>3</sub>)  $\delta$ : 8.10-8.00 (2H, m, Ar *H*), 7.63-7.40 (7H, m, Ar *H*), 5.34 (1H, s, CHOH), 5.02 (1H, d, *J* = 16.9 Hz, COCHH), 4.83 (1H, d, *J* = 16.9 Hz, COCHH); <sup>13</sup>C NMR (150 MHz; CDCl<sub>3</sub>)  $\delta$ : 202.7 (C=O), 171.4 (C=O), 163.1 (d, <sup>1</sup>*J*<sub>CF</sub> = 249.8 Hz), 139.4 (d, <sup>3</sup>*J*<sub>CF</sub> = 10.3 Hz), 133.9 (d, <sup>3</sup>*J*<sub>CF</sub> = 11.0 Hz), 131.6, 130.3, 129.2, 128.1, 123.1 (d, <sup>4</sup>*J*<sub>CF</sub> = 3.3 Hz), 116.3 (d, <sup>2</sup>*J*<sub>CF</sub> = 21.5 Hz), 114.0 (d, <sup>2</sup>*J*<sub>CF</sub> = 20.8 Hz), 76.9 (CHOH), 65.2 (CH<sub>2</sub>OH); <sup>19</sup>F NMR (300 MHz; CDCl<sub>3</sub>)  $\delta$ : - 111.6; *m/z* (HR ES+) found [MH]<sup>+</sup> 289.0871. C<sub>16</sub>H<sub>14</sub>O<sub>4</sub>F requires 289.0876.

HPLC analysis (Chiralpak AD column, isopropanol:hexane, 10:90, 1 mL/min) gave retention times of 10.9 minutes (*S*-isomer) and 13.1 minutes (*R*-isomer).

### ***Rac*-1,3-dihydroxy-1-(3-hydroxyphenyl)propan-2-one** (*Rac*-103)<sup>[85]</sup>



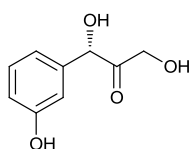
**Rac-103**

Li-HPA (0.110 g, 1.0 mmol) was dissolved in water:acetonitrile, 3:2 (10 mL total), at room temperature. 3-Hydroxybenzaldehyde (0.122 g, 1.0 mmol) and *N*-methylmorpholine (0.110 mL, 1.0 mmol) were added and the pH was adjusted to 7 with hydrochloric acid (1 M). The reaction was stirred overnight at room temperature and monitored by TLC analysis. The crude reaction mixture was then dry-loaded onto silica and purified by flash silica chromatography (EtOAc:hexane, 1:1) to give *rac*-**103** as a colourless oil (0.010 g, 6%), R<sub>f</sub> = 0.31 (EtOAc:hexane, 3:1).

$\nu_{\max}/\text{cm}^{-1}$  (neat): 3350, 2925, 2497, 1731, 1592; <sup>1</sup>H NMR (300 MHz; CDCl<sub>3</sub>)  $\delta$ : 7.18-7.10 (1H, m, Ar *H*), 6.87-6.73 (3H, m, Ar *H*), 5.39 (1H, s, CHOH), 4.45 (1H, d, *J* =

19.1 Hz, COCHH), 4.30 (1H, d,  $J = 19.1$  Hz, COCHH);  $^{13}\text{C}$  NMR (125 MHz;  $\text{CDCl}_3$ )  $\delta$ : 211.0 (C=O), 156.5, 137.7, 131.0, 123.0, 119.9, 114.5, 77.1 (CHOH), 65.0 (CH<sub>2</sub>OH);  $m/z$  (HR ES+) found  $[\text{MH}]^+$  183.0663.  $\text{C}_9\text{H}_{11}\text{O}_4$  requires 183.0673.

**(3S)-1,3-Dihydroxy-1-(3-hydroxyphenyl)propan-2-one (S-103)<sup>[85]</sup>**

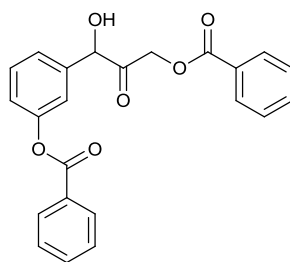


S-103

The standard biotransformation procedure was performed with F434A TK cell-free lysate (2 mL) and 3-hydroxybenzaldehyde (50 mM) for 48 hours. The crude reaction mixture was then dry-loaded onto silica and purified by flash silica chromatography (EtOAc:hexane, 1:1) to give the title compound as a colourless oil (0.011 g, 6%),  $[\alpha]_{\text{D}}^{20} = +93.3$  ( $c$  0.08, MeOH).

Characterisation data was as found for the racemic product (*rac*-103).

**3-(3-(Benzyloxy)-1-hydroxy-2-oxopropyl)phenyl benzoate (103-B)<sup>[85]</sup>**

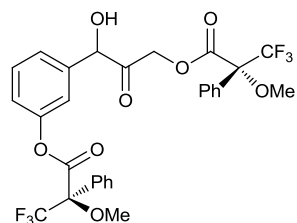


103-B

To a stirred solution of **103** (0.010 g, 0.05 mmol) in  $\text{CH}_2\text{Cl}_2$  (2 mL) was added 2,4,6-collidine (0.030 mL, 0.23 mmol) and benzoyl chloride (0.030 mL, 0.26 mmol). The reaction was stirred at room temperature overnight and monitored by TLC before being washed with HCl (2 M, 75 mL) and extracted with  $\text{CH}_2\text{Cl}_2$  (50 mL). The organic layer was dried over magnesium sulfate, filtered and product dry-loaded onto silica before being purified by flash silica chromatography (EtOAc:hexane, 2:8) to give **103-B** as a colourless oil (10 mg, 50%),  $R_f = 0.2$  (EtOAc:hexane, 3:7).

$^1\text{H}$  NMR (600 MHz;  $\text{CDCl}_3$ )  $\delta$ : 8.19 (2H, d,  $J = 7.9$  Hz, Ar  $H$ ), 8.12 (4H, d,  $J = 7.9$  Hz, Ar  $H$ ), 8.05 (2H, d,  $J = 7.9$  Hz, Ar  $H$ ), 7.68-7.26 (6H, m, Ar  $H$ ), 5.40 (1H, s,  $\text{CHOH}$ ), 5.10 (1H, d,  $J = 17.2$  Hz,  $\text{COCHH}$ ), 4.85 (1H, d,  $J = 17.2$  Hz,  $\text{COCHH}$ );  $^{13}\text{C}$  NMR (150 MHz;  $\text{CDCl}_3$ )  $\delta$ : 202.3 ( $\text{C}=\text{O}$ ), 171.6 ( $\text{C}=\text{O}$ ), 165.9 ( $\text{C}=\text{O}$ ), 165.1, 151.6, 138.7, 134.0, 133.9 (signals overlapping), 130.5, 130.3, 130.1, 128.8 (signals overlapping), 128.7, 128.6, 124.7, 122.7, 120.1, 78.4 ( $\text{CHOH}$ ), 65.7 ( $\text{CH}_2\text{OH}$ ).  
HPLC analysis (Chiralpak AD column, isopropanol:hexane, 20:80, 1 mL/min) gave retention times of 13.5 minutes ( $S$ -isomer) and 18.8 minutes ( $R$ -isomer).

***(R)*-3-(1-Hydroxy-2-oxo-3-(((*R*)-3,3,3-trifluoro-2-methoxy-2-phenylpropanoyl)oxy)propyl)phenyl 3,3,3-trifluoro-2-methoxy-2-phenylpropanoate (**103-C**)**

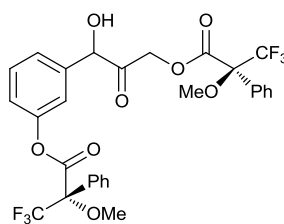


**103-C**

To a stirred solution of **103** (0.003 g, 0.02 mmol) in  $\text{CH}_2\text{Cl}_2$  (2 mL) was added 2,4,6-collidine (0.010 mL, 0.08 mmol) and ( $S$ )-MTPA-Cl (0.010 mL, 0.04 mmol). The reaction was stirred for 36 hours at room temperature before being dry loaded onto silica and purified by flash silica chromatography (EtOAc:hexane, 3:7) to give **103-C** as a colourless oil (1 mg, 8%),  $R_f = 0.14$  (EtOAc:hexane, 3:7).

$\nu_{\text{max}}/\text{cm}^{-1}$  (neat) 3420, 2930, 2855, 1734;  $^1\text{H}$  NMR (600 MHz;  $\text{CDCl}_3$ )  $\delta$ : 7.60–7.25 (14H, m, Ar), 5.20 (1H, s,  $\text{CHOH}$ ), 5.02 (1 H, d,  $J = 16.9$  Hz,  $\text{CHHO}$  ( $2R,3'R$ )), 4.95 (0.07H, d,  $J = 5.0$  Hz,  $\text{CHHO}$  ( $2S,3'R$ )), 4.88 (0.07H, d,  $J = 5.0$  Hz,  $\text{CHHO}$  ( $2S,3'R$ )), 4.74 (1H, d,  $J = 16.9$  Hz,  $\text{CHHO}$  ( $2R,3'R$ )), 3.62 (6H, s,  $\text{OCH}_3$ );  $^{13}\text{C}$  NMR (150 MHz;  $\text{CDCl}_3$ )  $\delta$ : 201.8 ( $\text{C}=\text{O}$ ), 166.6 ( $\text{C}=\text{O}$ ), 156.4 ( $\text{C}=\text{O}$ ), 138.5, 131.8, 131.1, 130.0, 129.8, 128.6, 127.5, 127.3, 77.1 ( $\text{CHOH}$ ), 66.5, 55.9 ( $\text{OCH}_3$ );  $^{19}\text{F}$  NMR (282 MHz;  $\text{CDCl}_3$ )  $\delta$ :  $-72.2$  ( $\text{CF}_3$ );  $m/z$  (ES+)  $[\text{MH}]^+$  found 615.09.  $\text{C}_{29}\text{H}_{25}\text{F}_6\text{O}_8$  requires 615.13.

**(S)-3-(1-Hydroxy-2-oxo-3-(((S)-3,3,3-trifluoro-2-methoxy-2-phenylpropanoyl)oxy)propyl)phenyl 3,3,3-trifluoro-2-methoxy-2-phenylpropanoate (103-D)<sup>[85]</sup>**

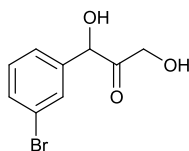


103-D

To a stirred solution of **103** (0.003 g, 0.02 mmol) in  $\text{CH}_2\text{Cl}_2$  (2 mL) was added 2,4,6-collidine (0.010 mL, 0.08 mmol) and (*R*)-MTPA-Cl (0.010 mL, 0.04 mmol). The reaction was stirred for 36 hours at room temperature before being dry-loaded onto silica gel and purified by flash silica chromatography (EtOAc:hexane, 3:7) to give **103-D** as a colourless oil (0.001 g, 8 %),  $R_f = 0.14$  (EtOAc:hexane, 3:7).

$\nu_{\text{max}}/\text{cm}^{-1}$  (neat) 3420, 2930, 2855, 1734;  $^1\text{H}$  NMR (600 MHz;  $\text{CDCl}_3$ )  $\delta$ : 7.60–7.24 (14H, m, Ar), 5.20 (1H, m, *CHOH*), 5.02 (0.3H, d,  $J = 16.9$  Hz, *CHHO* (2*S*,3'*S*)), 4.91 (0.82H, d,  $J = 16.9$  Hz, *CHHO* (2*R*,3'*S*)), 4.88 (0.82H, d,  $J = 16.9$  Hz, *CHHO* (2*R*,3'*S*)), 4.74 (0.3H, d,  $J = 16.9$  Hz, *CHHO* (2*S*,3'*S*)), 4.01–3.62 (6H, m,  $\text{OCH}_3$ );  $^{13}\text{C}$  NMR (150 MHz;  $\text{CDCl}_3$ )  $\delta$ : 205.3 (C=O), 166.9 (C=O), 159.2 (C=O), 132.0, 131.9, 131.1, 129.6, 129.8, 128.4, 127.1, 120.0, 71.2 (*CHOH*), 63.6 ( $\text{CH}_2\text{O}$ ), 57.1 ( $\text{OCH}_3$ );  $^{19}\text{F}$  NMR (282 MHz;  $\text{CDCl}_3$ )  $\delta$ : -72.2 ( $\text{CF}_3$ ).

**1-(3-Bromophenyl)-1,3-dihydroxypropan-2-one (104)**

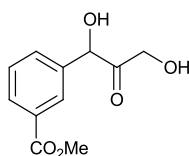


104

Li-HPA (0.110 g, 1.0 mmol) was dissolved in water:acetonitrile, 1:1 (10 mL total), at room temperature. 3-Bromobenzaldehyde (0.120 mL, 1.0 mmol) and *N*-methylmorpholine (0.110 mL, 1.0 mmol) were added and the pH was adjusted to 7 with hydrochloric acid (1 M). The reaction was stirred at room temperature for 24 hours and monitored by TLC analysis. The crude reaction mixture was then dry-

loaded onto silica and purified by flash silica chromatography (EtOAc:hexane, 3:7) to give **104** as a colourless oil (0.051 g, 20% yield),  $R_f = 0.29$  (EtOAc:hexane, 1:1).  $\nu_{\max}/\text{cm}^{-1}$  (neat): 3426, 2924, 2854, 1728, 1190;  $^1\text{H NMR}$  (500 MHz;  $\text{CDCl}_3$ )  $\delta$ : 7.85-7.07 (4H, m, Ar *H*), 5.21 (1H, s, *CHOH*), 4.36 (1H, d,  $J = 19.5$  Hz, *COCHH*), 4.26 (1H, d,  $J = 19.5$  Hz, *COCHH*);  $^{13}\text{C NMR}$  (150 MHz;  $\text{CDCl}_3$ )  $\delta$ : 208.3 ( $\text{C}=\text{O}$ ), 139.4, 132.4, 130.7, 129.8 (Signals overlapping), 125.5, 76.8 (*CHOH*), 65.0 ( $\text{CH}_2\text{OH}$ );  $m/z$  (HR ES+) found  $[\text{MH}]^+$  244.9817.  $\text{C}_9\text{H}_{10}\text{BrO}_3$  requires 244.9813.

***Rac*-methyl 3-(1,3-dihydroxy-2-oxopropyl)benzoate (*rac*-106)<sup>[79]</sup>**

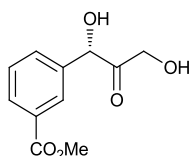


*Rac*-106

Li-HPA (0.110 g, 1.0 mmol) was dissolved in water:acetonitrile, 1:1 (10 mL total), at room temperature. Methyl-3-formylbenzoate (0.160 g, 1.0 mmol) and *N*-methylmorpholine (0.110 mL, 1.0 mmol) were added and the pH was adjusted to 7 with hydrochloric acid (1 M). The reaction was stirred at room temperature for 24 hours and monitored by TLC analysis. The crude reaction mixture was then dry-loaded onto silica and purified by flash silica chromatography (EtOAc:hexane, 3:7), to give *rac*-**106** as a colourless oil (0.064 g, 29% yield),  $R_f = 0.28$  (EtOAc:hexane, 1:1).

$\nu_{\max}/\text{cm}^{-1}$  (neat): 3441, 2954, 1719, 1272;  $^1\text{H NMR}$  (600 MHz;  $\text{CDCl}_3$ )  $\delta$ : 8.05 (2H, m, Ar *H*), 7.51 (2H, m, Ar *H*), 5.33 (1H, d,  $J = 3.9$  Hz, *CHOH*), 4.40 (1H, dd,  $J = 19.4$  Hz, 5.0 Hz, *COCHH*), 4.23 (1H, dd,  $J = 19.4$  Hz, 5.0 Hz, *COCHH*), 3.93 (4H, m,  $\text{OCH}_3$ , *OH*), 2.69 (1H, t,  $J = 5.0$  Hz, *OH*);  $^{13}\text{C NMR}$  (125 MHz;  $\text{CDCl}_3$ )  $\delta$ : 209.0 ( $\text{C}=\text{O}$ ), 166.5 ( $\text{C}=\text{O}$ ), 137.9, 131.4, 131.3, 130.5, 129.5, 128.2, 77.3 (*CHOH*), 65.3 ( $\text{CH}_2\text{OH}$ ), 52.5 ( $\text{OCH}_3$ );  $m/z$  (HR ES+) found  $[\text{MH}]^+$  225.0763.  $\text{C}_{11}\text{H}_{12}\text{O}_5$  requires 225.0756

**(3S)-Methyl 3-(1,3-dihydroxy-2-oxopropyl)benzoate (S-106)**

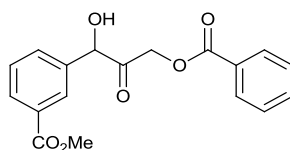


S-106

The standard biotransformation procedure was performed with S385T/D469T/R520Q TK cell-free lysate (4 mL) and methyl-3-formylbenzoate (25 mM) for 24 hours. The crude reaction mixture was then purified by flash silica chromatography (EtOAc:hexane, 1:4) to give S-106 as a colourless oil (0.040 g, 34%).

Characterisation data was as found for the racemic product (*rac*-106).

**Methyl 3-(3-(benzoyloxy)-1-hydroxy-2-oxopropyl)benzoate (106-B)<sup>[79]</sup>**



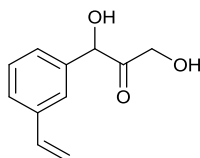
106-B

To a stirred solution of **106** (0.064 g, 0.29 mmol) in CH<sub>2</sub>Cl<sub>2</sub> (5 mL) was added 2,4,6-collidine (0.020 mL, 0.15 mmol) and benzoyl chloride (0.020 mL, 0.16 mmol). The reaction was stirred at room temperature overnight and followed by TLC analysis. The crude reaction mixture was then washed with HCl (2 M, 25 mL) and extracted with CH<sub>2</sub>Cl<sub>2</sub> (20 mL), before being dry-loaded onto silica and purified by flash silica chromatography (EtOAc:hexane, 1:9) to give **106-B** as a colourless oil (0.015 g, 27%), R<sub>f</sub> = 0.15 (EtOAc:hexane, 2:8).

$\nu_{\max}/\text{cm}^{-1}$  (neat): 3441, 3074, 2954, 1719, 1272; <sup>1</sup>H NMR (600 MHz; CDCl<sub>3</sub>)  $\delta$ : 8.19-8.01 (4H, m, Ar *H*), 7.40-7.26 (5H, m, Ar *H*), 5.42 (1H, s, *CHOH*), 5.03 (1H, d, *J* = 17.2 Hz, *COCHH*), 4.82 (1H, d, *J* = 17.2 Hz, *COCHH*), 3.91 (3H, s, *OCH*<sub>3</sub>); <sup>13</sup>C NMR (150 MHz; CDCl<sub>3</sub>)  $\delta$ : 203.0 (*C=O*), 171.2 (*C=O*), 166.5 (*C=O*), 137.6, 133.8,

131.7, 131.3, 130.5, 130.3, 130.1, 129.6, 129.2, 128.7, 77.7 (CHOH), 65.6 (CH<sub>2</sub>OH), 52.5 (OCH<sub>3</sub>); *m/z* (HR ES<sup>+</sup>) found [MH]<sup>+</sup> 329.1011. C<sub>18</sub>H<sub>17</sub>O<sub>6</sub> requires 329.1025. HPLC analysis (Chiralpak AD column, isopropanol:hexane, 10:90, 1 mL/min) gave retention times of 21.9 minutes (*S*-isomer) and 24.3 minutes (*R*-isomer).

### ***Rac*-1,3-dihydroxy-1-(3-vinylphenyl)propan-2-one (*Rac*-107)**



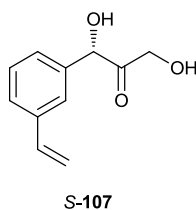
*Rac*-107

Li-HPA (0.110 g, 1.0 mmol) was dissolved in water:acetonitrile, 1:1 (10 mL total), at room temperature. 3-Vinylbenzaldehyde (0.130 mL, 1.0 mmol) and *N*-methylmorpholine (0.110 mL, 1.0 mmol) were added and the pH was adjusted to 7 with hydrochloric acid (1 M). The reaction was stirred at room temperature overnight and monitored by TLC analysis. The crude reaction mixture was then dry-loaded onto silica and purified by flash silica chromatography (EtOAc:hexane, 2:8) to give *rac*-**107** as a colourless oil (11 mg, 6%), *R<sub>f</sub>* = 0.30 (EtOAc:hexane, 1:1).

$\nu_{\max}/\text{cm}^{-1}$  (neat): 3404, 2922, 1726, 1652, 1276; <sup>1</sup>H NMR (600 MHz; CDCl<sub>3</sub>)  $\delta$ : 7.50-7.30 (4H, m, Ar *H*), 6.70 (1H, dd, *J* = 17.4 Hz, 10.9 Hz, CHCHH), 5.78 (1H, d, *J* = 17.4 Hz, CHCHH), 5.31 (1H, d, *J* = 10.9 Hz, CHCHH), 5.25 (1H, d, *J* = 3.7 Hz, CHOH), 4.37 (1H, dd, *J* = 19.5 Hz, 4.9 Hz, COCHH), 4.25 (1H, dd, *J* = 19.5 Hz, 4.9 Hz, COCHH), 3.82 (1H, d, *J* = 3.7 Hz, OH), 2.68 (1H, t, *J* = 4.9 Hz, OH); <sup>13</sup>C NMR (150 MHz; CDCl<sub>3</sub>)  $\delta$ : 209.0 (C=O), 138.8 (CHCH<sub>2</sub>), 136.2, 129.6 (signals overlapping), 127.1, 126.4, 124.8, 115.2 (CHCH<sub>2</sub>), 77.7 (CHOH), 65.2 (CH<sub>2</sub>OH); *m/z* (HR ES<sup>+</sup>) found [MH]<sup>+</sup> 193.0861. C<sub>11</sub>H<sub>13</sub>O<sub>3</sub> requires 193.0864.



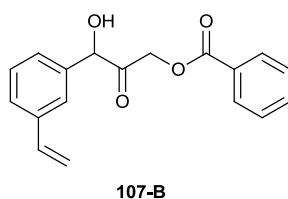
### **(3S)-1,3-Dihydroxy-1-(3-vinylphenyl)propan-2-one (S-107)**



The standard biotransformation procedure was performed with S385T/D469T/R520Q TK cell-free lysate (4 mL) and 3-vinylbenzaldehyde (25 mM) for 24 hours. Solvent was then removed and the crude product purified by flash silica chromatography (EtOAc:hexane, 1:4). Solvent was removed to give *S-107* as a colourless oil (0.005 g, 4 %).

Characterisation data was as found for the racemic product (*rac-107*)

### **3-Hydroxy-2-oxo-3-(3-vinylphenyl)propyl benzoate (107-B)**



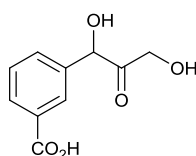
To a stirred solution of **107** (0.004 g, 0.02 mmol) in CH<sub>2</sub>Cl<sub>2</sub> (5 mL) was added 2,4,6-collidine (0.022 mL, 0.16 mmol) and benzoyl chloride (0.018 mL, 0.16 mmol). The reaction was followed by TLC analysis and stirred overnight at room temperature. The reaction was then washed with HCl (2 M, 25 mL) and extracted with CH<sub>2</sub>Cl<sub>2</sub> (20 mL), before being dry-loaded onto silica and purified by flash silica chromatography (EtOAc:hexane, 1:9), to give **107-B** as a colourless oil (0.002 g, 34% yield), R<sub>f</sub> = 0.20 (EtOAc:hexane, 2:8).

$\nu_{\max}/\text{cm}^{-1}$  (neat): 2927, 2677, 1686, 1292; <sup>1</sup>H NMR (600 MHz; CDCl<sub>3</sub>)  $\delta$ : 8.03-7.84 (2H, d,  $J = 7.8$  Hz, Ar  $H$ ), 7.60 (1H, t,  $J = 7.8$  Hz, Ar  $H$ ), 7.48-7.35 (6H, m, Ar  $H$ ) 6.69 (1H, dd,  $J = 17.7$  Hz, 10.8 Hz, CHCHH), 5.76 (1H, d,  $J = 17.7$  Hz, CHCHH), 5.35 (1H, s, CHOH), 5.29 (1H, d,  $J = 10.8$  Hz, CHCHH), 5.03 (1H, d,  $J = 17.1$  Hz, COCHH), 4.79 (1H, d,  $J = 17.1$  Hz, COCHH), <sup>13</sup>C NMR (150 MHz; CDCl<sub>3</sub>)  $\delta$ :

203.3 (C=O), 165.8 (C=O), 138.8 (CHCH<sub>2</sub>), 137.3, 136.2, 133.8, 130.0, 129.6, 128.9, 128.7, 127.2, 126.7, 125.4, 115.1 (CHCH<sub>2</sub>), 77.1 (CHOH), 65.4 (CH<sub>2</sub>OH); *m/z* (HR CI+) found [M-OH]<sup>+</sup> 279.1029. C<sub>18</sub>H<sub>15</sub>O<sub>3</sub> requires 279.1099.

HPLC analysis (Chiralpak AD column, isopropanol:hexane, 10:90, 1 mL/min) gave retention times of 13.5 minutes (*S*-isomer) and 16.4 minutes (*R*-isomer).

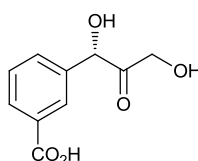
### **3-(1,3-Dihydroxy-2-oxopropyl)benzoic acid (*Rac*-108)**



**Rac-108**

Li-HPA (0.110 g, 1.0 mmol) was dissolved in water:acetonitrile, 1:1 (10 mL total), at room temperature. 3-Formylbenzoic acid (0.150 g, 1.0 mmol) and *N*-methylmorpholine (0.110 mL, 1.0 mmol) were added and the pH was adjusted to 7 with hydrochloric acid (1 M). The reaction was stirred at room temperature overnight, then the solvent was removed *in vacuo* and the crude mixture carried through to the benzylation reaction.

### **(3*S*)-(1,3-Dihydroxy-2-oxopropyl)benzoic acid (*S*-108)<sup>[91]</sup>**



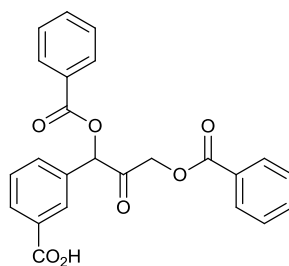
**S-108**

The standard biotransformation procedure was performed with D469T TK cell-free lysate (2 mL) and 3-formylbenzoic acid (50 mM) for 24 hours. The crude reaction mixture was then dry-loaded onto silica and the product purified by flash silica chromatography (CH<sub>2</sub>Cl<sub>2</sub>:MeOH, 9:1, then 8:2), to give *S*-108 as an amorphous green solid (0.200 g, 90%). *R<sub>f</sub>* = 0.57 (CH<sub>2</sub>Cl<sub>2</sub>:MeOH, 8:2).

Mp (Decomposed before melting), *R<sub>f</sub>* = 0.57 (CH<sub>2</sub>Cl<sub>2</sub>:MeOH, 4:1); *v*<sub>max</sub> (neat)/cm<sup>-1</sup> 3252, 2946, 2843, 1693, 1606; <sup>1</sup>H NMR (300 MHz; CD<sub>3</sub>OD) δ: 8.08-8.01 (1H, s, Ar

*H*), 7.96 (1H, dt,  $J = 7.7$  Hz, 1.4 Hz, Ar *H*), 7.61 (1H, d,  $J = 7.7$  Hz, Ar *H*), 7.45 (1H, t,  $J = 7.7$  Hz, Ar *H*), 5.36 (1H, s, *CHOH*), 4.46 (1H, d,  $J = 19.2$  Hz, *CHHOH*), 4.39 (1H, d,  $J = 19.2$  Hz, *CHHOH*);  $^{13}\text{C}$  NMR (125 MHz;  $\text{D}_2\text{O}$ )  $\delta$ : 211.2 ( $\text{C}=\text{O}$ ), 175.3 ( $\text{CO}_2\text{H}$ ), 137.7, 137.6, 130.5, 130.0, 129.7, 128.2, 77.2 (*CHOH*), 65.2 ( $\text{CH}_2\text{OH}$ );  $m/z$  (NSI-) 209 ( $[\text{M}-\text{H}]^-$ , 100%), 179 (27), 149 (27);  $m/z$  (NSI-) found  $[\text{M}-\text{H}]^-$  209.0453.  $\text{C}_{10}\text{H}_9\text{O}_5$  requires 209.0455.

### 3-(1,3-Bis(benzoyloxy)-2-oxopropyl)benzoic acid (**108-B**)



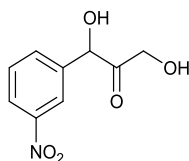
**108-B**

To a stirred solution of **108** (0.050 g, 0.24 mmol) in tetrahydrofuran (10 mL) was added 2,4,6-collidine (0.250 mL, 1.90 mmol) and benzoyl chloride (0.250 mL, 1.90 mmol). The reaction was followed by TLC analysis and stirred overnight at room temperature. Solvent was then removed under reduced pressure, and the solid was re-dissolved in  $\text{CH}_2\text{Cl}_2$  (30 mL) and washed with HCl (2 M, 25 mL). The product was extracted with further  $\text{CH}_2\text{Cl}_2$  (20 mL), before being dry-loaded onto silica and purified by flash silica chromatography (EtOAc:hexane, 1:9) to give **108-B** as a colourless oil (0.020 g, 20%),  $R_f = 0.14$  (EtOAc:hexane, 2:8).

$\nu_{\text{max}}/\text{cm}^{-1}$  (neat): 3066, 2927, 1789, 1721, 1691;  $^1\text{H}$  NMR (600 MHz;  $\text{CDCl}_3$ )  $\delta$ : 8.10-7.30 (14H, m, Ar *H*), 6.54 (1H, s, *CHO*), 5.36 (1H, d,  $J = 17.2$  Hz, *COCHH*); 5.00 (1H, d,  $J = 17.2$  Hz, *COCHH*)  $^{13}\text{C}$  NMR (150 MHz;  $\text{CDCl}_3$ )  $\delta$ : 197.9 ( $\text{C}=\text{O}$ ), 190.9 ( $\text{CO}_2\text{H}$ ), 169.6 ( $\text{C}=\text{O}$ ) 165.9 ( $\text{C}=\text{O}$ ), 134.8, 134.2, 134.1, 134.0, 133.9, 133.7, 131.7, 130.8, 130.3, 130.1, 130.0, 129.1, 128.8, 128.6, 78.4 (*CHOH*), 66.6 ( $\text{CH}_2\text{OH}$ );  $m/z$  (HR CI+) found  $[\text{MH}]^+$  419.1134.  $\text{C}_{24}\text{H}_{19}\text{O}_7$  requires 419.1130

HPLC analysis (Chiralpak AD column, isopropanol:hexane, 23:77, 1 mL/min) gave retention times of 33.2 minutes (*R*-isomer) and 37.0 minutes (*S*-isomer).

### 1,3-Dihydroxy-1-(3-nitrophenyl)propan-2-one (*Rac-109*)

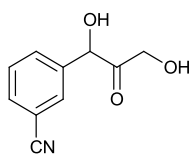


*Rac-109*

Li-HPA (0.110 g, 1.0 mmol) was dissolved in water:acetonitrile, 1:1 (10 mL total), at room temperature. 3-Nitrobenzaldehyde (0.150 g, 1.0 mmol) and *N*-methylmorpholine (0.110 mL, 1.0 mmol) were added and the pH was adjusted to 7 with hydrochloric acid (1 M). The reaction was stirred at room temperature for 24 hours and monitored by TLC analysis. The crude reaction mixture was then dry-loaded onto silica and purified by flash silica chromatography (EtOAc:hexane, 3:7) to give *rac-109* as a colourless oil (0.047 g, 22%),  $R_f = 0.28$  (EtOAc:hexane, 1:1).

$\nu_{\max}/\text{cm}^{-1}$  (neat): 3467, 2924, 2854, 1738, 1529;  $^1\text{H NMR}$  (600 MHz;  $\text{CDCl}_3$ )  $\delta$ : 8.50-8.25 (2H, m, Ar *H*), 7.80-7.60 (2H, m, Ar *H*), 5.41 (1H, s, *CHOH*), 4.44 (1H, d,  $J = 19.6$  Hz, *COCHH*), 4.33 (1H, d,  $J = 19.6$  Hz, *COCHH*);  $^{13}\text{C NMR}$  (150 MHz;  $\text{CDCl}_3$ )  $\delta$ : 208.1 (*C=O*), 147.2 (*C-NO}\_2*), 134.8, 132.8, 130.6, 129.5, 124.4, 77.4 (*CHOH*), 65.3 (*CH}\_2\text{OH}*);  $m/z$  (HR ES<sup>+</sup>) found  $[\text{MH}]^+$  212.0555.  $\text{C}_{16}\text{H}_{10}\text{O}_5\text{N}$  requires 212.0559.

### *Rac-3-(1,3-dihydroxy-2-oxopropyl)benzotrile (Rac-110)*

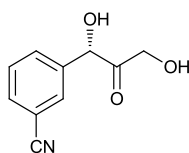


*Rac-110*

Li-HPA (0.110 g, 1.0 mmol) was dissolved in water:acetonitrile, 1:1 (10 mL total volume), at room temperature. 3-Formylbenzotrile (0.065 g, 0.5 mmol) and *N*-methylmorpholine (0.110 mL, 1.0 mmol) were added and the pH was adjusted to 7 with hydrochloric acid (1 M). The reaction was stirred at room temperature overnight and monitored by TLC analysis. The crude reaction mixture was then dry-

loaded onto silica and purified by flash silica chromatography (EtOAc:hexane, 3:7) to give *rac*-**110** as a colourless oil (0.010 g, 10%),  $R_f = 0.35$  (EtOAc:hexane, 1:1). Characterisation data was as found for the biotransformation product (*S*-**110**).

### **(3*S*)-(1,3-Dihydroxy-2-oxopropyl)benzonitrile (S-110)**

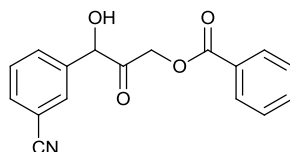


S-110

The standard biotransformation procedure was performed with S385T/D469T/R520Q TK cell-free lysate (4 mL) and 3-formylbenzonitrile (25 mM) for 24 hours. The crude reaction mixture was then dry-loaded onto silica and purified by flash silica chromatography (EtOAc:hexane, 4:6) to give *S*-**110** as a colourless oil (0.025 g, 26 %),  $R_f = 0.35$  (EtOAc:hexane, 7:3).

$\nu_{\max}/\text{cm}^{-1}$  (neat): 3409, 2904, 2232, 1727;  $^1\text{H}$  NMR (600 MHz;  $\text{CDCl}_3$ )  $\delta$ : 7.73 (1H, s, Ar *H*), 7.70 (1H, d,  $J = 7.7$  Hz, Ar *H*), 7.62 (1H, d,  $J = 7.7$  Hz, Ar *H*), 7.53 (1H, t,  $J = 7.7$  Hz, Ar *H*), 5.34 (1H, s, *CHOH*), 4.41 (1H, d,  $J = 19.8$  Hz, *CHHOH*), 4.30 (1H, d,  $J = 19.8$  Hz, *CHHOH*);  $^{13}\text{C}$  NMR (125 MHz;  $\text{CDCl}_3$ )  $\delta$ : 208.1 ( $\text{C}=\text{O}$ ), 139.0, 132.8, 131.3, 130.6, 130.1, 118.2 (CN), 113.5 ( $\text{C}-\text{CN}$ ), 76.8 (*CHOH*), 65.4 ( $\text{CH}_2\text{OH}$ );  $m/z$  (HR ES<sup>-</sup>) found  $[\text{M}-\text{H}]^-$  190.0494.  $\text{C}_{10}\text{H}_8\text{NO}_3$  requires 190.0504.

### 3-(3-Cyanophenyl)-3-hydroxy-2-oxopropyl benzoate (**110-B**)



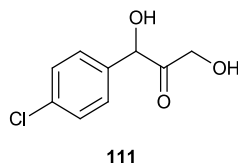
**110-B**

To a stirred solution of **110** (0.020 g, 0.10 mmol) in  $\text{CH}_2\text{Cl}_2$  (5 mL) was added 2,4,6-collidine (0.020 mL, 0.16 mmol) and benzoyl chloride (0.020 mL, 0.16 mmol). The reaction was followed by TLC analysis and stirred overnight at room temperature. The reaction was then washed with HCl (2 M, 25 mL) and extracted with  $\text{CH}_2\text{Cl}_2$  (20 mL), before being dry-loaded onto silica and purified by flash silica chromatography (EtOAc:hexane, 1:9) to give **110-B** as a colourless oil (0.010 g, 24%),  $R_f = 0.15$  (EtOAc:hexane, 2:8).

$\nu_{\text{max}}/\text{cm}^{-1}$  (neat): 3449, 2925, 2854, 2232, 1724, 1274;  $^1\text{H}$  NMR (600 MHz;  $\text{CDCl}_3$ )  $\delta$ : 8.10 (1H, d,  $J = 7.8$  Hz, Ar  $H$ ), 8.02 (2H, d,  $J = 7.8$  Hz, Ar  $H$ ), 7.70 (1H, s, Ar  $H$ ), 7.68 (1H, d,  $J = 7.8$  Hz, Ar  $H$ ), 7.62 (1H, t,  $J = 7.8$  Hz, Ar  $H$ ), 7.54 (1H, t,  $J = 7.8$  Hz, Ar  $H$ ), 7.47 (2H, t,  $J = 7.8$  Hz, Ar  $H$ ), 5.38 (1H, s,  $\text{CHOH}$ ), 5.01 (1H, d,  $J = 17.0$  Hz,  $\text{COCHH}$ ), 4.87 (1H, d,  $J = 17.0$  Hz,  $\text{COCHH}$ );  $^{13}\text{C}$  NMR (150 MHz;  $\text{CDCl}_3$ )  $\delta$ : 202.4 ( $\text{C}=\text{O}$ ), 165.8 ( $\text{C}=\text{O}$ ), 138.7, 134.0, 132.9, 131.6, 131.0, 130.2, 130.0, 128.8, 128.6, 118.2 (CN), 113.5 ( $\text{C-CN}$ ), 77.4 ( $\text{CHOH}$ ), 65.6 ( $\text{CH}_2\text{OH}$ );  $m/z$  (HR ES-) found  $[\text{M-H}]^-$  294.0778  $\text{C}_{17}\text{H}_{12}\text{NO}_4$  requires 294.0766;  $[\alpha]_D^{20}$  ( $S$ -**110-B**) = - 16.0 (c 0.15,  $\text{CH}_2\text{Cl}_2$ )

HPLC analysis (Chiralpak AD column, isopropanol:hexane, 10:90, 1 mL/min) gave retention times of 14.9 mins ( $S$ -isomer) and 19.5 mins ( $R$ -isomer).

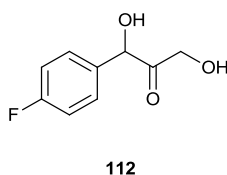
### 1-(4-Chlorophenyl)-1,3-dihydroxypropan-2-one (**111**)<sup>[79]</sup>



Li-HPA (0.110 g, 1.0 mmol) was dissolved in water:acetonitrile, 1:1 (5 mL total), at room temperature. 4-Chlorobenzaldehyde (0.141 g, 1.0 mmol) and *N*-methylmorpholine (0.110 mL, 1.0 mmol) were added and the pH was adjusted to 7 with hydrochloric acid (1 M). The reaction was stirred at room temperature and monitored by TLC analysis. The crude reaction mixture was then dry-loaded onto silica and purified by flash silica chromatography (EtOAc:hexane, 2:8) to give **111** as a colourless oil (0.002 g, 2%),  $R_f = 0.14$  (EtOAc:hexane, 1:1).

$\nu_{\max}/\text{cm}^{-1}$  (neat): 3344, 2923, 1728, 1598;  $^1\text{H NMR}$  (300 MHz;  $\text{CDCl}_3$ )  $\delta$ : 7.30-7.10 (4H, m, Ar *H*), 5.24 (1H, d,  $J = 3.5$  Hz, *CHOH*), 4.35 (1H, dd,  $J = 19.6$  Hz, 4.1 Hz, *COCHH*), 4.23 (1H, dd,  $J = 19.6$  Hz, 4.1 Hz, *COCHH*), 3.81 (1H, d,  $J = 3.5$  Hz, *OH*), 2.67 (1H, t,  $J = 4.1$  Hz, *OH*);  $^{13}\text{C NMR}$  (150 MHz;  $\text{CDCl}_3$ )  $\delta$ : 208.6 (*C=O*), 135.4 (signals overlapping), 128.9, 128.8, 77.3 (*CHOH*), 65.2 (*CH<sub>2</sub>OH*);  $m/z$  (HR EI+) found  $[\text{MH}]^+$  201.0313.  $\text{C}_9\text{H}_{10}\text{ClO}_3$  requires 201.0318.

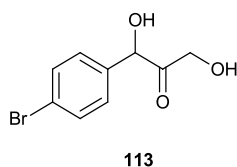
### 1-(4-Fluorophenyl)-1,3-dihydroxypropan-2-one (**112**)<sup>[79]</sup>



Li-HPA (0.110 g, 1.0 mmol) was dissolved in water:acetonitrile, 1:1 (5 mL total), at room temperature. 4-Fluorobenzaldehyde (0.124 g, 1.0 mmol) and *N*-methylmorpholine (0.110 mL, 1.0 mmol) were added and the pH was adjusted to 7 with hydrochloric acid (1 M). The reaction was stirred at room temperature for 24 hours and monitored by TLC analysis. Then the crude reaction mixture was dry-loaded onto silica and purified by flash silica chromatography (EtOAc:hexane, 2:8) to give **112** as a colourless oil (0.004 g, 2%),  $R_f = 0.37$  (EtOAc:hexane, 7:3).

$\nu_{\max}/\text{cm}^{-1}$  (neat): 3377, 2924, 1725, 1603, 1509;  $^1\text{H}$  NMR (300 MHz;  $\text{CDCl}_3$ )  $\delta$ : 7.30-7.11 (4H, m, Ar *H*), 5.25 (1H, d,  $J = 3.9$  Hz, *CHOH*), 4.35 (1H, dd,  $J = 19.8$  Hz, 5.0 Hz, *COCHH*), 4.25 (1H, dd,  $J = 19.8$  Hz, 5.0 Hz, *COCHH*), 3.80 (1H, d,  $J = 3.9$  Hz, *OH*), 2.67 (1H, t,  $J = 5.0$  Hz, *OH*),  $^{13}\text{C}$  NMR (125 MHz;  $\text{CDCl}_3$ )  $\delta$ : 208.9 (*C=O*); 163.2 (d,  $^1J_{\text{C-F}} = 247.0$  Hz, *C-F*), 133.2, 128.9 (d,  $^3J_{\text{C-F}} = 8.0$  Hz), 116.4 (d,  $^2J_{\text{C-F}} = 21.3$  Hz), 77.4 (*CHOH*), 65.2 (*CH}\_2\text{OH}*);  $^{19}\text{F}$  NMR (282 MHz;  $\text{CDCl}_3$ )  $\delta$ : -112.4;  $m/z$  (HR EI+) found (MH)<sup>+</sup> 185.0622.  $\text{C}_9\text{H}_{10}\text{FO}_3$  requires 185.0536.

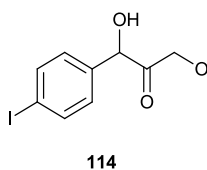
### 1-(4-Bromophenyl)-1,3-dihydroxypropan-2-one (**113**)<sup>[79]</sup>



Li-HPA (0.110 g, 1.0 mmol) was dissolved in water:acetonitrile, 3:2 (5 mL total), at room temperature. 4-Bromobenzaldehyde (0.190 g, 1.0 mmol) and *N*-methylmorpholine (0.110 mL, 1.0 mmol) were added and the pH was adjusted to 7 with hydrochloric acid (1 M). The reaction was stirred at room temperature for 24 hours and monitored by TLC analysis. The crude reaction mixture was then dry-loaded onto silica and purified by flash silica chromatography (EtOAc:hexane, 2:8) to give **113** as a colourless oil (0.002 g, 1%),  $R_f = 0.42$  (EtOAc:hexane, 7:3).

$\nu_{\max}/\text{cm}^{-1}$  (neat): 3390, 2923, 1725, 1590;  $^1\text{H}$  NMR (300 MHz;  $\text{CDCl}_3$ )  $\delta$ : 7.61-7.10 (4H, m, Ar *H*), 5.22 (1H, s, *CHOH*), 4.36 (1H, d,  $J = 19.8$  Hz, *COCHH*), 4.24 (1H, d,  $J = 19.8$  Hz, *COCHH*);  $^{13}\text{C}$  NMR (125 MHz;  $\text{CDCl}_3$ )  $\delta$ : 208.6 (*C=O*), 136.4 (*C-Br*), 132.5, 131.1, 128.7, 77.3 (*CHOH*), 65.2 (*CH}\_2\text{OH}*);  $m/z$  (HR EI+) found [MH]<sup>+</sup> 244.9811.  $\text{C}_9\text{H}_9\text{BrO}_3$  requires 244.9813.

### 1-(4-Iodophenyl)-1,3-dihydroxypropan-2-one (**114**)

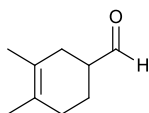




Li-HPA (0.110 g, 1.0 mmol) was dissolved in water:acetonitrile, 3:2 (5 mL total), at room temperature. 4-Iodobenzaldehyde (0.230 g, 1.0 mmol) and *N*-methylmorpholine (0.110 mL, 1.0 mmol) were added and the pH was adjusted to 7 with hydrochloric acid (1 M). The reaction was stirred at room temperature for 24 hours and monitored by TLC analysis. The crude reaction mixture was then dry-loaded onto silica and purified by flash silica chromatography (EtOAc:hexane, 2:8) to give **114** as a colourless oil (0.010 mg, 3%),  $R_f = 0.24$  (EtOAc:hexane, 1:1).

$^1\text{H}$  NMR (300 MHz;  $\text{CDCl}_3$ )  $\delta$ : 8.02-7.14 (4H, m, Ar *H*), 5.21 (1H, s, *CHOH*), 4.35 (1H, d,  $J = 18.3$  Hz, *COCHH*), 4.24 (1H, d,  $J = 18.3$  Hz, *COCHH*);  $^{13}\text{C}$  NMR (125 MHz;  $\text{CDCl}_3$ )  $\delta$ : 208.6 ( $\text{C}=\text{O}$ ), 138.5 ( $\text{C}-\text{I}$ ), 137.0, 130.9, 128.8, 77.3 (*CHOH*), 65.2 ( $\text{CH}_2\text{OH}$ );  $m/z$  (HR EI-) found  $[\text{M}-\text{H}]^-$  290.9525.  $\text{C}_9\text{H}_8\text{IO}_3$  requires 290.9518.

### 3,4-Dimethylcyclohex-3-enecarbaldehyde (**122**)

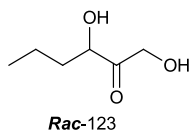


**122**

Acrolein (1.93 mL, 29.0 mmol), 2,3-dimethyl-1,3-butadiene (1.93 mL, 17.2 mmol) and zinc chloride (0.10 g, 0.68 mmol) were added together in a sealed tube and stirred at 60 °C behind a blast shield for 6 hours. The reaction was then allowed to cool and quenched with ice. The product was extracted with diethyl ether and purified by flash silica chromatography (EtOAc:hexane, 1:9) to afford **122** as a colourless liquid (1.32 g, 56%),  $R_f = 0.57$  (EtOAc:Hexane, 1:9).

$\nu_{\text{max}}/\text{cm}^{-1}$  (neat): 2923, 1720;  $^1\text{H}$  NMR (300 MHz;  $\text{CDCl}_3$ )  $\delta$ : 9.50 (1H, s, *CHO*), 2.30 (1H, m,  $\text{CH}_2\text{CHCHO}$ ), 2.10-1.70 (6H, m,  $\text{CH}_2\text{CHCH}_2\text{CH}_2$ ), 1.60-1.40 (6H, m,  $(\text{CH}_3)_2$ );  $^{13}\text{C}$  NMR (75 MHz;  $\text{CDCl}_3$ )  $\delta$ : 203.8 ( $\text{C}=\text{O}$ ), 125.7 ( $\text{CH}_3\text{C}$ ), 123.3 ( $\text{CH}_3\text{C}$ ), 46.8 ( $\text{CHCHO}$ ), 30.6 ( $\text{CH}_2$ ), 30.0 ( $\text{CH}_2$ ), 22.9 ( $\text{CH}_2$ ), 18.8 ( $\text{CH}_3$ ), 14.0 ( $\text{CH}_3$ );  $m/z$  (HR CI) found  $[\text{M}]^+$  138.1035.  $\text{C}_9\text{H}_{14}\text{O}$  requires 138.1045

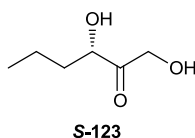
### ***Rac-1,3-dihydroxyoctan-2-one (Rac-123)***<sup>[26]</sup>



Li-HPA (0.110 g, 1.0 mmol) was dissolved in water (10 mL) at room temperature. Butanal (0.090 mL, 1.0 mmol) and *N*-methylmorpholine (0.110 mL, 1.0 mmol) were added and the pH was adjusted to 8 with hydrochloric acid (1 M). The reaction mixture was stirred at room temperature for 24 hours and monitored by TLC analysis. The crude reaction mixture was dry-loaded onto silica and purified by flash silica chromatography (EtOAc:hexane, 1:1) to give *rac-123* as a colourless solid (0.080 g, 56%),  $R_f = 0.30$  (EtOAc:hexane, 1:1).

Characterisation data was as found for the biotransformation product (*S-123*).

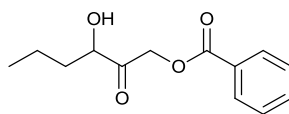
### ***(3S)-1,3-Dihydroxyhexan-2-one (S-123)***<sup>[26]</sup>



The standard biotransformation procedure was performed with D469Y/R520V TK cell-free lysate (4 mL) and butanal (50 mM) for 48 hours. The crude reaction mixture was then dry-loaded onto silica and purified by flash silica chromatography (EtOAc:hexane, 3:7). Solvent was removed to give *S-123* as a colourless oil (0.014 g, 11%),  $R_f = 0.25$  (EtOAc:hexane, 1:1).

$\nu_{\max}/\text{cm}^{-1}$  (neat): 3413, 2960, 2935, 2874, 1720;  $^1\text{H}$  NMR (600 MHz;  $\text{CDCl}_3$ )  $\delta$ : 4.50 (1H, d,  $J = 19.3$  Hz, COCHH), 4.39 (1H, d,  $J = 19.3$  Hz, COCHH), 4.31 (1H, dd,  $J = 8.0$  Hz, 3.8 Hz, CHOH), 1.76 (1H, m,  $\text{CH}_2\text{CHH}$ ), 1.58 (1H, m,  $\text{CH}_2\text{CHH}$ ), 1.43 (2H, m,  $\text{CH}_3\text{CH}_2$ ), 0.96 (1H, t,  $J = 7.1$  Hz,  $\text{CH}_3\text{CH}_2$ );  $^{13}\text{C}$  NMR (125 MHz;  $\text{CDCl}_3$ )  $\delta$ : 211.8 (C=O), 74.8 (CHOH), 65.6 ( $\text{CH}_2\text{OH}$ ), 36.4 ( $\text{CH}_2\text{CH}$ ) 18.1 ( $\text{CH}_3\text{CH}_2$ ), 13.9 ( $\text{CH}_3$ );  $m/z$  (HR ES<sup>+</sup>) found  $[\text{MH}]^+$  133.0866.  $\text{C}_6\text{H}_{13}\text{O}_3$  requires 133.0864.

### 3-Hydroxy-2-oxohexyl benzoate (**123-B**)



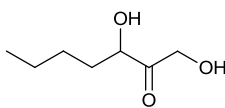
**123-B**

To a stirred solution of **123** (0.014 g, 0.10 mmol) in CH<sub>2</sub>Cl<sub>2</sub> (5 mL) was added 2,4,6-collidine (0.014 mL, 0.11 mmol) and benzoyl chloride (0.021 mL, 0.11 mmol). The reaction was stirred at room temperature overnight and followed by TLC analysis. The reaction was then washed with HCl (2 M, 25 mL) and extracted with CH<sub>2</sub>Cl<sub>2</sub> (20 mL), before being dry-loaded onto silica and purified by flash silica chromatography (EtOAc:hexane, 1:9) to give **123-B** as a colourless oil (0.022 g, 85%),  $R_f = 0.19$  (EtOAc:hexane, 2:8).

$\nu_{\max}/\text{cm}^{-1}$  (neat): 3480, 2960, 2925, 2854, 1724, 1275; <sup>1</sup>H NMR (500 MHz; CDCl<sub>3</sub>)  $\delta$ : 8.09 (2H, m, Ar *H*), 7.60 (1H, m, Ar *H*), 7.49 (2H, t,  $J = 7.8$  Hz, Ar *H*), 5.14 (1H, d,  $J = 17.2$  Hz, COCHH), 5.04 (1H, d,  $J = 17.2$  Hz, COCHH), 4.43 (1H, dd,  $J = 8.1$  Hz, 3.7 Hz, CHOH), 1.66 (1H, m, CH<sub>2</sub>CHH), 1.52 (1H, m, CH<sub>2</sub>CHH), 1.43 (2H, m, CH<sub>3</sub>CH<sub>2</sub>), 0.96 (1H, t,  $J = 7.3$  Hz, CH<sub>3</sub>CH<sub>2</sub>); <sup>13</sup>C NMR (125 MHz; CDCl<sub>3</sub>)  $\delta$ : 206.0 (C=O), 170.1 (C=O), 133.7, 129.8 (Signals overlapping), 128.6, 74.9 (CHOH), 66.1 (COCH<sub>2</sub>), 36.4 (CH<sub>2</sub>CH), 18.2 (CH<sub>2</sub>), 13.9 (CH<sub>3</sub>);  $m/z$  (HR ES<sup>+</sup>) found [MH]<sup>+</sup> 237.1118. C<sub>13</sub>H<sub>17</sub>O<sub>4</sub> requires 237.1126.

HPLC analysis (Chiralpak AD column, isopropanol:hexane, 3:97, 1 mL/min) gave retention times of 18.5 mins (*R*-isomer) and 20.5 mins (*S*-isomer).

### ***Rac-1,3-dihydroxyheptan-2-one (Rac-124)***<sup>[26]</sup>

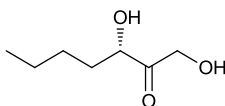


*Rac-124*

Li-HPA (0.110 g, 1.0 mmol) was dissolved in water (10 mL) at room temperature. Pentanal (0.106 mL, 1.0 mmol) and *N*-methylmorpholine (0.110 mL, 1.0 mmol) were added and the pH was adjusted to 8 with hydrochloric acid (1 M). The reaction was stirred at room temperature overnight and monitored by TLC analysis. The crude reaction mixture was then dry-loaded onto silica and purified by flash silica chromatography (EtOAc:hexane, 1:3) to give *rac-124* as a colourless solid (0.080 mg, 48%),  $R_f = 0.37$  (EtOAc:hexane, 1 : 1).

Characterisation data was as found for the biotransformation product.

### ***(3S)-1,3-Dihydroxyheptan-2-one (S-124)***<sup>[26]</sup>

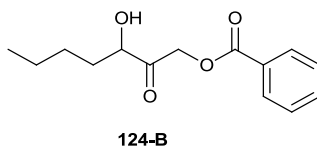


*S-124*

The standard biotransformation procedure was performed with D469Y/R520V TK cell-free lysate (2 mL) and pentanal (50 mM) for 48 hours. The crude reaction mixture was then purified by flash silica chromatography (EtOAc:hexane, 3:7) to give *S-124* as a colourless oil (0.015 mg, 10%),  $R_f = 0.25$  (EtOAc:hexane, 1:1).

$\nu_{\max}/\text{cm}^{-1}$  (neat): 3434, 3266, 2955, 1718;  $^1\text{H}$  NMR (500 MHz;  $\text{CDCl}_3$ )  $\delta$ : 4.49 (1H, d,  $J = 19.3$  Hz, COCHH), 4.39 (1H, d,  $J = 19.3$  Hz, COCHH) 4.30 (1H, dd,  $J = 7.9$  Hz, 3.9 Hz, CHOH), 2.96 (2H, br s, OH), 1.78 (1H, m,  $\text{CH}_2\text{CHH}$ ), 1.65-1.30 (5H, m,  $\text{CH}_3\text{CH}_2\text{CH}_2\text{CHH}$ ), 0.90 (3H, m,  $\text{CH}_3$ );  $^{13}\text{C}$  NMR (150 MHz;  $\text{CDCl}_3$ )  $\delta$ : 211.8 (C=O), 75.0 (CHOH), 65.6 ( $\text{CH}_2\text{OH}$ ), 34.0 ( $\text{CH}_2\text{CHOH}$ ), 29.8 ( $\text{CH}_3\text{CH}_2\text{CH}_2$ ), 26.0 ( $\text{CH}_3\text{CH}_2$ ), 13.9 ( $\text{CH}_3$ );  $m/z$  (HR ES+) found  $[\text{MH}]^+$  147.1027.  $\text{C}_7\text{H}_{15}\text{O}_3$  requires 147.1021.

### 3-Hydroxy-2-oxoheptyl benzoate (**124-B**)

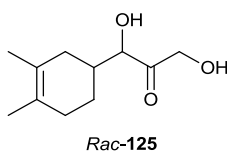


To a stirred solution of **124** (0.015 g, 0.10 mmol) in CH<sub>2</sub>Cl<sub>2</sub> (5 mL) was added 2,4,6-collidine (0.014 mL, 0.11 mmol) and benzoyl chloride (0.021 mL, 0.11 mmol). The reaction was stirred at room temperature overnight and followed by TLC analysis. The crude reaction mixture was then washed with HCl (2 M, 25 mL) and extracted with CH<sub>2</sub>Cl<sub>2</sub> (20 mL), before being dry-loaded onto silica and purified by flash silica chromatography (EtOAc:hexane, 1:9) to give **124-B** as a colourless oil (0.020 mg, 85%), R<sub>f</sub> = 0.20 (EtOAc : hexane, 2 : 8)).

$\nu_{\max}$  (neat)/cm<sup>-1</sup>: 3439, 2957, 2929, 2856, 1725, 1275; <sup>1</sup>H NMR (600 MHz; CDCl<sub>3</sub>)  $\delta$ : 8.10-8.01 (2H, m, Ar *H*), 7.61 (1H, m, Ar *H*), 7.48 (2H, m, Ar *H*), 5.13 (1H, d, *J* = 17.0 Hz, COCHH), 5.03 (1H, d, *J* = 17.0 Hz, COCHH), 4.41 (1H, dd, *J* = 8.0, 3.9 Hz, CHOH), 3.10 (1H, s, OH), 1.80-1.70 (1H, m, CH<sub>2</sub>CH<sub>2</sub>CHH), 1.65-1.30 (5H, m, CH<sub>3</sub>CH<sub>2</sub>CH<sub>2</sub>CHH), 0.90 (3H, t, *J* = 7.2 Hz, CH<sub>3</sub>); <sup>13</sup>C NMR (150 MHz; CDCl<sub>3</sub>)  $\delta$ : 206.0 (C=O), 169.8 (C=O), 133.8, 129.8 (Signals overlapping), 128.6, 75.1 (CHOH), 66.2 (CH<sub>2</sub>), 33.8 (CH<sub>2</sub>), 27.0 (CH<sub>2</sub>), 14.0 (CH<sub>3</sub>); *m/z* (HR ES<sup>+</sup>) found [MH]<sup>+</sup> 251.1285. C<sub>14</sub>H<sub>19</sub>O<sub>4</sub> requires 251.1283.

HPLC analysis (Chiralpak AD column, isopropanol:hexane, 3:97, 1 mL/min) gave retention times of 18.2 mins (*R*-isomer) and 20.9 mins (*S*-isomer).

### 1-(3,4-Dimethylcyclohex-3-en-1-yl)-1,3-dihydroxypropan-2-one (*Rac*-**125**)

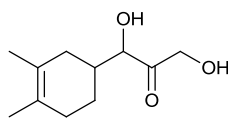


Li-HPA (0.110 g, 1.0 mmol) was dissolved in water:tetrahydrofuran, 1:1 (5 mL total), at room temperature. **122** (0.150 g, 1.1 mmol) and *N*-methylmorpholine (0.110 mL, 1.0 mmol) were added and the pH was adjusted to 7 with hydrochloric acid (1 M). The reaction was stirred at room temperature for 24 hours and monitored by

TLC analysis. The crude reaction mixture was then dry-loaded onto silica and purified by flash silica chromatography (EtOAc:hexane, 2:8) to give *rac*-**125** as a colourless oil (0.007 g, 4 %),  $R_f = 0.40$  (EtOAc:hexane, 1:1).

$\nu_{\max}/\text{cm}^{-1}$  (neat): 3456, 2893, 1721;  $^1\text{H NMR}$  (300 MHz;  $\text{CDCl}_3$ )  $\delta$ : 4.60-4.30 (2H, m,  $\text{CH}_2\text{OH}$ ), 4.31-4.20 (1H, m,  $\text{CHOH}$ ), 3.00-2.80 (1H, m,  $\text{CHCHOH}$ ), 2.11-1.72 (6H, m,  $\text{CH}_2\text{CHCH}_2\text{CH}_2$ ), 1.43-1.21 (6H, m,  $\text{CH}_3\text{CCCH}_3$ );  $^{13}\text{C NMR}$  (75 MHz;  $\text{CDCl}_3$ )  $\delta$ : 211.4 ( $\text{C}=\text{O}$ ), 125.7 ( $\text{CH}_3\text{C}$ ), 124.6 ( $\text{CH}_3\text{C}$ ), 77.3 ( $\text{CHOH}$ ), 66.2 ( $\text{CH}_2\text{OH}$ ), 38.8 ( $\text{CHCHOH}$ ), 34.4 ( $\text{CH}_2$ ), 31.6 ( $\text{CH}_2$ ), 22.9 ( $\text{CH}_2$ ), 19.2 ( $\text{CH}_3$ ), 18.8 ( $\text{CH}_3$ ).

### ***Biotrans-1-(3,4-dimethylcyclohex-3-en-1-yl)-1,3-dihydroxypropan-2-one (Biotrans-125)***

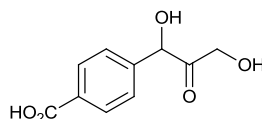


*Biotrans-125*

The standard biotransformation procedure was performed with F434A TK cell-free lysate (2 mL) and **122** (50 mM) for 48 hours. The crude reaction mixture was then dry-loaded onto silica and purified by flash silica chromatography (EtOAc:hexane, 2:8) to give biotrans-**125** as a colourless oil (0.013 g, 11 %).

Characterisation data was as found for racemic product (*rac*-**125**).

### ***4-(1,3-Dihydroxy-2-oxopropyl)benzoic acid (154)<sup>[91]</sup>***

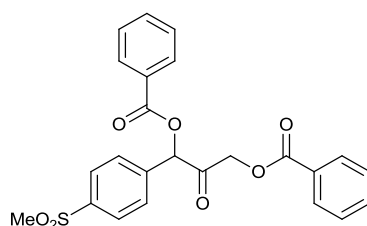


**154**

The standard biotransformation procedure was performed with S385Y/D469T/R520Q TK cell-free lysate (2 mL) and 4-formylbenzoic acid (50 mM) for 24 hours. The crude reaction mixture was then dry-loaded onto silica and purified by flash silica chromatography ( $\text{CH}_2\text{Cl}_2$ :MeOH, 9:1, then 8:2) to give **154** as a colourless oil (0.020 g, 10 %),  $R_f = 0.57$  ( $\text{CH}_2\text{Cl}_2$ :MeOH, 8:2).

$\nu_{\max}/\text{cm}^{-1}$  (neat): 3356, 2946, 1634, 1412;  $^1\text{H}$  NMR (600 MHz; MeOD)  $\delta$ : 8.02 (2H, d,  $J = 8.3$  Hz, Ar  $H$ ), 7.53 (2H, d,  $J = 8.3$  Hz, Ar  $H$ ), 5.35 (1H, s, CHOH), 4.42 (2H, app. t,  $J = 19.4$  Hz, CH<sub>2</sub>OH);  $^{13}\text{C}$  NMR (150 MHz; MeOD)  $\delta$ : 210.7 (C=O), 193.8 (CO<sub>2</sub>H), 144.9, 130.6 (signals overlapping), 127.8, 78.6 (CHOH), 65.9 (CH<sub>2</sub>OH);  $m/z$  (NSI-) 209 [M-H]<sup>-</sup>, 100%), 179 (15), 149 (86), 75 (47);  $m/z$  (NSI-) found [M-H]<sup>-</sup> 209.0453. C<sub>10</sub>H<sub>9</sub>O<sub>5</sub> requires 209.0455.

### **1-(4-(Methylsulfonyl)phenyl)-2-oxopropane-1,3-diyl dibenzoate (159-B)**



**159-B**

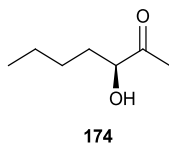
The standard biotransformation procedure was performed with S385Y/D469T/R520Q TK cell-free lysate (4 mL) and 4-(methylsulfonyl)benzaldehyde (50 mM) for 24 hours. Solvent was then removed and the crude product was redissolved in dichloromethane (20 mL) and 2,4,6-collidine (0.250 mL, 1.9 mmol) and benzoyl chloride (0.250 mL, 2.2 mmol) were added. The reaction was stirred at room temperature overnight and followed by TLC analysis. The crude reaction mixture was then washed with HCl (2 M, 50 mL) and the product extracted with further CH<sub>2</sub>Cl<sub>2</sub> (20 mL), before being dry-loaded onto silica and purified by flash silica chromatography (EtOAc:hexane, 15:85) to give **159-B** as a white powder (0.020 mg, 9%),  $R_f = 0.57$  (EtOAc : hexane, 1 : 1).

mp = 110-118 °C;  $\nu_{\max}/\text{cm}^{-1}$  (neat): 2962, 2927, 1723, 1600;  $^1\text{H}$  NMR (600 MHz; CDCl<sub>3</sub>)  $\delta$ : 8.12 (2H, d,  $J = 7.5$  Hz, Ar  $H$ ), 8.02 (4H, t,  $J = 8.0$  Hz, Ar  $H$ ), 7.76 (2H, d,  $J = 8.0$  Hz, Ar  $H$ ), 7.65 (1H, t,  $J = 7.5$  Hz, Ar  $H$ ), 7.60 (1H, t,  $J = 7.5$  Hz, Ar  $H$ ), 7.50 (2H, t,  $J = 8.0$  Hz, Ar  $H$ ), 7.45 (2H, t,  $J = 8.0$  Hz, Ar  $H$ ), 6.52 (1H, s, CHOH), 5.26 (1H, d,  $J = 17.2$  Hz, COCHH), 5.13 (1H, d,  $J = 17.2$  Hz, COCHH);  $^{13}\text{C}$  NMR (150 MHz; CDCl<sub>3</sub>)  $\delta$ : 207.2 (C=O), 197.6 (C=O), 165.7 (C=O), 141.7, 139.1, 134.3, 133.8, 130.1, 130.0, 128.9, 128.8, 128.7, 128.4 (signals overlapping), 78.1 (CHOH), 66.5

(CH<sub>2</sub>OH), 44.6 (SO<sub>2</sub>CH<sub>3</sub>); *m/z* (HR CI<sup>+</sup>) found [MH]<sup>+</sup> 453.0995. C<sub>24</sub>H<sub>20</sub>O<sub>7</sub>S requires 453.1008.

HPLC analysis (Chiralpak AD column, isopropanol:hexane, 18:82, 1 mL/min) gave retention times of 37.8 minutes (*R*-isomer) and 42.2 minutes (*S*-isomer)

### **(3S)-Hydroxyheptan-2-one (174)**

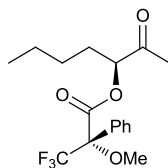


MgCl<sub>2</sub> (0.390 mL of 100 mg/mL solution, 0.4 mmol) was added to ThDP (0.022 g, 48 mmol) in water (10 mL) at pH 7. D469E TK cell-free lysate (2 mL) was added and the mixture was incubated for 20 minutes. In a separate flask, sodium pyruvate (0.110 g, 1.0 mmol) was dissolved in water (10 mL) with pentanal (0.106 mL, 1.0 mmol) and the pH adjusted to 7. This was then added to the enzyme suspension and stirred in an autotitrator for 18 hours and the reaction was followed by TLC analysis. The product was then extracted with Et<sub>2</sub>O (2 x 500 mL), and the organic layer was dried over magnesium sulfate, filtered and then dry-loaded onto silica before being purified by flash silica chromatography (Et<sub>2</sub>O:pentane, 5:95) to give **174** as a pale green oil (0.006g, 5%), R<sub>f</sub> = 0.20 (EtOAc:hexane, 1:9).

$\nu_{\max}/\text{cm}^{-1}$  (neat): 3450, 2957, 2927, 2859, 1714; <sup>1</sup>H NMR (600 MHz; CDCl<sub>3</sub>)  $\delta$ : 4.19 (1H, m, CHOH), 3.47 (1H, d, *J* = 4.7 Hz, CHOH), 2.20 (3H, s, COCH<sub>3</sub>), 1.84-1.25 (6H, m, CH<sub>2</sub>CH<sub>2</sub>CH<sub>2</sub>), 0.91 (3H, t *J* = 7.2 Hz, CH<sub>3</sub>CH<sub>2</sub>); <sup>13</sup>C NMR (150 MHz; CDCl<sub>3</sub>)  $\delta$ : 210.2 (C=O), 77.1 (CHOH), 33.6 (CH<sub>2</sub>), 26.9 (CH<sub>2</sub>), 25.5 (CH<sub>3</sub>) 22.2 (CH<sub>2</sub>), 15.4 (CH<sub>3</sub>), [ $\alpha$ ]<sub>D</sub><sup>20</sup> = +33.3 (*c* 0.30, Et<sub>2</sub>O).



**(S)-(S)-2-oxoheptan-3-yl-3,3,3-trifluoro-2-methoxy-2-phenylpropanoate (174-B)**

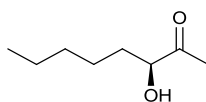


174-B

To a stirred solution of **174** (0.006 g, 0.05 mmol) in  $\text{CH}_2\text{Cl}_2$  (5 mL) was added triethylamine (0.020 mL, 0.14 mmol) and (*R*)-MTPA-Cl (0.020 mL, 0.1 mmol) and the reaction stirred at room temperature overnight. The crude reaction mixture was then dry-loaded onto silica and purified by flash silica chromatography (EtOAc:hexane, 5:95) to give **174-B** as a colourless oil (0.001 g, 6%),  $R_f = 0.5$  (EtOAc:hexane, 1:9).

$\nu_{\text{max}}/\text{cm}^{-1}$  (neat): 2948, 2862, 1753, 1732;  $^1\text{H NMR}$  (600 MHz;  $\text{CDCl}_3$ )  $\delta$ : 7.64 (2H, m, Ar *H*), 7.43 (3H, m, Ar *H*), 5.17 (1H, dd,  $J = 4.53$  Hz, 4.14 Hz, *CHO*), 3.64 (3H, s,  $\text{OCH}_3$ ), 2.21 (3H, s, (*2R,5S*),  $\text{COCH}_3$ ), 2.13 (0.04H, s, (*2R,5R*),  $\text{COCH}_3$ ), 1.79 (2H, m,  $\text{CH}_2\text{CHO}$ ) 1.24 (4H, m,  $\text{CH}_2\text{CH}_2$ ), 0.83 (3H, t,  $J = 7.14$  Hz,  $\text{CH}_3\text{CH}_2$ );  $^{13}\text{C NMR}$  (150 MHz;  $\text{CDCl}_3$ )  $\delta$ : 203.7 ( $\text{C}=\text{O}$ ), 166.6 ( $\text{C}=\text{O}$ ), 132.1, 129.8, 128.5, 127.6, 84.7 (q,  $^2J_{\text{CF}} = 22.4$  Hz), 80.5 (*CHO*), 55.8 ( $\text{OCH}_3$ ) 29.8 ( $\text{CH}_2$ ), 27.1 ( $\text{CH}_2$ ), 26.6 ( $\text{CH}_3$ ) 22.1 ( $\text{CH}_2$ ), 13.8 ( $\text{CH}_3$ );  $^{19}\text{F NMR}$  (282 MHz;  $\text{CDCl}_3$ )  $\delta$  -72.1 ( $\text{CF}_3$ );  $m/z$  (HR  $\text{CI}^+$ ) found  $[\text{MH}]^+$  347.1477.  $\text{C}_{17}\text{H}_{22}\text{O}_4\text{F}_3$  requires 347.1470.

**(3S)-Hydroxyoctan-2-one (175)**



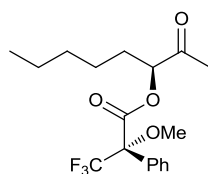
175

$\text{MgCl}_2$  (0.390 mL of 100 mg/mL solution, 0.4 mmol) was added to ThDP (0.022 g, 48  $\mu\text{mol}$ ) in water (10 mL) at pH 7. D469E TK cell-free lysate (2 mL) was added and the mixture was incubated for 20 minutes. In a separate flask, sodium pyruvate (0.110 g, 1.0 mmol) was dissolved in water (10 mL) with hexanal (0.122 mL, 1.0 mmol) and the pH adjusted to 7. This was then added to the enzyme suspension and

stirred in an autotitrator for 18 hours and the reaction was followed by TLC analysis. The product was then extracted with Et<sub>2</sub>O (2 x 500 mL), and the organic layer was dried over magnesium sulfate, filtered and the crude product was then dry-loaded onto silica and purified by flash silica chromatography (Et<sub>2</sub>O:pentane, 5:95) to give **175** as a pale green oil (0.007 g, 6%), R<sub>f</sub> = 0.20 (EtOAc:hexane, 1:9).

$\nu_{\max}/\text{cm}^{-1}$  (neat): 3449, 2956, 2926, 2858, 1716; <sup>1</sup>H NMR (600 MHz; CDCl<sub>3</sub>)  $\delta$ : 4.18 (1H, m, CHOH), 3.46 (1H, d, *J* = 4.9 Hz, CHOH), 2.19 (3H, s, COCH<sub>3</sub>), 1.83-1.20 (8H, m, CH<sub>2</sub>CH<sub>2</sub>CH<sub>2</sub>), 0.91 (3H, m, CH<sub>3</sub>CH<sub>2</sub>); <sup>13</sup>C NMR (150 MHz; CDCl<sub>3</sub>)  $\delta$ : 210.2 (C=O), 77.2 (CHOH), 33.7 (CH<sub>2</sub>), 32.0 (CH<sub>2</sub>), 25.4 (CH<sub>3</sub>), 24.5 (CH<sub>2</sub>), 22.5 (CH<sub>2</sub>), 14.2 (CH<sub>3</sub>), [ $\alpha$ ]<sub>D</sub><sup>20</sup> = +8.5 (*c* 0.35, Et<sub>2</sub>O).

**(S)-(S)-2-oxooctan-3-yl-3,3,3-trifluoro-2-methoxy-2-phenylpropanoate (175-B)**<sup>[104]</sup>

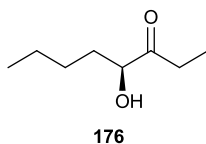


**175-B**

To a stirred solution of **175** (0.007 g, 0.05 mmol) in CH<sub>2</sub>Cl<sub>2</sub> (5 mL) was added triethylamine (0.020 mL, 0.14 mmol) and (*R*)-MTPA-Cl (0.020 mL, 0.1 mmol) and the reaction was stirred at room temperature overnight. The crude reaction mixture was then dry-loaded onto silica and purified by flash silica chromatography (EtOAc:hexane, 5:95) to give **175-B** as a colourless oil (0.001 g, 5%), R<sub>f</sub> = 0.5 (EtOAc:hexane, 1:9).

$\nu_{\max}/\text{cm}^{-1}$  (neat): 2930, 2856, 1717, 1667; <sup>1</sup>H NMR (600 MHz; CDCl<sub>3</sub>)  $\delta$ : 7.65 (2H, m, Ar *H*), 7.43 (3H, m, Ar *H*), 5.18 (1H, dd, *J* = 4.6 Hz, 4.1 Hz, CHO), 3.63 (3H, s, CF<sub>3</sub>COCH<sub>3</sub>), 2.22 (2.95 H, s, (2*R*,5*S*), COCH<sub>3</sub>), 2.13 (0.05 H, s, (2*R*,5*R*), COCH<sub>3</sub>) 1.83-1.05 (8H, m, (CH<sub>2</sub>)<sub>4</sub>), 0.82 (3H, m, CH<sub>3</sub>CH<sub>2</sub>); <sup>13</sup>C NMR (150 MHz; CDCl<sub>3</sub>)  $\delta$ : 203.7 (C=O), 166.5 (C=O), 132.1, 129.8, 128.5, 127.4, 84.7 (q, <sup>2</sup>J<sub>CF</sub> = 28.1 Hz), 80.7 (CHOCO), 55.7 (OCH<sub>3</sub>), 31.3 (CH<sub>2</sub>), 30.0 (CH<sub>2</sub>), 25.5 (CH<sub>2</sub>), 24.8 (CH<sub>3</sub>) 22.3 (CH<sub>2</sub>), 13.9 (CH<sub>3</sub>); *m/z* (HR CI<sup>+</sup>) found [MH]<sup>+</sup> 361.1636. C<sub>18</sub>H<sub>23</sub>O<sub>4</sub>F<sub>3</sub> requires 361.1621.

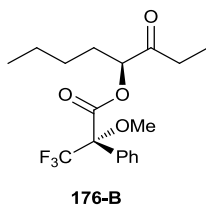
### (4S)-Hydroxyoctan-3-one (176)



MgCl<sub>2</sub> (0.390 mL of 100 mg/mL solution, 0.4 mmol) was added to ThDP (0.022 g, 48 μmol) in water (10 mL) at pH 7.5. S385T/D469T/R520Q TK cell free lysate (2 mL) was added and the mixture was incubated for 20 minutes. In a separate flask, 2-ketobutyric acid (0.102 g, 1.0 mmol) was dissolved in water (10 mL) with pentanal (0.106 mL, 1.0 mmol) and the pH adjusted to 7. This was then added to the enzyme suspension and stirred in an autotitrator for 18 hours and the reaction was followed by TLC analysis. The product was then extracted with Et<sub>2</sub>O (2 x 500 mL), and the organic layer was dried over magnesium sulfate, filtered and dry-loaded onto silica before being purified by flash silica chromatography (Et<sub>2</sub>O:hexane, 5:95) to give **176** as a pale green oil (0.006 g, 4%), R<sub>f</sub> = 0.21 (EtOAc:hexane, 1:9).

$\nu_{\max}/\text{cm}^{-1}$  (neat): 3502, 2953, 2850, 1712; <sup>1</sup>H NMR (600 MHz; CDCl<sub>3</sub>)  $\delta$ : 3.80 (1H, m, CHOH), 3.49 (1H, s, OH), 2.49 (2H, m, COCH<sub>2</sub>), 1.83 (1H, m, CHHCHOH), 1.54 (1H, m, CHHCHOH), 1.45-1.25 (4H, m, CH<sub>2</sub>CH<sub>2</sub>), 1.12 (3H, t, *J* = 7.4 Hz, COCH<sub>2</sub>CH<sub>3</sub>); 0.91 (3H, t, *J* = 7.2 Hz, CH<sub>3</sub>); <sup>13</sup>C NMR (150 MHz; CDCl<sub>3</sub>)  $\delta$ : 213.0 (C=O), 76.4 (CHOH), 34.2 (CH<sub>2</sub>), 31.3 (CH<sub>2</sub>), 26.5 (CH<sub>2</sub>), 22.7 (CH<sub>2</sub>), 14.3, (CH<sub>3</sub>), 7.6 (CH<sub>3</sub>); *m/z* (HR CI+) found [MH]<sup>+</sup> 145.1232. C<sub>8</sub>H<sub>17</sub>O<sub>2</sub> requires 145.1228. [ $\alpha$ ]<sub>D</sub><sup>20</sup> = + 83.3 (*c* 0.15, CDCl<sub>3</sub>).

### (S)-(S)-3-oxooctan-4-yl-3,3,3-trifluoro-2-methoxy-2-phenylpropanoate (176-B)

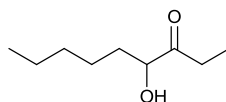


To a stirred solution of **176** (0.006 g, 0.04 mmol) in CH<sub>2</sub>Cl<sub>2</sub> (5 mL) was added triethylamine (0.020 mL, 0.14 mmol) and (*R*)-MTPA-Cl (0.020 mL, 0.1 mmol) and the reaction was stirred at room temperature overnight. The crude reaction mixture

was dry-loaded onto silica and purified by flash silica chromatography (EtOAc:hexane, 5:95) to give **176-B** as a colourless oil (0.001 g, 6%),  $R_f = 0.52$  (EtOAc:hexane, 1:9).

$\nu_{\max}/\text{cm}^{-1}$  (neat): 2938, 2857, 1753, 1715;  $^1\text{H NMR}$  (600 MHz;  $\text{CDCl}_3$ )  $\delta$ : 7.65-7.42 (5H, m, Ar H), 5.17 (1H, m, CHCO), 3.64 (3H, s, OCH<sub>3</sub>), 2.51 (2H, m, COCH<sub>2</sub>CH<sub>3</sub>), 1.84-1.18 (6H, m, CH<sub>2</sub>CH<sub>2</sub>CH<sub>2</sub>), 1.10 (3H, t,  $J = 7.3$  Hz, COCH<sub>2</sub>CH<sub>3</sub>), 0.82 (3H, t,  $J = 7.0$  Hz, CH<sub>3</sub>CH<sub>2</sub>);  $^{13}\text{C NMR}$  (150 MHz;  $\text{CDCl}_3$ )  $\delta$ : 206.5 (C=O), 166.5 (C=O), 132.1, 129.8, 128.9, 127.6, 84.7 (q,  $^2J_{\text{CF}} = 28.1$  Hz), 80.1 (CHO), 55.8 (OCH<sub>3</sub>) 33.9, (CH<sub>2</sub>), 29.8 (CH<sub>2</sub>), 27.1 (CH<sub>2</sub>), 25.4 (CH<sub>2</sub>), 14.3 (CH<sub>3</sub>), 7.4 (CH<sub>3</sub>);  $^{19}\text{F NMR}$  (282 MHz;  $\text{CDCl}_3$ )  $\delta$  -72.1 (CF<sub>3</sub>);  $m/z$  (HR CI+) found  $[\text{MH}]^+$  361.1627. C<sub>18</sub>H<sub>23</sub>F<sub>3</sub>O<sub>4</sub> requires 361.1633.

#### 4-hydroxynonan-3-one (177)



177

MgCl<sub>2</sub> (0.390 mL of 100 mg/mL solution, 0.4 mmol) was added to ThDP (0.022 g, 48 μmol) in water (10 mL) at pH 7. D469E/R520Q TK cell free lysate (2 mL) was added and the mixture was incubated for 20 minutes. In a separate flask, 2-ketobutyric acid (0.102 g, 1.0 mmol) was dissolved in water (10 mL) with hexanal (0.122 mL, 1.0 mmol) and the pH adjusted to 7. This was then added to the enzyme suspension and stirred in an autotitrator for 18 hours and the reaction was followed by TLC analysis. The product was then extracted with Et<sub>2</sub>O (2 x 500 mL), and the organic layer was dried over magnesium sulfate, filtered and dry-loaded onto silica before being purified by flash silica chromatography (Et<sub>2</sub>O:pentane, 5:95) to give **177** as a pale green oil (0.013 g, 8%),  $R_f = 0.21$  (EtOAc:hexane, 1:9).

$\nu_{\max}/\text{cm}^{-1}$  (neat): 3451, 2932, 2860, 1712;  $^1\text{H NMR}$  (300 MHz;  $\text{CDCl}_3$ )  $\delta$ : 4.19 (1H, m, CHOH), 2.49 (2H, m, COCH<sub>2</sub>), 1.40-0.74 (14H, m, CH<sub>3</sub>CH<sub>2</sub>CH<sub>2</sub>CH<sub>2</sub>CH<sub>2</sub>, COCH<sub>2</sub>CH<sub>3</sub>);  $^{13}\text{C NMR}$  (75 MHz;  $\text{CDCl}_3$ )  $\delta$ : 212.9 (C=O), 76.2 (CHOH), 34.1 (CH<sub>2</sub>), 33.8 (CH<sub>2</sub>), 31.7 (CH<sub>2</sub>), 31.1 (CH<sub>2</sub>), 24.5 (CH<sub>2</sub>), 22.3 (CH<sub>2</sub>), 7.6 (CH<sub>3</sub>);  $m/z$  (HR CI+) found  $[\text{MH}]^+$  159.1394. C<sub>9</sub>H<sub>19</sub>O<sub>2</sub> requires 159.1385,  $[\alpha]_D^{20} = +95.3$  (c 0.15,  $\text{CDCl}_3$ ).

## 9 References

- [1] P. Anastas, Warner, J., *Green Chemistry: Theory and Practice* Oxford University Press, **1998**.
- [2] L. Rosenthaler, *Biochem. Z.* **1908**, *14*, 238–253.
- [3] L. Hecquet, J. Bolte, C. Demuynck, *Tetrahedron* **1996**, *52*, 8223-8232.
- [4] V. J. Jensen, S. Rugh, *Method Enzymol.* **1987**, *136*, 356-370.
- [5] H. Griengl, H. Schwab, M. Fechter, *Trends Biotechnol.* **2000**, *18*, 252-256.
- [6] G. Hills, *Eur. J. Lipid Sci. Technol.* **2003**, *105*, 601-607.
- [7] C. K. Savile, J. M. Janey, E. C. Mundorff, J. C. Moore, S. Tam, W. R. Jarvis, J. C. Colbeck, A. Krebber, F. J. Fleitz, J. Brands, P. N. Devine, G. W. Huisman, G. J. Hughes, *Science* **2010**, *329*, 305-309.
- [8] S. K. Ma, J. Gruber, C. Davis, L. Newman, D. Gray, A. Wang, J. Grate, G. W. Huisman, R. A. Sheldon, *Green Chem.* **2010**, *12*, 81-86.
- [9] N. Urano, S. Fukui, S. Kumashiro, T. Ishige, S. Kita, K. Sakamoto, M. Kataoka, S. Shimizu, *J. Biosci. Bioeng.* **2011**, *111*, 266-271.
- [10] L. Hecquet, M. Lemaire, J. Bolte, C. Demuynck, *Tetrahedron Lett.* **1994**, *35*, 8791-8794.
- [11] D.-K. Ro, E. M. Paradise, M. Ouellet, K. J. Fisher, K. L. Newman, J. M. Ndungu, K. A. Ho, R. A. Eachus, T. S. Ham, J. Kirby, M. C. Y. Chang, S. T. Withers, Y. Shiba, R. Sarpong, J. D. Keasling, *Nature* **2006**, *440*, 940-943.
- [12] C. Y. Zhu, S. P. Cook, *J. Am. Chem. Soc.* **2012**, *134*, 13577-13579.
- [13] M. Muller, D. Gocke, M. Pohl, *Febs Journal* **2009**, *276*, 2894-2904.
- [14] M. Brovetto, D. Gamenara, P. S. Mendez, G. A. Seoane, *Chem. Rev.* **2011**, *111*, 4346-4403.
- [15] D. Meyer, L. Walter, G. Kolter, M. Pohl, M. Muller, K. Tittmann, *J. Am. Chem. Soc.* **2011**, *133*, 3609-3616.
- [16] J. M. Candy, R. G. Duggleby, *BBA-Protein Struct. M.* **1998**, *1385*, 323-338.
- [17] D. Dobritzsch, S. Konig, G. Schneider, G. G. Lu, *J. Biol. Chem.* **1998**, *273*, 20196-20204.
- [18] A. Y. Tsou, S. C. Ransom, J. A. Gerlt, D. D. Buechter, P. C. Babbitt, G. L. Kenyon, *Biochemistry* **1990**, *29*, 9856-9862.

- [19] M. S. Hasson, A. Muscate, M. J. McLeish, L. S. Polovnikova, J. A. Gerlt, G. L. Kenyon, G. A. Petsko, D. Ringe, *Biochemistry* **1998**, *37*, 9918-9930.
- [20] H. Iding, T. Dunnwald, L. Greiner, A. Liese, M. Muller, P. Siegert, J. Grotzinger, A. S. Demir, M. Pohl, *Chem. Eur. J.* **2000**, *6*, 1483-1495.
- [21] P. Dunkelmann, D. Kolter-Jung, A. Nitsche, A. S. Demir, P. Siegert, B. Lingen, M. Baumann, M. Pohl, M. Muller, *J. Am. Chem. Soc.* **2002**, *124*, 12084-12085.
- [22] E. Racker, *The Enzymes*, Vol. 5, Academic Press, New York, **1961**.
- [23] M. Sundstrom, Y. Lindqvist, G. Schneider, U. Hellman, H. Ronne, *J. Biol. Chem.* **1993**, *268*, 24346-24352.
- [24] G. Schneider, Y. Lindqvist, *BBA-Protein Struct. M.* **1998**, *1385*, 387-398.
- [25] N. J. Turner, *Curr. Opin. Biotechnol.* **2000**, *11*, 527-531.
- [26] A. Cázares, J. L. Galman, L. G. Crago, M. E. B. Smith, J. Strafford, L. Ríos-Solís, G. J. Lye, P. A. Dalby, H. C. Hailes, *Org. Biomol. Chem.* **2010**, *8*, 1301.
- [27] P. P. Philippov, I. K. Shestakova, N. K. Tikhomirova, G. A. Kochetov, *BBA-Enzymol.* **1980**, *613*, 359-369.
- [28] F. Paoletti, D. Aldinucci, *Arch. Biochem. Biophys.* **1986**, *245*, 212-219.
- [29] S. W. Masri, M. Ali, C. J. Gubler, *Comp. Biochem. Phys. B* **1988**, *90*, 167-172.
- [30] M. E. Kiely, E. L. Tan, T. Wood, *Can. J. Biochem.* **1969**, *47*, 455-460.
- [31] J. P. Blass, S. Piacentini, E. Boldizsar, A. Baker, *J. Neurochem.* **1982**, *39*, 729-733.
- [32] A. Mocali, F. Paoletti, *Eur. J. Biochem.* **1989**, *180*, 213-219.
- [33] M. Abedinia, R. Layfield, S. M. Jones, P. F. Nixon, J. S. Mattick, *Biochem. Biophys. Res. Commun.* **1992**, *183*, 1159-1166.
- [34] C. Demuynck, J. Bolte, L. Hecquet, V. Dalmas, *Tetrahedron Lett.* **1991**, *32*, 5085-5088.
- [35] G. R. Hobbs, M. D. Lilly, N. J. Turner, J. M. Ward, A. J. Willets, J. M. Woodley, *J. Chem. Soc., Perkin Trans. 1* **1993**, 165-166.
- [36] Y. Lindqvist, G. Schneider, U. Ermler, M. Sundstrom, *EMBO J.* **1992**, *11*, 2373-2379.
- [37] U. Nilsson, L. Meshalkina, Y. Lindqvist, G. Schneider, *J. Biol. Chem.* **1997**, *272*, 1864-1869.

- [38] L. Meshalkina, U. Nilsson, C. Wikner, T. Kostikowa, G. Schneider, *Eur. J. Biochem.* **1997**, *244*, 646-652.
- [39] C. Wikner, L. Meshalkina, U. Nilsson, M. Nikkola, Y. Lindqvist, M. Sundstrom, G. Schneider, *J. Biol. Chem.* **1994**, *269*, 32144-32150.
- [40] C. Wikner, U. Nilsson, L. Meshalkina, C. Udekwu, Y. Lindqvist, G. Schneider, *Biochemistry* **1997**, *36*, 15643-15649.
- [41] C. Wikner, L. Meshalkina, U. Nilsson, S. Backstrom, Y. Lindqvist, G. Schneider, *Eur. J. Biochem.* **1995**, *233*, 750-755.
- [42] U. Nilsson, L. Hecquet, T. Gefflaut, C. Guerard, G. Schneider, *FEBS Lett.* **1998**, *424*, 49-52.
- [43] A. Ranoux, S. K. Karmee, J. F. Jin, A. Bhaduri, A. Caiazzo, I. Arends, U. Hanefeld, *Chembiochem* **2012**, *13*, 1921-1931.
- [44] A. Ranoux, I. W. C. E. Arends, U. Hanefeld, *Tetrahedron Lett.* **2012**, *53*, 790-793.
- [45] G. A. Sprenger, M. Pohl, *J. Mol. Catal. B: Enzym.* **1999**, *6*, 145-159.
- [46] E. G. Hibbert, T. Senussi, S. J. Costelloe, W. Lei, M. E. B. Smith, J. M. Ward, H. C. Hailes, P. A. Dalby, *J. Biotechnol.* **2007**, *131*, 425-432.
- [47] E. G. Hibbert, T. Senussi, M. E. B. Smith, S. J. Costelloe, J. M. Ward, H. C. Hailes, P. A. Dalby, *J. Biotechnol.* **2008**, *134*, 240-245.
- [48] M. E. B. Smith, E. G. Hibbert, A. B. Jones, P. A. Dalby, H. C. Hailes, *Adv. Synth. Catal.* **2008**, *350*, 2631-2638.
- [49] D. Yi, T. Devamani, J. Abdoul-Zabar, F. Charmantray, V. Helaine, L. Hecquet, W.-D. Fessner, *Chembiochem* **2012**, *13*, 2290-2300.
- [50] M. E. B. Smith, K. Smithies, T. Senussi, P. A. Dalby, H. C. Hailes, *Eur. J. Org. Chem.* **2006**, *2006*, 1121-1123.
- [51] C. H. Wong, F. P. Mazonod, G. M. Whitesides, *J. Org. Chem.* **1983**, *48*, 3493-3497.
- [52] K. G. Morris, M. E. B. Smith, N. J. Turner, M. D. Lilly, R. K. Mitra, J. M. Woodley, *Tetrahedron: Asymmetry* **1996**, *7*, 2185-2188.
- [53] A. J. Humphrey, S. F. Parsons, M. E. B. Smith, N. J. Turner, *Tetrahedron Lett.* **2000**, *41*, 4481-4485.
- [54] R. K. Mitra, J. M. Woodley, M. D. Lilly, *Enzyme Microb. Technol.* **1998**, *22*, 64-70.

- [55] J. Bongs, D. Hahn, U. Schorken, G. A. Sprenger, U. Kragl, C. Wandrey, *Biotechnol. Lett.* **1997**, *19*, 213-215.
- [56] G. J. Lye, J. M. Woodley, *Trends Biotechnol.* **1999**, *17*, 395-402.
- [57] S. Brocklebank, J. M. Woodley, M. D. Lilly, *J. Mol. Catal. B: Enzym.* **1999**, *7*, 223-231.
- [58] B.-Y. Hwang, B.-K. Cho, H. Yun, K. Koteshwar, B.-G. Kim, *J. Mol. Catal. B: Enzym.* **2005**, *37*, 47-55.
- [59] J. N. Jansonius, *Curr. Opin. Struc. Biol.* **1998**, *8*, 759-769.
- [60] P. Christen, Metzler, D.E., *Transaminases*, Wiley, New York, **1985**.
- [61] P. K. Mehta, T. I. Hale, P. Christen, *Eur. J. Biochem.* **1993**, *214*, 549-561.
- [62] J. Ward, R. Wohlgemuth, *Curr. Org. Chem.* **2010**, *14*, 1914-1927.
- [63] K. Yonaha, S. Toyama, M. Yasuda, K. Soda, *FEBS Lett.* **1976**, *71*, 21-24.
- [64] K. Yonaha, S. Toyama, K. Soda, *Method Enzymol.* **1987**, *Volume 143*, 500-504.
- [65] J. S. Shin, B. G. Kim, *Biosci., Biotechnol., Biochem.* **2001**, *65*, 1782-1788.
- [66] U. Kaulmann, K. Smithies, M. E. B. Smith, H. C. Hailes, J. M. Ward, *Enzyme Microb. Technol.* **2007**, *41*, 628-637.
- [67] B. K. Cho, H. J. Cho, S. H. Park, H. Yun, B. G. Kim, *Biotechnol. Bioeng.* **2003**, *81*, 783-789.
- [68] D. Koszelewski, D. Clay, K. Faber, W. Kroutil, *J. Mol. Catal. B: Enzym.* **2009**, *60*, 191-194.
- [69] M. Fuchs, D. Koszelewski, K. Tauber, W. Kroutil, K. Faber, *Chem. Commun.* **2010**, *46*, 5500-5502.
- [70] F. M. Platt, G. R. Neises, R. A. Dwek, T. D. Butters, *J. Biol. Chem.* **1994**, *269*, 8362-8365.
- [71] A. El Nemr, *Tetrahedron* **2000**, *56*, 8579-8629.
- [72] C. F. Snook, J. A. Jones, Y. A. Hannun, *BBA-Mol. Cell. Biol. L.* **2006**, *1761*, 927-946.
- [73] G. Bhaskar, *Tetrahedron: Asymmetry* **2004**, *15*, 1279-1283.
- [74] C. U. Ingram, M. Bommer, M. E. B. Smith, P. A. Dalby, J. M. Ward, H. C. Hailes, G. J. Lye, *Biotechnol. Bioeng.* **2007**, *96*, 559-569.
- [75] K. Smithies, M. E. B. Smith, U. Kaulmann, J. L. Galman, J. M. Ward, H. C. Hailes, *Tetrahedron: Asymmetry* **2009**, *20*, 570-574.
- [76] Bhaskar, G., *Tetrahedron: Asymmetry* **2004**, *15*, 1279-1283.



- [77] S. George, S. V. Narina, A. Sudalai, *Tetrahedron* **2006**, *62*, 10202-10207.
- [78] B. O'Sullivan, H. Al-Bahrani, J. Lawrence, M. Campos, A. Cazares, F. Baganz, R. Wohlgemuth, H. C. Hailes, N. Szita, *J. Mol. Catal. B: Enzym.* **2012**, *77*, 1-8.
- [79] J. L. Galman, D. Steadman, L. D. Haigh, H. C. Hailes, *Org. Biomol. Chem.* **2012**, *10*, 2621.
- [80] S. R. Wilson, Y. Wu, *Organometallics* **1993**, *12*, 1478-1480.
- [81] S. R. Wilson, Q. Lu, M. L. Tulchinsky, Y. Wu, *J. Chem. Soc., Chem. Commun.* **1993**, 664-665.
- [82] K. Rohr, R. Mahrwald, *Org. Lett.* **2011**, *13*, 1878-1880.
- [83] J. L. Galman, H. C. Hailes, *Tetrahedron: Asymmetry* **2009**, *20*, 1828-1831.
- [84] M. E. B. Smith, U. Kaulmann, J. M. Ward, H. C. Hailes, *Biorg. Med. Chem.* **2006**, *14*, 7062-7065.
- [85] J. L. Galman, D. Steadman, S. Bacon, P. Morris, M. E. B. Smith, J. M. Ward, P. A. Dalby, H. C. Hailes, *Chem. Commun.* **2010**, *46*, 7608.
- [86] S. J. Costelloe, J. M. Ward, P. A. Dalby, *J. Mol. Evol.* **2008**, *66*, 36-49.
- [87] A. J. Humphrey, N. J. Turner, R. McCague, S. J. C. Taylor, *J. Chem. Soc.-Chem. Commun.* **1995**, 2475-2476.
- [88] J. Strafford, P. Payongsri, E. G. Hibbert, P. Morris, S. S. Batth, D. Steadman, M. E. B. Smith, J. M. Ward, H. C. Hailes, P. A. Dalby, *J. Biotechnol.* **2012**, *157*, 237-245.
- [89] M. Socolich, S. W. Lockless, W. P. Russ, H. Lee, K. H. Gardner, R. Ranganathan, *Nature* **2005**, *437*, 512-518.
- [90] P. Asztalos, C. Parthier, R. Golbik, M. Kleinschmidt, G. Hubner, M. S. Weiss, R. Friedemann, G. Wille, K. Tittmann, *Biochemistry* **2007**, *46*, 12037-12052.
- [91] P. Payongsri, D. Steadman, H. C. Hailes, P. A. Dalby, *Org. Biomol. Chem.* **2012**, *10*, 9021-9029.
- [92] J. Paramesvaran, E. G. Hibbert, A. J. Russell, P. A. Dalby, *Protein Eng. Des. Sel.* **2009**, *22*, 401-411.
- [93] E. Kühnel, D. D. P. Laffan, G. C. Lloyd-Jones, T. Martínez del Campo, I. R. Shepperson, J. L. Slaughter, *Angew. Chem. Int. Ed.* **2007**, *46*, 7075-7078.
- [94] N. Hashimoto, T. Aoyama, T. Shioiri, *Chem. Pharm. Bull.* **1981**, *29*, 1475-1478.

- [95] T. Aoyama, T. Shioiri, *Chem. Pharm. Bull.* **1981**, *29*, 3249-3255.
- [96] M. Kapoor, M. N. Gupta, *Process Biochem.* **2012**, *47*, 555-569.
- [97] J. S. Shin, B. G. Kim, *J. Org. Chem.* **2002**, *67*, 2848-2853.
- [98] F. Yasuhara, S. Yamaguchi, R. Kasai, O. Tanaka, *Tetrahedron Lett.* **1986**, *27*, 4033-4034.
- [99] E. Racker, G. Delahaba, I. G. Leder, *J. Am. Chem. Soc.* **1953**, *75*, 1010-1011.
- [100] P. Srere, J. R. Cooper, M. Tabachnick, E. Racker, *Arch. Biochem. Biophys.* **1958**, *74*, 295-305.
- [101] B. L. Horecker, P. Z. Smyrniotis, H. Klenow, *J. Biol. Chem.* **1953**, *205*, 661-682.
- [102] O. A. Esakova, L. E. Meshalkina, G. A. Kochetov, R. Golbik, *Biochemistry-Moscow* **2009**, *74*, 1234-1238.
- [103] G. Scheid, W. Kuit, E. Ruijter, Romano V. A. Orru, E. Henke, U. Bornscheuer, Ludger A. Wessjohann, *Eur. J. Org. Chem.* **2004**, *2004*, 1063-1074.
- [104] X. Shi, W. S. Leal, J. Meinwald, *Biorg. Med. Chem.* **1996**, *4*, 297-303.
- [105] W. S. Leal, X. W. Shi, K. Nakamuta, M. Ono, J. Meinwald, *P. Natl. Acad. Sci. USA* **1995**, *92*, 1038-1042.
- [106] A. Kurutsch, M. Richter, V. Brecht, G. A. Sprenger, M. Mueller, *J. Mol. Catal. B: Enzym.* **2009**, *61*, 56-66.
- [107] R. C. Simon, B. Grischek, F. Zepeck, A. Steinreiber, F. Belaj, W. Kroutil, *Angew. Chem. Int. Edit.* **2012**, *51*, 6713-6716.
- [108] J. L. Galman, D. Steadman, L. D. Haigh, H. C. Hailes, *Org. Biomol. Chem.* **2012**, *10*, 2621-2628.

## Appendix

1. Galman, J. L.; **Steadman, D.**; Bacon, S.; Morris, P.; Smith, M. E. B.; Ward, J. M.; Dalby, P. A.; Hailes, H. C.,  $\alpha,\alpha'$ -Dihydroxyketone formation using aromatic and heteroaromatic aldehydes with evolved transketolase enzymes (2010) *Chem. Commun.*, 46 (40), 7608.
2. Galman, J.L; **Steadman, D.**; Haigh, L.D.; Hailes, H.C., Investigating the reaction mechanism and organocatalytic synthesis of  $\alpha,\alpha'$ -dihydroxyketones (2012) *Org. Biomol. Chem.*, 10, 2621.
3. Payongsri, P.; **Steadman, D.**; Strafford, J.; MacMurray, A; Hailes, H.C; Dalby, P.A., Rational substrate and enzyme engineering of transketolase for aromatics (2012) *Org. Biomol. Chem.*, 10, 9021.











































